

Departamento de Tecnología de Alimentos



UNIVERSITAT  
POLITÈCNICA  
DE VALÈNCIA

**APLICACIÓN DE TECNOLOGÍAS EMERGENTES PARA  
LA OBTENCIÓN DE ZINC PROTOPORFIRINA Y  
PROTEÍNAS FUNCIONALES A PARTIR DE  
COPRODUCTOS CÁRNICOS**

**TESIS DOCTORAL**

Presentada por:

**Blanca Abril Gisbert**

Dirigida por:

**Dr. José Javier Benedito Fort**

**Dr. José Vicente García Pérez**

**Valencia, Enero 2023**



D. JOSE JAVIER BENEDITO FORT Y D. JOSE VICENTE GARCÍA PÉREZ,  
AMBOS CATEDRÁTICOS DE UNIVERSIDAD DEL DEPARTAMENTO DE  
TECNOLOGÍA DE ALIMENTOS DE LA UNIVERSITAT POLITÈCNICA DE VALÈNCIA

CERTIFICAN:

Que la memoria titulada “APLICACIÓN DE TECNOLOGÍAS EMERGENTES PARA LA OBTENCIÓN DE ZINC PROTOPORFIRINA Y PROTEINAS FUNCIONALES A PARTIR DE COPRODUCTOS CÁRNICOS”, presentada por Dña. Blanca Abril Gisbert para aspirar al grado de Doctora en Ciencia, Tecnología y Gestión Alimentaria y realizada bajo nuestra dirección en el Departamento de Tecnología de Alimentos de la Universitat Politècnica de València, cumple las condiciones adecuadas para su aceptación como Tesis Doctoral, por lo que

AUTORIZAN:

A la interesada a su presentación en el Departamento de Tecnología de Alimentos de la Universitat Politècnica de València.

Y para que conste a los efectos oportunos, presentamos la referida memoria firmando el presente certificado en Valencia, 2023.

Fdo. Dr. D. José Javier Benedito Fort

Fdo. Dr. D. José Vicente García Pérez



## **Agradecimientos**

*Aunque esta Tesis Doctoral lleva mi nombre, son muchas las personas que han aportado su granito de arena, y de una forma u otra han conseguido que salga a la luz.*

*En primer lugar, quiero agradecer a mis directores José Benedito Fort y José Vicente García Pérez por haberme dado la oportunidad de llevar a cabo esta Tesis Doctoral. Gracias por haberme introducido en el mundo de la Investigación, por vuestra guía, dedicación, por formarme y aprender tantísimo durante estos años de doctorado.*

*A Ricard Bou, para mí un director de tesis más. Gracias por haberme enseñado y ayudado tanto, desde el primer hasta el último día, por haberme transmitido tu pasión y haberme animado a seguir en momentos bajos.*

*A todos los profesores y técnicos del grupo ASPA. Ramón, gracias por los montajes y soluciones al instante, ahora sé un poquito más de ingeniería.*

*A todos mis compañeros del laboratorio del grupo ASPA (Paola, Nelson, Alba, Andrés, Sergio, Malike...) y en especial al Food Team: Virginia, Beatriz, Ángela, Marina y Lola, porque no me hubiera imaginado realizar una Tesis Doctoral sin vosotras. ¡Somos una piña! En particular agradecer a Virginia y a Beatriz por haberme escuchado y soportado en momentos de agobio y haber sabido transmitirme paz y calma. Por saber estar siempre. Es difícil explicar cómo en tan solo 4 años os habéis convertido en personas imprescindibles para mí.*

*A mis padres por todo su apoyo, confianza y cariño. Gracias por creer siempre en mí, por enseñarme el valor del esfuerzo y la constancia, sin vuestra ayuda hoy no estaría redactando mi Tesis Doctoral. A mi hermano Andrés por las risas, los ánimos y el apoyo cuando más lo he necesitado. Por preocuparte por mí. Por nuestros paseos y charradas cuando llegábamos al Puerto de Sagunto, los cuales eran curanderos. Eres el mejor hermano que puedo tener. ¡Os quiero!*

*Por último, pero no menos importante, a ti Álvaro. Gracias por apoyarme como lo has hecho, por tu comprensión y paciencia, especialmente durante estos últimos meses. Como dice nuestro Cholo "Nunca dejes de creer", gracias por creer en mí.*

**Blanca**



---

Abstract .....	XIII
Resumen .....	XX
Resum .....	XXVIII
<b>1. INTRODUCCIÓN.....</b>	<b>37</b>
<b>1.1. Hígado de cerdo .....</b>	<b>39</b>
1.1.1. Proteína del hígado .....	40
1.1.2. Ferroquelatasa de hígado de cerdo .....	42
<b>1.2. Estabilización de productos cárnicos mediante secado .....</b>	<b>44</b>
1.2.1. Cinéticas y modelos de secados.....	47
<b>1.3. Desodorización de alimentos .....</b>	<b>49</b>
1.3.1. Métodos empleados .....	50
<b>1.4. Características de la zinc protoporfirina e importancia en el sector .....</b>	<b>51</b>
cárnico.....	51
<b>1.5. Intensificación de la extracción de enzimas. Ultrasonidos .....</b>	<b>54</b>
<b>1.6. Intensificación de reacciones enzimáticas. Ultrasonidos .....</b>	<b>57</b>
<b>1.7. Justificación de la Tesis .....</b>	<b>60</b>
<b>2. OBJETIVOS .....</b>	<b>66</b>
<b>3. METODOLOGÍA.....</b>	<b>71</b>
<b>3.1. Plan de trabajo.....</b>	<b>73</b>
<b>3.2. Preparación de muestras .....</b>	<b>76</b>
3.2.1. Homogeneizado de hígado de cerdo .....	76
3.2.2. Hígado deshidratado .....	78
<b>3.3. Extracción de la enzima ferroquelatasa (FeQ): método convencional y por... ultrasonidos (US) .....</b>	<b>79</b>
<b>3.4. Formación de zinc protoporfirina (ZnPP) .....</b>	<b>80</b>

---

3.4.1. Formación de ZnPP a partir de extracto de FeQ .....	80
3.4.2. Formación de ZnPP a partir de homogeneizado de hígado obtenido..... de modo convencional y asistido por US .....	81
<b>3.5. Secado de hígado de cerdo .....</b>	<b>85</b>
3.5.1. Secado convectivo a baja temperatura .....	86
3.5.2. Secado convectivo a alta temperatura .....	86
3.5.3. Modelado de la cinética de secado.....	88
<b>3.6. Desgrasado de hígado de cerdo .....</b>	<b>89</b>
<b>3.7. Desodorización de hígado de cerdo .....</b>	<b>90</b>
3.7.1. Arrastre por vapor con aplicación de vacío .....	90
3.7.2. CO <sub>2</sub> supercrítico .....	91
<b>3.8. Análisis de compuestos orgánicos volátiles .....</b>	<b>93</b>
<b>3.9. Características fisicoquímicas .....</b>	<b>95</b>
3.9.1. Composición química .....	95
3.9.2. Medida de color.....	96
3.9.3. Análisis de calorimetría diferencial de barrido.....	96
<b>3.10. Propiedades tecno-funcionales .....</b>	<b>97</b>
3.10.1. Solubilidad de proteínas .....	97
3.10.2. Propiedades espumantes.....	97
3.10.3. Propiedades emulsionantes .....	98
<b>3.11. Análisis estadístico.....</b>	<b>99</b>
<b>4. RESULTADOS Y DISCUSIÓN.....</b>	<b>102</b>
<b>4.1. Capítulo 1. Aplicación de ultrasonidos para mejorar la formación del pigmento zinc protoporfirina a partir de hígado de cerdo como fuente de ferroquelatasa.....</b>	<b>104</b>
<i>'Ultrasound intensification of ferrochelatase extraction from pork liver as a strategy to improve zinc protoporphyrin formation'</i> .....	106



---

<i>'Influence of ultrasonic application on the enzymatic formation of zinc protoporphyrin'</i> .....	136
<b>4.2. Capítulo 2. Secado y desgrasado de hígado de cerdo</b> .....	<b>164</b>
<i>'Influence of pork liver drying on ferrochelataase activity for zinc protoporphyrin formation'</i> .....	166
<i>'Physicochemical and techno-functional properties of dried and defatted porcine liver'</i> .....	200
<b>4.3. Capítulo 3. Desodorización de hígado de cerdo</b> .....	<b>229</b>
<i>'Supercritical CO<sub>2</sub> deodorization of dried pork liver'</i> .....	231
<b>5. DISCUSIÓN GENERAL</b> .....	<b>268</b>
<b>6. CONCLUSIONES</b> .....	<b>282</b>
<b>7. RECOMENDACIONES</b> .....	<b>290</b>
<b>8. CONTRIBUCIONES CIENTÍFICAS</b> .....	<b>295</b>
<b>9. REFERENCIAS</b> .....	<b>300</b>
<b>ANEXOS</b> .....	<b>326</b>
<i>'Role of enzymatic reactions in meat processing and use of emergent technologies for process intensification'</i> .....	328



**ABSTRACT / RESUMEN / RESUM**



---

## APPLICATION OF EMERGING TECHNOLOGIES TO OBTAIN ZINC PROTOPORPHYRIN AND FUNCTIONAL PROTEINS FROM MEAT CO-PRODUCTS

Pork liver represents a relevant co-product of the pork industry. As a result of new consumer trends, there has been a decrease in its demand, so today it has a low commercial value. However, pork liver has excellent nutritional properties, has an elevated protein content of high biological and techno-functional value, is rich in minerals and vitamins and in turn, has a low fat content, so it can be considered an excellent product for food use. In addition, recent studies have shown that pork liver has high catalytic activity for the zinc protoporphyrin (ZnPP) formation due to the presence of the enzyme ferrochelatase (FeCH). ZnPP is a natural red colorant with high stability that has been identified in Parma Ham and also in other meat products. Its production at an industrial scale and its addition to meat products could be useful to improve its color, avoiding or minimizing the use of nitrites and nitrates. However, the enzymatic process of ZnPP formation is generally slow. In this sense, new technologies are emerging, such as power ultrasound (US), which have been applied to accelerate and intensify enzymatic reactions, through the improvement of the mass transfer phenomena. Moreover, US has also been used to facilitate the extraction of various compounds of interest, including enzymes. Therefore, from the technological point of view, the use of US may be interesting to improve the enzymatic process of ZnPP formation catalyzed by FeCH, obtained from pork liver.

One of the main problems presented by the pork liver is that it is a very perishable organ, due to its high water content. In addition, the liver contains volatile organic compounds (VOCs) that generate a strong unpleasant aroma, which causes an important consumer's rejection. However, the liver has a very interesting protein fraction from the nutritional and techno-functional point of view, so its use could be very convenient for the food industry. Therefore, in order to recover the protein fraction of the liver at an industrial level, its dehydration could be interesting. This could extend its shelf life, eliminating its majority component, the water, and would facilitate its handling and storage, for later use in applications such as the extraction of proteins and/or enzymes. In addition, the removal or reduction of the fat fraction would also facilitate

the recovery of the protein fraction, and limit degradation reactions, such as oxidation and lipid hydrolysis. However, it is important to determine how the reduction of water and fat can affect the techno-functional properties and quality of proteins. Hot air drying is one of the most important unit operations in food processing. Despite this, it can cause significant changes that can affect the quality of the product, especially when high temperatures are used. In this sense, an alternative to high temperature convective drying could be low temperature convective drying, which could improve the properties of the product. In general, for the removal of VOCs, vacuum steam distillation (VSD) or without vacuum application (SD) are used. The VSD technique is a treatment that uses water vapor at moderate temperatures and at low pressure, the steam drags the VOCs of the sample to be treated, which condense into a distillate (waste). On the other hand, extraction by supercritical CO<sub>2</sub> (SC-CO<sub>2</sub>) is a promising processing technology for the deodorization of meat products, since SC-CO<sub>2</sub> has been used as a solvent in food applications for its physicochemical properties, including low viscosity, liquid-like density and high diffusivity. In the literature, different works have described the ability of SC-CO<sub>2</sub> to eliminate VOCs in products such as fish sauce, water, truffles, lavender and thyme extracts, or vegetable protein isolates, among others. However, to date, this deodorization technology has not been applied in a matrix of animal origin such as pork liver.

In this context, the main objective of this PhD Thesis was to evaluate the viability of different emerging technologies for the revaluation of pork liver as a co-product of animal origin to obtain compounds of techno-functional interest. Thus, the effect of the US application was analyzed, using different times and modes of application (continuous and pulsed) on the FeCH extraction from the pork liver, determining the enzymatic activity by analyzing the kinetics of ZnPP formation and characterizing the acoustic field used and the energy efficiency of the different conditions tested. In addition, the feasibility of using US, applied at moderate and low intensities, was evaluated for the improvement of the enzymatic reaction of ZnPP formation catalyzed by FeCH from different substrates: homogenized pork liver (HLi) and homogenized pork liver, with the addition of oxyhemoglobin (HLi+OxyHb) from pork blood. The drying process in a wide range of temperatures (from -10 to 70 °C) and

defatting was also studied for the stabilization of the pork liver and its subsequent use for the FeCH extraction and the use of the protein fraction. Finally, the deodorization process of dried pork liver was evaluated using two techniques: VSD and extraction by SC-CO<sub>2</sub>.

The FeCH extraction was performed from thawed pork liver homogenized with a standard buffer solution at refrigeration temperature (4 °C), by conventional mechanical stirring (30 min) and by US-assisted extraction (400 W). The US treatments were performed with continuous and pulsed application (0.5 s ON / 0.5 s OFF) at different extraction times (1, 2.5 and 5 min). The enzymatic activity was evaluated by quantifying the ZnPP obtained from exogenous substrates (protoporphyrin IX and ZnSO<sub>4</sub>) at 37 °C, studying the formation kinetics for 120 min. In addition, the intensification of the enzymatic reaction of FeCH to form ZnPP was also investigated, by applying US in HLi and HLi+OxyHb. The ZnPP formation was carried out at 37 °C under anaerobic conditions, analyzing the amount formed at different incubation times (6, 12, 18, 24 and 48 h). The US application was carried out by means of an ultrasonic bath, using water as a transmitting element and the temperature was maintained constant by water recirculation. Two powers were applied: moderate (36.53 W/L) and low (7.05 W/L), the application was carried out intermittently (30 min ON, 30 min OFF). In this way, the process conditions that led to improve the interaction between the enzyme and the substrates of the enzymatic reaction and the subsequent diffusion of the ZnPP were sought by applying powers that did not involve the enzyme degradation. As for the drying treatments of pork liver, drying experiments were carried out in a wide temperature range (-10 to 70 °C). The influence of drying temperature on enzymatic activity and the apparent-FeCH concentration extracted from the liver after drying were evaluated. Both parameters were calculated from the kinetics of ZnPP formation, using extracts of pork liver dried at different temperatures and comparing it with the kinetics obtained from the extract of FeCH from raw pork liver. In addition to evaluating the influence of drying on the catalytic capacity of FeCH for the formation of ZnPP, the effect of drying temperature (moderate-high 70 °C and moderate-low 40 °C), as well as the subsequent defatting process, on the physicochemical properties of pork liver and techno-functional properties of the protein fraction of the liver, was studied. Once the

stabilization of the liver was carried out by means of drying, its possible deodorization, in order to eliminate the VOCs characteristic of the unpleasant aroma of the liver, was studied. The treatments were performed using two different techniques: deodorization by VSD and through SC-CO<sub>2</sub>. Once the deodorization process was carried out, the residual VOCs in the liver were analyzed, using the headspace solid phase microextraction technique, combined with gas chromatography (HS-SPME-GC/MS).

Experimental results showed that the US application greatly intensified the extraction of the FeCH enzyme from pork liver. Thus, the US application during the FeCH extraction led to an improvement in enzymatic activity and consequently to an increase in the formation of ZnPP. For example, when US was applied in continuous mode, it was observed that the enzymatic activity of the FeCH extracted increased by 33.3% for 1 min of US application (4314 J applied), 30.8% for 2.5 min (10785 J applied) and 25.6% for 5 min (21570 J applied), compared to conventional extraction. That the greatest enzymatic activity was obtained with the shortest time in continuous US application, shows that prolonged exposure to ultrasonic energy could lead to the degradation of the enzyme, probably due to the effects of cavitation in the medium. On the other hand, the pulsed US application for 5 min treatment increased the enzymatic activity by 10.3 % (7384 J applied) compared to the conventional method. However, when US was applied in pulsed mode for shorter times (1 and 2.5 min), enzymatic activity was lower by 12.8 % for 1 min (1476 J applied) and 10.3 % for 2 min (3690 J applied), compared to the conventional method. As is the case of many processes assisted by US, there is an energy threshold necessary to observe the US effects; thus, probably, in the case of pulsed US application at times lower than 5 min, no differences with conventional extraction were observed, as the necessary energy threshold was not reached. In addition to the significant increase in the enzymatic activity, the amount of ZnPP formed from the continuous US application increased by 24.6 % for 1 min, 14.9% for 2.5 min and 13.9% for 5 min, compared to conventional extraction. As for the pulsed US application, an increase of 4.8% of the amount ZnPP formed was observed for 5 min, however, for shorter extraction times, the ZnPP formed was similar to that obtained with conventional FeCH extracts. In this sense, both the US application time and the mode used (continuous/pulsed) turned out to be decisive in the performance



of FeCH extraction. Among all the conditions tested, the optimal was the continuous US application for 1 min. Therefore, the US are an intensification technique of great interest to improve the FeCH extraction from pork liver, providing greater enzymatic activity probably due to structural changes that could favor both the localization of substrates at the active site, the diffusion of the product, or both processes, and reducing the time with respect to the conventional extraction method.

As for the ZnPP formation assisted by US from HLi and HLi+OxyHb, the maximum ZnPP formed when US was applied at low power (7.05 W/L) was 0.405 mmol ZnPP/L in HLi and 0.449 mmol ZnPP/L in HLi+OxyHb, reaching this value at 12 h, while without US application the maximum was reached at 24 h, this being 0.322 mmol ZnPP/L in HLi and 0.430 mmol ZnPP/L in HLi+OxyHb. However, when US was applied at moderate power (36.53 W/L) it was only 0.037 mmol ZnPP/L at 24 h of incubation, because the temperature control system could not prevent the temperature increase in the reaction medium generated by the US application. For this power, the temperature of the reaction medium rose above the set point (37 °C), fluctuating around 50 °C, despite the fact that the temperature of the US bath was maintained at 37 °C. Thus, the US at low power caused a micro-agitation in the reaction medium, which improved the enzymatic activity, facilitating the contact of the FeCH enzyme with the substrates, as well as the diffusion of the ZnPP. Therefore, by applying US during the ZnPP formation enzymatic reaction, there is a reduction in the ZnPP formation time of 50% and an increase in the final ZnPP concentration achieved, being an effective method to intensify the ZnPP formation enzymatic reaction.

In relation to the drying of pork liver at different temperatures (from -10 to 70 °C), the results revealed that the increase in the drying temperature influenced both the enzymatic activity and the apparent-FeCH concentration. Thus, the optimal condition was found in the range of 10 to 20 °C, where the average value of enzymatic activity and apparent-FeCH concentration was 0.00065  $\mu\text{mol/L min}$  and 0.277  $\mu\text{mol/L min}$ , respectively. However, at extreme drying temperatures, the lowest values of enzymatic activity and apparent-FeCH concentration were obtained (0.0005  $\mu\text{mol/L min}$  and 0.021  $\mu\text{mol/L}$  and 0.00033  $\mu\text{mol/L min}$  and 0.072  $\mu\text{mol/L}$ , for -10 and 70 °C, respectively).

Therefore, the drying process at temperatures close to room temperature (between 10 and 20 °C) proved to be an effective method in stabilizing the pork liver for the subsequent FeCH extraction, maintaining the apparent-FeCH concentration with respect to raw pork liver.

The drying temperature also influenced the physicochemical and techno-functional properties of pork liver, with the temperature of 40 °C leading to lower protein degradation compared to pork liver dried at 70 °C. The defatting process contributed to improving certain techno-functional properties of the proteins, as the foaming capacity, obtaining an average value 397% higher in the defatted samples compared to the undefatted samples. Also, the stability of foaming in the dried-defatted samples at 40 °C was the highest (13.76 min). However, regarding the emulsifying capacity, there was no significant ( $p>0.05$ ) difference between the different samples analyzed (dried and dried-defatted). Therefore, the drying and defatting processes, applied to facilitate the extraction of the protein fraction, must be tuned according to the functional properties needs of the liver proteins obtained.

Regarding the removal of VOCs, the results showed that both deodorization techniques (VSD and SC-CO<sub>2</sub>) were effective in reducing and eliminating VOCs characteristic of the pork liver. Through VSD the concentration of VOCs was reduced on average by 67.55%, while by SC-CO<sub>2</sub> it was reduced by 81.25%, with respect to dried pork liver without deodorizing. In addition, after the SC-CO<sub>2</sub> application, VOCs characteristic of the unpleasant smell of pork liver such as (E,E)- 2,4-heptadienal (fish), 1-octen-3-ol (mushrooms) and 1-onanol (fat and green nature) were eliminated. In addition, supercritical CO<sub>2</sub> extraction reduced the fat content by 24.9 %, compared to the sample without deodorizing. Therefore, the SC-CO<sub>2</sub> can be a technique with high potential in the removal of VOCs in pork liver, improving the results of the conventional technique of VSD and enabling a simultaneous defatting of the samples.

Thus, it can be concluded that emerging technologies such as US improved the FeCH extraction process, as well as its enzymatic activity in the ZnPP formation. In addition, by drying and defatting the liver, it is possible to extend the shelf life of the liver, with the aim of revaluing this co-product for later use in various technological

applications in the food industry. Thus, from dried pork liver, FeCH with catalytic activity for the formation of the pigment ZnPP was extracted, and from the dried-defatted liver the protein fraction was recovered, which presented excellent physicochemical and techno-functional properties, of great interest since they have been obtained from a co-product of animal origin. Extraction by SC-CO<sub>2</sub> turned out to be an alternative to the conventional technique of VSD for the elimination of VOCs, in addition and simultaneously, the fat content was reduced.

In order to improve knowledge about the applications developed for the use of pork liver, it is recommended to delve into the following aspects not addressed in this PhD Thesis. Thus, it would be necessary to address the optimization of ultrasonic treatment by studying other relevant variables, such as liver-solvent ratio, temperature, pH or power density. It would also be interesting to deepen the search for other substrates that can be a source of FeCH for the formation of ZnPP and other emerging technologies that allow improving the enzymatic process of pigment formation. In addition, the US application could be studied to improve the ZnPP formation in raw-cured meat products to which an enzymatic extract rich in FeCH, from the pork liver, has been previously added, subjecting them to a moderate ultrasonic field for times between 12 and 24 h. Additionally, the use of other drying techniques that minimize or avoid exposure to oxygen, such as vacuum drying or freeze-drying, could be studied with the aim of preserving the catalytic activity of FeCH for the ZnPP formation. Finally, it is recommended to investigate about the treatment of SC-CO<sub>2</sub> combined with other emerging technologies such as US, which facilitate the extraction of VOCs on the solid matrix of the pork liver.

## APLICACIÓN DE TECNOLOGÍAS EMERGENTES PARA LA OBTENCIÓN DE ZINC PROTOPORFIRINA Y PROTEINAS FUNCIONALES A PARTIR DE COPRODUCTOS CÁRNICOS

El hígado de cerdo representa un coproducto relevante de la industria porcina. Como resultado de las nuevas tendencias de consumo, se ha producido una disminución de su demanda, por lo que hoy en día presenta un bajo valor comercial. Sin embargo, el hígado de cerdo tiene unas excelentes propiedades nutricionales, presenta un alto contenido en proteínas de elevado valor biológico y tecno-funcional, es rico en minerales y vitaminas y a su vez, tiene un bajo contenido en grasa, por lo que puede considerarse un excelente producto de uso alimentario. Además, estudios recientes han demostrado que el hígado de cerdo presenta alta actividad catalítica para la formación de zinc protoporfirina (ZnPP) debido a la presencia de la enzima ferroquelatasa (FeQ). La ZnPP es un colorante rojo natural y con alta estabilidad que se ha identificado en el Jamón de Parma y también en otros productos cárnicos. Su producción a nivel industrial y adición a productos cárnicos podría ser útil para mejorar su color, evitando o minimizando el uso de nitritos y nitratos. Sin embargo, el proceso enzimático de formación de ZnPP es, en general, lento. En este sentido, están surgiendo tecnologías emergentes, como los ultrasonidos de potencia (US), que han sido aplicados para acelerar e intensificar reacciones enzimáticas, a través de la mejora en los fenómenos de transferencia de materia. Por otra parte, los US también se han empleado para facilitar la extracción de diversos compuestos de interés, incluidas las enzimas. Por lo tanto, desde el punto de vista tecnológico, el uso de US puede resultar interesante para mejorar el proceso enzimático de formación de ZnPP catalizado por la FeQ, obtenida del hígado de cerdo.

Uno de los principales problemas que presenta el hígado de cerdo es que es un órgano muy perecedero, por su elevado contenido en agua. Además, el hígado contiene compuestos orgánicos volátiles (COVs) que generan un fuerte aroma desagradable, lo que provoca un alto rechazo por parte del consumidor. Sin embargo, el hígado tiene una fracción proteica muy interesante desde el punto de vista nutritivo y tecno-funcional, por lo que sería muy conveniente su aprovechamiento por parte de

la industria alimentaria. Por ello, con el fin de recuperar la fracción proteica del hígado a nivel industrial, podría ser interesante su deshidratación, para así prologar su vida útil, eliminando su componente mayoritario, que es el agua, lo que facilitaría su manejo y almacenamiento, para su posterior uso en aplicaciones como la extracción de proteínas y/o enzimas. Además, la eliminación o reducción de la fracción grasa también facilitaría la recuperación de la fracción proteica, y limitaría las reacciones de degradación, como la oxidación e hidrólisis lipídica. Sin embargo, es importante determinar cómo la reducción de agua y grasa puede afectar a las propiedades tecno-funcionales y a la calidad de las proteínas. El secado por aire caliente es una de las operaciones unitarias más importantes en el procesado de alimentos. A pesar de ello, puede provocar cambios significativos que pueden afectar a la calidad del producto, especialmente cuando se emplean temperaturas elevadas. En este sentido, una alternativa al secado convectivo a alta temperatura podría ser el secado convectivo a baja temperatura, que podría mejorar las propiedades del producto. En general, para la eliminación de COVs se usan tratamientos de arrastre por vapor con (AVV) o sin aplicación de vacío (AV). La técnica de AVV es un tratamiento que utiliza el vapor de agua a temperaturas moderadas y a baja presión, el vapor arrastra los COVs de la muestra a tratar, que se condensan en un destilado (vertido). Por otra parte, la extracción mediante CO<sub>2</sub> supercrítico (CO<sub>2</sub>-SC) es una tecnología de procesado prometedora para la desodorización de coproductos cárnicos, ya que el CO<sub>2</sub> supercrítico ha sido usado como solvente en aplicaciones alimentarias por sus propiedades fisicoquímicas incluyendo baja viscosidad, densidad similar a la de un líquido y alta difusividad. En bibliografía existen diferentes trabajos que han descrito la capacidad de eliminación de COVs del CO<sub>2</sub>-SC en productos como salsa de pescado, agua, trufas, extractos de lavanda y tomillo o aislados proteicos vegetales, entre otros. Sin embargo, hasta la fecha esta tecnología de desodorización no ha sido aplicada en una matriz de origen animal como es el hígado de cerdo.

En este contexto, el objetivo principal de esta Tesis Doctoral fue evaluar la viabilidad de diferentes tecnologías emergentes para la revalorización del hígado de cerdo como coproducto de origen animal para la obtención de compuestos de interés tecno-funcional. Así, se analizó el efecto de la aplicación de US, empleando diferentes

tiempos y modos de aplicación (continuo y pulsado) sobre la extracción de FeQ del hígado de cerdo, determinando la actividad de la enzima mediante el análisis de las cinéticas de formación de ZnPP y caracterizando el campo acústico empleado y la eficiencia energética de las diferentes condiciones ensayadas. Además, se evaluó la viabilidad del uso de US, aplicados a intensidades moderadas y bajas, para la mejora de la reacción enzimática de formación de ZnPP catalizada por FeQ a partir de diferentes sustratos: hígado de cerdo homogeneizado (Hhc) e hígado de cerdo homogeneizado, con adición de oxihemoglobina (Hhc+OxiHb) procedente de sangre porcina. También se estudió el proceso de secado en un amplio rango de temperaturas (de -10 a 70 °C) y de desgrasado para la estabilización del hígado de cerdo y su posterior uso para la extracción de FeQ y el aprovechamiento de la fracción proteica. Por último, se evaluó el proceso de desodorización del hígado de cerdo deshidratado mediante dos técnicas: AVV y la extracción mediante CO<sub>2</sub>-SC.

La extracción de FeQ se realizó a partir de hígado de cerdo descongelado homogeneizado con una solución tampón estándar a temperatura de refrigeración (4 °C), mediante agitación mecánica convencional (30 min) y mediante extracción asistida por US (400 W). Los tratamientos de US se realizaron con aplicación continua y pulsada (0.5 s ON / 0.5 s OFF), a diferentes tiempos de extracción (1, 2.5 y 5 min). La actividad enzimática se evaluó cuantificando la ZnPP obtenida a partir de sustratos exógenos (protoporfirina IX y ZnSO<sub>4</sub>) a 37 °C, estudiando la cinética de formación durante 120 min. Además, también se investigó la intensificación de la reacción enzimática de la FeQ para formar ZnPP, mediante la aplicación de US en Hhc y Hhc+OxiHb. La formación de ZnPP se llevó a cabo a 37 °C en condiciones de anaerobiosis, analizándose la cantidad formada a diferentes tiempos de incubación (6, 12, 18, 24 y 48 h). La aplicación de US se realizó mediante un baño ultrasónico, utilizando agua como elemento transmisor y se mantuvo la temperatura constante mediante la recirculación del agua. Se aplicaron dos potencias: una moderada (36.53 W/L) y otra baja (7.05 W/L), la aplicación se llevó a cabo de forma intermitente (30 min ON, 30 min OFF). De este modo, se buscaron las condiciones del proceso que condujeran a mejorar la interacción entre la enzima y los sustratos de la reacción enzimática y la posterior difusión de la ZnPP aplicando potencias que no llevaran

asociadas la degradación del enzima. En cuanto a los tratamientos de secado del hígado de cerdo, se realizaron experimentos de secado en un amplio rango de temperatura (-10 a 70 °C). Se evaluó la influencia de la temperatura de secado sobre la actividad enzimática y la concentración de FeQ aparente extraída del hígado tras su deshidratación. Ambos parámetros se calcularon a partir de la cinética de formación de ZnPP, usando extractos de hígado deshidratado a diferentes temperaturas y comparándolo con la cinética obtenida a partir del extracto de FeQ de hígado fresco. Además de evaluar la influencia del secado sobre la capacidad catalítica de la FeQ para la formación de ZnPP, se estudió el efecto de la temperatura de secado (moderada-alta 70 °C y moderada-baja 40 °C), así como el posterior proceso de desgrasado, sobre las propiedades fisicoquímicas del hígado de cerdo y tecno-funcionales de la fracción proteica del hígado. Una vez llevada a cabo la estabilización del hígado mediante el secado, se estudió su posible desodorización, con el fin de eliminar los COVs característicos del aroma desagradable del hígado. Los tratamientos se realizaron mediante dos técnicas diferentes: la desodorización por AVV y a través de CO<sub>2</sub>-SC. Una vez llevado a cabo el proceso de desodorización, se analizaron los COVs residuales en el hígado, mediante la técnica de micro-extracción en fase sólida, con espacio de cabeza, combinado con cromatografía de gases (HS-SPME-GC/MS).

Los resultados experimentales mostraron que la aplicación de US intensificó en gran medida la extracción de la enzima FeQ del hígado de cerdo. Así, la aplicación de US durante la extracción de FeQ condujo a una mejora de la actividad enzimática y consecuentemente a un aumento de la formación de ZnPP. Por ejemplo, cuando se aplicó US en modo continuo, se observó que la actividad enzimática de la FeQ extraída aumentó un 33.3 % para 1 min de aplicación de US (4314 J aplicados), un 30.8 % para 2.5 min (10785 J aplicados) y un 25.6 % para 5 min (21570 J aplicados), en comparación con la extracción convencional. Que la mayor actividad enzimática se obtuviera con el menor tiempo de aplicación de US en continuo, pone de manifiesto que una exposición prolongada a la energía ultrasónica, podría conducir a la degradación de la enzima, probablemente por los efectos de la cavitación en el medio. Por otra parte, la aplicación pulsada de US en el tratamiento de 5 min aumentó la actividad enzimática un 10.3 % (7384 J aplicados), en comparación con el método

convencional. Sin embargo, cuando se aplicaron US en modo pulsado para tiempos más cortos (1 y 2.5 min), la actividad enzimática fue inferior en un 12.8 % para 1 min (1476 J aplicados) y un 10.3 % para 2 min (3690 J aplicados), en comparación con el método convencional. Como es el caso de muchos procesos asistidos por US, existe un umbral de energía necesaria para observar el efecto de los mismos; así, probablemente, en el caso de la aplicación pulsada a tiempos menores de 5 min, no se observaron diferencias con la extracción convencional, al no alcanzarse el umbral energético necesario. Además del aumento significativo de la actividad enzimática, la cantidad formada de ZnPP a partir de la aplicación de US en modo continuo aumentó respecto a la extracción convencional, un 24.6 % para 1 min, un 14.9 % para 2.5 min y un 13.9 % para 5 min. En cuanto a la aplicación pulsada de US, se observó un aumento de un 4.8 % de cantidad formada de ZnPP para 5 min, sin embargo, para tiempos más cortos de extracción, la ZnPP formada fue similar a la obtenida con los extractos convencionales de FeQ. En este sentido, tanto el tiempo de aplicación de US, como el modo empleado (continuo/pulsado), resultaron ser determinantes en el rendimiento de la extracción de FeQ. Entre todas las condiciones ensayadas, la óptima fue la aplicación de US de forma continua durante 1 min. Por tanto, los US son una técnica de intensificación de gran interés para mejorar la extracción de FeQ del hígado de cerdo, proporcionando una mayor actividad enzimática probablemente debido a cambios estructurales que podrían favorecer tanto la localización de los sustratos en el sitio activo, la difusión del producto o ambos procesos y reduciendo el tiempo con respecto al método de extracción convencional.

En cuanto a la formación de ZnPP asistida por US a partir Hhc y de Hhc+OxiHb, el máximo de ZnPP formado cuando se aplicaron US a baja potencia (7.05 W/L) fue de 0.405 mmol ZnPP/L en Hhc y 0.449 mmol ZnPP/L en Hhc+OxiHb, alcanzándose este valor a las 12 h, mientras que sin aplicación de US el máximo se alcanzó a las 24 h, siendo éste de 0.322 mmol ZnPP/L en Hhc y 0.430 mmol ZnPP/L en Hhc+OxiHb. Sin embargo, cuando se aplicaron US a moderada potencia (36.53 W/L) fue solo de 0.037 mmol ZnPP/L a 24 h de incubación, debido a que el sistema de control de temperatura no pudo evitar el aumento de temperatura en el medio de reacción generado por la aplicación de US. Para esta potencia, la temperatura del



medio de reacción se elevó por encima del punto de consigna (37 °C), fluctuando alrededor de 50 °C, a pesar de que la temperatura del baño de US se mantuviera a 37 °C. Así pues, los US a baja potencia provocaron una micro agitación en el medio de reacción, que mejoró la actividad enzimática, facilitando el contacto de la enzima FeQ con los sustratos, así como la difusión de la ZnPP. Por lo tanto, mediante la aplicación de US durante la reacción enzimática de formación de ZnPP, se produce una reducción del tiempo de formación de ZnPP de un 50 % y un aumento de la concentración de ZnPP final alcanzada, siendo un método eficaz para intensificar la reacción enzimática de formación de ZnPP.

En relación al secado de hígado de cerdo a diferentes temperaturas (de -10 a 70 °C), los resultados revelaron que el aumento de la temperatura de secado influyó tanto en la actividad enzimática como en la concentración de FeQ aparente. Así, la condición óptima se encontró en el rango de 10 a 20 °C, donde el valor promedio de la actividad enzimática y la concentración de FeQ aparente fue de 0.00065  $\mu\text{mol/L}\cdot\text{min}$  y 0.277  $\mu\text{mol/L}\cdot\text{min}$ , respectivamente. Sin embargo, a las temperaturas extremas de secado se obtuvieron los valores más bajos de actividad enzimática y concentración de FeQ aparente (0.0005  $\mu\text{mol/L}\cdot\text{min}$  y 0.021  $\mu\text{mol/L}$  y 0.00033  $\mu\text{mol/L}\cdot\text{min}$  y 0.072  $\mu\text{mol/L}$ , para -10 y 70 °C, respectivamente). Por tanto, el proceso de secado a temperaturas cercanas a la temperatura ambiente (entre 10 y 20 °C), demostró ser un método eficaz en la estabilización del hígado de cerdo para la posterior extracción de FeQ, manteniéndose la concentración de FeQ aparente con respecto al hígado de cerdo fresco.

La temperatura de secado también influyó en las propiedades fisicoquímicas y tecno-funcionales del hígado de cerdo, siendo la temperatura de 40 °C la que conllevó una menor degradación de proteínas en comparación con el hígado de cerdo deshidratado a 70 °C. El proceso de desgrasado contribuyó a mejorar ciertas propiedades tecno-funcionales de las proteínas, como la capacidad espumante, obteniendo un valor promedio un 397 % mayor en las muestras desgrasadas respecto a las muestras sin desgrasar. También, la estabilidad de formación de espuma en las muestras deshidratadas-desgrasadas a 40 °C fue la más alta (13.76 min). Sin

embargo, respecto a la capacidad emulsionante no se vio afectada entre las diferentes muestras analizadas (deshidratadas y deshidratadas-desgrasadas). Por lo tanto, los procesos de secado y desgrasado, aplicados para facilitar la extracción de la fracción proteica, deben ajustarse de acuerdo con las necesidades de propiedades funcionales de las proteínas hepáticas obtenidas.

En cuanto a la eliminación de COVs, los resultados mostraron que ambas técnicas de desodorización (AVV y CO<sub>2</sub>-SC) fueron eficaces en la reducción y eliminación COVs característicos del hígado del cerdo. A través del AVV la concentración de COVs se redujo en su conjunto un 67.55 %, mientras que mediante CO<sub>2</sub>-SC se redujo un 81.25 %, con respecto al hígado de cerdo deshidratado sin desodorizar. Además, tras la aplicación de CO<sub>2</sub>-SC se eliminaron COVs característicos del olor desagradable del hígado de cerdo como (E,E)- 2,4-heptadienal (pescado), 1-octen-3-ol (setas) y 1-onanol (grasa y verde de naturaleza). Asimismo, mediante la extracción con CO<sub>2</sub> supercrítico se redujo el contenido de grasa un 24.9 %, en comparación con la muestra sin desodorizar. Por lo tanto, la aplicación de CO<sub>2</sub>-SC puede ser una técnica con alto potencial en la eliminación de COVs en hígado de cerdo, mejorando los resultados de la técnica convencional de AVV y posibilitando un desgrasado de las muestras de forma simultánea.

Así pues, se puede concluir que las tecnologías emergentes como los US mejoraron el proceso de extracción de FeQ, así como su actividad enzimática en la formación de ZnPP. Además, mediante el secado y desgrasado del hígado, es posible alargar la vida útil del hígado, con el objetivo de revalorizar este coproducto para su posterior uso en varias aplicaciones tecnológicas en la industria alimentaria. Así, a partir del hígado deshidratado se extrajo FeQ con actividad catalítica para la formación del pigmento ZnPP, y a partir del hígado deshidratado-desgrasado se recuperó la fracción proteica del hígado, la cual presentaba excelentes propiedades fisicoquímicas y tecno-funcionales, de elevado interés al haberse obtenido a partir de un coproducto de origen animal. La extracción mediante CO<sub>2</sub>-SC resultó ser una alternativa a la técnica convencional de AVV para la eliminación COVs, además, simultáneamente, se redujo el contenido en grasa.

Con el fin de mejorar el conocimiento sobre las aplicaciones desarrolladas para el aprovechamiento del hígado de cerdo, se recomienda profundizar en los siguientes aspectos no abordados en la presente Tesis Doctoral. Así, sería necesario abordar la optimización del tratamiento ultrasónico mediante el estudio de otras variables relevantes, como la relación hígado-solvente, la temperatura, el pH o la densidad de potencia. También sería interesante profundizar en la búsqueda de otros sustratos que puedan ser fuente de FeQ para la formación de ZnPP y de otras tecnologías emergentes que permitan mejorar el proceso enzimático de formación del pigmento. Además, se podría estudiar la aplicación de US para mejorar la formación de ZnPP en productos cárnicos crudo-curados a los que se les ha añadido previamente un extracto enzimático rico en FeQ, procedente del hígado de cerdo, sometiéndolos a un campo ultrasónico moderado durante tiempos comprendidos entre 12 y 24 h. Adicionalmente, se podría estudiar el uso de otras técnicas de secado que minimicen o eviten la exposición al oxígeno, como el secado a vacío o la liofilización, con el objetivo de preservar la actividad catalítica de la FeQ para la formación de ZnPP. Finalmente, se recomienda investigar más acerca del tratamiento de CO<sub>2</sub>-SC combinado con otras tecnologías emergentes como los US, que faciliten la extracción de un mayor número de COVs sobre la matriz sólida del hígado de cerdo.

## APLICACIÓ DE TECNOLOGIES EMERGENTS PER A L'OBTENCIÓ DE ZINC PROTOPORFIRINA I PROTEÏNES FUNCIONALS A PARTIR DE COPRODUCTES CÀRNICS

El fetge de porc representa un coproducte rellevant de la indústria porcina. Com a resultat de les noves tendències de consum, s'ha produït una disminució de la seua demanda, per la qual cosa hui en dia presenta un baix valor comercial. No obstant això, el fetge de porc té unes excel·lents propietats nutricionals, presenta un alt contingut en proteïnes d'elevat valor biològic i tecno-funcional, és ric en minerals i vitamines i al mateix temps, té un baix contingut en greix, per la qual cosa pot considerar-se un excel·lent producte d'ús alimentari. A més, estudis recents han demostrat que el fetge de porc presenta alta activitat catalítica per a la formació de zinc protoporfirina (ZnPP), a causa de la presència de l'enzim ferroquelatasa (FeQ). La ZnPP és un colorant roig natural i amb alta sensibilitat que s'ha identificat en el Pernil de Parma i també en altres productes càrnics. La seua producció a nivell industrial i addició a productes càrnics podria ser útil per a millorar el seu color, evitant o minimitzant l'ús de nitrats i nitrats. No obstant això, el procés enzimàtic de formació de ZnPP és, en general, lent. En este sentit, estan sorgint tecnologies emergents, com els ultrasons de potència (US), que han sigut aplicats per a accelerar i intensificar reaccions enzimàtiques, a través de la millora en els fenòmens de transferència de matèria. D'altra banda, els US també s'han emprat per a facilitar l'extracció de diversos compostos d'interés, incloses els enzims. Per tant, des del punt de vista tecnològic, l'ús de US pot resultar interessant per a millorar el procés enzimàtic de formació de ZnPP catalitzat per la FeQ obtinguda del fetge de porc.

Un dels principals problemes que presenta el fetge de porc és que és un òrgan molt perible, pel seu elevat contingut en aigua. A més, el fetge conté compostos orgànics volàtils (COVs) que generen un fort aroma desagradable, la qual cosa provoca un alt rebuig per part del consumidor. No obstant això, el fetge té una fracció proteica molt interessant des del punt de vista nutritiu i tecno-funcional, per la qual cosa seria molt convenient el seu aprofitament per part de la indústria alimentària. Per això, amb la finalitat de recuperar la fracció proteica del fetge a nivell industrial, podria ser

interessant la seua deshidratació, per a així prologar la seua vida útil, eliminant el seu component majoritari, que és l'aigua, la qual cosa facilitaria el seu maneig i emmagatzematge, per al seu posterior ús en aplicacions com l'extracció de proteïnes i/o enzims. A més, l'eliminació o reducció de la fracció grassa també facilitaria la recuperació de la fracció proteica, i limitaria les reaccions de degradació, com l'oxidació i hidròlisi lipídica. No obstant això, és important determinar com la reducció d'aigua i greix pot afectar les propietats tecno-funcionals i a la qualitat de les proteïnes. L'assecat per aire calent és una de les operacions unitàries més importants en el processament d'aliments. Malgrat això, pot provocar canvis significatius que poden afectar la qualitat del producte, especialment quan s'empren temperatures elevades. En este sentit, una alternativa a l'assecat convectiu a alta temperatura podria ser l'assecat convectiu a baixa temperatura, que podria millorar les propietats del producte. En general, per a l'eliminació de COVs s'usen tractaments d'arrossegament per vapor amb (AVV) o sense aplicació de buit (AV). La tècnica de AVV és un tractament que utilitza el vapor d'aigua, a temperatures moderades i a baixa pressió, el vapor arrosega els COVs de la mostra a tractar, que es condensen en un destil·lat (abocament). D'altra banda, l'extracció mitjançant CO<sub>2</sub> supercrític (CO<sub>2</sub>-SC) és una tecnologia de processament prometedora per a la desodoració de coproductes d'origen animal, ja que el CO<sub>2</sub> supercrític ha sigut usat com a solvent en aplicacions alimentaries per les seues propietats fisicoquímiques incloent baixa viscositat, densitat semblant a la d'un líquid i alta difusivitat. En bibliografia existeixen diferents treballs que han descrit la capacitat d'eliminació de COVs del CO<sub>2</sub>-SC en productes com la salsa de peix, aigua, tòfones, extractes de lavanda i timó o aïllats proteics vegetals, entre altres. No obstant això, fins hui esta tecnologia de desodoració no ha sigut aplicada en una matriu d'origen animal com és el fetge de porc.

En este context, l'objectiu principal d'esta Tesi Doctoral va ser avaluar la viabilitat de diferents tecnologies emergents per a la revaloració del fetge de porc com a coproducte d'origen animal per a l'obtenció de compostos d'interès tecno-funcional. Així, es va analitzar l'efecte de l'aplicació de US, emprant diferents temps i maneres d'aplicació (continu i premut) sobre l'extracció de FeQ del fetge de porc, determinant l'activitat de l'enzim mitjançant l'anàlisi de les cinètiques de formació de ZnPP i

caracteritzant el camp acústic emprat i l'eficiència energètica de les diferents condicions assajades. A més, es va avaluar la viabilitat de l'ús de US, aplicats a intensitats moderades i baixes, per a la millora de la reacció enzimàtica de formació de ZnPP catalitzada per FeQ a partir de diferents substrats: fetge de porc homogeneïtzat (Hfp) i fetge de porc homogeneïtzat, amb addició de oxihemoglobina (Hfp+OxiHb) procedent de sang porcina. També es va estudiar el procés d'assecat en un ampli rang de temperatures (de -10 a 70 °C) i de desgreixat per a l'estabilització del fetge de porc i el seu posterior ús per a l'extracció de FeQ i l'aprofitament de la fracció proteica. Finalment, es va avaluar el procés de desodoració del fetge de porc deshidratat mitjançant dues tècniques: AVV i l'extracció mitjançant CO<sub>2</sub>-SC.

L'extracció de FeQ es va realitzar a partir de fetge de porc descongelat homogeneïtzat amb una solució tampó estàndard a temperatura de refrigeració (4 °C), mitjançant agitació mecànica convencional (30 min) i mitjançant extracció assistida per US (400 W). Els tractaments de US es van realitzar amb aplicació contínua i polsada (0.5 s ON / 0.5 s OFF), a diferents temps d'extracció (1, 2.5 i 5 min). L'activitat enzimàtica es va avaluar quantificant la ZnPP obtinguda a partir de substrats exògens (protoporfirina IX i ZnSO<sub>4</sub>) a 37 °C, estudiant la cinètica de formació durant 120 min. A més, també es va investigar la intensificació de la reacció enzimàtica de la FeQ per a formar ZnPP, mitjançant l'aplicació de US en Hfp i Hfp+OxiHb. La formació de ZnPP es va dur a terme a 37 °C en condicions de anaerobiosi, analitzant-se la quantitat formada a diferents temps d'incubació (6, 12, 18, 24 i 48 h). L'aplicació de US es va realitzar mitjançant un bany ultrasònic, utilitzant aigua com a element transmissor i es va mantindre la temperatura constant mitjançant la recirculació de l'aigua. Es van aplicar dues potències: una moderada (36.53 W/L) i una altra baixa (7.05 W/L), l'aplicació es va dur a terme de manera intermitent (30 min ON, 30 min OFF). D'esta manera, es van buscar les condicions del procés que conduïren a millorar la interacció entre l'enzim i els substrats de la reacció enzimàtica i la posterior difusió de la ZnPP, aplicant potències que no dugueren associades la degradació de l'enzim. Pel que respecta als tractaments d'assecat del fetge de porc, es van realitzar experiments d'assecat en un ampli rang de temperatura (-10 a 70 °C). Es va avaluar la influència de la temperatura d'assecat sobre l'activitat enzimàtica i la concentració de FeQ aparent

extreta del fetge després de la seua deshidratació. Tots dos paràmetres es van calcular a partir de la cinètica de formació de ZnPP, usant extractes de fetge deshidratat a diferents temperatures i comparant-ho amb la cinètica obtinguda a partir de l'extracte de FeQ de fetge fresc. A més d'avaluar la influència de l'assecat sobre la capacitat catalítica de la FeQ per a la formació de ZnPP, es va estudiar l'efecte de la temperatura d'assecat (moderada-alta: 70 °C i moderada-baixa: 40 °C), així com el posterior procés de desgreixat sobre les propietats fisicoquímiques del fetge de porc i tecno-funcionals de la fracció proteica del fetge. Una vegada duta a terme l'estabilització del fetge mitjançant l'assecat, es va estudiar la seua possible desodoració, amb la finalitat d'eliminar els COVs característics de l'aroma desagradable del fetge. Els tractaments es van realitzar mitjançant dues tècniques diferents; la desodoració per AVV i a través de CO<sub>2</sub>-SC. Una vegada dut a terme el procés de desodoració, es van analitzar els COVs residuals en el fetge, mitjançant la tècnica de micro-extracció en fase sòlida, amb espai de cap, combinat amb cromatografia de gasos (HS-SPME-GC/MS).

Els resultats experimentals van mostrar que l'aplicació de US va intensificar en gran manera l'extracció de l'enzim FeQ del fetge de porc. Així, l'aplicació de US durant l'extracció de FeQ va conduir a una millora de l'activitat enzimàtica i conseqüentment a un augment de la formació de ZnPP. Per exemple, quan es va aplicar US en manera contínua, es va observar que l'activitat enzimàtica de la FeQ extreta va augmentar un 33.3 % per a 1 min d'aplicació de US (4314 J aplicats), un 30.8 % per a 2.5 min (10785 J aplicats) i un 25.6 % per a 5 min (21570 J aplicats), en comparació amb l'extracció convencional. Que la major activitat enzimàtica s'obtinguera amb el menor temps d'aplicació de US en continu, posa de manifest que una exposició prolongada a l'energia ultrasònica, podria conduir a la degradació de l'enzim, probablement pels efectes de la cavitació en el medi. D'altra banda, l'aplicació polsada de US en el tractament de 5 min va augmentar l'activitat enzimàtica un 10.3% (7384 J aplicats), en comparació amb el mètode convencional. No obstant això, quan es van aplicar US en manera polsada per a temps més curts (1 i 2.5 min), l'activitat enzimàtica va ser inferior en un 12.8 % per a 1 min (1476 J aplicats) i un 10.3 % per a 2 min (3690 J aplicats), en comparació amb el mètode convencional. Com és el cas de molts processos assistits per US, existeix un llindar d'energia necessària per a observar l'efecte d'estos;

així, probablement, en el cas de l'aplicació polsada a temps menors de 5 min, no es van observar diferències amb l'extracció convencional, al no aconseguir-se el lliandar energètic necessari. A més de l'augment significatiu de l'activitat enzimàtica, la quantitat formada de ZnPP a partir de l'aplicació de US en manera contínua va augmentar respecte a l'extracció convencional, un 24.6 % per a 1 min, un 14.9 % per a 2.5 min i un 13.9 % per a 5 min. Quant a l'aplicació polsada de US, es va observar un augment d'un 4.8% de quantitat formada de ZnPP per a 5 min, no obstant això, per a temps més curts d'extracció, la ZnPP formada va ser similar a l'obtinguda amb els extractes convencionals de FeQ. En este sentit, tant el temps d'aplicació de US, com la manera emprada (continu/polsat), van resultar ser determinants en el rendiment de l'extracció de FeQ. Entre totes les condicions assajades, l'òptima va ser l'aplicació de US de manera contínua durant 1 min. Per tant, els US són una tècnica d'intensificació de gran interès per a millorar l'extracció de FeQ del fetge de porc, proporcionant una major activitat enzimàtica probablement a causa de canvis estructurals que podrien afavorir tant la localització dels substrats en el lloc actiu, la difusió del producte o ambdós processos i estalviant temps respecte al mètode d'extracció convencional.

Pel que respecta a la formació de ZnPP assistida per US a partir Hfp i de Hfp+OxiHb, el màxim de ZnPP format quan es van aplicar US a baixa potència (7.05 W/L) va ser de 0.405 mmol ZnPP/L en Hfp i 0.449 mmol ZnPP/L en Hfp+OxiHb, aconseguint-se este valor a les 12 h, mentre que sense aplicació de US el màxim es va aconseguir a les 24 h, sent este de 0.322 mmol ZnPP / L en Hfp i 0.430 mmol ZnPP/L en Hfp+OxiHb. No obstant això, quan van aplicar US a moderada potència (36.53 W/L) va ser sol de 0.037 mmol ZnPP/L a 24 h d'incubació, pel fet que el sistema de control de temperatura no va poder evitar l'augment de temperatura en el medi de reacció generat per l'aplicació de US. Per a esta potència, la temperatura del medi de reacció es va elevar per damunt del punt de consigna (37 °C), fluctuant al voltant de 50 °C, tot i que la temperatura del bany de US es mantinguer a 37 °C. Pel que, els US a baixa potència van provocar una micro agitació en el medi de reacció, que va millorar l'activitat enzimàtica, facilitant el contacte de l'enzim FeQ amb els substrats, així com la difusió de la ZnPP. Per tant, mitjançant l'aplicació de US durant la reacció enzimàtica de formació de ZnPP, es produeix una reducció del temps de formació de



ZnPP d'un 50 % i un augment de la concentració de ZnPP final aconseguida, sent un mètode eficaç per a intensificar la reacció enzimàtica de formació de ZnPP.

En relació a l'assecat de fetge de porc a diferents temperatures (-10 a 70 °C), els resultats van revelar que l'augment de la temperatura d'assecat va influir tant en la activitat enzimàtica com en la concentració de FeQ aparent. Així, la condició òptima es va trobar en el rang de 10 a 20 °C, on el valor mitjà de la activitat enzimàtica i la concentració de FeQ aparent va ser de 0.00065  $\mu\text{mol/L}\cdot\text{min}$  i 0.277  $\mu\text{mol/L}$ , respectivament. No obstant això, a les temperatures extremes d'assecat es van obtenir els valors més baixos de l'activitat enzimàtica i la concentració de FeQ aparent (0.0005  $\mu\text{mol/L}\cdot\text{min}$  i 0.021  $\mu\text{mol/L}$  i 0.00033  $\mu\text{mol/L}\cdot\text{min}$  i 0.072  $\mu\text{mol/L}$ , per a -10 i 70 °C, respectivament). Per tant, el procés d'assecat a temperatures pròximes a la temperatura ambient (entre 10 i 20 °C), va demostrar ser un mètode eficaç en l'estabilització del fetge de porc per a la posterior extracció de FeQ, mantenint-se la concentració de FeQ aparent respecte al fetge de porc fresc.

La temperatura d'assecat també va influir en les propietats fisicoquímiques i tecno-funcionals del fetge de porc, sent la temperatura de 40 °C la que va comportar una menor degradació de proteïnes en comparació amb el fetge porcí deshidratat a 70 °C. El procés de desgreixat va contribuir a millorar unes certes propietats tecno-funcionals de les proteïnes, com la capacitat espumant, obtenint un valor mitjà d'un 397% major en les mostres desgreixades respecte a les mostres sense desgreixar. També, l'estabilitat de formació d'espuma en les mostres deshidratades-desgreixades a 40 °C va ser la més alta (13.76 min). No obstant això, respecte a la capacitat emulsionant, no es va veure afectat entre les diferents mostres analitzades (deshidratades i deshidratades-desgreixades). Per tant, els processos d'assecat i desgreixat, aplicats per a facilitar l'extracció de la fracció proteica, han d'ajustar-se d'acord amb les necessitats de propietats funcionals de les proteïnes hepàtiques obtingudes.

Pel que fa a l'eliminació de COVs, els resultats van mostrar que totes dues tècniques de desodoració (AVV i CO<sub>2</sub>-SC) van ser eficaces en la reducció i eliminació COVs característics del fetge del porc. A través de la AVV la concentració de COVs es

va reduir en el seu conjunt un 67.55%, mentre que mitjançant CO<sub>2</sub>-SC es va reduir un 81.25%, respecte al fetge de porc deshidratat sense desodoritzar. A més, després de l'aplicació de CO<sub>2</sub>-SC es van eliminar COVs característics de l'olor desagradable del fetge de porc com (E,E)- 2,4-heptadienal (peix), 1-octen-3-ol (bolets) i 1-onanol (grassa i verd de naturalesa). Així mateix, mitjançant l'extracció amb CO<sub>2</sub> supercrític es va reduir el contingut de greix un 24.9 %, en comparació amb la mostra sense desodoritzar. Per tant, l'aplicació de CO<sub>2</sub>-SC pot ser una tècnica amb alt potencial en l'eliminació de COVs en fetge de porc, millorant els resultats de la tècnica convencional de AVV i possibilitant un desgreixat de les mostres de manera simultània.

Així doncs, es pot concloure que les tecnologies emergents com els US van millorar de manera general el procés d'extracció de FeQ, així com la seua activitat enzimàtica en la formació de ZnPP. A més, mitjançant l'assecat i desgreixat del fetge, és possible allargar la vida útil del fetge, amb l'objectiu de revaloritzar este coproducte pel seu posterior ús en diverses aplicacions tecnològiques en la indústria alimentària. Així, a partir del fetge deshidratat es va extraure FeQ amb activitat catalítica per a la formació del pigment ZnPP, i a partir del fetge deshidratat-desgreixat es va recuperar la fracció proteica del fetge, la qual presentava excel·lents propietats fisicoquímiques i tecno-funcionals, d'elevat interès en haver-se obtingut a partir d'un coproducte d' origen animal. L'extracció mitjançant CO<sub>2</sub>-SC va resultar ser una alternativa a la tècnica convencional de AVV per a l'eliminació COVs, a més, simultàniament, es va reduir el contingut en greix.

Amb la finalitat de millorar el coneixement sobre les aplicacions desenvolupades per a l'aprofitament del fetge de porc, es recomana aprofundir en els següents aspectes no abordats en la present Tesi Doctoral. Per a comprendre millor l'extracció i l'activitat de la FeQ, seria necessari abordar l'optimització del tractament ultrasònic mitjançant l'estudi de l'efecte de variables de procés rellevants, com la relació fetge-solvent, la temperatura, el pH o la densitat de potència. També seria interessant aprofundir en la cerca de substrats que puguen ser font de FeQ per a la formació de ZnPP i d'altres tecnologies emergents que permeten millorar el procés enzimàtic de formació del pigment. A més, es podria estudiar l'aplicació de US per a millorar la formació de ZnPP

en productes càrnics cru-curats als quals se'ls ha afegit prèviament un extracte enzimàtic ric en FeQ, procedent del fetge de porc, sotmetent-los a un camp ultrasònic moderat durant temps compresos entre 12 i 24 h. Addicionalment, es podria estudiar l'ús d'altres tècniques d'assecat que minimitzen o eviten l'exposició a l'oxigen, com l'assecat a buit o la liofilització, amb l'objectiu de preservar l'activitat catalítica de la FeQ per a la formació de ZnPP. Finalment, es recomana investigar més sobre el tractament de CO<sub>2</sub>-SC combinat amb altres tecnologies emergents com els US, que faciliten l'extracció d'un major nombre de COVs sobre la matriu sòlida del fetge de porc.



# **1. INTRODUCCIÓN**



## 1.1 Hígado de cerdo

En general, el uso de coproductos de origen animal comestibles para consumo humano en Europa ha disminuido a lo largo del siglo XXI (FAO, 2021). Sin embargo, en España, el consumo de coproductos, subproductos y despojos de origen animal ha aumentado de un 2 % en 2010 a un 2.4 % en 2020 (MAPA, 2020). Esta tendencia puede vincularse a factores como cultura, religión, cambios en la dieta, así como la tendencia del consumo que va asociado a consumidores con bajos ingresos, ya que se tratan de productos de bajo valor comercial (Nollet y Toldrá, 2011).

Actualmente, no existen datos que indiquen la producción de hígado de cerdo, pero cada año se sacrifican en la Unión Europea (UE) alrededor de 330 millones de animales (bovinos, ovinos, porcinos y caprinos), lo que genera más de 17 millones de toneladas de coproductos de origen animal (EFPRA, 2021). En España, se sacrificaron más de 58 millones de cerdos en el 2021, que resultaron en 5 millones de toneladas de peso de canales (MAGRAMA, 2022). Estos datos sitúan al porcino como la especie ganadera con mayor producción de carne y proporciona una idea de la magnitud del problema económico y ambiental que supone la gestión de los coproductos y subproductos asociados que se generan. En particular, estos datos ponen de manifiesto el elevado volumen de hígado generado dentro de la industria porcina, que podría alcanzar las 87000 toneladas de hígado de cerdo al año en nuestro país. El hígado es un coproducto de bajo valor añadido, debido a la baja demanda que presenta por parte de los consumidores (Aspevik *et al.*, 2017). Su comercialización en fresco tiene un reducido mercado de consumo, siendo su principal uso actual la elaboración de productos de pasta de hígado (paté) y la alimentación animal (Zou *et al.*, 2021). Sin embargo, el hígado de cerdo es un coproducto interesante desde el punto de vista nutricional, ya que es rico en proteínas (22.05 g /100 g hígado fresco), bajo en grasas (2.94 g /100 g hígado fresco) y además presenta una excelente fuente de minerales como el hierro y el manganeso y de vitaminas, destacando la riboflavina, niacina, vitamina B12, vitamina B6, folacina, ácido ascórbico y vitamina A (Seong *et al.*, 2014).

Entre las excelentes propiedades nutricionales, destaca su elevado contenido de proteína, que podría ser hidrolizada para la generación de péptidos bioactivos con

actividad antioxidante y/o antimicrobiana (Lafarga y Hayes, 2014; Mora *et al.*, 2014). Asimismo, otros compuestos como la vitamina B12 o la heparina porcina podrían ser de interés para la industria farmacéutica (Seong *et al.*, 2014; Toldrá *et al.*, 2016). Por último, estudios recientes han demostrado que el hígado de cerdo presenta alta actividad catalítica para la formación de zinc protoporfirina (ZnPP), a partir de la enzima ferroquelatasa (FeQ) presente en el mismo (De Maere *et al.*, 2017). La ZnPP es un pigmento rojo natural que, debido a su estabilidad a la luz y al calor, podría ser útil como medio para mejorar el color de los productos cárnicos, evitando o minimizando el uso de nitritos y nitratos (Wakamatsu *et al.*, 2015).

El gran volumen de desperdicios (vísceras y despojos) y coproductos de origen animal, supone un impacto negativo en el medio ambiente, así como económico para las empresas del sector. En este sentido, resulta de gran interés la búsqueda de nuevos usos para los coproductos de origen animal con interesantes propiedades nutricionales y tecno-funcionales, como el hígado de cerdo, que permitan su revalorización, contribuyendo así a una mejora ambiental y económica para el sector (Echegaray *et al.*, 2018).

Los procesos de transformación y/o pretratamiento del hígado de cerdo son esenciales para la obtención de compuestos de interés, como el aprovechamiento de su fracción proteica o la formación del pigmento ZnPP. En primer lugar, debido a la elevada actividad de agua del hígado, puede ser necesario una etapa previa de estabilización mediante deshidratación para facilitar su almacenamiento. Además, para el aprovechamiento de la fracción proteica, es conveniente eliminar la fracción grasa, ya que puede desencadenar reacciones de oxidación y enranciamiento, que provoquen olor y sabor desagradables, así como un acortamiento de la vida útil. Por último, destacar la necesidad de la eliminación de compuestos volátiles característicos del hígado, que generan un olor desagradable para el consumidor y que de no ser eliminados pueden trasladarse a la fracción proteica obtenida.

### **1.1.1 Proteína del hígado de cerdo**

En la actualidad, la creciente escasez de alimentos a nivel mundial se ha convertido en un estímulo para que la industria alimentaria se replantee estrategias de



revalorización de coproductos y subproductos de origen animal, con el objetivo de maximizar el aprovechamiento de los recursos existentes (Maluf *et al.*, 2020). Una forma de potenciar el uso de coproductos de origen animal como el hígado, es a partir de su fracción proteica, la cual ha demostrado tener excelentes propiedades nutricionales, al contener todos los aminoácidos esenciales, y propiedades tecno-funcionales (emulsionantes, gelificantes y espumantes) (Sánchez-Torres *et al.*, 2022). Por lo tanto, además de los beneficios ambientales y económicos que se derivan de la revalorización del hígado de cerdo, la recuperación de su fracción proteica supone una alternativa de calidad para su uso en alimentación. Esto es particularmente relevante en los países en desarrollo, donde la desnutrición por deficiencia de proteínas es un problema importante porque muchas personas no pueden permitirse comprar productos proteicos de alta calidad de origen animal o vegetal. Así, el uso del hígado de cerdo y sus proteínas en la cadena alimentaria, pueden generar importantes beneficios ambientales, económicos y nutricionales. Por otro lado, la obtención de proteínas funcionales a partir de hígado tiene un elevado interés, ya que sería una alternativa libre de alérgenos a las proteínas no cárnicas (Zou *et al.*, 2017). Además, la transformación de la fracción proteica en hidrolizados proteicos, mediante procesos enzimáticos, tiene aplicaciones industriales con implicaciones en la salud, como son los péptidos bioactivos con actividad antioxidante, antimicrobiana y nutraceútica (Verma *et al.*, 2019).

Los péptidos bioactivos se pueden obtener de diferentes fuentes; estos podrían provenir de proteínas dietéticas, que luego se descomponen en el tracto gastrointestinal para liberar péptidos bioactivos, o pueden aislarse directamente de varias fuentes naturales (Pearman *et al.*, 2020). Estas fuentes incluyen proteínas de origen vegetal como la soja y los garbanzos (Capriotti *et al.*, 2015; Xue *et al.*, 2015) y proteínas animales, a partir de coproductos y desechos de la industria cárnica (Di Bernardini *et al.*, 2011), entre los que cabría destacar el hígado de cerdo (Shimizu *et al.*, 2006).

En cuanto a las aplicaciones industriales que tienen los péptidos bioactivos, destacar aquellas que aprovechan su actividad antioxidante. En este sentido, la degradación de los lípidos implica la formación de compuestos volátiles como

aldehídos, cetonas y alcoholes, que son los principales contribuyentes de los sabores y aromas indeseables en la carne (Domínguez *et al.*, 2019a). El método más común de inhibir la oxidación de lípidos es la adición de antioxidantes naturales o sintéticos (Amaral *et al.*, 2018). Por lo tanto, una de las posibles alternativas a la adición de antioxidantes de otro origen, podría ser el empleo de péptidos bioactivos con actividad antioxidante extraídos de fuentes naturales, como son los coproductos de origen animal con elevado contenido proteico (Peighambardoust *et al.*, 2021). Así, Borrajo *et al.* (2021) estudiaron que los hidrolizados proteicos obtenidos a partir de hígado de cerdo, mediante la reacción enzimática catalizada por bromelina, presentaron una buena actividad antioxidante y, por lo tanto, podrían utilizarse como un antioxidante natural para extender la vida útil de las hamburguesas de cerdo. Además, a partir de hígado de cerdo y de las enzimas comerciales Alcalase 2.4L™ y Novo Pro-D™, se obtuvieron hidrolizados de proteínas, que pueden dar lugar a la formación de compuestos bioactivos, como antioxidantes, antimicrobianos, antihipertensivos, antitrombóticos, inmunomoduladores, hipolipemiantes y anticancerígenos, los cuales pueden emplearse para emplearse en desarrollo de nuevos productos (Maluf *et al.*, 2020). Otras aplicaciones de estos hidrolizados proteicos se encuentran en fórmulas nutricionales para dietas especiales en adultos, para personas mayores que necesitan suplementos proteicos extra, en fórmulas para lactantes con alergias a las proteínas intactas de los alimentos o con trastornos metabólicos congénitos y nutracéuticos (Aspevik *et al.*, 2017).

### 1.1.2 Ferroquelatasa de hígado de cerdo

La ferroquelatasa (FeQ; EC. 4.99.1.1.), también denominada Zn-quelatasa o hemo sintasa, es la enzima endógena responsable de la formación de zinc protoporfirina (ZnPP) en la carne (Benedini *et al.*, 2008), estando activa durante todo el procesado del jamón de Parma (producto típico del norte de Italia) (Adamsen *et al.*, 2006). Está ubicada en la membrana interna de las mitocondrias de las células eucariotas y actúa insertando un átomo de hierro ( $Fe^{2+}$ ) en la protoporfirina IX (PPIX), en el paso final de la biosíntesis del grupo hemo (UNIPROT, 2021) (Figura 1). Es una proteína sensible a los efectos de metales pesados (especialmente plomo ( $Pb^{2+}$ )) y, por supuesto, a la falta de  $Fe^{2+}$ . En este último caso, es cuando se ha demostrado que

puede incorporar zinc ( $Zn^{2+}$ ) a la PPIX, en lugar de  $Fe^{2+}$ , formando el complejo zinc (II) protoporfirina IX (Crowell *et al.*, 2006).

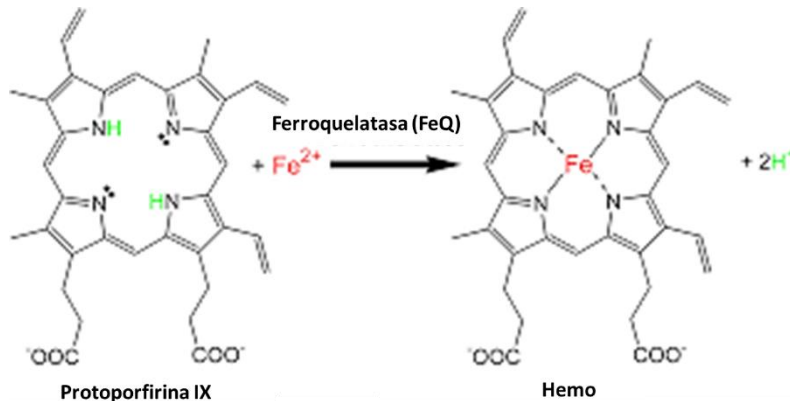


Figura 1. Reacción catalizada por la ferroquelatasa en presencia de hierro

El color de los productos cárnicos curados, generalmente se logra mediante la adición de nitratos y nitritos, donde el nitrosil-hemocromo es el responsable del color rojo característico. Sin embargo, en los jamones curados sin nitrificantes, como el jamón de Parma, el pigmento rojo característico y estable es la ZnPP (Parolari *et al.*, 2016), cuya formación está catalizada por la FeQ (Wakamatsu *et al.*, 2004a).

La formación enzimática de ZnPP en carne puede verse afectada por varios factores. Por ejemplo, Wakamatsu *et al.* (2007) observaron que la presencia de oxígeno disminuye la formación de ZnPP en la carne, aunque a diferencia del músculo, el oxígeno en el hígado de cerdo no parece inhibir la formación de ZnPP (Wakamatsu *et al.*, 2015). En extractos de carne fresca, Benedini *et al.* (2008) encontraron que la actividad enzimática depende de la temperatura, con un aumento de la misma de un 1554.5 % al pasar de 10 °C (0.22 unidades de actividad enzimática/g carne seca) a 37 °C (3.64 unidades de actividad enzimática/g de carne seca). Los mismos autores indicaron que la formación de ZnPP se ve favorecida por la presencia de altas cantidades de NaCl. Sin embargo, Becker *et al.* (2012) encontraron que un contenido

elevado de NaCl limitaba la formación de ZnPP en productos cárnicos. En relación al pH, Chau *et al.* (2010) observaron que la enzima tiene su óptimo de actividad para eliminar el átomo de Fe<sup>2+</sup> de la porfirina en el rango de pH 5.5 - 6.0 mientras que la inserción de Zn<sup>2+</sup> se ve favorecida en pH neutro o básico (7.5 - 8.0). Estos últimos autores también demostraron que la presencia de ácidos grasos y fosfolípidos aumenta la actividad de la FeQ, aunque el mecanismo de actuación no está claro, se considera que actúan activando la reacción enzimática de eliminación del átomo de hierro de la porfirina.

Alternativamente a la obtención del pigmento formado en matrices cárnicas, como el hígado de cerdo, podría ser de interés la purificación de la FeQ o la obtención de una fracción con elevada actividad de FeQ. Esto permitiría abordar la obtención de ZnPP a partir de otros substratos, como coproductos de origen animal, como la sangre, previa separación de la hemoglobina (Graham, 2001; Taketani y Tokunaga, 2005) o bien la adición directa de FeQ sobre productos cárnicos. En este sentido, Ishikawa *et al.* (2006) estudiaron la formación *in vitro* de ZnPP a partir de la enzima extraída del corazón de cerdo. Esta estrategia tendría la ventaja de poder asegurar un mejor control de las condiciones de formación de ZnPP. Además, el desarrollo de un ingrediente con un color rojo estable basado en ZnPP, o bien de una fracción con elevada actividad de FeQ que facilite su formación, pueden conducir al desarrollo de una nueva gama de productos.

## **1.2 Estabilización de productos cárnicos mediante secado**

Los productos cárnicos se caracterizan por tener un contenido de humedad elevado que condiciona su vida útil, y que los hace susceptibles de sufrir reacciones de degradación tanto enzimáticas como microbiológicas. Por ello, se requieren tratamientos de conservación que permitan mantener sus propiedades durante el almacenamiento y posibiliten su aprovechamiento posterior (Uribe *et al.*, 2014; Saavedra *et al.*, 2017). Los métodos de conservación más extendidos en la industria alimentaria se pueden clasificar en métodos de conservación por frío, como la refrigeración o la congelación, tratamientos térmicos, como la esterilización o

pasteurización, o no térmicos empleando nuevas tecnologías, como las altas presiones o los campos eléctricos, envasado en atmósferas controladas, incorporación de aditivos y conservación por reducción de la actividad de agua, entre los que destaca el secado y salado.

El secado de los productos cárnicos se ha realizado desde la antigüedad, colocando la carne, generalmente salada, al aire libre para que se deshidrata, por efecto del aire que estaba a temperatura elevada y a humedad relativa baja. Sin embargo, debido a la variabilidad de las condiciones climáticas, y por razones de seguridad alimentaria, hoy en día estas prácticas ancestrales han sido sustituidas por procesos de secado bajo condiciones controladas (Petrova *et al.*, 2015).

El proceso de secado es promovido por la diferencia de potencial químico del agua cuando se expone el producto a un fluido (aire caliente o frío, dependiendo de la temperatura de secado) con un potencial químico menor, por tanto, el agua del interior del alimento migra hacia la superficie, donde se evapora y se transporta hacia el medio que le rodea. Sin embargo, la carne es muy propensa a sufrir encostramiento durante el secado, desarrollando una capa seca externa que dificulta la salida de la humedad interna. Así, para evitar este fenómeno, el secado de la carne suele realizarse bajo condiciones de convección natural o forzada de carácter moderado, provocando cambios estructurales y de composición química, que se producirán en un mayor o menor grado, en función de la temperatura aplicada y el tiempo de exposición al secado (Fito *et al.*, 2001). Por tanto, la determinación de las mejores condiciones de secado resulta fundamental para la conservación de los compuestos de interés.

En los coproductos de origen animal de alto valor proteico, como es el hígado de cerdo, se puede aplicar el proceso de secado para prolongar la vida útil y facilitar el manejo y almacenamiento del hígado antes de su posterior uso en aplicaciones como la extracción de su fracción proteica (Sánchez-Torres *et al.*, 2021). Cabe destacar que, además del proceso de secado, la eliminación posterior de la fracción grasa facilitaría la recuperación de la fracción proteica, y limitaría las reacciones de degradación que acortan la vida útil y comprometen al sabor y al aroma, como la oxidación lipídica y el enranciamiento. A partir de ambos procesos se obtendría una fracción proteica con un

mayor grado de pureza, con el objetivo de aprovechar las características nutricionales y las propiedades tecno-funcionales de las proteínas (Vioquet *et al.*, 2001). Además, el desgrasado también podría facilitar la eliminación de aromas no deseables del hígado, que facilitarían su uso posterior como ingrediente. En cuanto a la temperatura aplicada en los procesos de secado de productos cárnicos, se pueden emplear dos tecnologías de secado por convección: el secado a baja temperatura y el secado a alta temperatura o por aire caliente. El secado a baja temperatura se define como el proceso llevado a cabo a temperaturas iguales o inferiores a las condiciones de temperatura ambiente estándar (20 °C) (Santacatalina *et al.*, 2014). Además, el proceso de secado a baja temperatura, por debajo de 0 °C, punto de congelación del agua pura, es conocido también como liofilización atmosférica (Bhatta *et al.*, 2020). Mediante el secado se reduce la cantidad de agua no adsorbida disponible y, por tanto, el agua no puede intervenir como vehículo de reacciones químicas y bioquímicas ni favorecer el crecimiento microbiológico (Barreiro y Sandoval, 2006). Por otro lado, el secado a baja temperatura hace que los compuestos termolábiles se conserven en gran medida, siendo uno de los métodos de conservación más respetuosos para la carne y los productos cárnicos, ya que, en comparación con otros métodos, produce una pérdida mínima de calidad durante el almacenamiento a largo plazo (Soyer *et al.*, 2010). Por otro lado, el secado a alta temperatura se define como el proceso realizado a temperaturas por encima de las condiciones de temperatura ambiente estándar (20 °C). Tras el secado, además de la estabilización del producto, el volumen y el peso del mismo disminuyen significativamente, dando lugar a menores costes de transporte y almacenamiento de los productos deshidratados, en comparación con los frescos (Aksoy *et al.*, 2019). Sin embargo, este procedimiento produce cambios físicos (color, textura, sabor, ...), químicos (pérdidas de compuestos bioactivos, vitaminas, ...) y estructurales (modificaciones en macromoléculas como polisacáridos y proteínas), que afectan negativamente a las propiedades nutricionales y a la calidad del producto final (Saavedra *et al.*, 2017; Martins *et al.*, 2019). Estas modificaciones dependerán principalmente de la temperatura empleada, que también influye en el tiempo de tratamiento y en el coste energético del proceso (Li *et al.*, 2012).

Por todo ello, es esencial establecer las condiciones óptimas del proceso de secado, desde el punto de vista de eficiencia del proceso y calidad del producto, para lo cual es necesario conocer las cinéticas de secado y así poder llevar a cabo una modelización matemática del proceso.

### **1.2.1 Cinéticas y modelos de secado**

Generalmente, en el secado por convección se pueden distinguir tres etapas, una de velocidad de secado creciente, otra de velocidad de secado constante y la última de velocidad de secado decreciente (Traffano-Schiffo *et al.*, 2014). En la etapa de velocidad creciente, el producto se calienta y aumenta la velocidad de evaporación del agua de la superficie del producto, es el periodo en el cual el producto se adapta a las condiciones expuestas. En la etapa de velocidad constante el movimiento del agua dentro del sólido es lo bastante rápido como para mantener saturada la superficie. La velocidad de secado está controlada por la evaporación del agua y su transferencia desde la superficie saturada del material hasta el medio que lo rodea, estando el proceso controlado por la convección o resistencia externa a la transferencia de materia. Esta etapa finaliza cuando el contenido en humedad del producto desciende por debajo de la humedad crítica y la superficie del producto ya no está completamente saturada. Así en la última etapa, de velocidad decreciente, la superficie del sólido deja de estar saturada, es decir aparecen zonas secas, y el proceso pasa también a estar controlado por la resistencia interna a la transferencia de materia debido a la difusión del agua (García-Pérez, 2007).

A través de la modelización matemática se lleva a cabo el análisis de los fenómenos que ocurren en los procesos alimentarios. Además, la modelización permite mejorar la comprensión de la dinámica del proceso y así desarrollar una estrategia de control del mismo (Taylor *et al.*, 2016). Así, mediante el uso de modelos, el coste y tiempo implicados en los estudios experimentales puede verse reducido. Un modelo matemático debe tener en cuenta la descripción del sistema del alimento, los mecanismos de los procesos que tienen lugar y las ecuaciones de los cambios de propiedad (energía, materia y cantidad de movimiento). Sin embargo, se debe resaltar que los modelos son aproximaciones de la realidad. Los modelos utilizados para

predecir los tiempos de secado pueden variar desde ecuaciones analíticas simples, basadas en una serie de aproximaciones y suposiciones, hasta formulaciones complejas que requieren el uso de métodos numéricos para su resolución. En este sentido, para modelizar un proceso de deshidratación de un producto podemos diferenciar dos tipos de modelos a aplicar de forma general modelos difusionales o empíricos (Freire *et al.*, 2014).

Los modelos difusionales están basados en las leyes del transporte difusional de agua. El modelo difusivo fue formulado por Lewis (1921) y posteriormente desarrollado por Sherwood (1929). La principal ventaja de estos modelos es que son fáciles de formular y además proporcionan resultados razonablemente buenos. Por contra, la facilidad de la formulación conlleva el tener que realizar una serie de simplificaciones. Por ello, en la formulación aparece el coeficiente de difusividad efectiva, que incluye el efecto de hipótesis conocidas, así como fenómenos desconocidos que no se consideran en el modelo (Mulet, 1994). Al emplear un modelo difusivo para describir los mecanismos de transporte, las ecuaciones empleadas se deducen a partir de la ley de Fick.

Los modelos empíricos no pretenden describir como tiene lugar el proceso y sólo interpretan de forma empírica los datos, son útiles en cuestiones de diseño cuando los problemas son excesivamente complicados (Van Boekel, 2008). Entre los modelos empíricos cabe destacar el modelo de Weibull. El modelo empírico de Weibull es un modelo de distribución probabilística muy utilizado en procesos complejos de alta variabilidad como lo son los procesos de secado (Barbosa *et al.*, 2022). Su utilización en tecnología de alimentos se centra en la descripción de procesos degradativos, ya que la deshidratación de un alimento se puede considerar como un fallo del sistema alimento al someterse a unas condiciones determinadas de estrés (Hardy y Jideani, 2017). La forma más habitual del modelo de Weibull que se utiliza en procesos de secado se muestra en la Ecuación 1.



$$W_t = W_e + (W_0 - W_e) \cdot \exp\left[-\left(\frac{t}{\beta}\right)^\alpha\right] \quad (\text{Ecuación 1})$$

Donde  $W_t$  es el contenido de humedad en el tiempo “t”, (kg agua/kg materia seca),  $W_e$  es el contenido de humedad de equilibrio (kg agua/kg materia seca) y  $W_0$  es el contenido de humedad inicial (kg agua/kg materia seca), t es el tiempo (s) y  $\beta$  (s) y  $\alpha$  (adimensional) son los parámetros cinéticos y de forma del modelo, respectivamente.

Cuando el valor de  $\alpha$  es igual a 1, el modelo corresponde a una cinética de primer orden, con una tasa de pérdida de agua constante. Cuando  $\alpha > 1$ , la velocidad de reacción del modelo de Weibull aumenta en función del tiempo y decrece cuando  $\alpha < 1$  (Marabi *et al.*, 2003).  $\beta$  es el parámetro cinético considerado como la constante de la velocidad de reacción, teniendo una relación inversa con la velocidad del proceso (Blasco *et al.*, 2006), es decir, si  $\beta$  disminuye, aumenta la velocidad del proceso. Así, el modelo de Weibull se ha utilizado para evaluar el efecto de variables como temperatura, velocidad del aire y tamaño de partícula de la cinética de secado a partir de la variación de las constantes cinéticas.

### 1.3 Desodorización de alimentos

El sabor y el aroma son unas de las características más significativas de la palatabilidad de la carne y, eventualmente, pueden afectar tanto a la aceptación de un producto cárnico por parte del consumidor, como a los hábitos de compra (Ramalingam *et al.*, 2019). En general, el consumo de coproductos y vísceras está limitado debido a su aroma y sabor característico, el cual dificulta su aceptabilidad y consumo, a pesar de ser productos saludables (Llauger *et al.*, 2021). Ante esta problemática y para poder revalorizar los coproductos de la industria, se podrían aplicar técnicas de desodorización, que consisten en la eliminación o reducción de la concentración de aquellos compuestos orgánicos volátiles (COVs) asociados a un olor desagradable. Estudios previos han aplicado la desodorización en otros productos como aceites

vegetales (soja, colza, maíz y girasol) (Liu *et al.*, 2021) o de pescado (de Oliveira *et al.*, 2016). También se ha aplicado al pescado (Li *et al.*, 2020) y especias (Silva *et al.*, 2005), entre otros alimentos. Sin embargo, la aplicación de técnicas de desodorización en carnes o derivados cárnicos no ha sido abordada hasta la fecha.

### 1.3.1 Métodos empleados

Actualmente, una técnica muy empleada para la eliminación de aromas indeseados en alimentos es el arrastre por vapor, con (AVV) o sin aplicación de vacío (AV), en la que se aplican temperaturas moderadas o altas con una baja presión y el vapor de agua arrastra vapores y COVs de la muestra a tratar, los cuales posteriormente son condensados y eliminados (Silva *et al.*, 2005). Una de las alternativas a la desodorización convencional podría ser la extracción de COVs mediante CO<sub>2</sub> supercrítico (CO<sub>2</sub>-SC).

La extracción con CO<sub>2</sub>-SC es una alternativa muy ventajosa, ya que se trata de un proceso limpio y respetuoso con el medio ambiente, al no generar efluentes orgánicos ni acuosos (Zhao *et al.*, 2022). Las técnicas de extracción con CO<sub>2</sub>-SC presentan ventajas sobre los métodos convencionales con disolventes orgánicos, como son disponer de una baja temperatura crítica (31 °C), una baja tensión superficial, una baja viscosidad, densidad similar a la de un líquido, una mejor selectividad y emplear un disolvente no tóxico, no inflamable, económico y fácilmente eliminable de la matriz a procesar (Asiri y Isloor, 2019). Al ser fácilmente eliminable de la matriz, esta podría tener un nuevo uso. Aunque la aplicación de esta técnica es relativamente costosa, las numerosas ventajas que presenta compensan el mayor costo de su uso y están en línea con la demanda de tecnologías de extracción limpias y seguras (Vafaei *et al.*, 2022). Además, en el campo de la desodorización de coproductos de origen animal, el CO<sub>2</sub>-SC presenta una gran ventaja frente a la técnica convencional de arrastre por vapor, ya que permitiría realizar simultáneamente la desodorización y la separación de la grasa. Hasta el momento, el CO<sub>2</sub>-SC se ha utilizado en la industria alimentaria como tecnología de extracción de compuestos como colorantes, ejemplo de ello el licopeno de la piel del tomate (Pellicanò *et al.*, 2019), componentes bioactivos, ácidos grasos mono y poliinsaturados a partir de vísceras, y filetes de pescado (Kuvendziev *et al.*, 2018),

saborizantes como aceites esenciales de plantas aromáticas (Yousefi *et al.*, 2019) y la cafeína del café o del té (Zabot, 2020). A partir de una matriz de origen animal también se ha realizado la extracción de compuestos como escualeno de hígado de tiburón (Catchpole *et al.*, 1997), lípidos de hígado de vacuno (Kang *et al.*, 2017) y de pollo (Ilias *et al.*, 2021), vitaminas como la vitamina A y  $\beta$  caroteno de hígado de ternera (Burri *et al.*, 1997) y antioxidantes como la etoxiquina de carne de vacuno (Brannegan *et al.*, 2001). Además de extraer compuestos de interés nutricional, el CO<sub>2</sub>-SC se ha utilizado para reducir el contenido graso de fuentes alimentarias ricas en proteínas como la carne y el pescado (King, 2014). Finalmente, esta tecnología se ha aplicado con el objetivo de extraer compuestos orgánicos volátiles (COVs) que generan aromas indeseables en productos alimenticios como en agua potable (Kobayashi *et al.*, 2006), en harina de guisante (Vatansever y Hall, 2020) o en salsa de pescado (Shimoda *et al.*, 2000), así como para extraer COVs deseables en polvo de chirimoya (Panadare *et al.*, 2021), en trufas (Tejedor-Calvo *et al.*, 2021), en extractos de lavandina y tomillo (Oszagyan *et al.*, 1996). Sin embargo, hasta la fecha no se ha abordado su estudio sobre la extracción de COVs en la industria cárnica, como es el caso del hígado de cerdo. Además, las aplicaciones que se pueden encontrar en la bibliografía relativas a la desodorización mediante CO<sub>2</sub>-SC se han desarrollado sobre líquidos o pastas, no habiéndose encontrado aplicaciones de extracción de COVs en matrices completamente sólidas, como es el caso del hígado de cerdo deshidratado.

#### **1.4 Características de la zinc protoporfirina e importancia en el sector cárnico**

El color es uno de los parámetros de calidad más importantes que influyen en la aceptabilidad de la carne por parte del consumidor (Pateiro *et al.*, 2018). Los consumidores se sienten atraídos por la apariencia de la carne, ya que asocian el color rojo brillante con un producto cárnico más fresco, saludable y de mayor calidad. Sin embargo, la carne es propensa a sufrir variaciones de color resultantes de la formación de desoximioglobina (rojo púrpura), oximioglobina (rojo cereza) y metamioglobina (marrón) a través de reacciones redox de la mioglobina (Tomasevic *et al.*, 2021). Por lo tanto, mantener el color de la carne fresca es crucial para asegurar la aceptación del

consumidor (Kadim, 2015).

Dentro de las posibles funciones tecnológicas que pueden tener los distintos compuestos obtenidos a partir coproductos y subproductos de origen animal, las relativas a la formación y estabilidad del color, tienen especial interés, puesto que éste es determinante en las decisiones de compra. En general, se consideraba que las ferroporfirinas eran las únicas responsables del característico color rojo de los productos cárnicos. Sin embargo, Wakamatsu *et al.* (2004a) identificaron la ZnPP como pigmento derivado de la ferroprotoporfirina responsable del color característico del jamón de Parma, en cuya producción no se añaden agentes de curado. Además de en el jamón de Parma, De Maere *et al.* (2017) estudiaron ocho fuentes de carne (pollo, pavo, cerdo, cordero, ternera, caballo e hígado de cerdo). Su presencia también ha sido descrita en jamón curado (Moller *et al.*, 2007; Laursen *et al.*, 2008).

La zinc protoporfirina (ZnPP) es un pigmento prácticamente similar al grupo hemo desde un punto de vista químico con la salvedad de que el átomo de hierro ( $\text{Fe}^{2+}$ ) del anillo porfirínico ha sido sustituido por un átomo de zinc ( $\text{Zn}^{2+}$ ). Este pigmento tiene un gran interés tecnológico por su color y su elevada estabilidad frente a la luz y el calor, entre otros factores de procesado (Adamsen *et al.*, 2004; De Maere *et al.*, 2017). Por este motivo, la ZnPP podría ser útil para mejorar el color de los productos cárnicos, tanto curados como frescos, presentando además una elevada similitud a las ferroporfirinas (De Maere *et al.*, 2017). Además, a diferencia del grupo hemo, el complejo ZnPP presenta una gran fluorescencia y es fácilmente detectable en pequeñas cantidades. Su nombre completo sería zinc (II) protoporfirina IX y su estructura aparece representada en la Figura 2.

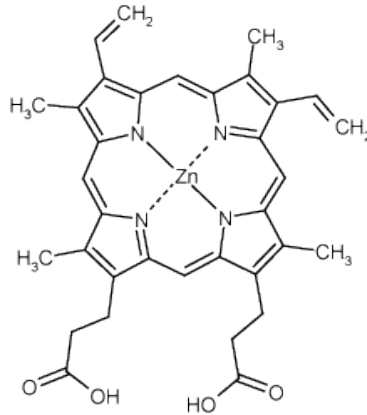


Figura 2. Estructura química de zinc (II) protoporfirina IX

Aunque los mecanismos relativos a la formación de ZnPP no han sido completamente descritos, se conoce que ésta depende de enzimas endógenas de la carne, destacando la enzima ferroquelatasa (FeQ), principal responsable de la formación de ZnPP en productos cárnicos (Adamsen *et al.*, 2004; Wakamatsu *et al.*, 2007; Benedini *et al.*, 2008; Chau *et al.*, 2011). Wakamatsu *et al.* (2004b) determinaron que bajo condiciones anaeróbicas y en presencia de microorganismos y enzimas endógenas propias de la carne, se formaba ZnPP. Además, Camadro y Labbe (1982) y Taketani y Tokunaga (1981) observaron que el pH óptimo de la actividad de la FeQ para la formación de ZnPP era entre 7.5 y 8.0, estudiado en levadura y en hígado de rata, respectivamente. Sin embargo, Benedini *et al.* (2008) demostraron que en el músculo porcino *post-mortem* (*Longissimus dorsi*) a pH relativamente bajo (5.5 - 6) y en presencia de  $Zn^{2+}$ , se favorecía la formación de ZnPP, mientras Wakamatsu *et al.* (2019) estudió el pH óptimo de 20 músculos porcinos (del hombro, del lomo y de la pierna), el cual se encontraba entre 4.75 y 5.5 dependiendo de la temperatura de incubación. En relación al pH, en extractos de corazón porcino, la formación de ZnPP también se favorecía a pH entre 5.5 y 6.0 (Ishikawa *et al.*, 2006). Por otro lado, Wakamatsu *et al.* (2015) investigaron las propiedades formadoras de ZnPP de varios

órganos internos de cerdo y pollo (hígado, corazón, riñón, bazo, etc.), encontrando que los órganos porcinos resultaron tener mayor actividad enzimática de formación de ZnPP que los de pollo. Además, entre todos los órganos porcinos, el hígado demostró la mayor capacidad enzimática para formar ZnPP, incluso a un valor de pH menor (pH 4.5) que en el músculo esquelético (pH de 4.75 a 6.0). Por lo tanto, la contribución de la FeQ en la inserción del  $Zn^{2+}$  a la protoporfirina IX (PPIX) para la formación de ZnPP sigue siendo contradictoria. Además, Becker *et al.* (2012) también pusieron de manifiesto que la ZnPP se podría formar en homogeneizados de cerdo a través de reacciones no enzimáticas. En este mismo sentido, Wakamatsu *et al.* (2022) afirmaron que la FeQ estaba involucrada en la formación de ZnPP, pero no estaba claro si la FeQ forma parte del proceso de eliminación del  $Fe^{2+}$  del grupo hemo o en la inserción del  $Zn^{2+}$  en la protoporfirina IX, o en ambos procesos. Por lo que, no están completamente elucidados los mecanismos de la formación de ZnPP hasta la fecha, probablemente debido a la complejidad bioquímica de su formación.

### **1.5 Intensificación de la extracción de enzimas. Ultrasonidos.**

En los últimos años, la extracción de compuestos de interés biotecnológico, como las enzimas, a partir de productos biológicos se ha convertido en un proceso muy extendido, debido a su gran interés para la industria alimentaria. La extracción de la ferroquelatasa (FeQ) a partir del hígado de cerdo, constituye un ejemplo de extracción sólido-líquido. La extracción sólido-líquido, es un proceso de separación que implica la transferencia de solutos de una matriz sólida a un solvente. En este sentido, la transferencia de materia durante la extracción sólido-líquido se define como la difusión de un sólido heterogéneo en un medio (refinado) que representa a la fase extraíble, en contacto con una solución que es el medio líquido homogéneo (extracto) compuesto principalmente por el disolvente en el cual se recupera el compuesto a extraer (Rodríguez-Jimenes *et al.*, 2013). Además, la transferencia de materia durante los procesos de extracción sólido-líquido involucra cuatro etapas entre sus dos fases:

1. La penetración del disolvente de extracción en la matriz sólida extraíble.

2. La disolución del compuesto extraíble a partir de la matriz sólida hacia el disolvente.
3. La transferencia de materia por difusividad del compuesto extraíble a través de la matriz sólida.
4. La transferencia de materia desde la interfase de la matriz sólida hacia el disolvente situado en el exterior por convección.

Los procesos de extracción tienen como objetivo aislar el compuesto de interés, como puede ser una enzima, del medio circundante. En las enzimas intracelulares, como es la FeQ del hígado de cerdo, el proceso de extracción y recuperación de la enzima considera la obtención de la enzima por ruptura celular, la separación de la matriz celular o biológica (que contiene la enzima) del medio circundante y la purificación de la enzima (Taipa *et al.*, 2019) o concentración de la fracción enzimática.

La ruptura celular con el fin de liberar la enzima al medio circundante puede llevarse a cabo mediante los siguientes métodos, los cuales se clasifican en métodos físicos (molienda de perlas, ultrasonicadores, homogeneizadores a alta presión etc.), métodos químicos (fluidos supercríticos, ozono, surfactantes, álcalis fuertes, solventes orgánicos) y métodos enzimáticos (Phong *et al.*, 2018). Posteriormente, para la separación de la matriz celular o biológica del medio circundante se utilizan los procesos de extracción sólido-líquido, siendo las operaciones más empleadas la filtración y la centrifugación. Por último, para la purificación de la enzima se debe concentrar el extracto enzimático y eliminar cualquier componente que interfiera en su posterior aplicación. Las técnicas de concentración dependerán fundamentalmente de las propiedades fisicoquímicas (pH, temperatura, solubilidad y fuerza iónica) de la enzima a recuperar. Algunos de los métodos más utilizados para estos fines son: precipitación con sales "salting-out", la cual es inducida por el cambio de pH o por el potencial iónico, precipitación por la adición de disolventes orgánicos inertes o polímeros, que producen interacción entre los grupos hidrofóbicos del disolvente y los de la enzima, disminuyendo la constante dieléctrica y el poder de solvatación, contribuyendo a la precipitación de la enzima en la interfase (Gimenes *et al.*, 2021) y filtración por

membrana (Rajeeva y Lele, 2011). Mediante la aplicación de ultrasonidos de potencia (US) es posible una mejora en la penetración del disolvente en la matriz celular y una alteración de su estructura (ruptura celular), lo que puede dar lugar a una intensificación en la transferencia de materia (Khadhraoui *et al.*, 2021). Este hecho se debe a que durante la aplicación de US en medio líquido se producen efectos rápidos y sucesivos de rarefacción y descompresión. A frecuencias adecuadas, los ciclos de rarefacción exceden a las fuerzas de atracción de las moléculas de agua, formándose burbujas de cavitación a partir de un núcleo gaseoso presente en la muestra. Estas burbujas se distribuyen por todo el líquido y aumentan de tamaño hasta que finalmente colapsan, dando lugar al fenómeno de cavitación (Li *et al.*, 2021). La explosión de estas burbujas produce acumulaciones de energía en determinados puntos, generando temperaturas y presiones extremas que producen altas tensiones de ondas de energía y turbulencia en la zona de cavitación, lo que origina unos esfuerzos cortantes muy elevados capaces de romper las células liberando su contenido al exterior (Martínez-Solano *et al.*, 2021). Además de intensificar la ruptura celular, la interacción de los US en la interfase sólido-líquido puede producir una micro-agitación en el medio que rodea al sólido, la cual conlleva la reducción del espesor de la capa límite de difusión y, por lo tanto, de la resistencia externa a la transferencia de materia (Guimarães *et al.*, 2020). Por otro lado, en la matriz sólida las compresiones y expansiones del material producidas por las ondas de US generan el llamado “efecto esponja” el cual produce la salida de líquido del interior de la muestra y la entrada de fluidos del exterior, por lo que se mejora la difusión de solutos dentro de la matriz sólida, pudiendo afectar en la resistencia interna a la transferencia de materia (Allahdad *et al.*, 2019).

El interés en el desarrollo de las extracciones asistidas con US recae en la posibilidad de reducir el tiempo de extracción, al mismo tiempo que puede aumentar el rendimiento (Kumar *et al.*, 2021). Además, en algunos casos, incluso podrían sustituirse los solventes orgánicos normalmente empleados para las extracciones, por otros solventes reconocidos generalmente como seguros o “GRAS” (FDA, 2021), lo que reportaría beneficios económicos, medioambientales y de seguridad alimentaria (Wen *et al.*, 2018).



Esta tecnología ha demostrado ser interesante en la extracción de numerosos compuestos a partir de diversos alimentos y matrices naturales (Chemat *et al.*, 2017). En este sentido, se ha empleado para la extracción de compuestos bioactivos y funcionales como los carotenoides (licopeno) del tomate (Li *et al.*, 2022), pectinas de la cáscara de la chirimoya (Shivamathi *et al.*, 2019), antocianinas de las patatas (*Solanum tuberosum L.*) (Carrera *et al.*, 2021), antioxidantes de frutas como el cerezo silvestre o chokeberry (*Aronia Melanocarpa L.*) (Vázquez-Espinosa *et al.*, 2019) o insulina extraída a partir de materiales alimenticios vegetales (Zhu *et al.*, 2016). Los US también se han utilizado para la extracción de aceites de vegetales a partir de avellana molida (Wong *et al.*, 2019) o de semillas de chía (Rosas-Mendoza *et al.*, 2017). Entre los números compuestos que se pueden extraer utilizando la técnica de los US se incluyen las enzimas. Así pues, se ha empleado US para la extracción de enzimas proteolíticas como pectinasas (Amid *et al.*, 2016), lipolíticas como las lipasas (Nunes *et al.*, 2021), enzimas hidrolíticas y oxidativas (Szabo *et al.*, 2015), así como enzimas hidrolíticas de origen fúngico como la xilanasa derivada del *Penicillium purpurogenum* (Sunkar *et al.*, 2020) entre otras muchas. Cabe indicar que, el tratamiento de US también conlleva modificaciones sobre la estructura de la matriz sólida, así como de la propia enzima, que pueden afectar a sus usos posteriores. Sin embargo, la extracción asistida por US de FeQ de hígado de cerdo, con el objetivo de reducir el tiempo de extracción y aumentar el rendimiento en la formación de zinc protoporfirina (ZnPP), no ha sido abordada previamente. En este sentido, usando niveles de energía ultrasónica moderados se podría favorecer la transferencia de la enzima desde el hígado al solvente, sin llegar a afectar a su estructura, y por lo tanto a su capacidad catalítica.

## **1.6 Intensificación de reacciones enzimáticas. Ultrasonidos.**

En el Anexo I, se incluye el artículo “Role of enzymatic reactions in meat processing and use of emergent technologies for process intensification”, donde se hace una descripción detallada de los aspectos más destacados de la intensificación de las reacciones enzimáticas mediante diferentes técnicas emergentes, entre las que se encuentran los ultrasonidos de potencia (US). Las reacciones enzimáticas suelen

presentar limitaciones en la transferencia de materia, lo que puede influir en la unión del sustrato al sitio activo de la enzima, dando lugar a un proceso lento, o también la difusión del producto, afectando a la velocidad de reemplazo del sitio activo. Además, la transferencia de materia de las reacciones enzimáticas depende de factores como la concentración de sustrato, la forma de la enzima o la viscosidad, temperatura y pH del medio de reacción, que puede cambiar durante la reacción con la formación del producto (Siddiqui *et al.*, 2022). En este sentido, la aplicación de US en las reacciones enzimáticas puede provocar una intensificación del proceso, proporcionando una mayor eficiencia respecto a los métodos convencionales. Mediante la aplicación de US tienen lugar mecanismos de cavitación y micro-agitación, anteriormente mencionados en el apartado 1.5, que mejoran la transferencia de materia y calor y también facilitan la liberación del contenido intracelular al solvente de extracción, es decir promueven el movimiento de las moléculas favoreciendo su difusión (Wang *et al.*, 2020), el contacto enzima-sustrato y por lo tanto, acelerando el proceso de formación del producto de la reacción enzimática, y también su salida del sitio activo.

La bibliografía relativa a la intensificación de reacciones enzimáticas mediante US se puede clasificar en dos grandes grupos, aquellos trabajos que realizan un pretratamiento de sustrato y/o enzima mediante US y aquellos que aplican los US durante la reacción enzimática (Wang *et al.*, 2018). En el primer caso, las ondas de choque y los radicales libres inducidos por los US pueden provocar la reducción del tamaño de partícula del sustrato y alterar las interacciones entre el sustrato y la enzima. Estos efectos, dan como resultado el consiguiente aumento del área de contacto efectiva de la enzima con los sustratos, reduciendo las limitaciones de transferencia de materia y mejorando indirectamente la actividad catalítica (Priya y Gogate, 2021). El segundo enfoque implica el uso de US durante toda la reacción enzimática. Aquí, la energía aportada por los US acelera la velocidad de reacción, pero el mecanismo por el cual esto ocurre no es evidente. Una posible hipótesis podría estar relacionada con que la energía ultrasónica aplicada afectaría a la conformación y estructura de la enzima o sustrato, lo que podría facilitar la unión enzima-sustrato (Yu *et al.*, 2013). Además, los US podrían aumentar la movilidad de la enzima y el sustrato, reduciendo la energía de activación, lo que favorecería que ambos se pusieran en contacto y por lo tanto, que

tuviera lugar la reacción enzimática (Waghmare y Rathod, 2016).

La aplicación de US durante la reacción enzimática ha sido utilizada para la intensificación de reacciones enzimáticas de hidrólisis en alimentos, en concreto en reacciones enzimáticas relacionadas con la hidrólisis de carbohidratos, lípidos y proteínas. Por ejemplo, a partir de la  $\beta$ -galactosidasa de *Kluyveromyces marzianus* se logró una hidrólisis de lactosa en la leche del 90 % empleando US (37 °C, pH 6.7, 20 W y 20 kHz), en comparación con el 84 % sin sonicación (Şener *et al.*, 2006). Asimismo, se mejoró la velocidad de reacción de hidrólisis de carbohidratos con invertasa en un 33 % empleando US (25 Hz, 22 W/L, 40 °C), en comparación con el tratamiento sin US (de Souza Soares *et al.*, 2019). En cuanto a las reacciones enzimáticas de hidrólisis de lípidos intensificadas mediante US, la actividad de la lipasa mostró un aumento del 12 % después del procesamiento con US (25 kHz, 22 W/L, 40 °C, 1 h de incubación), en comparación con la reacción enzimática sin US, en las mismas condiciones (de Souza Soares *et al.*, 2020). Por último, en cuanto a reacciones de hidrólisis de proteínas, Chen *et al.* (2017) reportaron que, en salsa de soja, la aplicación de US mejoró el grado de hidrólisis proteica del 10.46 % y recuperación enzimática del 57 %, sin tratamiento de US (20 min, 50 °C), a un grado de hidrólisis del 15.44 % y recuperación del 61.94 %, con el tratamiento de US (126.4 W/cm<sup>2</sup>, 20 min, 50 °C). Sin embargo, otra estrategia posible por la cual se podrían mejorar las reacciones enzimáticas es la aplicación de US de baja o moderada potencia con el fin de inducir una cavitación leve, o solo una micro-agitación, y promover la unión de los sustratos con los sitios activos, o incluso la difusión del producto sin alterar la estructura enzimática.

La aplicación de US en reacciones enzimáticas puede resultar muy interesante desde el punto de vista tecnológico, sin embargo, para que el proceso sea viable, es necesario determinar las condiciones óptimas de aplicación, como son la temperatura del proceso, la potencia, la intensidad y el tiempo de aplicación (Delgado-Povedano y De Castro, 2015; Bansode y Rathod, 2017; Nadar y Rathod, 2017). Esta tecnología se engloba dentro de las consideradas como “verdes”, ya que emplea menos solventes y menor consumo de energía. Además, debido a que la transferencia de energía acústica al medio es instantánea y bastante homogénea, es posible una reducción del tiempo de

proceso y aumentar el rendimiento de la reacción.

## 1.7 Justificación de la Tesis

En los últimos años, se ha producido un creciente consumo de productos cárnicos, lo que ha estimulado su producción en Europa. El elevado volumen de producción de carne ha conllevado una gran generación de subproductos, desperdicios y coproductos de origen animal, los cuales están contribuyendo a provocar un impacto negativo en el medio ambiente y económico para las empresas del sector. Por este motivo, cualquier actuación dirigida a revalorizar los coproductos de origen animal es de gran interés para esta industria, tanto desde el punto de vista económico, como medioambiental. Además, la revalorización de coproductos es una demanda histórica de amplio consenso social.

A pesar del elevado incremento de la producción y consumo de productos cárnicos, durante las últimas décadas se ha puesto de manifiesto el problema del déficit de proteína, que se deriva de la tasa de crecimiento demográfico y del incremento del consumo de proteína animal, tanto en países desarrollados como en vías de desarrollo (Henchion *et al.*, 2017). Por esta razón, las necesidades de proteína, junto con el coste medioambiental de la producción de animales de carne, hacen que sea necesario plantear el máximo aprovechamiento de todos los recursos que potencialmente contengan proteínas de alto valor biológico.

La mayoría de los coproductos, como el hígado tienen un escaso valor comercial, si bien son interesantes desde un punto de vista nutricional y tecnológico (Zou *et al.*, 2021). En este sentido, el valor nutricional de los coproductos de origen animal es en muchos casos comparable al de la carne magra (Soladoye *et al.*, 2022), siendo fuentes de proteínas de alta calidad, con excelentes propiedades tecnofuncionales. Por ello, la obtención de proteínas funcionales a partir de hígado tiene un elevado interés, ya que sería una alternativa libre de alérgenos a las proteínas no cárnicas. Actualmente, la mayor parte del consumo de coproductos está ligado al uso como ingrediente en la elaboración de productos cárnicos tradicionales como el paté

(de hígado), las morcillas (de sangre) (Lynch *et al.*, 2018), destinados a la elaboración de piensos o utilizados como abonos y enmiendas. El uso alternativo o valorización de órganos no es fácil, principalmente debido a una baja estabilidad biológica (Nollet y Toldrá, 2011) y a las propiedades organolépticas que presentan, en concreto el aroma y sabor. En este sentido, el aroma es una de las características más importantes de los alimentos, que determina la aceptación del consumidor y sus hábitos de compra (Miller, 2020). Por lo tanto, los procesos de recuperación y valorización no sólo deben mantener las propiedades funcionales del compuesto objetivo a extraer, sino que además deben cumplir con las exigentes expectativas de los consumidores en materia de seguridad y calidad alimentaria.

El panel de expertos de la EFSA ha confirmado la seguridad de los nitratos y nitritos que se añaden a los alimentos (EFSA *et al.*, 2017). Sin embargo, niveles elevados de nitratos y nitritos pueden dar lugar a la formación de metahemoglobina y, en el producto, compuestos nitrosilados, algunos de los cuales pueden ser carcinogénicos (Shahidi y Pegg, 2017). La mayoría de los productos cárnicos crudo-curados se producen en la actualidad añadiendo nitratos y nitritos, ya que la reacción del nitrito con la mioglobina del músculo de la carne da lugar a la nitrosilmioglobina, un compuesto rojo característico. Sin embargo, en productos cárnicos curados sin adición de agentes nitrificante, como en el jamón de Parma italiano, el pigmento color rojo característico y estable es la zinc protoporfirina (ZnPP) (Parolari, 1996; Wakamatsu *et al.*, 2004). Así, la ZnPP es catalizada a partir de la reacción enzimática de la enzima ferroquelatasa (FeQ) (Wakamatsu *et al.*, 2004). La FeQ se encuentra de forma natural en numerosas fuentes cárnicas, destacando el hígado de cerdo (Wakamatsu *et al.*, 2015). En condiciones anaeróbicas es posible obtener ZnPP a partir de hígado de cerdo, ya que el hígado es fuente de zinc ( $Zn^{2+}$ ) y protoporfirina IX, sustratos de la reacción enzimática. La extracción de fracciones ricas de FeQ del hígado resulta de gran interés para ser adicionada posteriormente a productos cárnicos crudo-curados o fermentados, donde tendría lugar la reacción enzimática de formación de ZnPP, pigmento que mejoraría la formación de su color típico, minimizando el uso de nitratos y nitritos (De Maere *et al.*, 2017). Además, el extracto de FeQ podría ser empleado en la formación de ZnPP a partir de coproductos de origen animal que sean fuente del

sustrato de la reacción, como es la hemoglobina de la sangre, la cual está formada por 4 grupos hemo, compuestos por la protoporfirina IX y el ion ferroso ( $\text{Fe}^{2+}$ ).

El uso de tecnologías emergentes como los ultrasonidos de potencia (US) ya ha demostrado tener éxito en la intensificación de reacciones enzimáticas en productos alimentarios, intensificando el proceso de extracción de enzimas y mejorando la actividad enzimática (Nadar y Rathod, 2017). Por lo tanto, la aplicación de US a una baja intensidad podría utilizarse para incrementar la actividad de FeQ en la formación de ZnPP, ya que se trata de una reacción enzimática de larga duración (Bou *et al.*, 2022), por lo que puede resultar de gran interés para incrementar la actividad enzimática y reducir el tiempo de proceso. Además, los US han sido aplicados para la extracción de compuestos de interés, como las enzimas, en diferentes matrices (Rodrigues *et al.*, 2015). Sin embargo, la extracción asistida por US de FeQ no ha sido abordada previamente y podría permitir la intensificación del proceso. Para incrementar la velocidad y el rendimiento de extracción de FeQ, se necesitarán niveles de energía ultrasónica que favorezcan la transferencia de la enzima al medio líquido, sin afectar su estructura.

Para llevar a cabo la estabilización del hígado de cerdo se precisa de una etapa previa de deshidratación siendo la más utilizada a nivel industrial, el secado convectivo o por aire forzado. Además, para poder aislar y extraer los compuestos de interés como son las proteínas funcionales es necesaria una etapa posterior al secado de desgrasado del hígado, con el objetivo de evitar reacciones de oxidación y enranciamiento, que provoquen una reducción de la vida útil, así como olores y sabores desagradables. El secado, además de reducir el contenido de agua, facilita la manipulación, transporte y almacenamiento. Las temperaturas de secado utilizadas, así como el tiempo de exposición durante el secado podrían afectar a la actividad enzimática de la FeQ para la formación del pigmento ZnPP, a las propiedades fisicoquímicas del hígado, a las propiedades tecno-funcionales de las proteínas, así como a la calidad final del producto para su posterior aprovechamiento. Por esta razón, es necesario determinar las condiciones de secado más favorables, según el uso posterior del hígado de cerdo. La modelización de las cinéticas de secado permite evaluar el efecto de los parámetros de

secado y optimizar el proceso según el objetivo final del producto (Taheri-Garavand *et al.*, 2018).

En el momento actual, una de las técnicas empleadas para la eliminación de aromas indeseados en alimentos es el arrastre por vapor (AV). Sin embargo, una de las alternativas es la extracción mediante CO<sub>2</sub> supercrítico (CO<sub>2</sub>-SC), una tecnología de extracción limpia y segura (Vafaei *et al.*, 2022), que además permite realizar simultáneamente la desodorización y la separación de la grasa de la matriz tratada. Si bien la aplicación de esta técnica a una matriz alimentaria es relativamente costosa, su uso presenta numerosas ventajas (bajas temperaturas, eliminación de solventes orgánicos, ausencia de O<sub>2</sub>) que permitirían compensar el mayor coste que representa el uso de esta tecnología. Aunque el mayor número de aplicaciones de extracción de grasas mediante CO<sub>2</sub>-SC se encuentra en matrices vegetales, también se ha empleado para reducir el contenido en grasa y colesterol de carnes y pescados (King, 2014) y la extracción de diversos componentes a partir de hígados (Catchpole *et al.*, 1997; Kang *et al.*, 2017). Shimoda *et al.* (2000) aplicaron CO<sub>2</sub>-SC en la desodorización de salsa de pescado para eliminar su aroma desagradable. Sin embargo, hasta el momento, el CO<sub>2</sub>-SC no ha sido aplicado para la desodorización de matrices cárnicas. En este contexto, se considera que el uso de CO<sub>2</sub>-SC podría ser una tecnología interesante para eliminar el aroma característico del hígado de cerdo, motivo de rechazo fundamental por parte de la mayoría de los consumidores (Llauger *et al.*, 2021).

En el marco de esta Tesis Doctoral se pretende avanzar en la intensificación del proceso de formación enzimática del pigmento ZnPP a partir de hígado de cerdo, así como en la extracción de la enzima FeQ mediante la aplicación de US. Además, la adición del extracto enzimático de FeQ a una fuente adicional de sustrato de reacción como es la hemoglobina porcina, conllevaría un aumento de la formación de ZnPP, con un posible uso posterior del pigmento en el desarrollo de productos cárnicos con un etiquetado “más limpio” e incluyendo la reducción o incluso eliminación de las sales nitrificantes. En cuanto a la estabilización del hígado de cerdo se persigue avanzar en el conocimiento científico de los factores implicados en la estabilización mediante el secado y el desgrasado del mismo, para la posterior obtención de proteínas funcionales

de alto valor biológico. Finalmente, respecto a la desodorización, con la aplicación de CO<sub>2</sub> supercrítico se pretende reducir y eliminar la mayor cantidad de compuestos volátiles característicos del aroma desagradable de hígado de cerdo fresco. Destacar que, esta Tesis Doctoral se ha realizado en el marco del proyecto “Obtención de pigmentos basados en la zinc protoporfirina y de proteínas funcionales a partir de coproductos cárnicos” financiado por “Ministerio de Economía y Competitividad (MINECO) e Instituto Nacional de Investigación y Tecnología Agraria y Alimentaria (INIA)”. Por último, resaltar la ayuda predoctoral recibida por la Universidad Politécnica de Valencia para la formación de Doctores (PAID-01-21) que ha financiado su realización.





## **2. OBJETIVOS**



El objetivo principal de esta Tesis Doctoral fue evaluar la viabilidad de diferentes tecnologías emergentes para la revalorización de coproductos porcinos en compuestos de interés tecno-funcional.

Para lograr este objetivo, se establecieron los siguientes objetivos particulares:

1. Analizar el efecto de la aplicación de ultrasonidos de potencia (US), empleando diferentes tiempos y modos de aplicación (continuo y pulsado), sobre la extracción de la enzima ferroquelatasa (FeQ) del hígado de cerdo, determinando la actividad de la enzima mediante el análisis de las cinéticas de formación de zinc protoporfirina (ZnPP) y caracterizando el campo acústico empleado y la eficiencia energética de las diferentes condiciones ensayadas.
2. Evaluar la viabilidad del uso de US, aplicados a intensidades moderadas y bajas, para la mejora de la reacción enzimática de formación de ZnPP catalizada por FeQ, a partir de diferentes sustratos: hígado de cerdo homogeneizado (Hhc) e hígado de cerdo homogeneizado, con adición de oxihemoglobina porcina (Hhc+OxiHb). Además, se determinará la idoneidad de la adición de diferentes antimicrobianos (antibióticos y ácidos) en la reacción de formación del pigmento ZnPP.
3. Determinar la influencia de la temperatura de secado (de -10 a 70 °C) sobre la actividad de FeQ obtenida a partir del hígado de cerdo deshidratado. Para lo cual se modelizarán las cinéticas de secado de hígado de cerdo y evaluará la actividad de la enzima y la concentración de FeQ aparente mediante el análisis de las cinéticas de formación de ZnPP.
4. Analizar el efecto del secado, a moderada-baja (40 °C) y a moderada-alta (70 °C) temperatura, sobre las propiedades fisicoquímicas y tecno-funcionales del hígado de cerdo.
5. Evaluar el efecto del desgrasado del hígado de cerdo deshidratado a temperatura moderada-baja (40 °C) y moderada-alta (70 °C), sobre sus propiedades fisicoquímicas y tecno-funcionales.

6. Evaluar la viabilidad del uso de arrastre de vapor con aplicación de vacío (AVV) y el tratamiento con dióxido de carbono en estado supercrítico (CO<sub>2</sub>-SC) para la reducción y eliminación de compuestos orgánicos volátiles (COVs) de hígado de cerdo deshidratado.
7. Determinar los cambios composicionales del hígado de cerdo deshidratado tras ser sometido a la desodorización mediante AVV y CO<sub>2</sub>-SC.



## **3. METODOLOGÍA**





### 3.1 Plan de trabajo

El plan de trabajo de la presente Tesis Doctoral (Figura 1) se diseñó en base a los objetivos planteados. Así, el plan experimental se dividió en cinco secciones dando lugar a los tres capítulos en los que se ha estructurado el apartado de Resultados y Discusión. Estos capítulos corresponden a los tres procesos estudiados para la revalorización del hígado de cerdo, mejora de la reacción enzimática de formación de zinc protoporfirina (ZnPP) catalizada por la ferroquelatasa (FeQ) (Capítulo 1), secado y desgrasado (Capítulo 2) y desodorización del hígado (Capítulo 3).

El primer capítulo está compuesto por dos secciones. En primer lugar, se estudió la viabilidad de la aplicación de ultrasonidos de potencia (US), en modo continuo y pulsado, a diferentes tiempos, sobre la extracción de FeQ del hígado de cerdo. El contenido y actividad de la FeQ se determinó mediante el estudio de la cinética de formación de ZnPP. Además, se analizó como afectaban las condiciones de extracción de FeQ (tiempo de reacción y el modo de extracción: convencional, US en continuo y US en modo pulsado) sobre la cinética de formación de ZnPP (Sección 1.1, Capítulo 1). En segundo lugar, se evaluó la viabilidad del uso de US, aplicados a intensidades moderadas y bajas, en la reacción enzimática de formación de ZnPP catalizada por FeQ, a partir de diferentes sustratos: hígado de cerdo homogeneizado (Hhc) e hígado de cerdo homogeneizado con adición de oxihemoglobina porcina (Hhc+OxiHb), para determinar si la aplicación de US tuvo un efecto significativo en la concentración de ZnPP de cada homogeneizado (Hhc y Hhc+OxiHb). Finalmente, se analizó el efecto de la adición de antimicrobianos en el medio de reacción (antibióticos y ácidos orgánicos) sobre la cinética de formación de ZnPP (Sección 1.2, Capítulo 1).

El segundo capítulo está formado por dos secciones, en la primera (Sección 2.1, Capítulo 2), se modelizaron las cinéticas de secado, con el objetivo de determinar la influencia de la temperatura de secado (de -10 a 70 °C), sobre la actividad de la FeQ (medida a través de la cinética de formación de ZnPP), obtenida a partir del hígado de cerdo deshidratado. En la segunda sección, se modelizó las cinéticas de secado para

determinar el efecto de la temperatura de secado, moderada-baja (40 °C) y moderada-alta (70 °C), así como el posterior proceso de desgrasado, sobre las propiedades fisicoquímicas del hígado de cerdo y tecno-funcionales de las proteínas del hígado (Sección 2.2, Capítulo 2). Las cinéticas de secado a diferentes temperaturas del Capítulo 2, se describieron mediante el modelo de Weibull y se analizó la influencia de la temperatura en sus parámetros.

En el tercer capítulo del plan experimental (Sección 3.1, Capítulo 3) se evaluó la efectividad de dos técnicas de desodorización, arrastre por vapor con aplicación de vacío (AVV) y la desodorización mediante CO<sub>2</sub> supercrítico (CO<sub>2</sub>-SC) sobre la eliminación de COVs que confieren el aroma desagradable del hígado de cerdo. Los COVs presentes en las muestras tras el proceso de desodorización, se analizaron mediante la técnica de micro-extracción en fase sólida, con espacio de cabeza, combinado con cromatografía de gases y detección por espectrómetro de masas (HS-SPME-GC/MS).

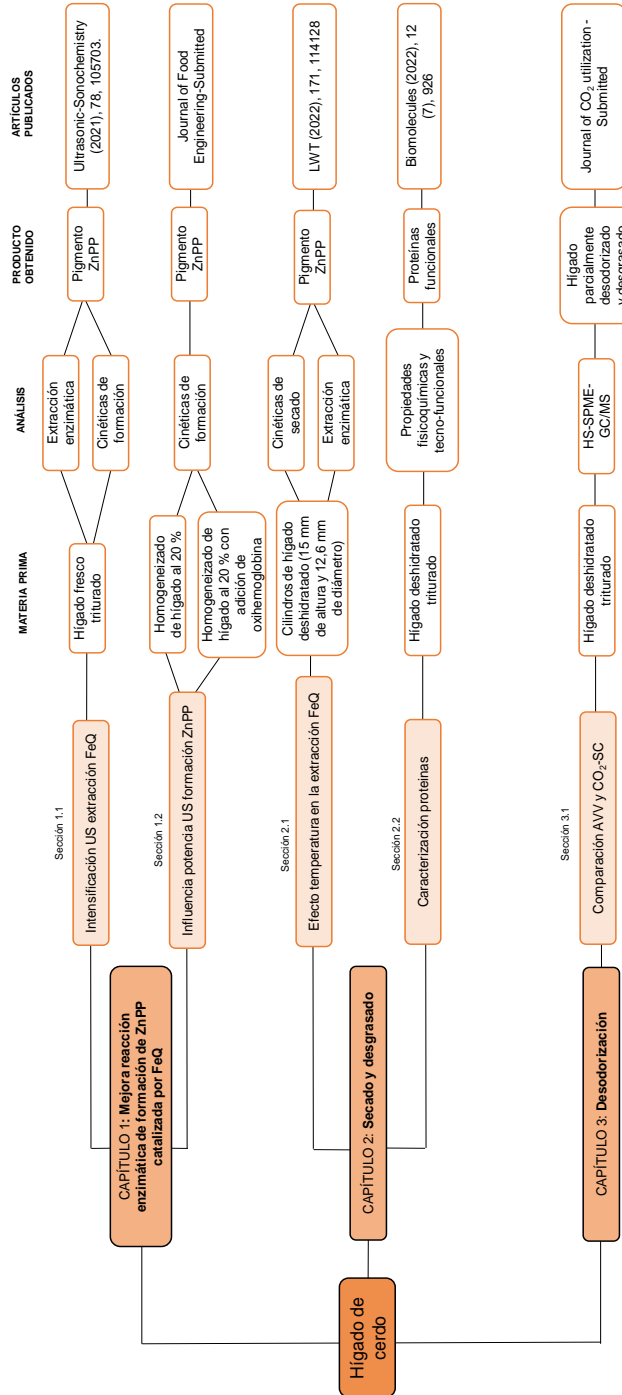


Figura 1. Plan de trabajo

## 3.2 Preparación de muestras

La materia prima utilizada fue hígado de cerdo procedente del matadero “Carnes de Teruel S.A.” (D.O. Jamón de Teruel, España). Los hígados de cerdo se transportaron a una temperatura inferior a 4 °C y se procesaron en menos de dos horas.

### 3.2.1 Homogeneizado de hígado de cerdo

Los hígados de cerdo fresco se trituraron para su homogeneización (Blixer 2, Robot Coupe, Vincennes Cedex, Francia), se envasaron en porciones de 30 g en bolsas de vacío (200 x 300 PA/PE, Sacoliva, Castellar del Vallès, Barcelona) y se almacenaron a -20 °C hasta su procesado. Una hora antes de su preparación se mantuvieron los hígados a 4 °C para una mejor manipulación.

Para llevar a cabo el proceso de formación de ZnPP a partir del homogeneizado de hígado fue necesario realizar un homogeneizado al 20 % de hígado de cerdo. Para ello, se utilizaron dos medios de reacción: con antibióticos y con ácidos orgánicos.

Para la formación de homogeneizado de hígado de cerdo al 20 % en un medio de reacción con antibióticos, el hígado de cerdo se diluyó con agua destilada y una mezcla de tres antibióticos: penicilina G potásica (140 µg/mL, concentración final), sulfato de estreptomicina (500 µg/mL, concentración final) y sulfato de gentamicina (100 µg/mL, concentración final).

El homogeneizado de hígado de cerdo utilizando el medio de reacción con ácidos orgánicos, se llevó a cabo con el fin de eliminar los antibióticos del homogeneizado final, ya que su uso no está aceptado en la industria alimentaria. Para ello se utilizaron ácido ascórbico y ácido acético, que son conservantes aceptados en la industria alimentaria para evitar el crecimiento microbiano. Para obtener un 20 % final de hígado en el homogeneizado, se preparó una solución que contenía 0.1 g de ácido ascórbico/100 mL de agua destilada y 250 µL de ácido acético, y se ajustó el pH a 4.16 con NaOH 1 N. Posteriormente, se tomaron 20 g de hígado previamente homogeneizados y conservados a 4 °C durante 1 h, se pesaron en un vaso de

precipitados y se completaron hasta 100 mL de la solución ácida. Ambas soluciones finales (con antibióticos y con ácidos orgánicos), se homogeneizaron (DI 25 Basic Homogenizer, IKA, Alemania) durante 1 min a 4 °C y 8000 rpm. Finalmente, el pH del homogeneizado al 20 % se ajustó a  $4.8 \pm 0.05$  con ácido clorhídrico (HCl) 1 N. Durante todo el procedimiento, el hígado de cerdo homogeneizado se protegió de la luz y se mantuvo en frío.

### **3.2.1.1 Homogeneizado de hígado de cerdo con adición de oxihemoglobina**

- ***Oxihemoglobina obtenida a partir de patrones comerciales de hemoglobina***

La solución de oxihemoglobina (OxiHb) se preparó según lo descrito por Bou *et al.* (2010). En primer lugar, se disolvieron 0.16 g del polvo liofilizado de hemoglobina porcina (Hb) (H4131, Sigma Aldrich, Canadá) en 3 mL de tampón fosfato frío (50 mM, pH 7.3, 4 °C). La Hb se redujo a OxiHb mediante la adición de cristales de ditionito de sodio (proporción 1:0.8 p/p) y se agitó en vórtex a 4 °C. Para eliminar el ditionito, se pasaron 2.5 mL de OxiHb a través de una columna de desalinización PD-10 desechable (17-0851-01, GE Healthcare Life Sciences). Luego, se pasaron 4 mL de tampón fosfato (50 mM, pH 7.3, 4 °C) a la fase estacionaria para eluir la OxiHb de la columna.

- ***Oxihemoglobina obtenida a partir de sangre de cerdo***

La sangre se obtuvo de cerdos sacrificados de acuerdo a los procedimientos estándar. Se recogieron aproximadamente 100 mL de sangre en un frasco que contenía trifosfato sódico con el objetivo de evitar la coagulación. La Hb se extrajo de los glóbulos rojos siguiendo el procedimiento descrito por Bou *et al.* (2019). Para reducir la solución de Hb a OxiHb, se añadieron cristales de ditionito de sodio (proporción 1:0.3 p/p). La mezcla se agitó en vórtex a 4 °C y se eliminó el ditionito pasando 2.5 mL de solución de OxiHb a una columna de desalinización desechable PD-10. Luego, se pasaron 4 mL de tampón Tris 50 mM (pH 8.5) a la fase estacionaria para eluir la OxiHb de la columna.

Para preparar ambos homogeneizados de hígado de cerdo con adición de OxiHb obtenida a partir de patrones comerciales de Hb y de OxiHb extraída a partir de sangre de cerdo (Hhc+OxiHb), se añadieron 2.5 mL de la solución de OxiHb con un rendimiento mínimo del 90 %. El porcentaje de OxiHb se calculó midiendo la absorbancia a 523 nm (punto isosbético), según lo descrito por Snell y Marini, (1988). El medio de reacción utilizado para el Hhc+OxiHb fue elaborado con ácidos orgánicos (para contener el crecimiento microbiano), preparación que ya ha sido descrita en el apartado 3.2.1. Por último, la solución final se homogeneizó en vórtex durante 45 s y se ajustó el pH a  $4.8 \pm 0.05$  con HCl 1 N.

### **3.2.2 Hígado deshidratado**

Los hígados de cerdo frescos se acondicionaron para su posterior deshidratación. Para ello, en primer lugar, se separaron sus 4 lóbulos principales: lateral derecho, lateral izquierdo, medial derecho y medial izquierdo. En segundo lugar, cada lóbulo se dividió en 2 partes, y todas las partes obtenidas se envasaron al vacío (200 x 300 PA/PE, Sacoliva, Castellar del Vallès, Barcelona), etiquetadas con un número correspondiente al hígado y al lóbulo, y se almacenaron a -20 °C hasta su procesado.

Para cada experimento de secado, se sacaron 2 partes envasadas a vacío del congelador (-20 °C), evitando coger dos partes de un mismo hígado y se atemperaron a 2 °C durante dos horas para facilitar su posterior manipulación. Con ayuda de una herramienta de uso doméstico, fabricada en el laboratorio, se obtuvieron cilindros de dimensiones estandarizadas (12.6 mm de diámetro x 15 mm de altura). La parte restante del hígado fue homogeneizada y se utilizó para determinar el contenido de humedad inicial y medir la actividad enzimática de FeQ (Sección 2.1, Figura 1). En los experimentos de secado en secadero de convección a alta y baja temperatura, se necesitaron 20 muestras cilíndricas para cada secado con un peso total de  $43 \pm 0.5$  g. En cambio, para los secados en estufa de convección se utilizaron 8 muestras cilíndricas para cada secado, con un peso total de  $15 \pm 0.5$  g.

### 3.3 Extracción de la enzima ferroquelatasa (FeQ): método convencional y asistido por ultrasonidos (US)

El proceso de extracción de ferroquelatasa (FeQ) a partir de hígado de cerdo se basó en el procedimiento descrito por Parolari *et al.* (2009), con pequeñas modificaciones (Sección 1.1 y 2.1, Figura 1). En la Sección 1.1 se homogeneizaron 4 g de hígado de cerdo molido descongelado (5 h, 20 °C) (Homogenizer DI 25 Basic, IKA, Alemania) con 100 mL de tampón de extracción durante 1 min a 4 °C y 8000 rpm, evitando la formación de espuma, utilizando un vaso de precipitado de vidrio de 200 mL. El tampón de extracción contenía Tris-HCl 50 mM, Glicerol 20 % (p/v), KCl 0.8 % (p/v) y Triton X-100 1 % (p/v) (Sigma Aldrich), y se ajustó a pH 8 con NaOH. La extracción convencional, sin aplicación de US, se llevó a cabo usando un agitador magnético (Magnetic Stirrer Hot Plate SM3, STUART, UK), la mezcla de hígado/disolvente se colocó en un vaso de precipitados de vidrio de 100 mL y la extracción se llevó a cabo durante 30 min. La temperatura se mantuvo a  $4 \pm 2$  °C para minimizar la degradación térmica de la enzima durante la extracción. En la Sección 2.1 se siguió el mismo procedimiento de extracción convencional descrito, a diferencia de que los volúmenes utilizados fueron menores, se homogeneizó 1 g de hígado de cerdo descongelado o de hígado deshidratado reconstituido a su humedad inicial (70 %) con 25 mL de tampón de extracción, utilizando un vaso de precipitados de vidrio 50 mL.

Como alternativa al método convencional, la extracción también se realizó con asistencia de ultrasonidos (US), utilizando un dispositivo tipo sonda (UP400S, HIELSCHER, Alemania), suministrando la máxima potencia disponible (400 W) a una frecuencia de 24 kHz y utilizando un sonotrodo de 2.2 cm de diámetro. La mezcla de hígado/disolvente se colocó en un vaso de precipitados de vidrio encamisado de 300 mL, protegido de la luz y la punta del sonotrodo ultrasónico se sumergió 1 cm. Se aplicó US durante diferentes tiempos (1, 2.5 y 5 min), en modo de operación continuo (100 % de frecuencia) y pulsado (50 % de frecuencia). La aplicación de US pulsada (50 % de frecuencia) consistió en pulsos de 0.5 s ON / 0.5 s OFF. En este caso, el control de la temperatura era más crítico que en el modo convencional, porque la cavitación generada por los ultrasonidos podía provocar un aumento rápido de la temperatura. Para evitar alcanzar altas temperaturas, a las que se podría inactivar la FeQ, se

bombé una solución de glicol (20 %) (SUK-0220, Shurho, México) a  $-20\text{ }^{\circ}\text{C}$ , que se hizo pasar a través de la camisa del vaso de precipitados que contenía la solución de extracción. La temperatura se controló mediante un sistema ON-OFF compuesto por un termopar tipo K conectado a un controlador de procesos (E5CN-R2MT-500, Omron, Japón), que actuó sobre la bomba para recircular la solución de glicol. Para cada condición de extracción (convencional, US continuo y US pulsado), se realizaron cinco repeticiones.

Para separar la fracción enzimática, la solución de extracción se centrifugó durante 10 min a 12500 rpm y  $4\text{ }^{\circ}\text{C}$  (Medifriger BL-S, SELECTA, España) y se filtró el sobrenadante (Whatman 597, GE LIFE SCIENCE, US), para ser utilizado como el extracto enzimático de FeQ.

### **3.4 Formación de zinc protoporfirina (ZnPP)**

#### **3.4.1 Formación de ZnPP a partir de extracto de FeQ**

Para cuantificar la concentración de ZnPP formada a partir de los extractos de FeQ de hígado de cerdo previamente extraídos siguiendo la metodología detallada en el apartado 3.3. se llevó a cabo la reacción enzimática de formación de ZnPP catalizada por el extracto de FeQ, siguiendo el procedimiento experimental desarrollado por Parolari *et al.* (2009) (Sección 1.1 y 2.1, Figura 1). La reacción enzimática tuvo lugar en microtubos incubados a  $37 \pm 0.5\text{ }^{\circ}\text{C}$  en baño María. En cada microtubo se introdujeron los siguientes reactivos: 35  $\mu\text{L}$  de EDTA 50 mM (solo al blanco), 250  $\mu\text{L}$  de  $\text{ZnSO}_4$  400  $\mu\text{M}$  en tampón Tris-HCl 360 mM, ajustado a pH 8, 200  $\mu\text{L}$  de ATP 25 mM en NaCl al 20 % (p/v) y 50  $\mu\text{L}$  de protoporfirina IX 0.25 mM en tampón Tris-HCl 360 mM, ajustado a pH 7, siguiendo este orden, y por último, se adicionó 300  $\mu\text{L}$  de extracto de FeQ de hígado de cerdo a las muestras. Con estos reactivos se prepararon dos lotes diferentes: muestras y blancos. En el lote de blancos, se agregaron 300  $\mu\text{L}$  del tampón de extracción en lugar del extracto enzimático para que la reacción enzimática no tuviera lugar. El valor del blanco se restó al de cada muestra para corregir cualquier señal fluorimétrica de fondo de los reactivos. Los microtubos se incubaron a diferentes tiempos (0, 15, 30, 45, 60, 90, 105 y 120 min) con el fin de



estudiar la cinética de la reacción. La cinética de formación de ZnPP se llevó a cabo por triplicado para cada muestra de extracto de FeQ de hígado de cerdo (Sección 1.1 y 2.1, Figura 1). Después de la incubación, la reacción enzimática se paró añadiendo a cada muestra 35  $\mu$ L de EDTA 50 mM en baño de hielo, quelante de la reacción enzimática. Tras parar la reacción enzimática, se añadió etanol absoluto frío (840  $\mu$ L) a los microtubos para la clarificación del pigmento y evitar interferencias en la medida de su espectro. Seguidamente las muestras se centrifugaron durante 30 min a 13200 rpm y 4 °C (5415R, EPPENDORF, Alemania). Finalmente, 200  $\mu$ L del sobrenadante clarificado fue sometido al análisis de fluorescencia utilizando un fluorímetro de placa de 96 pocillos (Infinite 200 Microplate Reader, TECAN, Suiza), ajustado al rango de 420 nm de excitación y 590 nm de emisión (Wakamatsu *et al.*, 2007). Cada extracto se analizó por duplicado.

### **3.4.2 Formación de ZnPP a partir de homogeneizado de hígado obtenido por el método convencional y asistido por US**

En cuanto a la cinética de formación de ZnPP a partir de homogeneizado (de hígado y de hígado con adición de oxihemoglobina, apartado 3.2.1), se siguió la metodología experimental previamente descrita por Bou *et al.* (2022), con modificaciones menores (Sección 1.2, Figura 1). La formación de ZnPP requiere un medio anaerobio y una temperatura óptima de 37 °C. Así, los medios de reacción descritos en el apartado 3.2.1, se colocaron en frascos de vidrio opaco (10 x 2 x 2 cm) de 15 mL de capacidad (Figura 2). Posteriormente, los frascos de vidrio se sumergieron en agua (800 mL) utilizando una jarra de anaerobiosis (HP0011, OXOID, Argentina) de 3.5 L en la que se indujeron condiciones anaeróbicas mediante sobres que generan una atmósfera de CO<sub>2</sub> (Anaerobic System BR 38, Oxoid Ltd., Hampshire, Inglaterra). La jarra de anaerobiosis se colocó a 6 cm del fondo de un baño ultrasónico (15 L ATG15160, ATU, España). Las muestras se incubaron a diferentes tiempos (0, 6, 12, 18, 24 y 48 h) con el fin de estudiar las cinéticas de formación de ZnPP.

El control de temperatura para formación de ZnPP por el método convencional y asistido por US se llevó a cabo utilizando un montaje experimental similar al descrito por Contreras *et al.* (2018) (Figura 2), el cual se basaba en la recirculación de agua

utilizando las conexiones superior e inferior del baño ultrasónico (5, Figura 2). Así, el agua de salida se conducía a un depósito de reserva (5 L) (3, Figura 2), equipado con un termostato de circulación (Digiterm TFT-200, Selecta, España) (2, Figura 2), que mantenía el líquido a 50 °C en agitación, además el líquido del baño también podía ser impulsado (3.5 L/min) a través de un intercambiador de calor de placas (EL852, Cervecería Mas Malta, España) (4, Figura 2). Como refrigerante en el intercambiador de calor se utilizó una solución de glicol (40 % p/v), que era proporcionada por una unidad de refrigeración a 2 °C (1190s, Circ Refrigerador, US) (1, Figura 2). La corriente de agua de salida del intercambiador de calor se introducía en el baño de agua por su conexión inferior, cerrando el circuito. Se implementó un control ON-OFF empleando un sensor Pt-100 colocado en el centro del frasco de vidrio opaco (6, Figura 2) conectado a un controlador de proceso (E5CK, Omron, Japón) (8, Figura 1), que actuaba sobre dos bombas de agua (10 y 11, Figura 2). El sistema de control actuó en dos modos: modo calentamiento y refrigeración. En el modo calentamiento, el agua pasaba del depósito de reserva, a 50 °C, al baño ultrasónico impulsada por la bomba de calentamiento (10, Figura 2), hasta alcanzar una temperatura de 37 °C (punto de consigna) en el frasco de vidrio. Cuando el sensor Pt-100 conectado al controlador de proceso detectaba que la temperatura en el frasco de vidrio era superior a 37 °C, se ponía en marcha el modo de enfriamiento, por lo que la bomba de enfriamiento (11, Figura 2) actuaba succionando el agua del baño ultrasónico, haciéndola pasar por el intercambiador, donde el agua era enfriada por la solución de glicol que recirculaba procedente de la unidad de refrigeración. Así, el agua era impulsada desde el intercambiador al baño ultrasónico para mantener una temperatura de 37 °C en el frasco de vidrio. Para la formación de ZnPP asistida por ultrasonidos (US), el modo de calentamiento solo funcionó hasta que se alcanzó la temperatura de 37 °C en el frasco de vidrio, ya que posteriormente, el calor proporcionado por los US hizo que solo fuera necesario el modo de enfriamiento.

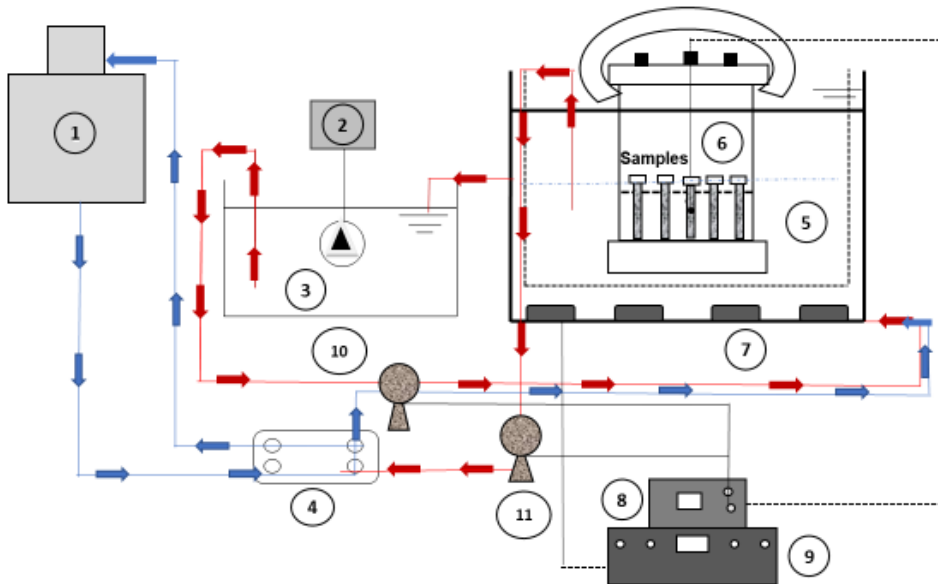


Figura 2. Esquema del baño ultrasónico con control de temperatura. 1, unidad de refrigeración; 2, termostato de circulación; 3, depósito de agua; 4, intercambiador de calor de placas; 5, baño ultrasónico; 6, jarra anaeróbica; 7, transductores ultrasónicos; 8, controlador de procesos; 9, generador y amplificador ultrasónico; 10, bomba de calentamiento; 11, bomba de enfriamiento.

En la cinética de formación de ZnPP asistida por US se aplicaron dos potencias ultrasónicas diferentes, modulando la amplitud del generador ultrasónico (GAT600W ATU, España). Así, las potencias reales (medidas por calorimetría de acuerdo al procedimiento propuesto por Ahmad-Qasem *et al.* (2013)) suministradas en los medios de reacción fueron 7.05 W/L (baja) y 36.53 W/L (moderada) y la aplicación se realizó en ambos casos en modo pulsado (30 min ON y 30 min OFF). La cinética de formación de ZnPP obtenida mediante el método convencional y asistida por US se realizó por triplicado.

Antes de llevar a cabo la cuantificación de la cantidad de ZnPP formada, se llevó a cabo su separación del medio de reacción. Para ello, se colocó 1 g del medio de reacción en tubos de centrífuga de 38 mL resistentes a disolventes (Nalgene Centrifuge Ware, PPCO), que se mantuvieron en hielo y protegidos de la luz. En cada tubo se agregaron 10 mL del solvente de extracción (dimetil sulfóxido (DMSO), acetato de etilo (AcOEt) y ácido acético glacial en una proporción de 1:10:2 v/v) y la mezcla se

homogeneizó por 30 s con un agitador vórtex (Velp Scientifica, 2 x 3 Advanced Vortex Mixer, Italia) y se mantuvo en frío a 4 °C y en oscuridad durante 20 min. A continuación, se centrifugó durante 20 min a 3100 rpm y 4 °C (Medifriger BL-S, SELECTA, España) y se filtró el sobrenadante (Whatman597, GE LIFE SCIENCE, EE. UU.). Posteriormente, el filtrado se recogió en matraces volumétricos color ámbar de 10 mL de capacidad. El filtrado se llevó a un volumen de 10 mL con el solvente de extracción. Finalmente, 200 µL de la muestra filtrada se midieron por fluorescencia siguiendo la misma metodología que se ha descrito en el apartado 3.4.1. Cada muestra se analizó por duplicado.

Para cuantificar la concentración de ZnPP se obtuvieron dos curvas de calibración, una para la ZnPP formada a partir del extracto de FeQ obtenido y otra para cuantificar la ZnPP formada a partir del homogeneizado de hígado de cerdo, debido a que el medio de reacción y los reactivos necesarios para la obtención de la ZnPP fueron diferentes, como se ha detallado en los apartados 3.2 y 3.3.

- **Cuantificación de ZnPP formada a partir de FeQ extraída del hígado**

Para obtener la curva de calibración, fue necesario la preparación de diferentes diluciones (0 µmol/L - 18 µmol/L) a partir de ZnPP concentrado (Sigma-Aldrich) utilizando el tampón de extracción descrito en el apartado 3.3, como medio de dilución. La curva de calibración ( $r^2=0.995$ ) se muestra en la Ecuación 1.

$$P = \frac{F - 1451}{6502} \quad (\text{Ecuación 1})$$

Donde F es la fluorescencia (RFU) medida con el equipo y P es la concentración de ZnPP formada (µmol/L)

- **Cuantificación de ZnPP formada a partir de homogeneizado de hígado**

Para realizar la curva de calibración se prepararon diferentes diluciones desde 0.02 hasta 2 mg/L- a partir de ZnPP concentrado (Sigma-Aldrich), utilizando el disolvente de extracción 1:10:2 (dimetilo sulfóxido, acetato de etilo: ácido acético

glacial) como medio de dilución. La curva de calibración ( $r^2= 0.998$ ) se muestra en la Ecuación 2.

$$P = \frac{F - 8724}{22935} \quad (\text{Ecuación 2})$$

Donde F es la fluorescencia (RFU) y P es la concentración de ZnPP formada (mg/L)

A partir del aumento en la cantidad de ZnPP, la velocidad de reacción se calculó como la cantidad de producto formado por unidad de tiempo (r, Ecuación 3) ( $\mu\text{mol de ZnPP/ L} \cdot \text{min}$ ) (Fersht, 1997).

$$r = \frac{dP}{dt} \quad (\text{Ecuación 3})$$

Donde P es la concentración de ZnPP ( $\mu\text{mol/L}$ ) y t es el tiempo (min).

Con el fin de comparar los resultados experimentales obtenidos con otros estudios, los valores de la velocidad de reacción también se expresaron como actividad enzimática específica (SEA,  $\text{nmol de ZnPP/g de materia seca} \cdot \text{min}$ ), considerando la masa de hígado utilizada para cada extracción.

### 3.5 Secado de hígado de cerdo

En los siguientes apartados se describen los dispositivos utilizados en este trabajo para la realización de las experiencias de secado, dependiendo de la temperatura empleada. Así, a partir de la temperatura estándar establecida ( $20\text{ }^\circ\text{C}$ ) (Santacatalina *et al.*, 2014), se definieron dos tipos de secado convectivo. El secado convectivo a baja temperatura, el cual se realizó a temperaturas iguales o inferiores a la temperatura estándar ( $20, 10, 0$  y  $-10\text{ }^\circ\text{C}$ ) y el secado convectivo a alta temperatura, es decir, a temperaturas superiores a la temperatura estándar establecida ( $30, 40, 50, 60, 70$  y  $105\text{ }^\circ\text{C}$ ).

### **3.5.1 Secado convectivo a baja temperatura**

El equipo de secado utilizado en este trabajo (Sección 2.1, Figura 1) consistía en un secadero convectivo a escala de laboratorio con control de temperatura y velocidad del aire (García-Pérez *et al.*, 2012). Estaba formado por una cámara de secado constituida por un cilindro portamuestras de aluminio (diámetro interno 10 cm, altura 31 cm y espesor 1 cm), dentro del cual se colocaban las muestras cilíndricas de hígado descritas anteriormente en el apartado 3.2.2. Durante las experiencias de secado, el portamuestras era pesado automáticamente a intervalos de tiempo preestablecidos mediante una balanza conectada a un ordenador. Un ventilador centrífugo (COT-100, Soler & Palau, España) fue el encargado de impulsar el flujo de aire a través de la cámara de secado y la velocidad del aire se midió con un anemómetro ( $2 \pm 0.1$  m/s; 1468, Wilh. Lambrecht GmbH, Alemania). El flujo de aire fue controlado por un controlador lógico programable (PLC) (cFP-2220, National Instruments, EE. UU.) utilizando un algoritmo PID (proporcional-integral-derivado) y actuando sobre un variador de frecuencia (MX2, Omron, Japón). La temperatura del aire se logró mediante un intercambiador de calor y resistencias eléctricas. El flujo de aire se enfriaba a su paso por el intercambiador de calor (área  $13 \text{ m}^2$ , espacio entre aletas 9 mm; Frimetal, España) que se conectaba a un equipo de refrigeración y posteriormente, las resistencias eléctricas calentaban para alcanzar la temperatura deseada. La humedad relativa del aire de secado se mantuvo por debajo del 15 %, pasando el flujo de aire a través de un lecho de material desecante (perlas de secado, tamaño de partícula de 6-8 mm, Rung Rueng Cosulting, Tailandia). Las bandejas se reemplazaban periódicamente por un nuevo material desecante regenerado en estufa a  $150 \text{ }^\circ\text{C}$  (ED 115, Binder GmbH, Alemania).

### **3.5.2 Secado convectivo a alta temperatura**

Los experimentos de secado a alta temperatura se llevaron a cabo a través de un secadero convectivo completamente automático y también utilizando una estufa convectiva.

### **3.5.2.1 Secado en secadero convectivo de aire caliente**

Los experimentos de secado a alta temperatura a temperaturas de 30, 40, 50, 60 y 70 °C se realizaron en un secadero convectivo a escala de laboratorio con control de temperatura y velocidad del aire (García-Pérez *et al.*, 2011) (Sección 2.1, Figura 1). Estaba formado por en una cámara de secado compuesta por un cilindro de aluminio (diámetro interno 10 cm, altura 31 cm y espesor 1 cm), donde se ubicaba el portamuestras, en el cual se colocaban las 20 muestras cilíndricas descritas en el apartado 3.2.2. La instalación de calefacción del secadero constaba de un sistema de ventilación, que disponía de un ventilador centrífugo de media presión (COT-100, Soler & Palau, Barcelona, España) que impulsaba el aire al interior de la cámara de secado, a través de las resistencias eléctricas. La velocidad del aire ( $2 \pm 0.1$  m/s) se midió con un anemómetro de rueda alada (Wilh, Lambrecht GmbH, Göttingen, Alemania). El peso de la muestra se midió y registró de forma automática regularmente a través de una balanza conectada a un ordenador.

### **3.5.2.2 Secado en estufa convectiva de aire caliente**

Los experimentos de secado con el objetivo de realizar un tratamiento posterior (desgrasado o desodorizado), se realizaron a temperatura moderada-baja (40 °C), moderada-alta (70 °C) y alta (105 °C), utilizando un horno convectivo (FD 56, Binder, Alemania) con una velocidad de aire de 1.3 m/s (Sección 2.2 y 3.1, Figura 1). Así, 8 muestras de hígado de cerdo cilíndricas, obtenidas tal y como se describe en el apartado 3.2.2, se colocaron en un crisol de porcelana, que se pesó cada 15 min.

Todos los experimentos de secado se realizaron por triplicado y se completaron cuando las muestras perdieron el 70 % del peso inicial. Posteriormente, se molieron y se determinó el contenido final de humedad, con el objetivo de obtener una muestra representativa de cada experimento de secado. Finalmente, las muestras se envasaron al vacío en bolsas PA/PE de 200 x 300 (Sacoliva, Castellar del Vallès, Barcelona) y fueron almacenadas a  $4 \pm 2$  °C hasta su posterior análisis (actividad enzimática, propiedades fisicoquímicas y tecno-funcionales) y/o procesado (desgrasado y desodorizado).

### 3.5.3 Modelado de la cinética de secado

Para la descripción matemática de las cinéticas de secado de hígado de cerdo se utilizó el modelo empírico de Weibull (Ecuación 4, Cunha *et al.*, 1998).

$$W_t = W_e + (W_0 - W_e) \cdot \exp\left[-\left(\frac{t}{\beta}\right)^\alpha\right] \quad (\text{Ecuación 4})$$

Donde  $W_t$  es el contenido de humedad medio en el tiempo  $t$  (kg agua/kg materia seca),  $W_e$  es el contenido de humedad de equilibrio (kg agua/kg materia seca) y  $W_0$  es el contenido de humedad inicial (kg agua/kg materia seca),  $t$  es el tiempo (s) y  $\beta$  (s) y  $\alpha$  son los parámetros cinéticos y de forma del modelo, respectivamente.  $W_e$  fue estimada a partir de los datos de equilibrio obtenidos por Sánchez-Torres *et al.* (2021).

Cuando el valor de  $\alpha$  es igual a 1, el modelo representa una cinética de primer orden, con una velocidad de pérdida de agua constante. Cuando  $\alpha > 1$ , la velocidad de reacción del modelo de Weibull aumenta en función del tiempo y decrece cuando  $\alpha < 1$  (Marabi *et al.*, 2003). El modelo de Weibull (Ecuación 4) se ajustó a los datos experimentales identificando los parámetros cinéticos y de forma ( $\beta$  y  $\alpha$ ) mediante un procedimiento de optimización que minimiza la suma de las diferencias al cuadrado entre los contenidos de humedad experimentales y calculados de las muestras. Para ello se utilizó el algoritmo de optimización no lineal del Gradiente Reducido Generalizado (GRG), disponible en la hoja de cálculo Microsoft Excel™ de MS Office 2019 (García-Pérez, 2007). Se determinó el porcentaje de error cuadrático medio (%MRE, Ecuación 5) y la varianza explicada (%VAR, Ecuación 6) para evaluar la bondad de ajuste del modelo.

$$\%MRE = \frac{100}{N} \left[ \sum_{i=1}^N \frac{|W_{\text{exp}} - W_{\text{cal}}|}{W_{\text{exp}}} \right] \quad (\text{Ecuación 5})$$

$$\%VAR = \left[ 1 - \frac{S_{xy}^2}{S_y^2} \right] \cdot 100 \quad (\text{Ecuación 6})$$



Donde  $W_{\text{exp}}$  y  $W_{\text{cal}}$  son la humedad media experimental y estimada, respectivamente;  $N$  es el número de datos experimentales y  $S_{xy}$  y  $S_y$  son las desviaciones estándar de la estimación y de la muestra, respectivamente.

### 3.6 Desgrasado de hígado de cerdo

Para el desgrasado del hígado de cerdo, una vez deshidratado a 40 °C o a 70 °C mediante el secado en estufa de convección, como se ha descrito anteriormente en el apartado 3.5.2.2, se utilizó el método estándar 991.36 (AOAC, 1996), basado en el uso de un equipo Soxhlet y un solvente orgánico (Sección 2.2, Figura 1). Para ello, se pesaron 3 g de hígado deshidratado y molido. Luego, las muestras se colocaron en un cartucho de papel filtro (material poroso). Posteriormente, la muestra se colocó en la cámara del extractor Soxhlet, que constaba de un matraz-balón (previamente desecado durante 1 h a 125 °C, para eliminar la humedad ambiental), la cámara del extractor Soxhlet (donde se insertó el cartucho), un condensador y un baño de agua a una temperatura superior de 70 °C (punto de ebullición del disolvente orgánico utilizado). En cada extractor se utilizaron 75 mL de disolvente orgánico, éter de petróleo ( $C_6H_6$ ). Así, el disolvente calentado, situado en el matraz-balón sumergido en el baño de agua se evaporaba llegando al condensador y caía sobre el cartucho de muestra, extrayéndose la grasa. El disolvente condensado volvió al matraz de ebullición y el proceso se llevó a cabo de forma continua durante 5 h. Posteriormente, los balones que contenían la grasa disuelta en el disolvente orgánico se rotoevaporaron para separar el solvente de la grasa. Para eliminar el disolvente del hígado deshidratado una vez desgrasado, los cartuchos se colocaron en una estufa de vacío a 70 °C durante 4 h. Posteriormente, se extrajo del cartucho el hígado de cerdo deshidratado-desgrasado y luego, las réplicas de cada temperatura se molieron y mezclaron con el objetivo de obtener muestras representativas para realizar los análisis fisicoquímicos y tecno-funcionales.

Los experimentos de desgrasado se realizaron por triplicado a ambas temperaturas de secado (40 y 70 °C). Finalmente, las muestras se envasaron al vacío en bolsas de PA/PE y fueron almacenadas en refrigeración a 4 °C hasta su caracterización.

### **3.7 Desodorización de hígado de cerdo**

Una vez llevado a cabo el proceso de deshidratación de los hígados de cerdo a 105 °C detallado en el apartado 3.5.2.2, se trituraron y homogeneizaron las muestras para realizar el tratamiento de desodorización, de eliminación de compuestos orgánicos volátiles (COVs) del hígado de cerdo deshidratado. El proceso se llevó a cabo mediante dos técnicas diferentes: arrastre por vapor con aplicación de vacío (AVV) y la extracción con CO<sub>2</sub> supercrítico (CO<sub>2</sub>-SC) (Sección 3.1, Figura 1).

#### **3.7.1 Arrastre por vapor con aplicación de vacío**

Para llevar a cabo la desodorización mediante arrastre por vapor con aplicación de vacío (AVV), se utilizó el montaje experimental que se muestra en la Figura 3.

El balón de destilación (2, Figura 3), con 2 L de agua destilada, se colocó en el baño de agua (HB digital 115, IKA, Alemania) (1, Figura 3), el cual se mantuvo a 80 °C. El balón estaba unido a la columna de destilación (3, Figura 3) en la que se introdujeron 3 g de muestra de hígado de cerdo deshidratado, en cartuchos de papel de filtro. Así, el vapor generado del baño de agua a 80 °C ascendía por la columna pasando sobre la muestra con un caudal de 0.19 g/s. Posteriormente, el vapor de agua pasaba a un condensador (4, Figura 3), el cual estaba conectado a un equipo de frío (5, Figura 3) y a la bomba de vacío (MZ 2C, Vacuubrand, Alemania) (7, Figura 3) (0.07 mbar) que permitía una evaporación del agua a  $42 \pm 2$  °C. El condensado se recogió en el balón pequeño de destilación (6, Figura 3). Además, se utilizó una trampa de agua (8, Figura 3) para evitar que el vapor llegara a la bomba de vacío. Tras la operación, se midió el volumen de agua recogido durante el proceso de desodorización para conocer el vapor generado (alrededor de 1100-1200 mL).

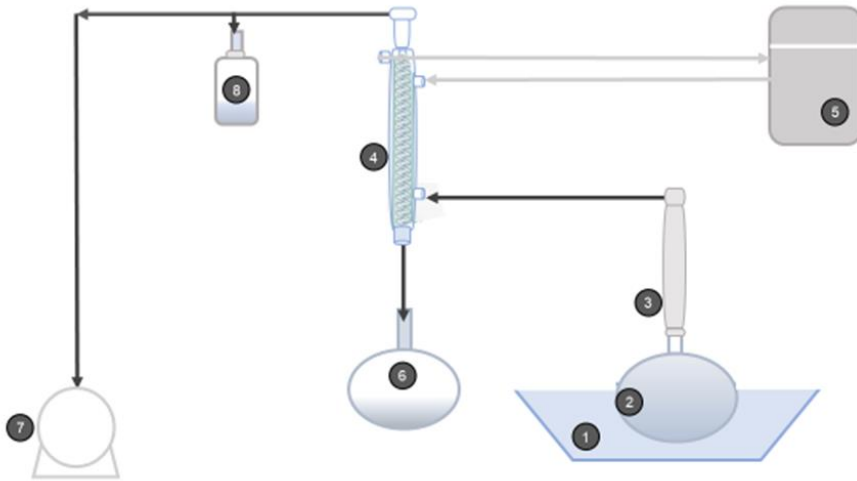


Figura 3. Esquema del sistema de arrastre por vapor con aplicación de vacío: 1- baño de agua; 2- balón de destilación; 3- columna de destilación; 4- condensador; 5- equipo de frío; 6- balón pequeño de destilación; 7- bomba de vacío; 8- trampa de agua.

El tiempo de desodorización se fijó en 90 minutos. La desodorización por AVV se realizó por triplicado. Posteriormente, las réplicas de hígado de cerdo deshidratadas y desodorizadas se extrajeron del cartucho de papel y se almacenaron congeladas (-20 °C) hasta su posterior análisis de COVs y composicional.

### 3.7.2 CO<sub>2</sub> supercrítico

Los tratamientos con CO<sub>2</sub> supercrítico (CO<sub>2</sub>-SC) para eliminar los COVs del hígado de cerdo deshidratado se realizaron con un equipo a escala de laboratorio (Figura 4). En primer lugar, se realizó un diseño experimental de tipo Box Behnken para la optimización de las condiciones de desodorización, se incluyeron las siguientes variables: presión (200, 325 y 450 bar), temperatura (35, 50 y 65 °C) y tiempo a aplicar (30, 60 y 90 min). El diseño involucró tres niveles para cada factor y tres repeticiones en el punto central (15 tratamientos experimentales). El caudal de CO<sub>2</sub> fue constante durante todas las experiencias, siendo de  $1 \pm 0.05$  kg CO<sub>2</sub>/h. En la Figura 4 se muestra el sistema, que constaba de un depósito (1, Figura 4) donde se introducía un recipiente de acero inoxidable (2, Figura 4) con 30 g de muestra (previamente deshidratada y

homogeneizada). El recipiente de acero inoxidable estaba compuesto de una superficie de rejillas y un filtro de papel a ambos lados del tanque, para evitar la pérdida de muestra y permitir la entrada y salida de CO<sub>2</sub> supercrítico, el cual se recirculaba de acuerdo a las condiciones de temperatura, presión y tiempo establecidas. El depósito que contenía el recipiente con la muestra a desodorizar se sumergió en un baño de agua termostático (3, Figura 4), para mantener la temperatura del proceso. También el sistema constaba de un tanque de CO<sub>2</sub> (5, Figura 4), un tanque de enfriamiento de CO<sub>2</sub> a -18 °C (6, Figura 4) y una bomba dosificadora de diafragma (LDB, LEWA, Tokio, Japón) para lograr la presión deseada en el recipiente de desodorización (7, Figura 4). Además, se dotó al sistema de un tanque separador (4, Figura 4) en el que se introdujeron 90 g de carbón activo para absorber los compuestos volátiles de la muestra a desodorizar (Pui *et al.*, 2019). Para medir la temperatura y presión de la muestra durante todo el proceso, se instaló un manómetro y un termopar tipo K en el interior del recipiente (8, Figura 4).

El CO<sub>2</sub> fue bombeado desde el tanque de enfriamiento (6, Figura 4) al recipiente de desodorización (1, Figura 4), donde se ubicó la muestra a desodorizar, pasando del estado líquido al supercrítico. El CO<sub>2</sub> supercrítico se convirtió en vapor y pasó por el tanque separador con carbón activo (4, Figura 4), un compuesto que retuvo los COVs de la muestra de hígado. El CO<sub>2</sub> se convirtió en líquido al pasarlo por el depósito de enfriamiento (6, Figura 4) y recircularlo. Posteriormente, las muestras de hígado de cerdo deshidratado-desodorizado fueron extraídas del contenedor de acero inoxidable y almacenadas congeladas (-20 °C) hasta su análisis de COVs y composicional.

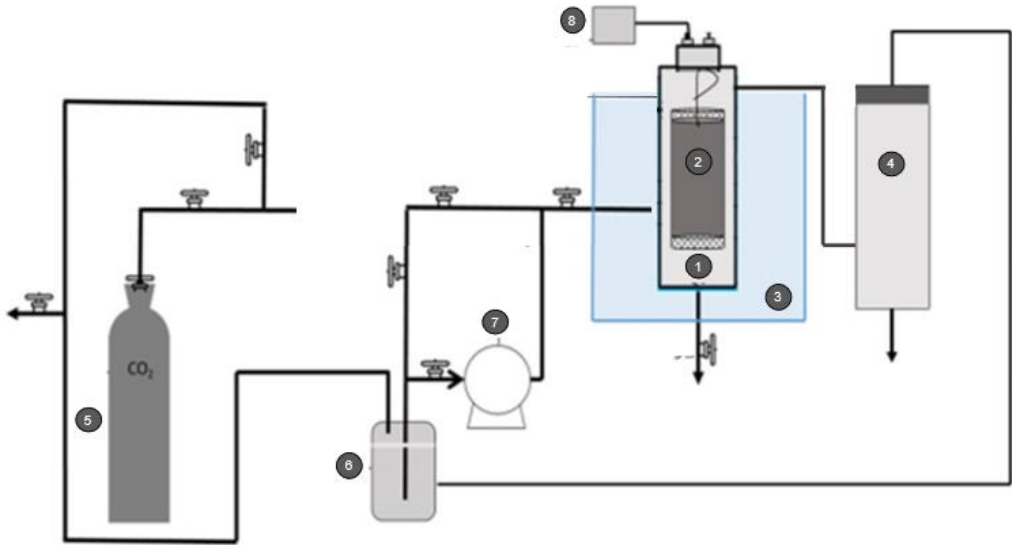


Figura 4. Esquema del equipo de CO<sub>2</sub> supercrítico. 1- recipiente, 2- tanque de acero inoxidable con muestra, 3- baño termostático, 4- tanque separador con carbón activo, 5- Tanque de CO<sub>2</sub>, 6- tanque de enfriamiento, 7-bomba, 8-grupo de generación de energía.

### 3.8 Análisis de compuestos orgánicos volátiles

Para el análisis de compuestos orgánicos volátiles (COVs) se siguió la metodología previamente descrita por Domínguez *et al.* (2019b), consistente en una micro-extracción en fase sólida con espacio de cabeza (HS-SPME), acoplada a cromatografía de gases (GC) y detección por espectrómetro de masas (MS) (HS-SPME-GC/MS) (Sección 3.1, Figura 1).

Para el HS-SPME se utilizó fibra de sílice fundida de 10 mm de largo recubierta con una capa de divinilbenceno, carboxeno y polidimetilsiloxano de 50/30 mm de espesor (Supelco, Bellefonte, PA, EEUU). Antes de realizar el análisis, la fibra se acondicionó con calor a 270 °C durante 30 minutos. Para realizar la extracción se introdujeron  $1 \pm 0.02$  g en viales de 20 mL (Agilent Technologies, Santa Clara, CA, EE.

UU.) y se enroscaron con un disco de goma laminada de teflón. Las muestras se equilibraron durante 15 min a 37 °C para garantizar una temperatura y un espacio de cabeza homogéneos. Luego, las extracciones se realizaron a 37 °C durante 30 min.

Una vez finalizada la extracción, la fibra se transfirió a la zona de inyección del sistema formado por el cromatógrafo de gases y el espectrómetro de masas (GC-MS). La fibra HS-SPME fue desorbida y mantenida en el sitio de inyección (modo sin división y una presión de helio de 9.59 psi) a 260 °C durante 8 minutos. Después de cada inyección, la fibra se lavó y acondicionó a 270 °C durante 2 min para asegurar que estuviera limpia antes de la siguiente extracción. Se utilizó helio como gas portador con un caudal constante de 1.2 mL/min (9.59 psi). La columna que se utilizó para la separación de los componentes volátiles fue una columna capilar DB-624 de 30 m de largo, 250 µm de ancho y 1.4 µm de espesor de película (J&W Scientific, Folsom, CA, EE. UU.). Se realizó un precalentamiento para alcanzar una temperatura isotérmica de 40 °C durante 10 min, seguido de un primer calentamiento donde la temperatura subió hasta 200 °C a 5 °C/min. Finalmente, se realizó un segundo calentamiento donde la temperatura subió hasta 250 °C a 20 °C/min, la cual se mantuvo durante 5 min. El análisis duró 49.5 min.

En cuanto a las condiciones del MS, la línea de transferencia se mantuvo a 260 °C. La fuente de iones utilizada fue The Extraction Source Xtr EI 350 (Agilent Technologies, Santa Clara, CA, EEUU). El espectro de masas se obtuvo utilizando el detector de masas selectivo 5977B trabajando con una energía electrónica de 70 eV, con un voltaje multiplicador de electrones de alrededor de 900 V (factor de ganancia = 1) y obteniendo 2.9 scans/s en el rango m/z 40–550 en el modo de adquisición de escaneo. La fuente de masas se mantuvo a 230 °C mientras que el cuadrupolo de masas se ajustó a 150 °C.

Tras el análisis cromatográfico, todos los datos obtenidos se estudiaron con el software MassHunter Quantitative Analysis B.07.01. Se realizó una comparación de estos con información bibliográfica. La integración de las áreas de los picos se realizó con el algoritmo Agile2a, mientras que el pico de detección se obtuvo por deconvolución. Los compuestos se identificaron comparando los espectros de masas

obtenidos con los publicados en la base de datos NIST14. Los compuestos se consideraron correctamente identificados cuando tenían un factor de concordancia superior al 85 %.

A partir de los cromatogramas se determinó la cantidad de cada compuesto por el área de sus picos, los cuales se expresaron en unidades de área (UA). Para calcular el porcentaje de COVs para las diferentes familias de compuestos químicos, se calculó la relación entre las UA de cada familia de COVs y el área total (suma de las UA de todos los COVs detectados) para cada una de las muestras analizadas. Mientras que para calcular cómo afecta la desodorización al contenido de COVs, la pérdida (% UA) para cada familia de COVs se calculó como la relación entre las UA de cada familia de compuestos químicos de las muestras desodorizadas (AVV y CO<sub>2</sub>-SC) y las UA del hígado de cerdo deshidratado.

### **3.9 Características fisicoquímicas**

#### **3.9.1 Composición química**

Se utilizaron métodos estándar para analizar la composición química del hígado de cerdo deshidratado, deshidratado-desgrasado (Sección 2.2, Figura 1) y deshidratado-desodorizado mediante AVV y CO<sub>2</sub>-SC (Sección 3.1, Figura 1). Cada muestra se analizó por triplicado. Los contenidos de humedad, ceniza, proteína y grasa se determinaron siguiendo los procedimientos de la Asociación de Químicos Analíticos Oficiales (AOAC, 2000). Los contenidos de humedad y ceniza se determinaron gravimétricamente utilizando un horno de aire caliente y un horno de mufla, respectivamente. El contenido de proteínas se estimó a partir del nitrógeno Kjeldahl total (TKN x 6.25) utilizando un sistema de digestión Gerhardt KB20 (C. Gerhardt GmbH & Co. KG, Königswinter, Alemania) y una unidad de destilación Büchi K-314 (Büchi Labortechnik AG, Flawil, Suiza). El contenido de grasa total se determinó gravimétricamente por extracción Soxhlet con éter dietílico.

### 3.9.2 Medida de color

El color de las muestras de hígado deshidratado y deshidratado-desgrasado se midió determinando los parámetros de color CIE  $L^*$ ,  $a^*$  y  $b^*$ , representando  $L^*$  la luminosidad en una escala de 0 (oscuro) a 100 (blanco);  $a^*$  el contenido rojo/verde; y  $b^*$  el contenido amarillo/azul, utilizando un Minolta Chroma Meter CR-300 con un tubo de proyección de luz de vidrio CR-A33f (Minolta Co, Ltd., Osaka, Japón) (Sección 2.2, Figura 1). Las medidas se realizaron utilizando iluminación difusa, una fuente de luz D65 y un observador estándar de 2°. El colorímetro había sido calibrado utilizando una placa de cerámica blanca estándar ( $L^*=97.15$ ,  $a^*=-5.28$  y  $b^*=+7.82$ ). El color de cada muestra se midió por triplicado. Las coordenadas angulares de Cromo ( $C^*$ ) y el ángulo Hue, de tonalidad ( $H^\circ$ ) se calcularon de acuerdo con la Ecuación 7 y la Ecuación 8, respectivamente.

$$C^* = \sqrt{(a^{*2} + b^{*2})} \quad (\text{Ecuación 7})$$

$$H^\circ = \tan^{-1} \left( \frac{b^*}{a^*} \right) \quad (\text{Ecuación 8})$$

### 3.9.3 Análisis de calorimetría diferencial de barrido

Los análisis de calorimetría diferencial de barrido (DSC) de las muestras se realizaron en un calorímetro DSC Q 2000 (TA Instruments, New Castle, Delaware, Estados Unidos), bajo un programa de calentamiento de 20 a 100 °C y a una velocidad de calentamiento de 3 °C/min (Sección 2.2, Figura 1). Se analizaron soluciones de muestras de hígado deshidratado y deshidratado-desgrasado reconstituido al mismo porcentaje de proteína (p/v) que el hígado de cerdo fresco (19.20 %). A partir de los termogramas DSC (curva de flujo de calor en función de la temperatura), se calculó por integración el área de los picos de transición endotérmica y, utilizando una línea base recta, se calculó la variación de la entalpía de transición global de la desnaturalización de la proteína ( $\Delta H$ , J/g muestra). También se obtuvo la temperatura inicial del pico endotérmico ( $T_i$ ) y las temperaturas de desnaturalización ( $T_{d1}$  y  $T_{d2}$ ),



considerando que se corresponden a las temperaturas a las que se registraron en los termogramas el mínimo de los dos principales picos endotérmicos de desnaturalización. Para la determinación de los diferentes parámetros, se utilizó el software “Universal Analysis” de TA Instruments.

### **3.10 Propiedades tecno-funcionales.**

#### **3.10.1 Solubilidad de proteínas**

La solubilidad de la proteína de muestras de hígado de cerdo deshidratado y deshidratado-desgrasado se analizó mediante el método descrito por Morr *et al.* (1985) con ligeras modificaciones (Sección 2.2, Figura 1). Se diluyó 1 g de muestras de hígado de cerdo molido, en agua destilada (100 mL). Las soluciones se agitaron durante 30 min en una placa de agitación magnética, evitando la formación de vórtices. Después de agitar, se centrifugaron alícuotas de las soluciones a 20000 × g durante 30 min a 20 °C (Sorvall RC-SC plus, DuPont Co., Newtown, CT, EE. UU.) y se decantaron. La solubilidad de la proteína se calculó como el porcentaje del contenido de proteína soluble en el sobrenadante en relación con el contenido de proteína total de las muestras de hígado deshidratado y deshidratado-desgrasado. Ambos contenidos de proteína se determinaron por el método Kjeldahl AOAC 954.01 (AOAC, 2000). Cada determinación se realizó por duplicado para cada condición estudiada.

#### **3.10.2 Propiedades espumantes**

Las propiedades espumantes se determinaron como se describe en Toldrà *et al.* (2019) (Sección 2.2, Figura 1). Se prepararon tres alícuotas de 200 mL de soluciones deshidratadas de proteína hepática (5 g/L) de cada muestra en agua destilada y luego se transfirieron a matraces volumétricos de 1000 mL. Las soluciones se batieron en un mezclador Braun Multimix M700 (Braun Española S.A., Barcelona, España) con dos batidores ( $\varnothing = 5$  cm) a 1000 rpm durante 10 min. Durante la mezcla, los matraces se colocaron en un plato giratorio para formar espumas homogéneas. Posteriormente, se determinó la capacidad espumante como el volumen (mL) de espuma después de 2 min en reposo. La estabilidad de la espuma se determinó utilizando un método gravimétrico de la siguiente manera: las cantidades medidas de

espuma se colocaron cuidadosamente en tres tamices secos de acero inoxidable para permitir que el líquido liberado se drenara, y la espuma restante se pesó cada 10 min durante un período de 60 min. Se trazó el porcentaje de espuma restante frente al tiempo y se calculó la estabilidad relativa de la espuma (RFS), definida como el tiempo (min) necesario para la desaparición del 50 % de la espuma inicial, ajustando los datos a una función de disminución exponencial utilizando la Ecuación 9.

$$y = B_0 \cdot \exp -(B_1 \cdot t) \quad (\text{Ecuación 9})$$

Donde  $y$  es el porcentaje de estabilidad de la espuma,  $B_0$  es el porcentaje de espuma inicial,  $t$  es el tiempo (min) y  $B_1$  la velocidad de desaparición de la espuma. Las medidas se realizaron por triplicado.

### 3.10.3 Propiedades emulsionantes

Las propiedades emulsionantes se determinaron según el método turbidimétrico descrito por Pearce y Kinsella (1978) y ligeramente modificado por Parés y Ledward (2001) (Sección 2.2, Figura 1). Con el objetivo de determinar las propiedades emulsionantes de las muestras de hígado deshidratado y deshidratado-desgrasado, se prepararon soluciones de 5 g/L (p/v) de proteína procedente de las muestras a estudiar. Posteriormente, se homogeneizaron 150 mL de solución de proteína de hígado junto con 50 mL de aceite de maíz comercial usando un homogeneizador de laboratorio (MFC Microfluidizer™ Series 5000, Microfluidics Corporation, Newton, MA, EE. UU.) a 12 MPa, que proporcionaba un caudal de salida de 40 L/h, durante 90 s, con recirculación. La temperatura se mantuvo a 20 °C. Las preparaciones se realizaron por triplicado para cada muestra. Las emulsiones se diluyeron 2500 veces con dodecilsulfato de sodio (SDS) al 0.1 %, inmediatamente después de la homogeneización ( $t=0$ ) y después de 10 min de reposo de la emulsión ( $t=10$ ). A continuación, se determinó la absorbancia de las emulsiones diluidas a 500 nm en un espectrofotómetro Cecil CE 7400 (Cecil Instruments Ltd., Cambridge, Inglaterra). Cada determinación se realizó por duplicado. Los resultados se expresaron como índice de actividad emulsionante (IAE) e índice de estabilidad de la emulsión (IEE). El IAE ( $\text{m}^2 \cdot \text{g}^{-1}$  de proteína) y el IEE (min) se calcularon mediante la Ecuación 10

y la Ecuación 11, respectivamente.

$$IAE = \frac{2 \cdot T}{\phi \cdot C} \quad (\text{Ecuación 10})$$

$$IEE = \frac{T \times \Delta t}{\Delta T} \quad (\text{Ecuación 11})$$

Donde T es la turbidez,  $\phi$  es la fracción de volumen de la fase dispersa (calculada como el volumen de la fase oleosa dividido por el volumen total de la emulsión), C es el peso de proteína por unidad de volumen de la fase acuosa antes de que se forme la emulsión, y  $\Delta T$  es el cambio en la turbidez (T) que ocurre durante el intervalo  $\Delta t$  (10 min).

### 3.11 Análisis estadístico

Los análisis estadísticos se realizaron con Statgraphics Centurion XVI (Statpoint Technologies Inc., Warrenton, VA, EE. UU.). Se empleó un ANOVA multifactorial para evaluar el efecto de las condiciones de extracción sobre el rendimiento de obtención de la enzima FeQ (Sección 1.1, Capítulo 1). La variable de respuesta o dependiente estudiada fue la concentración de ZnPP, mientras que los factores o variables independientes fueron el tiempo de reacción y el modo de extracción (convencional, US continuo y US pulsado). En la Sección 1.2, Capítulo 1, formación de ZnPP a partir de diferentes homogeneizados de hígado, se realizó un ANOVA multifactorial para examinar el efecto del medio de reacción (con antibióticos y con ácidos orgánicos) y el tiempo de reacción, sobre la concentración de ZnPP. Además, se utilizó un ANOVA de una vía para determinar si el modo de extracción (US o convencional), tuvo un efecto significativo en la concentración de ZnPP de cada homogeneizado (Hhc y Hhc+OxiHb).

En el Capítulo 2, se utilizó un ANOVA para evaluar la influencia de la temperatura de secado sobre la concentración de FeQ aparente y su actividad enzimática, así como sobre los parámetros del modelo de Weibull identificados.

Asimismo, a partir de un ANOVA se analizó la influencia de la temperatura de secado y el proceso de secado-desgrasado, sobre las características fisicoquímicas y tecno-funcionales del hígado procesado.

En el Capítulo 3 para estudiar la influencia de la temperatura, la presión y el tiempo en la eliminación o reducción de los COVs utilizando CO<sub>2</sub>-SC se empleó un diseño de superficie de respuesta (Box-Behnken). Además, para evaluar la importancia de las diferencias en la cantidad de COVs entre las diferentes muestras (hígado de cerdo fresco, deshidratado y deshidratado-desodorizado mediante AVV y CO<sub>2</sub>-SC) y en la composición entre las muestras deshidratadas y deshidratadas-desodorizadas mediante AVV y CO<sub>2</sub>-SC, se realizó un ANOVA.

Para todos los casos estudiados, englobados en los tres capítulos, las diferencias entre las medias se compararon mediante los intervalos LSD (Least Significant Difference) y se consideró un nivel de significación del 95 % ( $p < 0.05$ ).



## **4. RESULTADOS Y DISCUSIÓN**



# **CAPÍTULO 1**

*Aplicación de ultrasonidos para mejorar  
la formación del pigmento zinc  
protoporfirina a partir de hígado de  
cerdo como fuente de ferroquelatasa*





Ultrasonics Sonochemistry 78, (2021) - 105703

*Ultrasound intensification of Ferrochelatase extraction from pork liver as a strategy to improve ZINC-protoporphyrin formation*

---

Blanca Abril<sup>1</sup>, Eduardo A. Sánchez Torres<sup>1</sup>, Ricard Bou<sup>2</sup>, José Vicente García-Pérez<sup>1</sup> and José Benedito<sup>1</sup>

<sup>1</sup>Department of Food Technology, Universitat Politècnica de València, Camí de Vera, s/n, Valencia 46022, Spain

<sup>2</sup>IRTA, XaRTA, Food Technology, Finca Camps i Armet, Monells, Girona E-17121, Spain



## **Ultrasound intensification of Ferrochelatase extraction from pork liver as a strategy to improve ZINC-protoporphyrin formation**

### **Abstract**

The enzyme Ferrochelatase (FeCH), which is naturally present in pork liver, catalyses the formation of Zinc-protoporphyrin (ZnPP), a natural pigment responsible for the typical color of dry-cured Italian Parma ham. The aim of this study was to evaluate the feasibility of using high power ultrasound in continuous and pulsed modes to intensify the extraction of the enzyme FeCH from pork liver. US application during FeCH extraction led to an improved enzymatic activity and further increase in the formation of ZnPP. The optimal condition tested was that of 1 min in continuous US application, in which time the enzymatic activity increased by 33.3 % compared to conventional extraction (30 min). Pulsed US application required 5 min treatments to observe a significant intensification effect. Therefore, ultrasound is a potentially feasible technique as it increases the catalytic activity of FeCH and saves time compared to the conventional extraction method.

**Keywords:** Liver; ferrochelatase; zinc-protoporphyrin; colorant; ultrasound

## 1. Introduction

Nowadays, the pork industry is facing relevant challenges. Firstly, one of the most significant ones is linked to the large environmental load of animal protein production, which leads to the search for new protein sources with which to complement or replace meat products in the diet (Abbasi & Abassi, 2016). Secondly, the large amount of co-products and by-products generated in the pork industry are of low commercial value and represent a high impact in terms of waste treatment. However, some of these products, such as pork liver, possess high potential from a nutritional and technological point of view (Mackenzie *et al.*, 2016). Finally, another relevant issue that affects the cured meat industry is the use of nitrifying agents (E249, E250, E251 and E252), which have a threefold purpose: to achieve the characteristic color in dry-cured meat products due to the formation of nitrosomyoglobin, to inhibit pathogen microorganisms, especially *Clostridium botulinum*, and to enhance the flavour (Armenteros *et al.*, 2012). Nitrites are responsible for all of these functions, while nitrates can be a source of nitrite through the action of nitrate reductase. However, the use of these chemicals may be controversial because nitrites are precursors of the formation of methemoglobin and nitrosamines, recognized toxic substances (Walker, 1990). In Italian Parma ham manufacturing, the use of nitrates and nitrites is not allowed and microbial safety is ensured by an extended, 12-month minimum, manufacturing process. Thereby, the typical color of Parma ham is formed without adding nitrates and nitrites due to the formation of Zinc-protoporphyrin IX (ZnPP) which has a characteristic reddish color (Wakamatsu *et al.*, 2004a). There is evidence of ZnPP formation under anaerobic conditions and in the presence of endogenous microorganisms and meat enzymes in pork loin (Wakamatsu *et al.*, 2004b). Laursen *et al.* (2008) and Moller *et al.* (2007) also reported the presence of ZnPP in dry-cured Iberian and Parma ham. Wakamatsu *et al.* (2007) reported that the formation of ZnPP did not take place via the substitution of zinc in the heme group, but via the insertion of this atom into independently-formed Protoporphyrin IX. Therefore, it has to be considered that the formation of ZnPP is strongly influenced by the endogenous formation of Protoporphyrin IX. Benedini *et al.* (2009) found that fresh meat contains an enzyme, Ferroquelatase (FeCH), which promotes the formation of ZnPP in the presence of zinc and Protoporphyrin IX substrates at an optimum pH of 8. FeCH is a protein located in

the mitochondria, associated with the inner mitochondrial membrane in meat, which is highly resistant since it remains unaltered during dry-cured ham manufacturing. It has an optimum pH and temperature of 7.5-8 and 37-40 °C, respectively.

Pork liver is a co-product of the meat industry with a low market value, whose use has been limited to liver paste products and feed due to a lack of knowledge about its nutritional and technological functionality (Steen *et al.*, 2016). The liver, in addition to being a good source of protein, has a large number of enzymes and other valuable compounds that could be exploited industrially. Liver protein has special uses as a foaming agent and as a functional ingredient for the supply of nutrients in food (Zou *et al.*, 2018). Due to the high concentration of FeCH in the pork liver, its extracts could be used to catalyse the formation of ZnPP from hemoglobin or, when added to meat products, as a way to promote the formation and stability of redness. Previous studies about FeCH extraction had a marked analytical and biochemistry character since they were designed to separate and purify the enzyme for analysing its activity. Thus, Taketani & Tokunaga (1981) and Taketani & Tokunaga (1982) addressed the extraction of FeCH in rat and bovine liver by differential centrifugation from the purified mitochondrial fraction and the homogenized liver, respectively. High FeCH concentrations in the extracts would facilitate not only the further purification steps, if necessary, but also its direct and effective application for in-vivo and in-vitro ZnPP formation. For this purpose, efficient extraction processes must be developed to optimize the release of the enzyme from the internal cellular structures of the liver without being damaged. To our knowledge, this is the first study dealing with the intensification of the extraction process for industrial purposes.

Power ultrasound (US) is a technology that is frequently used to intensify the extraction of natural products, and as a strategy to increase the process rate or to obtain higher yields (Chemat *et al.*, 2017). In a liquid medium, the main effect linked to ultrasound application is the implosion of cavitation bubbles, which are formed due to the cycles of compression and rarefaction that, at a certain frequency, are provoked by high intensity ultrasound waves (Feng *et al.*, 2011; Shukla, 1992). Cavitation is characterized by high local heat and mechanical energy release, leading to a temperature rise and great turbulence, which positively induce a more intense solvent

penetration, structural alteration and improved mass and heat transfer (Mason, 1998; Awad *et al.*, 2012). As for the extraction of the molecules that are tightly attached to the solid matrix, ultrasound improves the cellular lysis that will release the compounds of interest (Patist & Bates, 2008). Both the physical phenomena associated with ultrasound extraction, as well as its performance, are mostly dependent on the process conditions used. As for the optimization of ultrasonic systems, the frequency, intensity, treatment time, shape and size of the vibrating surface of the emitter and of the treatment chamber are all essential, due to their effect on the energy released into the medium. As to the medium-related parameters, the temperature, solvent properties (density, viscosity, air dissolved, etc.), solid/liquid ratio and the nature of the matrix being treated are also key factors in solid-liquid extraction (Chemat *et al.*, 2017). Power ultrasound represents an alternative to conventional enzyme extraction methods, since it could improve the yield and rate of the process (Vilkhu *et al.*, 2008; Goula, 2013; Barba *et al.*, 2015; Dolatowski *et al.*, 2007; Soria & Villamiel, 2010; Delgado-Povedano and De Castro, 2015; Medina-Torres *et al.*, 2017). US technology increased the extraction yield of the pectinase enzyme from the guava shell (*Psidium guajava*) by 96.2%, also improving the enzymatic characteristics of the extracts (Amid *et al.*, 2016). Szabo *et al.* (2015) showed that the application of US in the extraction of ligninolytic and hydrolytic enzymes increased enzymatic activity by 129-413%. However, when applied at high power and for prolonged exposure times, US is also able to cause the alteration of the enzyme structure that can lead to its deactivation (Bansode & Rathod, 2017). In this regard, the effect of US on the protein structure of duck liver was also reported by Xu *et al.* (2021). So far, no literature has addressed the intensification of the enzyme extraction process in meat products using US or the extraction of FeCH from pork liver. Therefore, the objective of this study was to evaluate the feasibility of using US to improve the extraction of the FeCH enzyme from pork liver.

## **2. Materials and methods**

### **2.1. Raw material and sample preparation**

The raw material used was pork livers from the slaughterhouse “Carnes de Teruel S.A.” (D.O. Jamón de Teruel, Spain). The pork livers were transported at a temperature of under 4 °C and processed in the lab in less than 2 h. The fresh livers were ground for homogenization (Blixer 2, Robot Coupe, Vincennes Cedex, France),

packaged (30 g portions) in vacuum bags (200 x 300 PA/PE, Sacoliva, Castellar del Vallès, Barcelona) and stored at -20 °C until used.

## 2.2. Ferrochelatase extraction

The process of Ferrochelatase extraction carried out was based on the procedure described by Parolari *et al.* (2009). Firstly, 4 g of the milled thawed (5 h, 20 °C) pork liver were homogenized (Homogenizer DI 25 Basic, IKA, Germany) with 100 mL of extraction buffer for 1 min at 4°C and 8000 rpm, avoiding foam formation, using a 200 mL glass beaker. The extraction buffer contained Tris-HCl 50 mM, Glycerol 20 % (w/v), KCl 0.8 % (w/v) and Triton X-100 1 % (w/v) (Sigma Aldrich), and was adjusted to pH=8 with NaOH. Conventional extraction (CV) was carried out using a magnetic stirrer (Magnetic Stirrer Hot Plate SM3, STUART, UK), the liver/solvent mixture was placed into a 100 mL glass beaker and extraction was conducted for 30 min. Temperature was kept at  $4 \pm 2$  °C to minimize enzyme thermal deactivation during extraction.

As an alternative to the conventional method, once the sample was homogenized, the enzymatic extraction was also performed with ultrasound (US) assistance using a probe-like device (UP400S, HIELSCHER, Germany) supplying the maximum power available (400 W) at a frequency of 24 kHz and using a sonotrode of 2.2 cm in diameter. The liver/solvent mixture was placed into a 300 mL glass jacketed beaker, using a volume of 50 mL of liver/solvent mixture and the tip of the ultrasonic sonotrode was immersed for 1 cm. US was applied for different times (1, 2.5 and 5 min) in continuous (100 % frequency) and pulsed (50 % frequency) operation modes. Pulsed (50 % frequency) US application consisted of on and off pulses of 0.5 s. In this case, temperature control was more critical than in the conventional mode because the cavitation generated by ultrasound could lead to a fast temperature rise. To avoid reaching high temperatures at which the enzyme would be inactivated, a glycol solution (20 %) was pumped (SUK-0220, Shurho, Mexico) at -20°C through the walls of the jacketed-beaker containing the extraction solution. The temperature was controlled by using a K-type thermocouple wired to a process controller (on/off control) (E5CN-R2MT-500, Omron, Japan), which acted on the pump to recirculate the glycol-solution. The control system allowed to keep the temperature at  $10 \pm 2$  °C. For each extraction



condition (CV and US continuous and pulsed), five replications were carried out.

In order to separate the enzyme fraction, the extraction solution was centrifuged for 10 min at 12500 rpm and 4 °C (Medifriger BL-S, SELECTA, Spain) and the supernatant was filtered (Whatman 597, GE LIFE SCIENCE, USA) to be used as the FeCH enzyme extract.

### **2.3. Zinc-protoporphyrin formation kinetics**

Following the experimental procedure developed by Parolari *et al.* (2009), the enzymatic reaction of ZnPP formation catalyzed by the FeCH was conducted in microtubes incubated at  $37\pm 0.5$  °C in a water bath. The reactants used were as follows: 250 µL of ZnSO<sub>4</sub> 400 µM in Tris-HCl buffer 360 mM, adjusted to pH=8.0, 50 µL of protoporphyrin IX 0.25 mM in Tris-HCl buffer 360 mM, adjusted to pH=7.0, 200 µL of ATP 25 mM in NaCl at 20 % (w/v), 35 µL of EDTA 50 mM and 300 µL of FeCH enzyme extract from pork liver. With these reagents, two different batches were prepared: samples and blanks. In the batch of blanks, 300 µL of the extraction buffer was added instead of an enzyme extract (no enzymatic reaction). The blank value was subtracted from that of each sample to correct any background fluorimetric signal from the reagents. Microtubes were incubated at different times (0, 15, 30, 45, 60, 90, 105 and 120 min) for the purposes of monitoring the reaction kinetics.

Zinc-protoporphyrin (ZnPP) was quantified as the product of the reaction due to its ability to emit fluorescence (unlike myoglobin and nitrosylmyoglobin) with excitation and emission peaks at around 420 nm and 590 nm, respectively (Wakamatsu *et al.*, 2007). Fluorescence measurements were taken with a 96-well plate fluorometer (Infinite 200 Microplate Reader, TECAN, Switzerland) adjusted to the previously mentioned range. Before ZnPP quantification, cold absolute ethanol (840 µL) was added to the microtubes and then centrifuged for 30 min at 13200 rpm and 4 °C (5415R, EPPENDORF, Germany).

In order to quantify the ZnPP concentration (µmol/L), a calibration curve was obtained. For that purpose, different dilutions (0 µmol/L - 18 µmol/L) were prepared from concentrated ZnPP (Sigma-Aldrich) using the extraction buffer as dilution medium. The calibration curve ( $r^2=0.995$ ) is shown by Equation 1.

$$\text{ZnPP} = \frac{F - 1451}{6502} \quad (\text{Equation 1})$$

Where F is fluorescence (RFU) and ZnPP is the concentration of the product formed ( $\mu\text{mol/L}$ )

From the increase in the amount of ZnPP, the reaction rate was calculated as the product formation velocity ( $r$ ) ( $\mu\text{mol of ZnPP/ L x min}$ ) (Fersht, 1984). As shown in Equation 2, the velocity at which ZnPP is formed can be defined as the amount of product formed per unit of time.

$$r = \frac{dP}{dt} \quad (\text{Equation 2})$$

Where P is the ZnPP concentration ( $\mu\text{mol / L}$ ) and  $t$  is the time ( $\text{min}$ ).

With the aim of comparing the experimental results obtained with other studies, the reaction rate values can also be expressed as specific enzymatic activity (SEA,  $\text{nmol of ZnPP / g dry matter x min}$ ) by considering the mass of liver used for each extraction.

#### 2.4. Ultrasonic field characterization

In order to characterize the acoustic intensity applied to the solution, the calorimetric method was used (Cárcel et al., 2007). For this purpose, the temperature was measured with a type K thermocouple located in the center of the extraction beaker and recorded with an Agilent 34970A Data Acquisition/Switch Unit (4970 A, Hewlett-Packard Española, S. A., Madrid, Spain). Temperature data were transferred to a computer using proprietary software (Agilent BenchLink Data Logger 3).

The calorimetric measurement was taken in continuous mode (100 % cycle) and in pulsed mode (50% cycle). The experiments involved the measurement of temperature every 0.2 s for the first 2 min of US application. Equation 3 was used to determine the ultrasonic power.

$$P = M C_p \frac{dT}{dt} \quad (\text{Equation 3})$$

Where P (W) is the ultrasonic power, M (kg) the mass of the solution, Cp (J/Kg °C) the heat capacity (Cp of water was considered) and dT/dt the rate of temperature increase. The ultrasonic power was measured 5 times for every US mode tested

## 2.5. Statistical analysis

The influence of the extraction conditions was statistically evaluated by analysis of variance (multifactorial ANOVA) and the differences between the averages were compared by the LSD (Least Significant Difference) intervals. In every case, a significance level of 95 % ( $p < 0.05$ ) was considered. The response, or dependent, variable studied was ZnPP concentration, while the factors, or independent variables, were the reaction time and the extraction mode (conventional, continuous-ultrasound and pulsed-ultrasound). The analysis was performed by using Centurion XVI software (Statpoint Technologies Inc., Warrenton, VA, USA).

## 3. Results and discussion

### 3.1. Conventional FeCH extraction

Regardless of the procedure used for the FeCH extraction (conventional, CV or ultrasound-assisted, US), the ZnPP formation kinetics showed the same pattern (Figures 1 and 2). A linear, steady phase was preceded by an initial, burst phase. This initial phase is shown by a y-intercept of the linear relationship that is significantly ( $p < 0.05$ ) different from zero (Figure 1). The burst phase indicates an initial stage in the enzyme reaction at a very high rate, which is related to the first turnover of the active sites (Praestgaard *et al.*, 2011). Afterwards, the enzyme reaction enters the steady state phase in which a constant reaction rate is manifested, coinciding with the slope of the linear relationship (Figure 1). Thereby, and according to the Michaelis–Menten model, the slope of the linear fit for the steady state phase is proportional to the active enzyme concentration (E) and the product release rate constant ( $K_2$ ), while the y-intercept is only proportional to the active enzyme concentration (Sassa *et al.*, 2013). The extension of the initial burst phase ranged between 0 and 15 min, but it cannot be precisely assessed from the present experiments since the initial sampling time was 15

min. According to previous literature, the burst phase only generally covers the first seconds of the enzymatic reaction (Johnson, 2013); for this reason, its experimental assessment is, in many cases, extremely complex, and is not this study's aim. To our knowledge, previous literature has not identified the burst phase in ZnPP formation catalyzed by FeCH, since reaction rates have been computed at a single specific time, when the reaction is stopped, without analyzing the kinetic evolution. Thus, Taketani & Tokunaga (1982) reported that the Zn metal bound to protoporphyrin in the presence of bovine liver FeCH followed a Michaelis-Menten model illustrating the influence of the limiting substrate on the reaction rate, although no data is provided about the formation of ZnPP kinetics (ZnPP calculated at 30 min reaction).

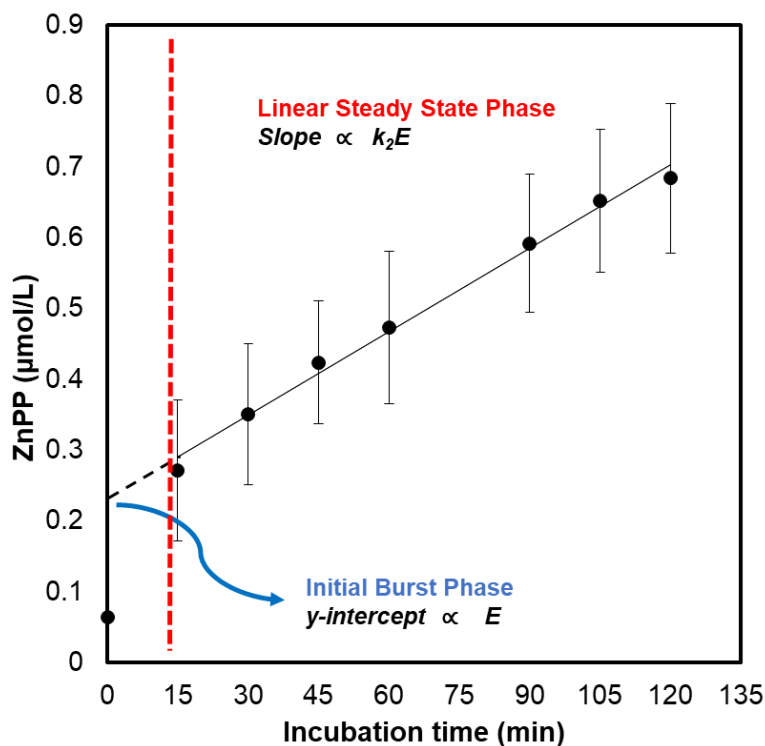


Figure 1. Kinetics of ZnPP formation using a FeCH extract from pork liver obtained by conventional extraction (CV, 30 min magnetic stirring). Average values  $\pm$  standard deviation are shown for each experimental time ( $t$ ).

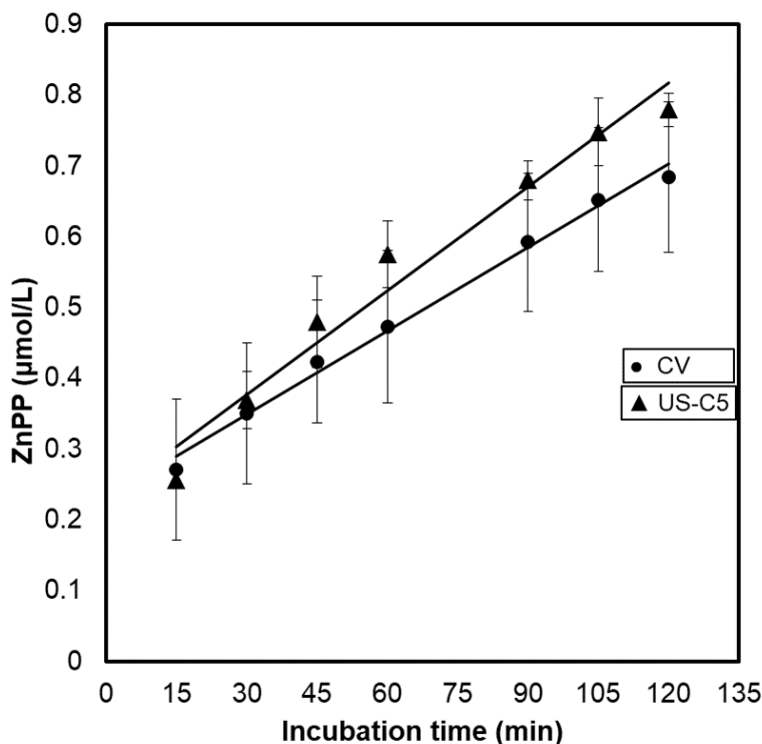


Figure 2. Kinetics of ZnPP formation using a FeCH extract from pork liver obtained by conventional (CV, 30 min magnetic stirring) and continuous ultrasound extraction for 5 min (US-C5). Average values  $\pm$  standard deviation are shown for each experimental time (t).

If what is considered is only the reaction rate at the steady phase (Figure 1), the specific enzymatic activity (SEA) was 7.6 nmol of ZnPP / g dry matter x min and the product formed at 120 min of 0.684  $\mu$ mol / L ZnPP. However, if the burst phase is not considered and the ZnPP formed at 45 min is used to calculate the SEA (De Maere *et al.*, 2016), a value of 18.2 nmol of ZnPP/ g dry matter x min is obtained. De Maere *et al.* (2016), reported a higher value of SEA for pork liver (123.81 nmol of ZnPP/ g dry matter x min) and a value of 31.51 nmol of ZnPP/ g dry matter x min for pork shoulder. Parolari *et al.* (2009) showed enzymatic activities ranging from 4.42 to 0.88 nmol of ZnPP / g dry matter x min throughout the different stages of Parma ham processing from green to dry-cured hams). On the other hand, in bovine liver, Taketani &

Tokunaga (1982) obtained a SEA of 18 nmol of ZnPP / h x mg of liver, a value much higher than that obtained in the present study (0.315 nmol of ZnPP/h x mg of liver, for a moisture of 71 gH<sub>2</sub>O/100g liver). This could be due to the fact that the reaction for the ZnPP formation was carried out using purified FeCH, obtained by solubilization, ammonium sulfate fractionation and blue Sepharose CL-6B chromatography while in the present study, an unpurified extract was used. The direct comparison of the values reported in this study and the ones found by De Maere *et al.* (2016) is complex, due to there being different factors, such as differences in the content of endogenous metals, (Fe<sup>2+</sup>, Co<sup>2+</sup>, Ni<sup>2+</sup>...) which are present in the mitochondrial membranes can modify the enzymatic activity, since they can serve as substrates, competing against and limiting the formation of ZnPP (Camadro *et al.*, 1984). In previous studies, ferrous ion (Fe<sup>2+</sup>) was already reported to lead to a competitive inhibition of the Zinc-chelatase activity and a decrease in the ZnPP formation catalyzed by FeCH from *Saccharomyces cerevisiae* (Camadro & Labbe, 1982). In this sense, Camadro *et al.* (1984) postulated that the FeCH capacity to synthesize ZnPP in human liver may be affected by the mitochondrial Fe<sup>2+</sup> reserve, which leads to the formation of Ferro-protoporphyrin instead of ZnPP and confirmed that Protoporphyrin IX consumption differed from the ZnPP formation. The influence of Fe<sup>2+</sup> was also evidenced by Nunez *et al.* (1983), who showed that when 2,2'-bipyridine was used to reduce endogenous Fe<sup>2+</sup> without affecting Zn<sup>2+</sup>, FeCH activity, in terms of ZnPP production, was increased (Marcus *et al.*, 1982; Rossi *et al.*, 1990). Finally, sample heterogeneity should also account for the differences in enzymatic activity; thus, Benedini *et al.* (2008) reported that the variation of FeCH concentration in pork loins reached 66 %, which was linked to different factors, such as the breed, feeding or slaughter technique.

### **3.2. Comparison between conventional and ultrasonically-assisted FeCH extraction**

Figure 2 compares the reaction kinetics of ZnPP formation using FeCH extracts obtained by two modes of extraction: conventional (CV, 30 min, agitation) and continuous, ultrasound-assisted for 5 min (US-C5). Ultrasound assistance during FeCH extraction did not alter the linear pattern found in the reaction kinetics. The CV and US-C5 linear fits presented similar y-intercepts but the use of ultrasound significantly

( $p < 0.05$ ) increased the slope, from 0.0039 to 0.0049  $\mu\text{mol}$  of ZnPP / L x min (Table 1). These facts confirm that the same amount of enzyme was extracted in both CV and US-C5 procedures, but ultrasound significantly ( $p < 0.05$ ) improved the performance of the enzyme. Thereby, the reaction rate was 25.7 % higher for the FeCH extract obtained with ultrasound assistance (Table 1), which amounts to a difference of 13.9 % (0.096  $\mu\text{mol}$  /L ZnPP) in the final ZnPP concentration at 120 min (Table 1) compared to the conventional method. Therefore, the experimental results highlighted that the enzyme extracted with ultrasound behaved differently to the one obtained by the conventional stirring procedure. This implies that ultrasound is inducing some conformational modification in the enzyme, improving its performance. No previous studies have addressed the influence of ultrasound on the extraction of FeCH but there is a wide number of applications for other enzymes. Thus, Li *et al.* (2015) studied the effects of the US-assisted extraction of pectinase, endoglucanase and xylanase collected from *Aspergillus japonicus* through solid state fermentation and obtained a maximum enzymatic activity increase of 1.2, 1.48 and 1.3, respectively. Szabo *et al.* (2015) applied US to extract various enzymes from *Trichoderma virens* and the enzymatic activity increased between 1.2 and 4.13 times compared to the conventional extraction mode, depending on the sonication parameters applied. Both previous studies presented similar values for the ultrasonic enhancement of the enzymatic activity to that found in the present study (1.31 increase). Ultrasound has also been applied to improve the extraction of enzymes from microbial cultures (Nadar *et al.*, 2017). In this sense, Avhad *et al.* (2014) used a 3-phase ultrasonically-assisted extraction partitioning to obtain fibrinolytic enzyme from *Bacillus sphaericus*, achieving 7 times more purity and activity than conventional extraction. Pakhale *et al.* (2016) reported that the application of ultrasound shortened the extraction time of serratiopeptidasa from *Serratia marcescens* to 5 min compared to the 60 min of conventional extraction and increased the enzyme activity. Therefore, previous literature supports the results achieved in this study, since ultrasound may dramatically speed-up the extraction process of the enzyme FeCH and additionally, improve its activity.

### 3.3. Influence of ultrasonic application time.

In order to evaluate the influence of US application time on FeCH extraction, times shorter than 5 min (1 and 2.5 min) were analyzed (Figure 3). Thus, the best performance was achieved by applying US for 1 min (US-C1). The maximum product formed was 0.852  $\mu\text{mol} / \text{L}$  ZnPP after 120 min (Table 1) and the reaction rate was 0.0052  $\mu\text{mol}$  of ZnPP / L x min (Table 1), which led to an increase of 24.6 % in the maximum product formed and 33.3 % in the reaction rate, compared to the values obtained using the conventional extraction mode (Table 1). Therefore, US extraction for 1 min involved a noticeable shortening in the process time compared to conventional stirring for 30 min, which is a relevant finding from an industrial point of view.

Table 1. Linear fit for steady state phase of ZnPP formation kinetics: slope (b), y-intercept (a) correlation coefficient (r) and  $\mu\text{mol}$  ZnPP / L at 120 min.

	<b>a</b> ( $\mu\text{M}$ ZnPP)	<b>b</b> ( $\frac{\mu\text{mol ZnPP}}{\text{L} \times \text{min}}$ )	<b>r</b>	<b>ZnPP*</b> ( $\frac{\mu\text{mol}}{\text{L}}$ )
<b>CV</b>	0.231 $\pm$ 0.094 <sub>AB</sub>	0.0039 $\pm$ 0.0001 <sub>Y</sub>	0.995	0.684
<b>US-C1</b>	0.262 $\pm$ 0.083 <sub>A</sub>	0.0052 $\pm$ 0.0013 <sub>Z</sub>	0.991	0.852
<b>US-C2.5</b>	0.180 $\pm$ 0.072 <sub>BC</sub>	0.0051 $\pm$ 0.0008 <sub>Z</sub>	0.993	0.786
<b>US-C5</b>	0.229 $\pm$ 0.110 <sub>AB</sub>	0.0049 $\pm$ 0.0015 <sub>Z</sub>	0.975	0.779
<b>US-P1</b>	0.155 $\pm$ 0.021 <sub>C</sub>	0.0034 $\pm$ 0.0004 <sub>X</sub>	0.991	0.565
<b>US-P2.5</b>	0.160 $\pm$ 0.036 <sub>C</sub>	0.0035 $\pm$ 0.0003 <sub>X</sub>	0.992	0.561
<b>US-P5</b>	0.226 $\pm$ 0.095 <sub>AB</sub>	0.0043 $\pm$ 0.0007 <sub>Y</sub>	0.984	0.717

\* Final ZnPP concentration at 120 min

For slope and y-intercept average values  $\pm$  LSD intervals are given.

(A, B, C) and (X, Y, Z) show homogeneous groups established from LSD intervals ( $p < 0.05$ ) for a and b, respectively



No significant ( $p > 0.05$ ) differences were found for the y-intercepts or the slopes identified in the linear fits for the US experiments at the different times (Table 1). This suggests that the same amount of enzyme was extracted and it acted in a very similar way. However, that the best performance was achieved with an extraction time of 1 min points to the fact that a prolonged exposure to the ultrasonic energy could lead to the degradation of the enzyme. Ultrasound waves released into the liquid medium at high intensity could cause a disruption to or modification in the structure of the enzymes due to the mechanical and thermal stress produced by the cavitation (Islam *et al.*, 2014; Wang *et al.*, 2018). The collapse of the cavitation bubbles generates very high localized temperatures and pressure shock waves (Mawson *et al.*, 2011), which may alter the structure of the enzymes (Raviyan *et al.*, 2005). Previous literature has not addressed a minimum temperature for the enzyme deactivation, but Koller *et al.* (1976) reported that the optimum temperatures for mouse and rat liver mitochondria FeCH were 45 and 50 °C, respectively. Thus, there is evidence of protein denaturation at temperatures of over 50 °C. Moreover, in barley leaves, FeCH activity was completely destroyed after a treatment of 1 min at 100 °C (Goldin & Little, 1969).

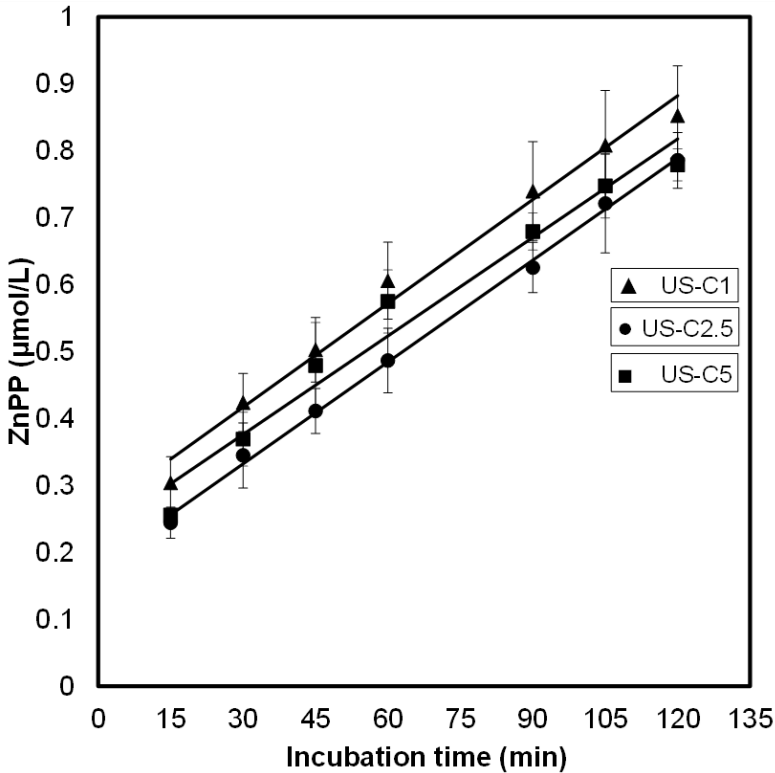


Figure 3. Kinetics of ZnPP formation using a FeCH extract from pork liver obtained by continuous ultrasound extraction for 1 min (US-C1), 2.5 min (US-C2.5) and 5 min (US-C5). Average values  $\pm$  standard deviation are shown for each experimental time (t).

### 3.4. Comparison between pulsed and continuous ultrasonic extraction

Pulsed ultrasound application (50 % frequency) (US-P) was tested (Figure 4) and compared to continuous (US-C) extraction at different times (1, 2.5 and 5 min). Figure 4A shows the product formation kinetics with enzyme extracts obtained with US-P application at different times. Among the conditions tested, the best performance was achieved with pulsed US application for 5 min. Thus, US-P5 conditions resulted in a maximum product formation of 0.717 ( $\mu\text{mol} / \text{L}$  ZnPP) (Table 1) due to a more pronounced reaction rate than in the CV experiments, which was evidenced in an increase of 10.3% in the slope of the linear fits (Table 1), while y-intercepts remained similar. However, when US-P was applied for shorter times (1 and 2.5 min), the

enzymatic activity for ZnPP formation evolved in a similar way to that in the conventional extracts of FeCH. This indicates that a very small amount of energy was introduced into the medium and did not cause any relevant modifications in the enzyme.

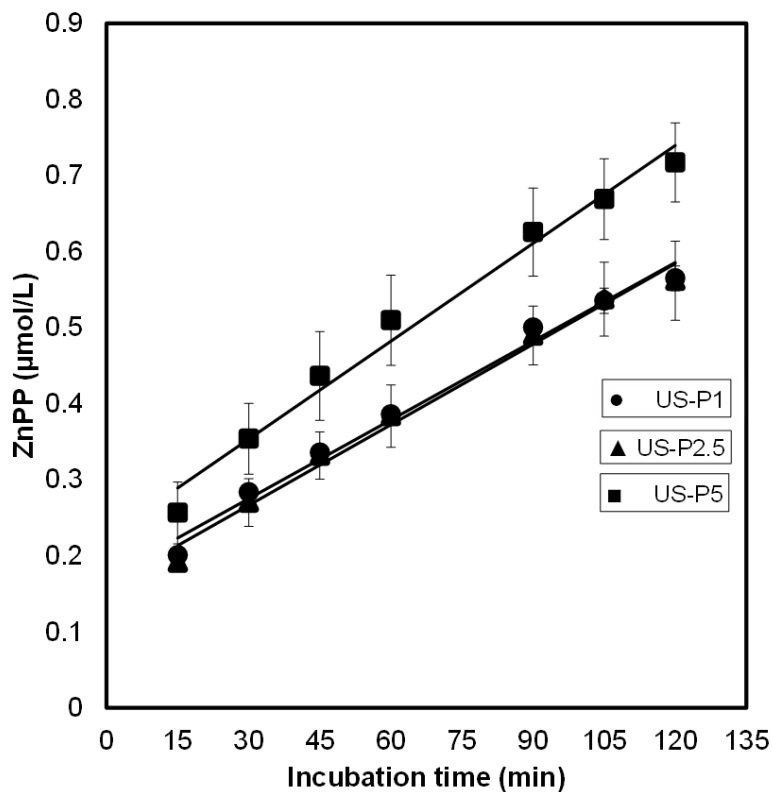


Figure 4. Kinetics of ZnPP formation using a FeCH extract from pork liver obtained by pulsed ultrasound extraction for 1 min (US-P1), 2.5 min (US-P2.5) and 5 min (US-P5). Average values  $\pm$  standard deviation are shown for each experimental time (t).

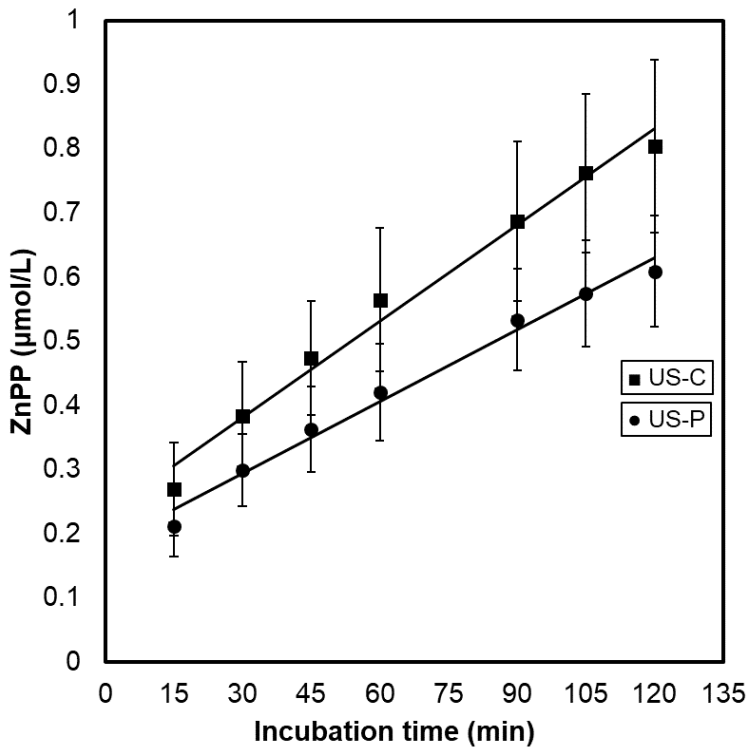


Figure 5. Kinetics of ZnPP formation using a FeCH extract from pork liver obtained by continuous ultrasound extraction (US-C) and pulsed ultrasound extraction (US-P). Average values for the different US application times (1, 2.5 and 5 min)  $\pm$  standard deviation are shown for each experimental time (t).

In general terms, pulsed US application was less efficient than continuous, as shown in Figure 5, in which average product formation kinetics for both application modes are shown for comparison purposes. Thus, pulsed US application involved a decrease in the maximum product formed ( $0.609 \mu\text{mol} / \text{L}$  ZnPP) compared to continuous US application ( $0.804 \mu\text{mol} / \text{L}$  ZnPP), as well as in the reaction rate (from  $0.0050$  to  $0.0037 \mu\text{mol} / \text{L} \times \text{min}$ ) (Figure 5). This is explained by a noticeable reduction in the average power released into the medium and, consequently, in the total energy supplied, which produces less intense effects, such as cavitation and stirring. In this sense, calorimetry tests revealed that pulsed ultrasound application (50% frequency) led to a 65.8% reduction in the power applied ( $24.6 \text{ W}$  in US-P vs  $71.9 \text{ W}$  in US-C). Therefore, a 50% reduction in the application time involved a proportionally

larger reduction in the energy released, since cavitation cycles are interrupted and a high portion of the energy is misspend. The observed differences between US-C and US-P application were dependent on the treatment time (Figures 6 A, B and C). The longer US was applied during FeCH extraction (Figure 6C), the smaller the differences between the pulsed and continuous modes. Thus, for an extraction time of 1 min, the average concentration of ZnPP was 33.8 % higher in continuous mode than in pulsed, whereas after 5 min, the concentration was only 7.1 % higher for the continuous method. As is the case for many ultrasound-assisted processes, there is probably an energy threshold value that is necessary to observe the effect of US; thus, until this threshold is not exceeded, no differences could be observed between the US-C or US-P compared to CV. On the other hand, it was necessary to apply 5 min treatments in pulsed mode (7380 J, Table 2) in order to obtain energy values greater than those of 1 min in continuous mode (the optimum time for the continuous US treatment, 4314 J, Table 2), which would explain why the difference between FeCH extraction in continuous and pulsed modes for 5 min treatments was minimal. Moreover, in terms of energy efficiency, which was defined as the increase in the ZnPP concentration (compared to the conventional treatment) divided by the ultrasonic energy applied (Table 2), US-C1 was the treatment showing the highest energy efficiency (0.0389  $\mu\text{M ZnPP/kJ}$ ), being 9 times higher than the US-C5 one (0.0044  $\mu\text{M ZnPP/kJ}$ ). On the other hand, US-P1 and US-P2 did not improve the ZnPP formation, compared to the CV treatment. Finally, the US-P5 obtained an energy efficiency value similar to US-C5. It is important to remark that the energy efficiency is a relevant aspect to be considered for the use of US in industrial applications.

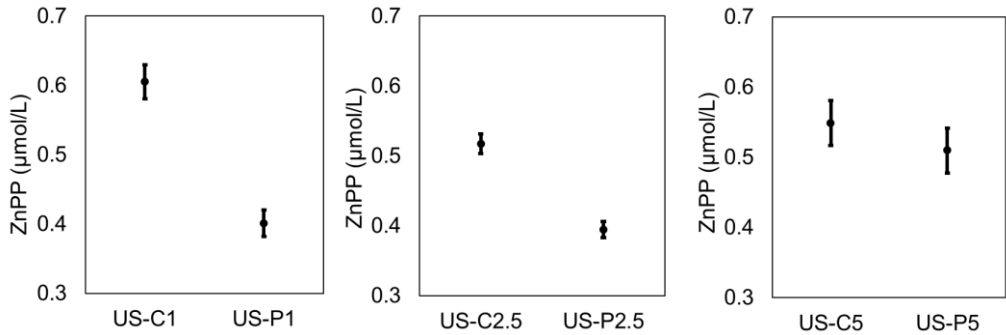


Figure 6. (A) Analysis of average values of ZnPP concentration and LSD intervals from multifactorial ANOVA (A) by continuous ultrasound extraction for 1 min (US-C1) and pulsed ultrasound extraction for 1 min (US-P1). (B) by continuous ultrasound extraction for 2.5 min (US-C2.5) and pulsed ultrasound extraction for 2.5 min (US-P2.5). (C) by continuous ultrasound extraction for 5 min (US-C5) and pulsed ultrasound extraction for 5 min (US-P5).

Table 2. Energy applied and energy efficiency in ultrasound applications.

Time (min)	Energy applied (J)		Energy efficiency* (µM ZnPP/kJ)	
	US-C	US-P	US-C	US-P
1	4314	1476	0.0389	-
2.5	10785	3690	0.0095	-
5	21570	7380	0.0044	0.0045

\*Calculated as the increase in the ZnPP concentration (compared to the conventional treatment) divided by the energy applied

- No increase compared to the conventional treatment

#### 4. Conclusions

Power ultrasound (US) application has proven to be an effective method for the intensification of Ferrochelataze (FeCH) extraction from pork liver, shortening the process time and improving the further formation of Zinc-protoporphyrin (ZnPP). Thus, the application of US improved the rate of ZnPP formation by up to 33.3 % compared

to conventional extraction. Ultrasound did not increase the amount of FeCH extracted but did improve its enzymatic activity. The best US application performance was achieved for 1 min of continuous treatment. It was evidenced that longer US application times of over 1 min could cause enzyme degradation. The pulsed US application system allowed the energy released into the medium to be modulated but, in general terms, led to a worsening of the extraction performance compared to continuous application. Further research should address the optimization of the ultrasonic treatment by exploring relevant process variables, such as the liver-solvent ratio, temperature, pH and power density. In addition, for future industrial applications, continuous US-assisted extraction has to be addressed for residence times of close to 1 min.

## Acknowledgements

The authors acknowledge the financial support from the “Ministerio de Economía y Competitividad (MINECO) and Instituto Nacional de Investigación y Tecnología Agraria y Alimentaria (INIA)” in Spain (Project RTA2017-00024-C04-03). The authors acknowledge the contribution of the undergraduate student Jose V. Pedrero-Gonzalez to the experimental work.

## References

- Abbasi, T., & Abbasi, S. A. (2016). Reducing the global environmental impact of livestock production: The minilivestock option. *Journal of Cleaner Production*, *112*, 1754-1766. <https://doi.org/10.1016/j.jclepro.2015.02.094>
- Amid, M., Murshid, F.S., Manap, M.Y. & Islam Sarker, Z. (2016). Optimization of ultrasound-assisted extraction of pectinase enzyme from guava (*Psidium guajava*) peel: Enzyme recovery, specific activity, temperature, and storage stability. *Preparative Biochemistry and Biotechnology*, *46*(1), 91-99. <https://doi.org/10.1080/10826068.2015.1031396>

- Armenteros, M., Aristoy, M. C., & Toldrá, F. (2012). Evolution of nitrate and nitrite during the processing of dry-cured ham with partial replacement of NaCl by other chloride salts. *Meat science*, 91(3), 378-381. <https://doi.org/10.1016/j.meatsci.2012.02.017>
- Avhad, D. N., Niphadkar, S. S., & Rathod, V. K. (2014). Ultrasound assisted three phase partitioning of a fibrinolytic enzyme. *Ultrasonics Sonochemistry*, 21(2), 628-633. <https://doi.org/10.1016/j.ultsonch.2013.10.002>
- Awad, T. S., Moharram, H. A., Shaltout, O. E., Asker, D., & Youssef, M. M. (2012). Applications of ultrasound in analysis, processing and quality control of food: A review. *Food Research International*, 48(2), 410-427. <https://doi.org/10.1016/j.foodres.2012.05.004>
- Bansode, S. R., & Rathod, V. K. (2017). An investigation of lipase catalysed sonochemical synthesis: A review. *Ultrasonics Sonochemistry*, 38, 503-529. <https://doi.org/10.1016/j.ultsonch.2017.02.028>
- Barba, F. J., Grimi, N., & Vorobiev, E. (2015). Evaluating the potential of cell disruption technologies for green selective extraction of antioxidant compounds from *Stevia rebaudiana* Bertoni leaves. *Journal of Food Engineering*, 149, 222-228. <https://doi.org/10.1016/j.jfoodeng.2014.10.028>
- Benedini, R., Raja, V., & Parolari, G. (2008). Zinc-protoporphyrin IX promoting activity in pork muscle. *LWT - Food Science and Technology*, 41(7), 1160-1166. <https://doi.org/10.1016/j.lwt.2007.08.005>
- Camadro, J. M., & Labbe, P. (1982). Kinetic studies of ferrochelatase in yeast. *Biochimica et Biophysica Acta (BBA) - Protein Structure and Molecular Enzymology*, 707(2), 280-288. [https://doi.org/10.1016/0167-4838\(82\)90362-4](https://doi.org/10.1016/0167-4838(82)90362-4)
- Camadro, J. M., Ibrahim, N. G., & Levere, R. D. (1984). Kinetic studies of human liver ferrochelatase. Role of endogenous metals. *The Journal of Biological Chemistry*, 259(9): 5678-5682



- Cárcel, J. A., Benedito, J., Rosselló, C., & Mulet, A. (2007). Influence of ultrasound intensity on mass transfer in apple immersed in a sucrose solution. *Journal of Food Engineering*, 78(2), 472-479. <https://doi.org/10.1016/j.jfoodeng.2005.10.018>
- Chemat, F., Rombaut, N., Sicaire, A. -, Meullemiestre, A., Fabiano-Tixier, A. -, & Abert-Vian, M. (2017). Ultrasound assisted extraction of food and natural products. mechanisms, techniques, combinations, protocols and applications. A review. *Ultrasonics Sonochemistry*, 34, 540-560. <https://doi.org/10.1016/j.ultsonch.2016.06.035>
- De Maere, H., Chollet, S., Claeys, E., Michiels, C., Govaert, M., De Mey, E., . . . Fraeye, I. (2017). In vitro zinc protoporphyrin IX formation in different meat sources related to potentially important intrinsic parameters. *Food and Bioprocess Technology*, 10(1), 131-142. <https://doi.org/10.1007/s11947-016-1804-0>
- Delgado-Povedano, M.M. & De Castro, M.D.L. (2015). A review on enzyme and ultrasound: A controversial but fruitful relationship. *Analytica Chimica Acta*, 889: 1-21. <https://doi.org/10.1016/j.aca.2015.05.004>
- Dolatowski, Z. J., Stadnik, J., & Stasiak, D. (2007). Applications of ultrasound in food technology. *Acta Scientiarum Polonorum Technologia Alimentaria*, 6(3), 88-99.
- Feng, H., Barbosa-Cánovas, G. V., & Weiss, J. (2011). Ultrasound technologies for food and bioprocessing (Vol. 1, p. 599). *New York: Springer*. doi 10.1007/978-1-4419-7472-3\_2,
- Fersht, A. (1984). *Enzyme Structure and Mechanism* (2nd ed). W H Freeman, New York. pp. 146 .
- Goldin, B. R., & Little, H. N. (1969). Metalloporphyrin chelatase from barley. *BBA - Enzymology*, 171(2), 321-332. [https://doi.org/10.1016/0005-2744\(69\)90165-X](https://doi.org/10.1016/0005-2744(69)90165-X)
- Goula, A. M. (2013). Ultrasound-assisted extraction of pomegranate seed oil–Kinetic modeling. *Journal of Food Engineering*, 117(4), 492-498. <https://doi.org/10.1016/j.jfoodeng.2012.10.009>

- Islam, M. N., Zhang, M., & Adhikari, B. (2014). The inactivation of enzymes by ultrasound-A review of potential mechanisms. *Food Reviews International*, 30(1), 1-21. <https://doi.org/10.1080/87559129.2013.853772>
- Johnson, K. A. (2013). A century of enzyme kinetic analysis, 1913 to 2013. *FEBS letters*, 587(17), 2753-2766. <https://doi.org/10.1016/j.febslet.2013.07.012>
- Koller, M. E., & Romslo, I. (1977). Studies on ferrochelatase activity of mitochondria and submitochondrial particles with special reference to regulatory function of mitochondrial inner membrane. *Biochimica et Biophysica Acta*, 461, 283–296. [https://doi.org/10.1016/0005-2728\(76\)90157-2](https://doi.org/10.1016/0005-2728(76)90157-2)
- Laursen, K., Adamsen, C.E., Laursen, J., Olsen, K. & Moller, J.K.S. (2008). Quantification of zinc-porphyrin in dry-cured ham products by spectroscopic methods Comparison of absorption, fluorescence and X-ray fluorescence spectroscopy. *Meat Science* 78: 336-341. <https://doi.org/10.1016/j.meatsci.2007.06.014>
- Li, P., Xia, J., Shan, Y., & Nie, Z. (2015). Comparative study of multi-enzyme production from typical agro-industrial residues and ultrasound-assisted extraction of crude enzyme in fermentation with *Aspergillus japonicus* PJ01. *Bioprocess and Biosystems Engineering*, 38(10): 2013–2022. <https://doi.org/10.1007/s00449-015-1442-3>
- Mackenzie, S. G., Leinonen, I., Ferguson, N., & Kyriazakis, I. (2016). Can the environmental impact of pig systems be reduced by utilising co-products as feed?. *Journal of Cleaner Production*, 115, 172-181. <https://doi.org/10.1016/j.jclepro.2015.12.074>
- Marcus, D. L., Ibrahim, N. G., & Freedman, M. L. (1982). Age-related decline in the biosynthesis of mitochondrial inner membrane proteins. *Experimental Gerontology*, 17(5): 333–341. [https://doi.org/10.1016/0531-5565\(82\)90033-X](https://doi.org/10.1016/0531-5565(82)90033-X)
- Mason, T. J. (1998). Power ultrasound in food processing-the way forward. *Ultrasound in food processing*, 105-126.

- Mawson, R., Gamage, M., Terefe, N. S., & Knoerzer, K. (2011). Ultrasound in enzyme activation and inactivation. *Springer, New York*, 369-404. [https://doi.org/10.1007/978-1-4419-7472-3\\_14](https://doi.org/10.1007/978-1-4419-7472-3_14)
- Medina-Torres, N., Ayora-Talavera, T., Espinosa-Andrews, H., Sánchez-Contreras, A., & Pacheco, N. (2017). Ultrasound Assisted Extraction for the Recovery of Phenolic Compounds from Vegetable Sources. *Agronomy*, 7(3): 47. <https://doi.org/10.3390/agronomy7030047>
- Moller, J.K.S., Adamsen, C.E., Catharino, R.R., Skibsted, L.H. & Eberlin, M.N. (2007). Mass spectrometric evidence for a zinc-porphyrin complex as the red pigment in dry-cured Iberian and Parma ham. *Meat Science* 75, 203-210. <https://doi.org/10.1016/j.meatsci.2006.07.005>
- Nadar, S. S., Pawar, R. G., & Rathod, V. K. (2017) Recent advances in enzyme extraction strategies: A comprehensive review. *International Journal of Biological Macromolecules*, 101, 931–957. <https://doi.org/10.1016/j.ijbiomac.2017.03.055>
- Nunez, M. T., Cole, E. S., & Glass, J. (1983). The reticulocyte plasma membrane pathway of iron uptake as determined by the mechanism of  $\alpha,\alpha'$ -dipyridyl inhibition. *Journal of Biological Chemistry*, 258(2), 1146-1151.
- Pakhale, S. V., & Bhagwat, S. S. (2016). Purification of serratiopeptidase from *serratia marcescens* NRRL B 23112 using ultrasound assisted three phase partitioning. *Ultrasonics Sonochemistry*, 31, 532-538. <https://doi.org/10.1016/j.ultsonch.2016.01.037>
- Patist, A., & Bates, D. (2008). Ultrasonic innovations in the food industry: From the laboratory to commercial production. *Innovative Food Science & Emerging Technologies*, 9(2): 147–154. <https://doi.org/10.1016/j.ifset.2007.07.004>

- Parolari, G., Benedini, R., & Toscani, T. (2009). Color Formation in Nitrite-Free Dried Hams as Related to Zn-Protoporphyrin IX and Zn-Chelatase Activity. *Journal of Food Science*, 74(6): 413–418. <https://doi.org/10.1111/j.1750-3841.2009.01193.x>
- Praestgaard, E., Elmerdahl, J., Murphy, L., Nymand, S., McFarland, K. C., Borch, K., & Westh, P. (2011). A kinetic model for the burst phase of processive cellulases. *FEBS Journal*, 278(9), 1547-1560. <https://doi.org/10.1111/j.1742-4658.2011.08078.x>
- Raviyan, P., Zhang, Z., & Feng, H. (2005). Ultrasonication for tomato pectinmethylesterase inactivation: effect of cavitation intensity and temperature on inactivation. *Journal of food engineering*, 70(2), 189-196. <https://doi.org/10.1016/j.jfoodeng.2004.09.028>
- Rossi, E., Attwood, P. V., Garcia-Webb, P., & Costin, K. A. (1990). Inhibition of human lymphocyte ferrochelatase activity by hemin. *Biochimica Et Biophysica Acta (BBA)/Protein Structure and Molecular*, 1038(3), 375-381. [https://doi.org/10.1016/0167-4838\(90\)90251-A](https://doi.org/10.1016/0167-4838(90)90251-A)
- Sassa, A., Beard, W. A., Shock, D. D., & Wilson, S. H. (2013). Steady-state, pre-steady-state, and single-turnover kinetic measurement for DNA glycosylase activity. *Journal of Visualized Experiments : JoVE*, (78) doi:10.3791/50695.
- Shukla, T.P. (1992). Microwave ultrasonics in food processing. *Cereal Foods World*, 37(4): 332.
- Soria, A. C., & Villamiel, M. (2010). Effect of ultrasound on the technological properties and bioactivity of food: A review. *Trends in Food Science and Technology*, 21(7), 323-331. <https://doi.org/10.1016/j.tifs.2010.04.003>
- Steen, L., Glorieux, S., Goemaere, O., Brijs, K., Paelinck, H., Foubert, I., & Fraeye, I. (2016). Functional properties of pork liver protein fractions. *Food and Bioprocess Technology*, 9(6), 970-980. <https://doi.org/10.1007/s11947-016-1685-2>

- Szabo, O. E., Csiszar, E., Toth, K., Szakacs, G., & Koczka, B. (2015). Ultrasound-assisted extraction and characterization of hydrolytic and oxidative enzymes produced by solid state fermentation. *Ultrasonics Sonochemistry*, 22, 249–256. <https://doi.org/10.1016/j.ultsonch.2014.07.001>
- Taketani, S., & Tokunaga, R. (1981). Rat liver ferrochelatase. Purification, properties, and stimulation by fatty acids. *Journal of Biological Chemistry*, 256(24), 12748-12753. [https://doi.org/10.1016/S0021-9258\(18\)42958-4](https://doi.org/10.1016/S0021-9258(18)42958-4)
- Taketani, S., & Tokunaga, R. (1982). Purification and substrate specificity of bovine Liver-Ferrochelatase. *European Journal of Biochemistry*, 127(3), 443-447. <https://doi.org/10.1111/j.1432-1033.1982.tb06892.x>
- Vilkhu, K., Mawson, R., Simons, L., & Bates, D. (2008). Applications and opportunities for ultrasound assisted extraction in the food industry—A review. *Innovative Food Science & Emerging Technologies*, 9(2), 161-169. <https://doi.org/10.1016/j.ifset.2007.04.014>
- Wakamatsu, J., Nishimura, T., & Hattori, A. (2004a). A Zn–porphyrin complex contributes to bright red color in Parma ham. *Meat Science*, 67(1): 95–100. <https://doi.org/10.1016/j.meatsci.2003.09.012>
- Wakamatsu J, Okui J, Ikeda Y, Nishimura T, Hattori A. (2004b). Establishment of a model experiment system to elucidate the mechanism by which Zn-protoporphyrin IX is formed in nitrite-free dry-cured ham. *Meat Science* 68, 313–317. <https://doi.org/10.1016/j.meatsci.2004.03.014>
- Wakamatsu, J., Okui, J., Hayashi, N., Nishimura, T., & Hattori, A. (2007). Zn protoporphyrin IX is formed not from heme but from protoporphyrin IX. *Meat Science*, 77(4): 580–586. <https://doi.org/10.1016/j.meatsci.2007.05.008>
- Walker, R. (1990). Nitrates, nitrites and N-nitrosocompounds: A review of the occurrence in food and diet and the toxicological implications. *Food Additives and Contaminants*, 7(6), 717-768. <https://doi.org/10.1080/02652039009373938>

- Wang, W., Chen, W., Zou, M., Lv, R., Wang, D., Hou, F., ... & Liu, D. (2018). Applications of power ultrasound in oriented modification and degradation of pectin: A review. *Journal of Food Engineering*, 234, 98-107. <https://doi.org/10.1016/j.jfoodeng.2018.04.016>
- Zou, Y., Bian, H., Li, P., Sun, Z., Sun, C., Zhang, M., Geng, Z. & Wang, D. (2018). Optimization and physicochemical properties of nutritional protein isolate from pork liver with ultrasound-assisted alkaline extraction. *Animal Science Journal*, 89(2), 456-466. <https://doi.org/10.1111/asj.12930>
- Xu, L., Xia, Q., Cao, J., He, J., Zhou, C., Guo, Y., & Pan, D. (2021). Ultrasonic effects on the headspace volatilome and protein isolate microstructure of duck liver, as well as their potential correlation mechanism. *Ultrasonics Sonochemistry*, 71. <https://doi.org/10.1016/j.ultsonch.2020.105358>



*Influence of ultrasonic application on the enzymatic formation of zinc protoporphyrin*

---

Blanca Abril<sup>1</sup>, Marina Contreras<sup>1</sup>, Ricard Bou<sup>2</sup>, Mar Llauger<sup>2</sup> José Vicente García-Pérez<sup>1</sup> and José Benedito<sup>1</sup>

<sup>1</sup>Department of Food Technology, Universitat Politècnica de València, Camí de Vera, s/n, Valencia 46022, Spain

<sup>2</sup>IRTA, XaRTA, Food Technology, Finca Camps i Armet, Monells, Girona E-17121, Spain





## **Influence of ultrasonic application on the enzymatic formation of zinc protoporphyrin**

### **Abstract**

Ferrochelatase (FeCH), present in pork liver, catalyses the formation of zinc-protoporphyrin (ZnPP), a stable purple-red pigment found in Parma ham. Kinetics of ZnPP formation is especially slow. Thus, the aim of this study was to improve the ZnPP production using power ultrasound (US) at low (7.05 W/L) and moderate power (36.53 W/L) in homogenised pork liver (HLi) and with added oxyhemoglobin (HLi+OxyHb). The ZnPP formation was performed at 37 °C, under anaerobic conditions, for different reaction times (6 to 48 h). Low power US proved to be an effective method with which to intensify ZnPP production; however, when a moderate power was applied, ZnPP formation was hindered. Thus, when US was applied at low power, it shortened the time needed to reach maximum ZnPP formation by 50 % and increased the yield by 25.77 % in the case of HLi and by 4.42 % in that of HLi+OxyHb when compared to the control experiments.

**Keywords:** Zinc-protoporphyrin, colorant, pork liver, ferrochelatase and power ultrasound

## 1. Introduction

The characteristic homogeneous stable redness of raw and dry-cured meat products is a determining factor in their quality, playing a key role in consumer preferences. This stable colour is usually achieved in dry cured meat products by adding nitrates and nitrites as colour enhancers and also as antimicrobial agents. The reaction of nitrite with the myoglobin of the meat muscle gives rise to nitrosylmyoglobin, a characteristic red compound. However, in long aged dry cured Italian hams (Parma ham), the red is formed without adding any nitrifying agent due to an enzymatic reaction by which zinc-protoporphyrin (ZnPP) is produced. Thus, ZnPP is the natural pigment that gives rise to the characteristic redness of Italian Parma ham (Wakamatsu *et al.*, 2004). Furthermore, ZnPP is stable to light, so its addition to dry cured or fermented meat products would enhance the formation of their typical colour, minimising the use of nitrates and nitrites (De Maere *et al.*, 2017).

ZnPP formation consists of two sequentially occurring mechanisms: i) the iron ( $\text{Fe}^{2+}$ ) is released from the heme group of oxymyoglobin to form protoporphyrin IX (PPIX), and ii) the ion zinc ( $\text{Zn}^{2+}$ ) is inserted into the porphyrin ring to form ZnPP (Ishikawa *et al.*, 2007). Wakamatsu *et al.* (2015) studied pork liver as a substrate for ZnPP formation, obtaining a high concentration of pigment. Pork liver is a coproduct obtained from the meat industry. Therefore, the revaluation of this low-value slaughterhouse coproduct would reduce the cost of disposal and the environmental associated impact (Verma *et al.*, 2022). Furthermore, it should be noted that previous studies examined the ZnPP formation in pork loin by adding an exogenous source of porphyrins from horse myoglobin, resulting in a greater amount of ZnPP (Wakamatsu *et al.*, 2007). The aforementioned mechanisms were also studied *in vitro* in mitochondria, and it was observed that the exogeneous oxymyoglobin porphyrins were a good substrate for the enzyme ferrochelatase (FeCH), a protein associated with the inner mitochondrial membrane that catalyses the ZnPP formation (Ishikawa *et al.*, 2007) Furthermore, Zhai *et al.* (2022) added commercial porcine hemoglobin (Hb) to Parma ham, which produced a higher formation of ZnPP, this fact indicated that Hb was an interesting substrate to generate ZnPP. They observed an increase in nonheme iron content with the formation of ZnPP from Hb, indicating that the release of iron ions

from the heme group was a crucial step in the formation of ZnPP. In this regard, the addition of an exogenous substrate such as Hb, obtained from pork blood, to the ZnPP formation reactions would be of great interest, since pork blood is a coproduct of the meat industry characterized by its high volume and environmental impact (Alvarez *et al.*, 2012). Parolari *et al.* (2016) postulated that the ZnPP formation in the Italian Parma ham curing process is catalysed by FeCH. However, there was also evidence that ZnPP formation could take place through other mechanisms, such as non-enzymatic reactions (Becker *et al.*, 2012; Parolari *et al.*, 2016). Although the mechanisms related to the ZnPP formation have not been fully elucidated, not only does the presence of endogenous enzymes, such as FeCH (Wakamatsu *et al.*, 2004), play a key-role, but the physicochemical parameters, such as pH and temperature, also seem to be of paramount importance (Benedini *et al.*, 2008; Ishikawa *et al.*, 2007).

Bou *et al.* (2022) studied the ZnPP formation from FeCH in Serrano ham, observing that the formation began after 12 days of salting, in the so-called resting period, once the temperature was rose from 4 to 16 °C, and was continued during curing (12 months). Therefore, the ZnPP formation catalysed by FeCH could be considered a slow process dependent on both extrinsic (temperature, salt concentration and time) and intrinsic factors of the meat (pH and concentration and availability of enzymes and substrates). Thus, the search for alternatives to accelerate the ZnPP formation process, such as the use of emerging technologies, would be of great interest for subsequent industrial applications.

Power ultrasound (US) has been used to intensify enzymatic reactions (Lerin *et al.*, 2011). It was used to improve the enzymatic hydrolysis of different substrates (Muñoz-Almagro *et al.*, 2017; Priya & Gogate, 2021), and has also been applied to improve the extraction of enzymes. In this sense, in a previous study, Abril *et al.* (2021) observed that high power US application improved the FeCH extraction from pork liver compared to mechanical stirring. In these applications, the great energy release caused by the acoustic waves (Khan *et al.*, 2021) helps to improve both hydrolysis and the enzyme extraction from the inner cell (Yao *et al.*, 2020), but the high power may also cause enzyme denaturation. However, another plausible strategy by which to improve the enzymatic reaction is low or moderate power US application in order to induce a

mild cavitation, or only a micro-stirring, and promote the union of the substrates with the active sites, or even product diffusion without altering the enzyme structure. Abril *et al.* (2021) postulated that the rate of ZnPP formation catalysed by the FeCH, using exogenous porphyrins and  $Zn^{2+}$ , was controlled by the product diffusion in the steady phase. In this context, this study aims to assess the feasibility of using power ultrasound, applied at moderate and low intensities, to improve the enzymatic reaction of the ZnPP formation catalysed by FeCH using different substrates: homogenised pork liver, and homogenised pork liver with added oxyhemoglobin from pork blood.

## **2. Materials and methods**

### **2.1. Preparation of homogenised pork liver**

Raw pork livers were transported at below 4 °C from an industrial slaughterhouse to the laboratory and processed in less than 2 h after slaughter. Afterwards, the pork livers were homogenised for 5 min (Blixer 2, Robot Coupe, Vincennes Cedex, France), immediately vacuum packaged (30 g portions) in plastic film 200 x 300 PA/PE (Sacoliva, Castellar del Vallès, Barcelona) and stored at -20 °C until use.

### **2.2. Preparation of oxyhemoglobin from hemoglobin standars**

The oxyhemoglobin (OxyHb) solution was prepared as described by Bou *et al.* (2010). Firstly, 0.16 g of porcine hemoglobin (Hb) lyophilised powder (H4131, Sigma Aldrich, Canada) were dissolved in 3 mL of cold phosphate buffer (50 mM, pH 7.3, 4 °C). Hb was reduced to OxyHb by the addition of sodium dithionite crystals (ratio 1:0.8 w/w) and vortexing at 4 °C. In order to remove dithionite, 2.5 mL of the OxyHb solution were passed through a disposable PD-10 desalting column (17-0851-01, GE Healthcare Life Sciences). Then, 4 mL of phosphate buffer (50 mM, pH 7.3, 4 °C) was passed into the stationary phase to elute the OxyHb out of the column. The amount of Hb was calculated by measuring the absorbance at 523 nm (isosbestic point), as described by Snell & Marini, (1988) whereas the percentage of OxyHb was calculated as described by Benesch *et al.* (1973). Only those solutions containing a minimum yield of 90 % of OxyHb were used in subsequent experiments.

### 2.3. Preparation of oxyhemoglobin from pork blood

Blood was removed from pigs sacrificed according to standard procedures. Approximately 100 mL of blood was collected in a bottle containing sodium triphosphate to avoid coagulation. Hb was extracted from red blood cells following the procedure described by Bou *et al.* (2019). In order to reduce Hb solution to OxyHb, sodium dithionite crystals were added (ratio 1:0.3 w/w). The mixture was vortexed at 4 °C, and it was removed by passing 2.5 mL of OxyHb solution to a disposable PD-10 desalting column. Then, 4 mL of 50 mM Tris buffer (pH 8.5) was passed into the stationary phase to elute the OxyHb out of the column. Finally, the percentage of OxyHb was calculated as described in section 2.2 and only samples with a minimum OxyHb content of 90% were considered.

### 2.4. Preparation of different reaction media

In order to investigate the ZnPP formation, 4 types of samples were prepared. Homogenized pork liver (HLi) with two different types of preservatives, antibiotics and organic acids, to study their influence on the ZnPP formation reaction. In addition, and using organic acids as preservatives, homogenised pork liver with added oxyhemoglobin from hemoglobin standards and homogenised pork liver with added oxyhemoglobin extracted from pork blood, were considered.

#### 2.4.1. Homogenised pork liver with added antibiotics

The homogenised pork liver, previously prepared and stored at -20 °C, was kept at 4 °C for 1 h before preparation. From preliminary experiments, the final homogenate contained 20 % pork liver; therefore, it was diluted with distilled water and a mixture of three antibiotics: potassium penicillin G (140 µg/mL), streptomycin sulfate (500 µg/mL), and gentamicin sulfate (100 µg/mL), to control microbial growth. The homogenised pork liver was protected from the light and kept on ice. The final solution was homogenised (DI 25 Basic Homogenizer, IKA, Germany) for 1 min at 4 °C and 8000 rpm. Finally, from preliminary experiments, the pH of the 20 % liver homogenate was adjusted to  $4.8 \pm 0.05$  with HCl 1 N.

#### 2.4.2. Homogenised pork liver with organic acids

Antibiotics are not allowed in the food industry, and in order to eliminate them

from the final homogenate, it was prepared with added organic acids. Therefore, ascorbic and acetic acids, preservatives which are accepted in the food industry as a means of preventing microbial growth, were considered. In order to obtain a final amount of liver in the homogenate of 20 %, a solution containing 0.1 g ascorbic acid and 250  $\mu$ L acetic acid/ 100 mL distilled water was prepared, and the pH was adjusted to 4.16 with NaOH 1 N. Subsequently, 20 g of liver that had been previously homogenised and kept at 4 °C for 1 h were weighed in a glass beaker and made up to 100 mL of the organic acid solution. The final solution was homogenised (DI 25 Basic Homogeniser, IKA, Germany) for 1 min at 4 °C and 8000 rpm. Finally, the pH of the 20 % liver homogenate was adjusted to  $4.8 \pm 0.05$  with HCl 1 N.

#### **2.4.3. Homogenised pork liver with added oxyhemoglobin from hemoglobin standards and from pork blood**

To prepare the homogenate of pork liver with added OxyHb, OxyHb obtained from commercial Hb as described in section 2.2 was first used, to better understand the effect of adding this pure and controlled substrate to the ZnPP formation reaction. Subsequently, OxyHb was obtained from pork blood (section 2.3), with the aim of studying the possibility of using this important meat co-product in the ZnPP formation. 2.5 mL of the OxyHb solution, obtained as described in sections 2.2 and 2.3, respectively, were added to the 100 mL of homogenised pork liver reaction medium with organic acids previously described in section 2.4.2. The final solution was homogenised using a vortex for 45 s and the pH was adjusted to  $4.8 \pm 0.05$  with HCl 1 N.

#### **2.5. Formation of zinc protoporphyrin: Conventional (CV) and Ultrasonic-assited (US)**

The kinetics of ZnPP formation were carried out following the experimental methodology previously described by Bou *et al.* (2022), with minor modifications. ZnPP formation requires an anaerobic medium and an optimal temperature of 37 °C. Thus, the reaction media described in section 2.4 were placed in opaque glass bottles (10 cm height x 2 cm diameter) of 15 mL capacity. Afterwards, the bottles were immersed in water (800 mL) placed inside a 3.5 L Anaerobic Jar (HP0011, OXOID, Argentina) in which anaerobic conditions were forced (Anaerobic System BR 38, Oxoid Ltd.,

Hampshire, England). The jar was placed (Figure 1) at 6 cm from the bottom of an ultrasonic bath (15 L ATG15160, ATU, Spain). The samples were incubated at different times (0, 6, 12, 18, 24 and 48 h) in order to study the ZnPP formation kinetics.

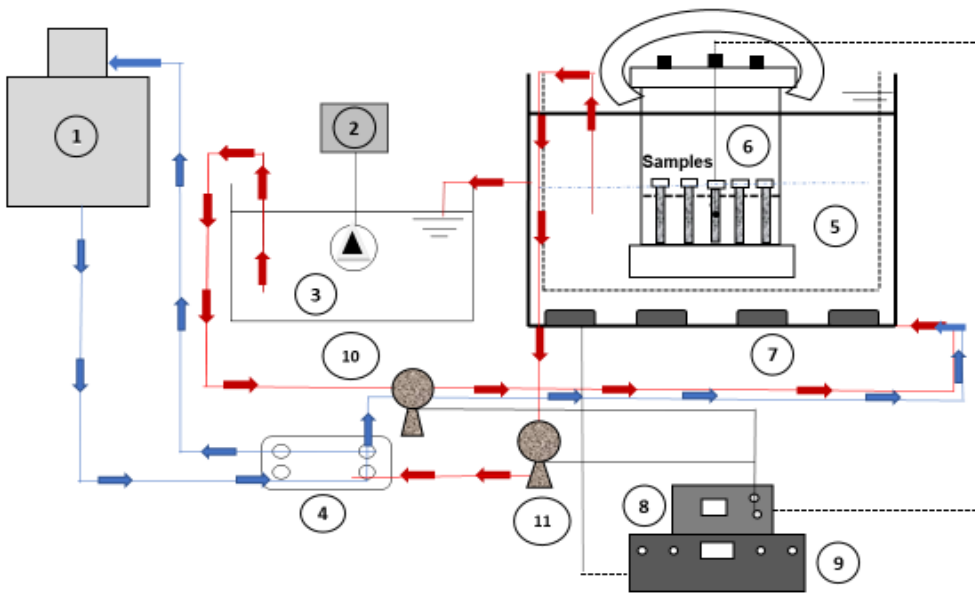


Figure 1. Scheme of the ultrasonic bath with temperature control. 1, Cooling unit; 2, Circulating thermostat; 3, Water reservoir tank; 4, Plate heat exchanger; 5, Ultrasonic bath; 6, Anaerobic jar; 7, Ultrasonic transducers; 8, Process Controller; 9, Ultrasonic generator and amplifier; 10, Heat pump; 11, Cooling pump.

The temperature control in conventional (CV) and ultrasonic-assisted (US) experiments was carried out using a similar experimental set-up to that described by Contreras *et al.* (2018) (Figure 1), which was based on water recirculation using the upper and lower connections of the ultrasonic bath (5, Figure 1). Thus, the outlet water stream was driven to a reservoir tank (5 L) (3, Figure 1) equipped with a circulating thermostat (Digitem TFT-200, Selecta, Spain) (2, Figure1), which kept the liquid at 50 °C in agitation while impelling it (3.5 L/min) through a plate heat exchanger (EL852, Mas Malta Brewery, Spain) (4, Figure 1). As a coolant, a glycol solution (40 % w/v) provided by a cooling unit at 2 °C (1190s, Circ Refrigerator, USA) (1, Figure 1) was used in the heat exchanger. The output water stream from the heat exchanger was



placed into the water bath using its lower connection, closing the water loop. An ON-OFF control strategy was implemented. To do this, a Pt-100 sensor placed in the centre of one of the opaque glass bottles (6, Figure 1) was connected to a process controller (E5CK, Omron, Japan) (8, Figure 1) that acted on the water circuit unit. The control system acted in two modes: heating and cooling. In the heating mode, the water passed from the reservoir bath to the ultrasonic bath through the heat pump (10, Figure 1) until a temperature of 37 °C (the set point) was reached in the glass bottle. When the Pt-100 sensor connected to the process controller detected that the temperature was higher than 37 °C in the glass bottle, the cooling mode was used. Thus, the cooling pump (11, Figure 1) acted by sucking the water from the ultrasonic bath and passing it through the heat exchanger, where the water was cooled by the glycol water that was recirculated from the cooling equipment. Subsequently, the water was driven by the cooling pump towards the ultrasonic bath in order to maintain a temperature of 37 °C in the glass bottle. In the case of ultrasonic (US) assisted ZnPP formation, the heating mode only worked until the temperature of 37 °C was reached in the glass bottle, since after that, the heat provided by US made only the cooling mode necessary. The ZnPP formation kinetics in CV and US modes were performed in triplicate.

As far as the kinetics of US-assisted ZnPP formation are concerned by, two different ultrasonic powers were tested by modulating the wave amplitude in the ultrasonic generator (GAT600W ATU, Spain) (9, Figure 1). Thus, the actual powers supplied in the reaction media were 7.05 W/L (low) and 36.53 W/L (moderate) and the application was carried out in both cases in pulsed mode (30 min on and 30 min off). The actual power supplied in the reaction media was experimentally assessed using the calorimetric method (Cárcel *et al.*, 2007; Ahmad-Qasem *et al.*, 2013). For that purpose, the change in the temperature in the opaque glass bottles was measured by placing a type-K thermocouple in the centre of one bottle filled with 15 mL of water. The thermocouple was connected to a datalogger unit (34970A, Agilent, U.S.A.), and the data were saved and analysed in a PC (Agilent BenchLink Data Logger 3). Equation 1 was used to determine the ultrasonic power.

$$P = (M \times C_p) \times \left( \frac{dT}{dt} \right) \quad (\text{Equation 1})$$

Where P (W) is the ultrasonic power, M (kg) the mass of the reaction media,  $C_p$  (J/kg °C) the heat capacity (water) and  $dT/dt$  the rate of temperature change (Equation 1). The ultrasonic power was measured 5 times for every power tested and expressed as power density (W/L).

## 2.6. Extraction and quantification of zinc-protoporphyrin

The measurement of ZnPP formation requires its prior separation from the reaction media. For that purpose, 1 g of the reaction media was placed into solvent-resistant 38 mL centrifuge tubes (Nalgene Centrifuge Ware, PPCO), which were kept on ice and protected from the light. In each tube, 10 mL of the extraction solvent (dimethyl sulfoxide (DMSO), ethyl acetate (AcOEt) and glacial acetic acid in a ratio of 1:10:2 v/v/v) were added and the mixture was homogenised for 30 s with a vortex (Velp scientifica, 2 x 3 Advanced Vortex Mixer, Italy) and kept cold at 4 °C and in the dark for 20 min. Then, it was centrifuged for 20 min at 3100 rpm and 4 °C (Medifriger BL-S, SELECTA, Spain) and the supernatant was filtered (Whatman597, GE LIFE SCIENCE, USA). Subsequently, the filtrate was collected in 10 mL amber volumetric flasks. The filtrate was made up to a volume of 10 mL with the extraction solvent. Finally, the ZnPP concentration was measured following the methodology proposed by Wakamatsu *et al.* (2004). A 96-well plate fluorimeter (Infinite 200 Microplate Reader, TECAN, Switzerland) was used, which was adjusted to excitation and fluorescence emission peaks of 420 nm and 590 nm, respectively.

In order to quantify the ZnPP concentration (mg/L), a calibration curve of ZnPP was obtained. For that purpose, different dilutions of up to 2 mg/L were prepared from concentrated ZnPP (Sigma-Aldrich) using the reaction media as dilution medium. The calibration curve ( $r^2= 0.998$ ) is shown in Equation 2.

$$\text{ZnPP} = \frac{F - 8724}{22935} \quad (\text{Equation 2})$$

Where F is the fluorescence (RFU) and ZnPP is the concentration of the product formed (mg/L).

## 2.7. Statistical analysis

An analysis of variance (ANOVA) was carried out to examine the effect of the reaction medium (with antibiotics and with organic acids) and the reaction time on the ZnPP concentration. In addition, a one-way ANOVA was used to determine whether the effect of the US application had a significant effect on the ZnPP concentration of each homogenate (HLi and HLi+OxyHb). Fisher's least significant difference (LSD) procedure was used to discriminate between means ( $p < 0.05$ ). The analyses were performed using Centurion XVI software (Statpoint Technologies Inc., Warrenton, VA, USA).

## 3. Results and discusión

### 3.1. Conventional ZnPP formation from homogenised pork liver

Experiments were carried out on two types of homogenised pork liver: i) with antibiotics and ii) with ascorbic and acetic acids as preservatives. The two reaction media sought to inhibit the microbial growth during the ZnPP formation kinetics. Figure 2 shows the ZnPP formation kinetics carried out under anaerobic conditions for 48 h. For HLi with antibiotics, the ZnPP concentration increase during incubation followed an almost linear pattern up to 24 h ( $r = 0.991$ ), when the maximum concentration ( $\text{ZnPP}_{\text{max}}$ ) was reached (0.352 mmol/L). The average ZnPP formation rate from 0 to 24 h was 0.0151 mmol/L·h. After 24 h, the ZnPP concentration decreased slowly (0.0014 mmol/L·h). Wakamatsu *et al.* (2015) also studied the ZnPP formation in pork liver at 20% in a reaction medium with antibiotics, at pH 4.5, at 37 °C and during 5 days of anaerobic incubation. They observed that after 24 h of incubation the maximum concentration of ZnPP was reached. When studying homogenised Parma ham (*Biceps femoris*), Becker *et al.* (2012) reported that the maximum ZnPP concentration was

reached after 48 h. Meanwhile, Wakamatsu *et al.* (2007) reported that the ZnPP<sub>max</sub> in homogenised pork loin samples increased rapidly up to 72 h, which is consistent with the time reported for the pork *Longissimus lumborum* (Khozroughi *et al.*, 2017). However, the results obtained regarding the ZnPP formation in the HLi of the present study were obtained in less time (24 h). This could be due to the fact that the amount of substrate (porphyrins and Zn<sup>2+</sup>) and/or FeCH in pork liver is higher than in pork muscles, such as *Longissimus* and *Biceps femoris* (Wakamatsu *et al.*, 2007; Becker *et al.*, 2012; Khozroughi *et al.*, 2017). Moreover, the higher rate could also be ascribed to the state/structure of the reaction medium, which is solid (intact muscle fibers) in the muscles and liquid (dissolved unstructured tissue) in the liver homogenate. After 24 h, there is a trend towards lower ZnPP, which may be attributed to the instability of the ZnPP, leading to its degradation. On the other hand, Wakamatsu *et al.* (2019) studied how the pH of the reaction medium affected the formation of ZnPP in twenty types of pork muscles, observing that the optimal value for ZnPP formation was 4.75, a similar value to the pH considered in the present study (the HLi remained at pH 4.8 ± 0.05 throughout the incubation). However, Wakamatsu *et al.* (2019) postulated that the endogenous myoglobin (source of porphyrins for the ZnPP formation) was degraded during incubation at pH 4.75, limiting the formation of ZnPP.

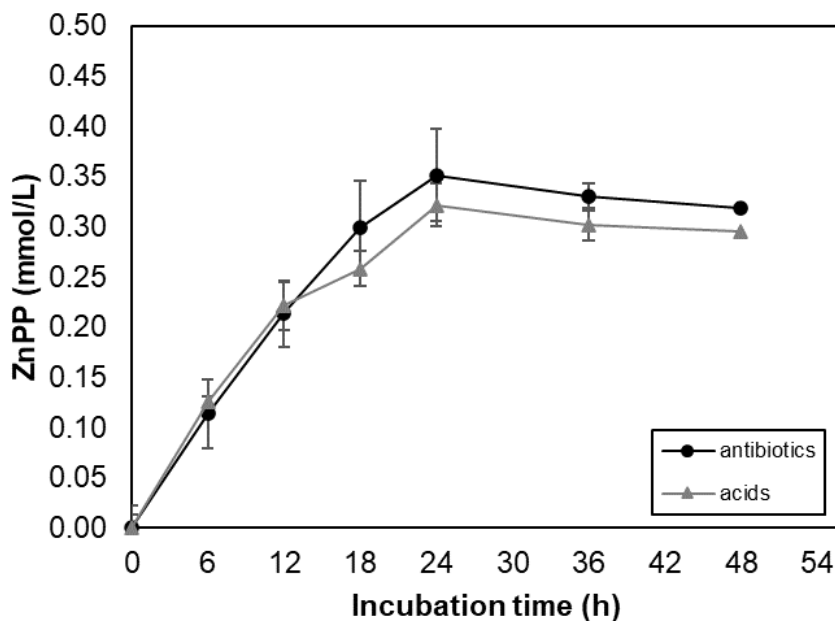


Figure 2. Conventional (without ultrasound) kinetics of ZnPP formation in homogenised pork liver reaction medium with antibiotics and acids. Average values  $\pm$  standard deviation are shown for each experimental incubation time (t).

As observed in Figure 2, the addition of acetic and ascorbic acids in the reaction medium, as microbial inhibitors, had an almost negligible impact on the ZnPP formation kinetics. Thus, the ZnPP concentration reached in the medium with organic acids was slightly lower (but not significantly,  $p > 0.05$ ) than that reached in the medium with antibiotics after 12 h of incubation, i.e., the ZnPP reached after 24 h was 0.321 mmol/L with acids compared to 0.352 mmol/L with antibiotics. Thereby, it could be postulated that the addition of organic acids to the HLi reaction medium could be very interesting as a substitute for antibiotics for the purposes of microbial growth control. Although it is true that microbial growth quantification has not been carried out in this study, if there has been, it has been minimal since the microorganisms have not interfered with the ZnPP formation. Nonetheless, the microbiological safety of the ZnPP formation process with organic acids has been addressed in previous studies and it was found that the initial total viable counts (unpublished data) were maintained. Therefore, it would be of great interest for future complementary studies to analyse the microbiota of the

homogenate after anaerobic incubation and its likely inactivation using emerging techniques (Mañas & Pagán, 2005).

### **3.2. Effect of power ultrasound (US) on the kinetics of ZnPP formation from homogenised pork liver**

The effect of US application on the ZnPP formation kinetics was studied at moderate-36.53 W/L (Figure 3) and low-7.05 W/L power (Figure 4) in HLi with organic acids. As Figure 3 illustrates, when a moderate power (36.53 W/L) was applied, the temperature control system was not able to prevent the temperature increase in the reaction medium related to US application. Thus, the temperature rose above the set-point of 37 °C and fluctuated at around 50 °C in the reaction medium, despite the temperature in the bulk water of the ultrasonic bath being kept at 37 °C. The increase in temperature and the ultrasonic application hindered the ZnPP formation, as observed in Figure 3, and only 0.037 mmol/L was obtained after 24h of incubation. These results were consistent with those reported by Becker *et al.* (2012) when analysing homogenised pork meat, who observed that above 60 °C no ZnPP formation was manifested. However, Numata & Wakamatsu (2005) reported that the optimum temperature of ZnPP formation in the liver was 55 °C (maximum ZnPP formation in only 3h), but the optimum pH for that temperature was found to be 6. Therefore, the results found at moderate power in the present study could be due to the temperature-pH combination, but also to a negative effect of the ultrasonic field, which could alter the enzyme integrity and the enzyme-substrate interaction. In addition, Dailey *et al.* (1994) studied the denaturation temperature profile of mammalian FeCH, showing that it denatures from 40 °C upwards. Therefore, the temperature profile (Figure 3) at moderate US power could have led to a thermal denaturation of FeCH during the process of ZnPP formation. Tian *et al.* (2004) also observed the same result in the enzymatic reaction of trypsin when they increased the US power (from 20 to 100 W/mL) for short treatment times (from 1 to 20 min), due to the rise in the temperature and pressure and to the formation of free radicals induced by the thermal dissociation of water due to US application, which affected the conformation of the enzyme and its stability. Therefore, depending on the US power applied, the structure of the enzymes

could be altered, affecting their stability and leading to their denaturation (Nadar & Rathod, 2017).

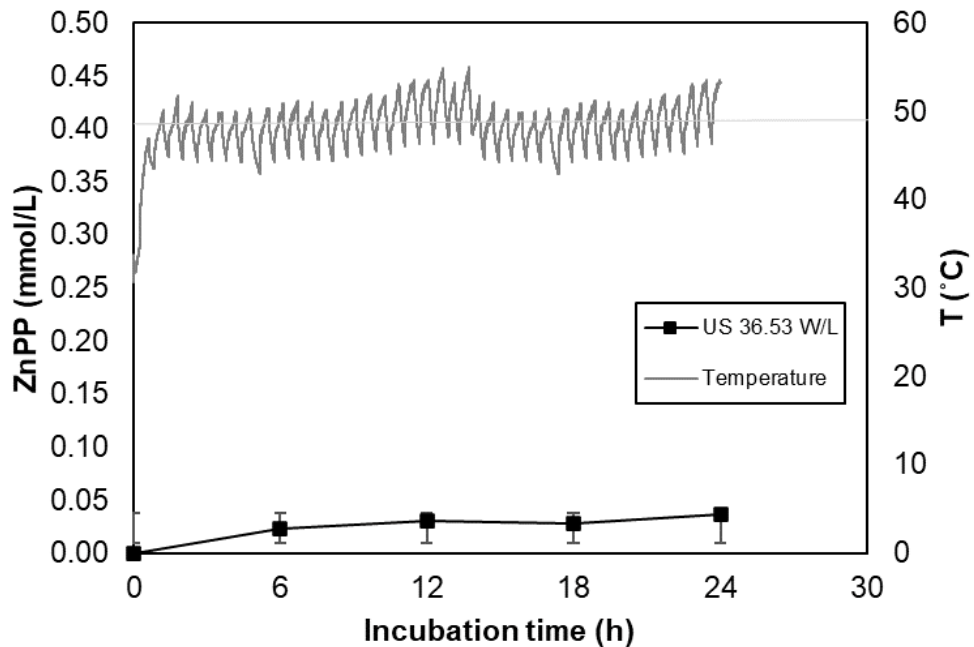


Figure 3. Kinetics of moderate power (36.53 W/L) ultrasound (US) assisted ZnPP formation in homogenised pork liver reaction medium (HLi) with organic acids and temperature (T) evolution in the reaction medium. Average values  $\pm$  standard deviation are shown for each experimental time (t).

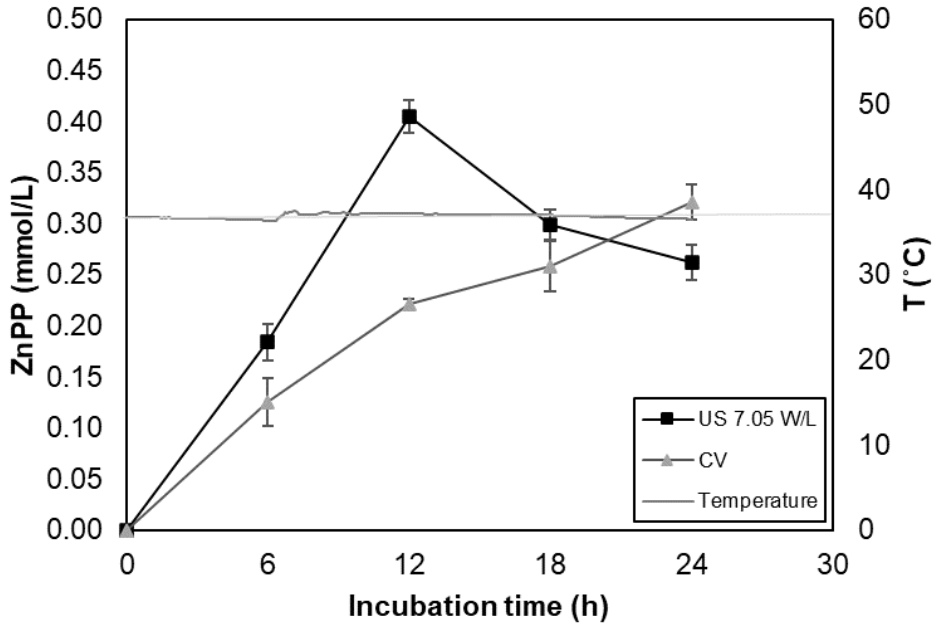


Figure 4. Kinetics of low power (7.05 W/L) ultrasound (US) assisted and conventional mode (CV), without US, ZnPP formation in homogenised pork liver reaction medium with organic acids (HLi) and temperature (T) evolution in the reaction medium. Average values  $\pm$  standard deviation are shown for each experimental time (t).

However, when the applied ultrasonic power was low (7.05 W/L), heat generation was less intense, and the temperature control system was able to keep a constant temperature of 37 °C in the reaction medium, as observed in Figure 4. Thus, low power (7.05 W/L) US application permitted the acceleration of the ZnPP formation when compared to CV mode. Therefore, the ZnPP<sub>max</sub> (0.405 mmol/L) was reached after 12 h, which represents 50 % less time than when using the CV mode (ZnPP<sub>max</sub> at 24 h). This could be linked to the fact that US energy improved the FeCH activity and promoted the ZnPP diffusion, obtaining a higher concentration in a shorter time by applying US (Abril *et al.*, 2021). Thus, low power US application caused an ultrasonic microagitation of the reaction medium that could favour the contact of FeCH with the substrates, as well as the ZnPP diffusion. The fact that US improves the enzymatic activity by facilitating the enzyme-substrate contact was previously reported by Yu *et al.* (2013) when studying the tyrosinase enzyme; this was activated with the US treatment, shortening the time of the first phase of the enzymatic reaction, which



consists of the binding of the substrates with the enzyme. In addition, as illustrated in Figure 4, the  $ZnPP_{max}$  reached when the low power (0.405 mmol/L) US was applied was significantly higher, 25.77 % more than in the case of CV kinetics (0.321 mmol/L). This could be explained by considering the simultaneous processes of formation and degradation of the ZnPP; thus, the concentration measured would be the net concentration, computed from the difference between the accumulated ZnPP formed and degraded at that time. Thereby, the  $ZnPP_{max}$  did not account for the total amount formed, but to the net, and its time location marked the moment when the rate of degradation was higher than that of formation. Another hypothesis that could explain this behaviour considers that the degradation occurs to the substrates of the reaction, the porphyrins, which degrade over time (Wakamatsu *et al.*, 2019). This substrate degradation could partly explain why  $ZnPP_{max}$  in CV experiments is not reached, as they have slower kinetics than US processing. If Figures 2 and 4 are compared, it may be elucidated that the net rate of ZnPP degradation was almost one order higher when US was applied; in CV mode, 0.0011 mmol/Lh in HLi was obtained, with respect to low power US application, in which 0.0119 mmol/Lh was found. Therefore, in the same way that US stimulates FeCH activity (Abril *et al.*, 2021), ZnPP degradation processes are also accelerated. So, when the  $ZnPP_{max}$  is achieved, the degradation of ZnPP is accelerated more drastically when US is applied. Further studies should address the mechanisms for ZnPP degradation and why US intensifies them.

### **3.3. Conventional and ultrasonic-assisted kinetics of ZnPP formation from homogenised pork liver with added oxyhemoglobin**

Once the kinetics of ZnPP formation from homogenised pork liver were addressed, the impact on ZnPP formation of the addition of oxyhemoglobin (OxyHb), as a substrate of protoporphyrin IX (PPIX), to the HLi with organic acid medium, was analysed. Two different external sources of OxyHb were used, one produced from a commercial pure chemical standard (Figure 5) and one extracted from pork blood (Figure 6). Thereby, conventional (CV) and low power ultrasonic-assisted (US) ZnPP formation kinetics were tested in the HLi+OxyHb reaction medium.

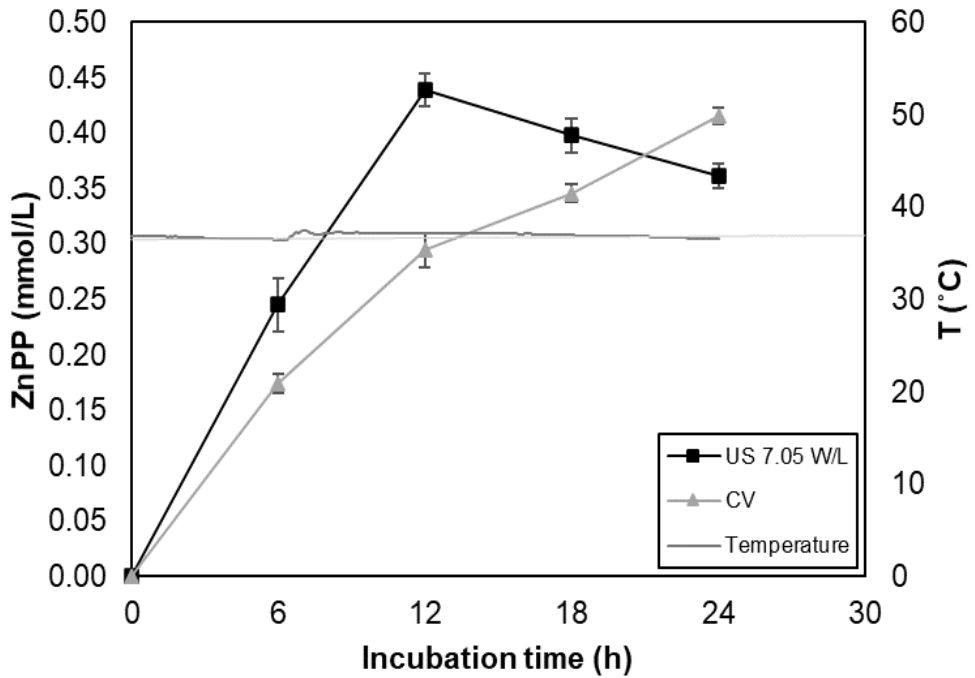


Figure 5. Kinetics of low power (7.05 W/L) ultrasound (US) assisted and conventional mode (CV), without US, ZnPP formation in homogenised pork liver with added OxyHb from commercial pure chemical standards (HLi+OxyHb) and temperature (T) evolution in the reaction medium. Average values  $\pm$  standard deviation are shown for each experimental time (t).

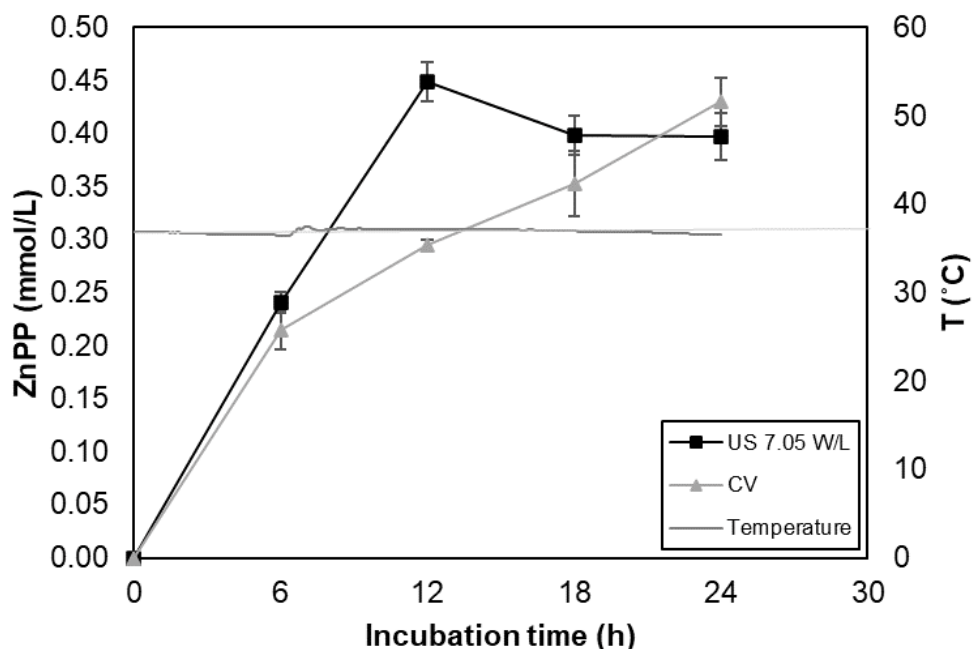


Figure 6. Kinetics of low power (7.05 W/L) ultrasound (US) assisted and conventional mode (CV), without US, ZnPP formation in homogenised pork liver with added OxyHb extracted from pork blood (HLi+OxyHb) and temperature (T) evolution in the reaction medium. Average values  $\pm$  standard deviation are shown for each experimental.

As for CV ZnPP formation kinetics, HLi+OxyHb was found to behave similarly to HLi, as illustrated in Figures 5 and 6. Thus, the highest ZnPP concentration was reached after 24 h and no significant differences ( $p > 0.05$ ) were found between the OxyHb from commercial pure chemical standards (0.415 mmol/L) (Figure 5) and the OxyHb extracted from pork blood (0.430 mmol/L) (Figure 6). Thereby, the addition of the OxyHb to HLi involved a moderate increase in the quantity of ZnPP formed (0.321 mmol/L for only HLi). Therefore, for any future industrial application, it could be of great interest to use the OxyHb extracted from pork blood, since as happens for liver, it is a co-product of low commercial value in the meat industry (Muflih *et al.*, 2017).

The US assisted ZnPP formation kinetics in HLi+OxyHb followed the same pattern as in HLi. Once again, low power US application (7.05 W/L) shortened the time needed to reach the  $ZnPP_{max}$  (12 h) by 50 %, compared to CV kinetics (24 h). As in the

case of CV kinetics, no significant ( $p>0.05$ ) differences were found between the ZnPP<sub>max</sub> obtained from HLi medium with added commercial pure chemical standards and that extracted from pork blood OxyHb (0.439 and 0.449 mmol/L, respectively). In addition, it should be noted that unlike the kinetics obtained from HLi, US application led only to a slight increase (4.42 %) in the ZnPP<sub>max</sub> reached from pork blood OxyHb with respect to ZnPP<sub>max</sub> obtained from CV mode (0.430 mmol/L in HLi OxyHb). This could be related to an additional degrading effect of OxyHb (Wakamatsu *et al.*, 2019) associated with US application, since low power US application intensifies the chemical reactions, shortening the process times (Rokhina *et al.*, 2009). In this regard, the oxidation reaction of OxyHb to MetHb could be limited, since the ZnPP formation took place in anaerobiosis. However, the US application could have promoted the reactions of the OxyHb with the hydrogen (H) present in the reaction medium and, consequently, could have given rise to other degradation products of the heme group (Nagababu *et al.*, 2010).

#### 4. Conclusions

US application could be considered an interesting alternative method to enhance the FeCH enzymatic activity, promoting ZnPP formation, in both pork liver homogenates (HLi and HLi+OxyHb). However, the effect of US mainly depends on the applied ultrasonic power. Thus, moderate power US application (36.53 W/L) largely reduced the ZnPP formation, which could be linked to the joint degradation effect of the rise in temperature above the target (37 °C) and the ultrasonic field. However, low power US application (7.05 W/L) was an effective method for the intensification of the enzymatic reaction, shortening the ZnPP formation time by 50 % and obtaining a higher ZnPP.

The present study could contribute to the sustainable production of a new natural ingredient from two co-products of the meat industry (liver and blood) that would offer interesting colouring properties. The use of the ZnPP pigment would permit the reduction in the quantity of chemical additives added (nitrates / nitrites) during the manufacturing of meat products. However, more research is needed into the application of this ultrasonic intensification for colour enhancement purposes in meat products, such as dry-cured ham or loin.

## Acknowledgements

The authors acknowledge the financial support from the “Ministerio de Economía y Competitividad (MINECO) and Instituto Nacional de Investigación y Tecnología Agraria y Alimentaria (INIA)” in Spain (Project RTA2017-00024-C04-03). The authors acknowledge the contribution of the slaughterhouse "Carnes de Teruel S.A." (D.O. Jamón de Teruel, Spain) for the supply of pork livers.

## References

- Abril, B., Sanchez-Torres, E. A., Bou, R., Garcia-Perez, J. V., & Benedito, J. (2021). Ultrasound intensification of Ferrochelataze extraction from pork liver as a strategy to improve ZINC-protoporphyrin formation. *Ultrasonics Sonochemistry*, *78*, 105703. <https://doi.org/10.1016/j.ultsonch.2021.105703>
- Ahmad-Qasem, M. H., Cánovas, J., Barrajón-Catalán, E., Micol, V., Cárcel, J. A., & García-Pérez, J. V. (2013). Kinetic and compositional study of phenolic extraction from olive leaves (var. Serrana) by using power ultrasound. *Innovative Food Science & Emerging Technologies*, *17*, 120-129. <https://doi.org/10.1016/j.ifset.2012.11.008>
- Alvarez, C., Rendueles, M., & Diaz, M. (2012). The yield of peptides and amino acids following acid hydrolysis of haemoglobin from porcine blood. *Animal Production Science*, *52*(5), 313-320. <https://doi.org/10.1071/AN11218>
- Becker, E. M., Westermann, S., Hansson, M., & Skibsted, L. H. (2012). Parallel enzymatic and non-enzymatic formation of zinc protoporphyrin IX in pork. *Food Chemistry*, *130*(4), 832-840. <https://doi.org/10.1016/j.foodchem.2011.07.090>
- Benedini, R., Raja, V., & Parolari, G. (2008). Zinc-protoporphyrin IX promoting activity in pork muscle. *LWT - Food Science and Technology*, *41*(7), 1160–1166. <https://doi.org/10.1016/j.lwt.2007.08.005>

- Benesch, R. E., Benesch, R., & Yung, S. (1973). Equations for the spectrophotometric analysis of hemoglobin mixtures. *Analytical biochemistry*, 55(1), 245-248. [https://doi.org/10.1016/0003-2697\(73\)90309-6](https://doi.org/10.1016/0003-2697(73)90309-6)
- Bou, R., Hanquet, N., Codony, R., Guardiola, F., & Decker, E. A. (2010). Effect of heating oxyhemoglobin and methemoglobin on microsomes oxidation. *Meat science*, 85(1), 47-53. <https://doi.org/10.1016/j.meatsci.2009.12.002>
- Bou, R., Llauger, M., Josse, R., & García-Regueiro, J. A. (2019). Effect of high hydrostatic pressure on the oxidation of washed muscle with added chicken hemoglobin. *Food chemistry*, 292, 227-236. <https://doi.org/10.1016/j.foodchem.2019.04.067>
- Bou, R., Llauger, M., Arnau, J., Olmos, A., & Fulladosa, E. (2022). Formation of Zn-protoporphyrin during the elaboration process of non-nitrified serrano dry-cured hams and its relationship with lipolysis. *Food Chemistry*, 374, 131730. <https://doi.org/10.1016/j.foodchem.2021.131730>
- Cárcel, J. A., Benedito, J., Bon, J., & Mulet, A. (2007). High intensity ultrasound effects on meat brining. *Meat Science*, 76(4), 611-619. <https://doi.org/10.1016/j.meatsci.2007.01.022>
- Contreras, M., Benedito, J., Bon, J., & Garcia-Perez, J. V. (2018). Accelerated mild heating of dry-cured ham by applying power ultrasound in a liquid medium. *Innovative Food Science and Emerging Technologies*, 50, 94-101. <https://doi.org/10.1016/j.ifset.2018.10.010>
- Dailey, H. A., Sellers, V. M., & Dailey, T. A. (1994). Mammalian ferrochelatase. Expression and characterization of normal and two human protoporphyrin ferrochelatases. *Journal of Biological Chemistry*, 269(1), 390-395. [https://doi.org/10.1016/S0021-9258\(17\)42362-3](https://doi.org/10.1016/S0021-9258(17)42362-3)

- De Maere, H., Chollet, S., Claeys, E., Michiels, C., Govaert, M., De Mey, E., ... & Fraeye, I. (2017). In vitro zinc protoporphyrin IX formation in different meat sources related to potentially important intrinsic parameters. *Food and bioprocess technology*, *10*(1), 131-142. <https://doi.org/10.1007/s11947-016-1804-0>
- Ishikawa, H., Kawabuchi, T., Kawakami, Y., Sato, M., Numata, M., & Matsumoto, K. (2007). Formation of zinc protoporphyrin IX and protoporphyrin IX from oxymyoglobin in porcine heart mitochondria. *Food science and technology research*, *13*(1), 85-88. doi: 10.3136/fstr.13.85
- Khan, M. K., Imran, M., Ahmad, M. H., Hassan, S., & Sattar, S. (2021). Ultrasound for beverage processing. In *Design and Optimization of Innovative Food Processing Techniques Assisted by Ultrasound*, 189-215 Academic Press. <https://doi.org/10.1016/B978-0-12-818275-8.00007-6>
- Khozroughi, A. G., Jander, E., Schirrmann, M., Rawel, H., Kroh, L. W., & Schlüter, O. (2017). The role of myoglobin degradation in the formation of zinc protoporphyrin IX in the longissimus lumborum of pork. *LWT-Food Science and Technology*, *85*, 22-27. <https://doi.org/10.1016/j.lwt.2017.06.047>
- Lerin, L. A., Feiten, M. C., Richetti, A., Toniazzo, G., Treichel, H., Mazutti, M. A., Vladimir Oliveira, J., Oestreicher, E. G., & De Oliveira, D. (2011). Enzymatic synthesis of ascorbyl palmitate in ultrasound-assisted system: Process optimization and kinetic evaluation. *Ultrasonics Sonochemistry*, *18*(5), 988–996. <https://doi.org/10.1016/j.ultsonch.2010.12.013>
- Mañas, P., & Pagán, R. (2005). Microbial inactivation by new technologies of food preservation. *Journal of applied microbiology*, *98*(6), 1387-1399. [10.1111/j.1365-2672.2005.02561.x](https://doi.org/10.1111/j.1365-2672.2005.02561.x)
- Muflih, B. K., Ahmad, N. S., Jamaludin, M. A., & Nordin, N. F. H. (2017). The concept and component of contaminated animals (Al-Jallalah Animals). *International Food Research Journal*, *24*(Suppl.).

- Muñoz-Almagro, N., Montilla, A., Moreno, F. J., & Villamiel, M. (2017). Modification of citrus and apple pectin by power ultrasound: Effects of acid and enzymatic treatment. *Ultrasonics sonochemistry*, 38, 807-819. <https://doi.org/10.1016/j.ultsonch.2016.11.039>
- Nadar, S. S., & Rathod, V. K. (2017). Ultrasound assisted intensification of enzyme activity and its properties: a mini-review. *World Journal of Microbiology and Biotechnology*, 33(9), 1-12. <https://doi.org/10.1007/s11274-017-2322-6>
- Nagababu, E., Mohanty, J. G., Bhamidipaty, S., Ostera, G. R., & Rifkind, J. M. (2010). Role of the membrane in the formation of heme degradation products in red blood cells. *Life sciences*, 86(3-4), 133-138. <https://doi.org/10.1016/j.lfs.2009.11.015>
- Numata, M., & Wakamatsu, J. (2005). U.S. Patent Application No. 10/503,338.
- Parolari, G., Aguzzoni, A., & Toscani, T. (2016). Effects of processing temperature on color properties of dry-cured hams made without nitrite. *Foods*, 5(2), 33. <https://doi.org/10.3390/foods5020033>
- Priya, & Gogate, P. R. (2021). Ultrasound-Assisted Intensification of Activity of Free and Immobilized Enzymes: A Review. *Industrial & Engineering Chemistry Research*, 60(27), 9650-9668. <https://doi.org/10.1021/acs.iecr.1c01217>
- Rokhina, E. V., Lens, P., & Virkutyte, J. (2009). Low-frequency ultrasound in biotechnology: state of the art. *Trends in biotechnology*, 27(5), 298-306. <https://doi.org/10.1016/j.tibtech.2009.02.001>
- Snell, S. M., & Marini, M.A. (1988). A convenient spectroscopic method for the estimation of hemoglobin concentrations in cell-free solutions. *Journal of biochemical and biophysical methods*, 17(1), 25-33. [https://doi.org/10.1016/0165-022X\(88\)90075-9](https://doi.org/10.1016/0165-022X(88)90075-9)
- Tian, Z. M., Wan, M. X., Wang, S. P., & Kang, J. Q. (2004). Effects of ultrasound and additives on the function and structure of trypsin. *Ultrasonics Sonochemistry*, 11(6), 399-404. <https://doi.org/10.1016/j.ultsonch.2003.09.004>



- Verma, A. K., Chatli, M. K., Mehta, N., & Kumar, P. (2022). Antimicrobial and antioxidant potential of papain liver hydrolysate in meat emulsion model at chilling storage under aerobic packaging condition. *Waste and Biomass Valorization*, 13(1), 417-429. <https://doi.org/10.1016/B978-0-12-820563-1.00017-2>
- Wakamatsu, J., Okui, J., Ikeda, Y., Nishimura, T., & Hattori, A. (2004). Establishment of a model experiment system to elucidate the mechanism by which Zn-protoporphyrin IX is formed in nitrite-free dry-cured ham. *Meat Science*, 68(2), 313-317. <https://doi.org/10.1016/j.meatsci.2004.03.014>
- Wakamatsu, J. I., Okui, J., Hayashi, N., Nishimura, T., & Hattori, A. (2007). Zn protoporphyrin IX is formed not from heme but from protoporphyrin IX. *Meat Science*, 77(4), 580-586. <https://doi.org/10.1016/j.meatsci.2007.05.008>
- Wakamatsu, J. I., Murakami, N., & Nishimura, T. (2015). A comparative study of zinc protoporphyrin IX-forming properties of animal by-products as sources for improving the color of meat products. *Animal Science Journal*, 86(5), 547-552. <https://doi.org/10.1111/asj.12326>
- Wakamatsu, J. I., Akter, M., Honma, F., Hayakawa, T., Kumura, H., & Nishimura, T. (2019). Optimal pH of zinc protoporphyrin IX formation in porcine muscles: Effects of muscle fiber type and myoglobin content. *LWT*, 101, 599-606. <https://doi.org/10.1016/j.lwt.2018.11.040>
- Yao, Y., Pan, Y., & Liu, S. (2020). Power ultrasound and its applications: A state-of-the-art review. *Ultrasonics sonochemistry*, 62, 104722. <https://doi.org/10.1016/j.ultsonch.2019.104722>
- Yu, Z. L., Zeng, W. C., & Lu, X. L. (2013). Influence of ultrasound to the activity of tyrosinase. *Ultrasonics sonochemistry*, 20(3), 805-809. doi: <https://doi.org/10.1016/j.ultsonch.2012.11.006>

Zhai, Y., Wang, H. C., Hayakawa, T., Kumura, H., & Wakamatsu, J. I. (2022). Zinc protoporphyrin IX predominantly exists as a complex non-enzymatically bound to apo-hemoglobin in Parma ham. *Food Chemistry*, 395, 133604. <https://doi.org/10.1016/j.foodchem.2022.133604>



## **CAPÍTULO 2**

*Secado y desgrasado de hígado de cerdo*



*Influence of pork liver drying on ferrochelatase activity for zinc protoporphyrin formation*

---

Blanca Abril<sup>1</sup>, Eduardo A. Sánchez Torres<sup>1</sup>, Ricard Bou<sup>2</sup>, José Benedito<sup>1</sup>  
and José Vicente García-Pérez<sup>1</sup>

<sup>1</sup>Department of Food Technology, Universitat Politècnica de València, Camí de Vera, s/n, Valencia 46022, Spain

<sup>2</sup>IRTA, XaRTA, Food Technology, Finca Camps i Armet, Monells, Girona E-17121, Spain



## **Influence of pork liver drying on ferrochelatase activity for zinc protoporphyrin formation**

### **Abstract**

Pork liver contains an endogenous enzyme, ferrochelatase (FeCH), which catalyses the formation of zinc protoporphyrin (ZnPP), a natural pigment of great interest for the meat industry. The aim of this study was to analyse the effect of pork liver drying (from -10 to 70 °C), as a stabilisation method, on the FeCH activity (EA) and the apparent concentration ( $EC_{app}$ ). Drying temperatures close to room conditions (from 10 to 20 °C) allowed to preserve well the  $EC_{app}$ , while the EA was slightly lower (-15.2 %) than in raw liver. However, when drying was conducted at extreme conditions (-10 and 70 °C), the lowest values of  $EC_{app}$  and EA were manifested. Therefore, the drying process at moderate temperatures close to room conditions (10 – 20 °C) was considered to be an effective method for FeCH preservation since it was possible to stabilise the liver and the loss of FeCH activity was minimised.

**Keywords:** Ferrochelatase; zinc protoporphyrin; drying; pork liver; coproduct, revalorisation



## 1. Introduction

Currently, there is increasing demand for natural ingredients, thereby avoiding the use of chemicals in the food industry. In this context, zinc protoporphyrin (ZnPP) could be considered a natural ingredient with noticeable technological properties. ZnPP is a compound found in red blood cells, similar to the heme group, except that the iron atom (Fe) of the porphyrin ring has been replaced by a zinc atom (Zn). Furthermore, unlike the heme group, the ZnPP complex exhibits a high level of fluorescence and is easily detectable in small amounts. ZnPP is of great technological interest due to its reddish colour and its high degree of light and thermal stability (Morita *et al.*, 1996; Adamsen *et al.*, 2004). Wakamatsu *et al.* (2004a) postulated the ZnPP formation in Parma ham, this compound being responsible for the characteristic purple-red colour of this type of ham, which is manufactured using neither nitrates nor nitrites. Therefore, the use of ZnPP as a colorant for the purposes of improving the colour of meat products, both dry-cured and cooked, is of great interest at industrial level.

The ZnPP formation is catalysed by the enzyme ferrochelatase (FeCH), which facilitates the replacement of the Fe atom, present in the heme group, by the Zn atom (Chau *et al.*, 2010; Chau *et al.*, 2011). Taketani & Tokunaga (1982) found that the FeCH could be extracted from the bovine liver to obtain ZnPP. In addition, subsequent studies demonstrated that one of the most interesting sources of FeCH, from which it is possible to obtain the ZnPP pigment, was pork liver (Wakamatsu *et al.*, 2015). Nowadays, pork liver is a co-product of the meat industry; it is of low commercial value and is mainly used for the production of pâtés and animal feed (Estévez *et al.*, 2004). In slaughterhouses, large quantities of co-products and residues, such as liver, heart, kidney, skin, blood or bones, are generated. Every year, around 330 million animals (cows, sheep, pigs and goats) are slaughtered in the EU, which generates more than 17 million tons of meat co-products (EFPRA, 2021). The management of co-products, as well as the elimination of waste from the meat industry, is becoming a serious concern, contributing to environmental pollution. For this reason, it is necessary to seek new uses for meat co-products that allow their revaluation, thus contributing to the concept of circular economy (Echegaray *et al.*, 2018). In this context, pork liver extracts

with a high degree of FeCH activity are postulated as potential food ingredients for the meat industry, due to their ability to catalyse ZnPP formation (Abril *et al.*, 2021). However, liver is a perishable product due to its large amount of water and heavy microbial load. Consequently, drying represents a necessary stage in the stabilisation of pork liver in order to prolong its shelf life at a moderate cost. This would facilitate both the FeCH extraction and the subsequent valorisation of the protein fraction.

Convective drying, using forced air, is the most popular dehydration technique in the food industry. During drying, the moisture is removed by evaporation or sublimation, depending on the process temperature (Santacatalina *et al.*, 2011). Sanchez-Torres *et al.* (2021) recently reported the sorption isotherms of pork liver, which are essential for the optimal design of its drying process, allowing the subsequent extraction of enzymes or protein fractions. Drying reduces the water availability for enzymatic and microbial degradation (Baque *et al.*, 201). However, drying may affect the structure and activity of food enzymes (Oyinloye & Yoon, 2020). Enzyme degradation will depend on the stress caused during drying, which is mainly dependent on the drying temperature and time. Temperature is a key factor for enzymes since, in some cases, they maintain their activity at temperatures below 4 °C (known as cold-adapted enzymes), while other enzymes are active at temperatures above 95 °C (known as thermostable enzymes) (Kuddus, 2019). On the one hand, heat exposure may reduce the enzymatic activity due to the denaturation of the protein structure (Guiné, 2018). Thus, Perdana *et al.* (2012) carried out a study into the influence of drying on the  $\beta$ -galactosidase enzyme in the maltodextrin matrix, observing that the enzymes are heat sensitive and, therefore, can be partially or completely inactivated during drying, depending on the temperature applied. These authors observed that the  $\beta$ -galactosidase inactivation is more intense (inactivation rate 0.001 mol-s<sup>-1</sup>) at the beginning of drying and reported a reduction of only 3% in the enzymatic activity caused by spray drying. On the other hand, drying at low temperatures may also cause a decrease in the enzyme activity (Roy & Gupta, 2004) due to the fact that this type of drying involves lengthy exposure to the stress characteristic. Thus, Parra Vergara (2013) observed a significant decrease in the activity of the peroxidase enzyme in lyophilised broccoli (10.50 % residual peroxidase enzyme activity, UPOD) compared to

the fresh broccoli. In this context, an analysis of the effect of temperature on pork liver drying, as a pre-treatment to the further FeCH extraction, would help us gain insight not only into the drying process, but also into the impact on the activity of the extracted enzyme. In this regard, there have been no previous references addressing the drying of pork liver or other meat co-products for further enzyme extraction over a wide temperature range. Therefore, the objective of this study was to assess the impact of temperature (from -10 to 70 °C) on the drying kinetics of liver and the FeCH activity for ZnPP formation obtained from the dehydrated product.

## **2. Materials and methods**

### **2.1. Raw material and sample preparation**

Raw pork livers were obtained from the slaughterhouse “Carnes de Teruel S.A.” (D.O. Jamón de Teruel, Spain) and transported to the laboratory in refrigeration ( $4 \pm 2$  °C). The initial preparation of the pork liver firstly consisted of the separation of its 4 main lobes: the right lateral, left lateral, right medial and left medial. Secondly, each lobe was divided into 2 parts, and all the obtained parts were vacuum packaged (200 × 300 PA/PE, Sacoliva, Castellar del Vallès, Barcelona), labelled with a number corresponding to the liver and the lobe and stored at -20 °C until used in the drying experiments. For each drying experiment, 2 parts were taken out of the freezer (-20 °C), avoiding taking parts from the same liver and kept in refrigeration ( $4 \pm 2$  °C) for two hours before use. Afterwards, cylindrical samples (15 mm in height and 12.6 mm in diameter) were obtained using a household tool and the remaining part of the liver was homogenized and used to determine the initial moisture content and FeCH activity, as explained in sections 2.5 y 2.6. For each drying process, 20 cylindrical samples were placed into a custom sample holder inside the drying chamber, weighing  $43 \pm 0.5$  g.

### **2.2. Determination of moisture content**

The moisture content was determined using the AOAC method nº 940.44 (AOAC, 1997). Approximately 3 g of liver were homogenised by grinding (Manta BL201, 200W, Spain). Then, 2 g of sand were mixed with 3 g of the sample and placed into a convective oven (ED 115, Binder GmbH, Alemania) at 105 °C for 24 h. Afterwards, the

samples were placed into a desiccator for tempering before weighing. The moisture content was determined in triplicate for each experimental run.

### 2.3. Convective drying at low and high temperatures

The two types of convective drying processes were defined from the standard room conditions (20 °C) (Santacatalina *et al.*, 2014). Low temperature drying was carried out at temperatures equal to or lower than the standard room conditions (20, 10, 0 and -10 °C) whereas high temperature drying was carried out at temperatures above the standard room conditions (30, 40, 50, 60 and 70 °C).

The drying experiments were carried out in two different convective driers with temperature and air velocity control, which have already been described in the literature (García-Pérez *et al.*, 2011; García-Pérez *et al.*, 2012). The weight of the sample was automatically measured and recorded at regular time intervals. High temperature drying experiments were carried out in the drying chamber, which was made up of an aluminium cylinder (internal diameter 10 cm, height 31 cm, and thickness 1 cm) where the sample holder was located. The heating set-up consisted of a ventilation system, which had a medium pressure centrifugal fan (COT-100, Soler & Palau, Spain) that drove the drying air into the drying chamber, previous to which it had passed through the heating resistors controlled by a PID algorithm from a PLC (PLC CQM41, OMRON, Japan). Air velocity ( $2 \pm 0.1$  m/s) was measured by a winged wheel anemometer (1468, Wilh, Lambrecht GmbH, Germany).

As regards low temperature drying, the experiments were carried out in a drying chamber comprised of an aluminium cylinder (internal diameter 10 cm, height 31 cm, and thickness 1 cm) inside which the cylindrical liver samples were placed in the sample holder. A centrifugal fan (COT-100, Soler & Palau, Spain) was in charge of driving the air flow through the drying chamber and the air velocity was measured with an anemometer (1468, Wilh. Lambrecht GmbH, Germany). The airflow was controlled by a PLC (cFP-2220, National Instruments, USA) using a PID algorithm and acting on a frequency inverter (MX2, Omron, Japan). The air temperature was modified by combining a heat exchanger and electric resistors. The airflow was cooled down as it passed through the heat exchanger (area 13 m<sup>2</sup>, fin space 9 mm; Frimetal, Spain) which

was connected to refrigeration equipment and, subsequently, the electrical resistors adjusted the desired temperature using a PID algorithm. The relative humidity of the drying air was kept below 15 % by passing the airflow through a set of trays with a bed of desiccant material (drying bead height 1.5 cm, particle size 6-8 mm, Rung Rueng Cosulting, Thailand). The trays were periodically refilled with new desiccant material regenerated in an oven at 150 °C (ED 115, Binder GmbH, Germany).

The drying experiments were conducted in triplicate and completed when the samples lost 70 % of their initial weight. Subsequently, they were ground and the final moisture content was determined. Finally, the samples were vacuum packed and stored at  $4 \pm 2$  °C until the enzymatic activity was measured.

#### 2.4. Drying kinetics and mathematical model fitting

Mathematical modelling of the drying kinetics is necessary to assess the influence of the drying temperature and predict the behaviour of the material under different process conditions. The empirical Weibull model was used to compute the influence of the temperature on the drying time. Equation 1 illustrates the probabilistic distribution of Weibull used to describe the evolution of moisture during drying (Cunha *et al.*, 1998).

$$W_t = W_e + (W_0 - W_e) \cdot \exp\left[-\left(\frac{t}{\beta}\right)^\alpha\right] \quad (\text{Equation 1})$$

Where  $W_t$  is the average moisture content (kg water/kg dry matter) at time  $t$  (s),  $W_e$  is the equilibrium moisture content (kg water/kg dry matter) and  $W_0$  is the initial moisture content (kg water/kg dry matter). As for the Weibull distribution model,  $\beta$  is the kinetic parameter (s), having an inverse relationship with the drying rate; that is, the higher the  $\beta$ , the slower the process.  $\alpha$ , meanwhile, is the shape parameter, reflecting the behaviour of the sample during drying (Cunha *et al.*, 1998). The shape parameter is related to the velocity of the mass transfer at the beginning; thus, the lower the  $\alpha$  value, the faster the initial drying rate (Buzrul, 2022). If  $\alpha > 1$ , this indicates an initial

delay in the drying process and  $\alpha = 1$  means that the model presents a first order kinetics.

The parameters of the Weibull model were identified by minimising the sum of the squared differences between the experimental and calculated moisture using the Solver Microsoft Excel™ tool, available in the Microsoft Excel spreadsheet, which uses the Generalised Reduced Gradient optimisation method (GRG) (García-Pérez, 2007). The percentages of the mean relative error (%MRE, Equation 2) and explained variance (%VAR, Equation 3) were computed to assess the goodness of the fit.

$$\%MRE = \frac{100}{N} \left[ \sum_{i=1}^N \frac{|W_{exp} - W_{cal}|}{W_{exp}} \right] \quad (\text{Equation 2})$$

$$\%VAR = \left[ 1 - \frac{S_{xy}^2}{S_y^2} \right] \cdot 100 \quad (\text{Equation 3})$$

Where  $W_{exp}$  and  $W_{cal}$  are the experimental and the estimated moisture, respectively;  $N$  is the number of experimental data and  $S_{xy}$  and  $S_y$  are the standard deviations of the estimation and the sample deviation, respectively.

From simulated drying kinetics at the different temperatures, the drying time required to reach a moisture content of 0.10 kg water/kg dry matter (70 % loss of the initial weight) was computed using the identified Weibull parameters in order to better compare the influence of the temperature. This approach minimises the experimental error of computing the drying time from experimental data. The kinetic parameter of the Weibull model (inverse of  $\beta$ ) presents an Arrhenius-type relationship with the temperature (Meziane, 2011), as shown by Equation 4.

$$\frac{1}{\beta} = \frac{1}{\beta_0} \exp\left(\frac{-E_a}{RT}\right) \quad (\text{Equation 4})$$

Where  $1/\beta_0$  ( $s^{-1}$ ) is the pre-exponential factor,  $E_a$  (kJ/mol) the activation energy,  $R$  (kJ/mol K) the universal gas constant and  $T$  (K) the drying temperature.

## 2.5. Ferrochelatase extraction

The Ferrochelatase (FeCH) enzyme was extracted from raw pork liver following the methodology proposed by Abril *et al.* (2021), whereas some minor modifications in this methodology were introduced when FeCH was extracted from the dried liver due to the moisture reconstitution. Firstly, 3 g of dried pork liver was ground (Blixer 2, Robot Coupe USA, Inc., Jackson Ms, USA). Secondly, the ground dried pork liver was rehydrated with distilled water (0.7 g of water per 0.3 g of dried liver) until it reached its initial moisture content. Thus, 1 g of raw or reconstituted dried liver was homogenised (Homogeniser DI 25 Basic, IKA, Germany) with 25 mL of extraction buffer at 4 °C for 1 min, at 8000 rpm, using a 50 mL glass beaker. The extraction buffer was made up of 50 mM Tris-HCl, 20 % Glycerol (w/v), 0.8 % KCl (w/v) and 1 % Triton X-100 (w/v) (Sigma Aldrich) and was adjusted to pH= 8 with NaOH. Secondly, FeCH extraction was carried out by stirring for 30 min using a magnetic stirrer (SM3, STUART, UK). Subsequently, the FeCH extract was kept at  $4 \pm 2$  °C in order to avoid modifications in the enzyme. Finally, in order to separate the enzyme fraction, the sample was centrifuged for 10 min at 12500 rpm and at 4 °C (Medifriger BL-S, SELECTA, Spain), and then the obtained supernatant was filtered (Whatman 597, GE LIFE SCIENCE, United States). This fraction containing the FeCH was used as the enzyme source in the formation kinetics of ZnPP.

## 2.6. Zinc-protoporphyrin formation kinetics

ZnPP formation kinetics were carried out following the experimental method described by Abril *et al.* (2021). The enzymatic reaction was produced in microtubes of 2 mL, incubated at  $37 \pm 0.5$  °C in a water bath. Thus, the FeCH fraction obtained from the liver extract (300 µL) was mixed with the two substrates: Zinc (250 µL ZnSO<sub>4</sub> in Tris-HCl buffer, adjusted to pH=8.0), and the protoporphyrin source (50 µL Protoporphyrin IX in Tris-HCl buffer, adjusted to pH=7.0). In addition, ATP (200 µL of ATP solution in 20 % NaCl, w/v) was also added to the mixture. Blank samples were used to detect any background fluorometric signal from the reagents and were prepared by adding all the reagents except the 300 µL of the FeCH fraction (liver extract).

The microtubes were incubated at different times (0, 15, 30, 45, 60, 90, 105, 120 min) to determine the reaction kinetics of ZnPP formation. The enzymatic reaction was stopped by adding 35  $\mu\text{L}$  of EDTA and 840  $\mu\text{L}$  of cold absolute ethanol. Then, the samples were centrifugated for 30 min at 13200 rpm and 4  $^{\circ}\text{C}$  (5415R, EPPENDORF, Germany) and, subsequently, the obtained supernatant was measured by fluorescence (200  $\mu\text{L}$ ). Fluorescent analyses were carried out as described by Wakamatsu *et al.* (2004b), with minor modifications. The fluorescence spectrum of ZnPP was measured from 420 to 590 nm for the purposes of excitation using a spectrofluorophotometer with an 96-well plate (Infinite 200 Microplate Reader, TECAN, Switzerland). In order to determine the concentration of ZnPP ( $\mu\text{M}$ ), the calibration curve reported by Abril *et al.* (2021) was considered. ZnPP formation kinetics were carried out in triplicate for pork liver dried at the different temperatures, while it was also performed using the remaining raw pork liver in each drying run.

Abril *et al.* (2021) defined the enzyme activity, expressed in terms of the product formation rate, as the derivative of ZnPP concentration with time, as shown in Equation 5.

$$EA = \frac{dP}{dt} \quad (\text{Equation 5})$$

Where EA is the enzyme activity ( $\mu\text{M}/\text{min}$ ), P the ZnPP concentration ( $\mu\text{M}$ ), and t the time (min).

Using a FeCH source from raw pork liver, Abril *et al.* (2021) observed two phases in the kinetics of ZnPP formation: i) an initial burst phase during the first 15 min followed by ii) a steady rate phase. The burst phase indicates an initial stage in the enzyme reaction which occurs at a very high rate, related to the first turnover of the active sites (Praestgaard *et al.*, 2011). Afterwards, the enzyme reaction enters the steady state phase in which a constant reaction rate is manifested, coinciding with the slope of the linear relationship and computing the enzyme activity (EA). Meanwhile, the y-intercept would represent the ZnPP concentration formed during the first turnover of the enzyme, being directly proportional to the active enzyme concentration and possibly



postulated as an apparent-FeCH concentration ( $EC_{app}$ ,  $\mu\text{M}$ ) (Sassa *et al.*, 2013).

## 2.7. Statistical analysis

The influence of the drying temperature on the FeCH concentration and enzyme activity was statistically evaluated by analysis of variance (ANOVA). Fisher's least significant difference (LSD) procedure was used to identify the differences between the averages with a confidence interval of 95 % ( $p < 0.05$ ). The Statistical analysis was performed by using Centurion XVI software (Statpoint Technologies Inc., Warrenton, VA, USA).

## 3. Results and discussion

### 3.1. Drying of pork liver at different temperatures

In order to evaluate the influence of air temperature on drying kinetics, experiments were carried out at temperatures ranging from  $-10$  to  $70$  °C. As stated in Section 2.4., an experimental moisture content of  $0.10$  kg water/kg dry matter (70 % loss of the initial weight) was set to determine the drying time. The results obtained for the experiments showed that the air temperature affected the drying kinetics, shortening the drying time (Figures 1A and 2A). Thus, the drying times necessary to achieve a 70 % loss in the initial weight ranged between  $838.8$  h at  $-10$  °C and  $12.1$  h at  $70$  °C (Table 1). This large time difference can be explained if we consider that, the water changes from a solid to a vapour state in the atmospheric drying experiment ( $-10$  °C), a phenomenon known as sublimation, and further diffusion of the vapour through the drying solid occurs at very low temperatures (García-Pérez *et al.*, 2012). However, in the case of experiments performed above the freezing point of water ( $0$  °C), molecules in a liquid state move by diffusion through the solid being dried and the phase change from liquid to gas occurs at the air-solid interface. The use of temperatures above the freezing point of water may be of great interest since the prior freezing of the sample is not required. Moreover, the freezing of the sample can lead to the degradation of its internal structure brought about by the growth of ice crystals (Santacatalina *et al.*, 2016).

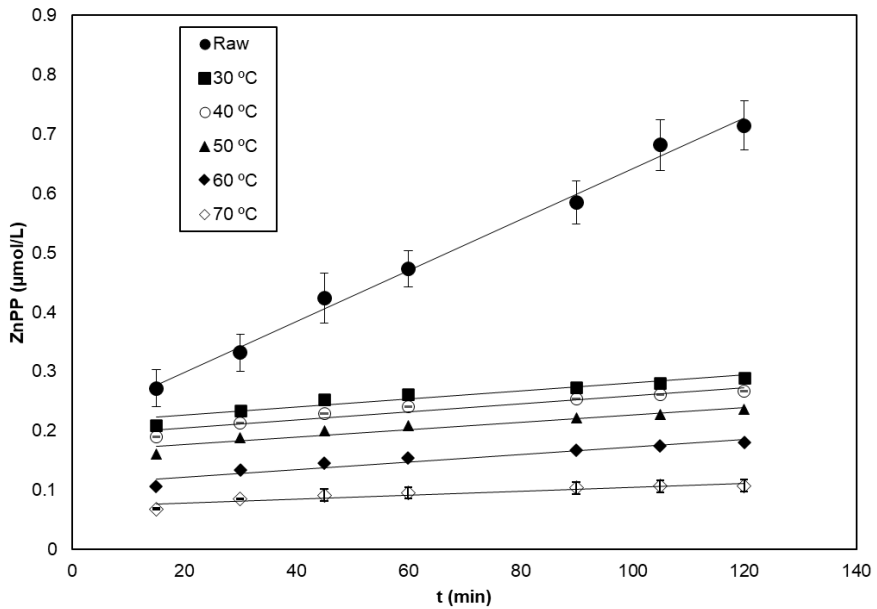
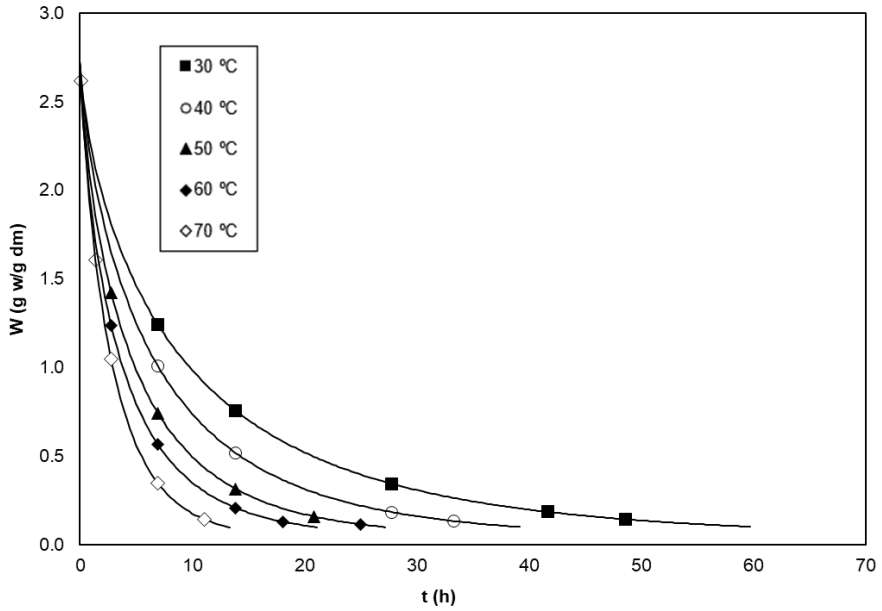


Figure 1. Experimental and simulated (Weibull model) drying kinetics of pork liver at high temperatures (A) and the kinetics of ZnPP formation using dried and raw pork livers as sources of FeCH (B).

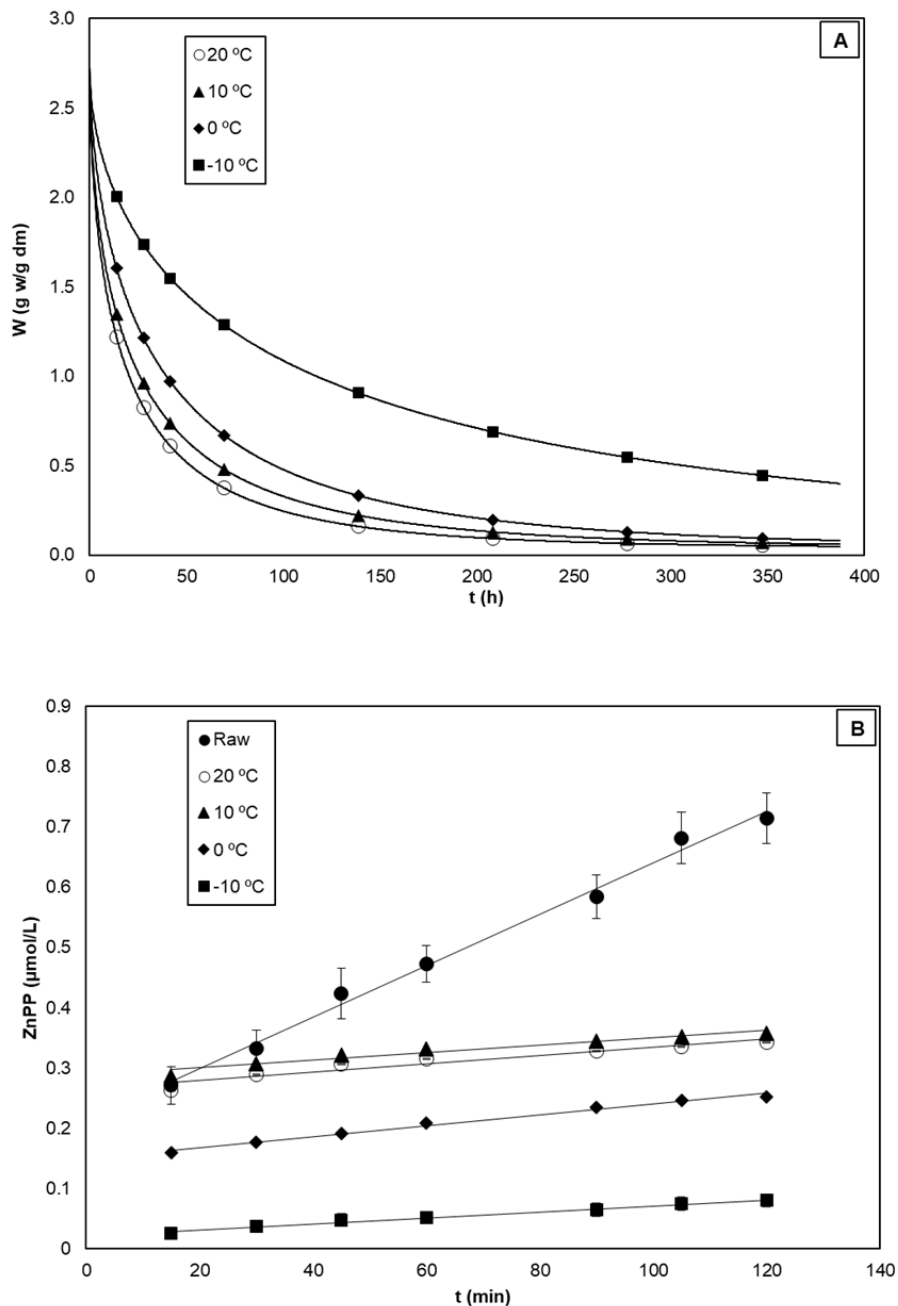


Figure 2. Experimental and simulated (Weibull model) drying kinetics of pork liver at low temperatures (A) and the kinetics of ZnPP formation using dried and raw pork livers as sources of FeCH (B).

Table 1. Drying time and Weibull model parameters at different temperatures for the drying of pork liver.

<b>T</b> (°C)	<b>t*</b> (h)	<b>α</b>	<b>β</b> (10 <sup>3</sup> s)	<b>%VAR</b>	<b>%MRE</b>
<b>-10</b>	838.8 ± 68.9	0.56±0.01	402.3±2.2	99.9 ± 0.1	1.00±0.33
<b>0</b>	325.1 ± 79.2	0.61±0.02	136.9 ± 4.4	99.9 ± 0.1	1.61±0.94
<b>10</b>	225.6 ± 25.9	0.57±0.01	89.2 ± 8.7	99.9 ± 0.1	1.21±0.72
<b>20</b>	180.6 ± 55.9	0.58±0.03	61.3 ± 7.5	99.9 ± 0.1	1.06±0.40
<b>30</b>	64.5 ± 13.4	0.7 ± 0.03	33.9 ± 3.9	99.8 ± 0.1	2.39±0.69
<b>40</b>	40.1 ± 12.1	0.76±0.06	24.4 ± 2.8	99.7 ± 0.2	3.03±0.66
<b>50</b>	38.1 ± 12.4	0.77±0.03	17.1 ± 1.7	99.5 ± 0.2	4.22±0.54
<b>60</b>	19.5 ± 8.4	0.77±0.06	13.2 ± 3.7	99.3 ± 0.8	5.67±1.02
<b>70</b>	12.1 ± 3.7	0.87±0.08	10.2 ± 1.5	99.4 ± 0.7	3.28±0.87

\* t (h) represents the drying time needed to obtain a moisture ratio of 0.10 kg water/ kg dry matter. Weibull parameters ( $\alpha$  and  $\beta$ ) and statistical parameters (%VAR and %MRE). For Weibull parameters, %VAR and %MRE average values  $\pm$  LSD intervals are given. For t (h) average values  $\pm$  SD is given.

Drying kinetics at different temperatures (-10, 0, 10, 20, 30, 40, 50, 60 y 70 °C) were modelled using the Weibull empirical equation (Table 1). The Weibull model allowed a satisfactory description of the drying kinetics, reporting percentages of explained variance (%VAR) of over 99 %, which represents an adequate figure, particularly considering the high degree of experimental variability found in the drying of biological materials. In addition, %MRE values were lower than 10 % (García-Pérez, 2007), which also indicates a reasonable fitting capability.

The figures of the  $\alpha$  parameter showed an upward trend towards the value of 1 as the temperature increased (Figure 3). It is worth noting that its value increased almost linearly with the temperature from 0.56 at -10 °C to 0.87 at 70 °C, obtaining intermediate values of 0.72 and 0.76 for temperatures of 30 and 40 °C, respectively

(Table 1). This indicates that the drying kinetics approaches a first order kinetic progressively as the temperature rises. Therefore, it seems evident that there is a modification of the mass transfer controlling pattern as higher temperatures are used. A first order kinetic indicates that the drying rate is constant, which would mean a complete control of mass transfer by convection. This hypothesis seems consistent with the previous literature. Thus, Simal *et al.* (2005) used the Weibull model, also frequently known as the Page model, for the mathematical description of the drying kinetics of kiwi at different drying temperatures, from 30 to 90 °C, comparing its fitting ability with the theoretical diffusion model. It was found that as the drying temperature increased, the fitting ability of the diffusion model decreased, which denotes that moisture removal deviates from an entirely diffusion control. The temperature rise leads to an exponential increase in the diffusion rate, following an Arrhenius type relationship, leading to a rise in the amount of water on the product surface and giving more relevance to the convection, which also increases in line with the temperature but at a lower magnitude than the diffusion mechanisms. This was not observed by Simal *et al.* (2005) since a constant shape parameter was assumed; moreover, in the present study, a lower air velocity was used than that employed in the kiwi fruit drying kinetics modelled by Simal *et al.* (2005) ( $3 \text{ m}\cdot\text{s}^{-1}$ ) and, therefore, external transport plays an even greater role in drying kinetics.

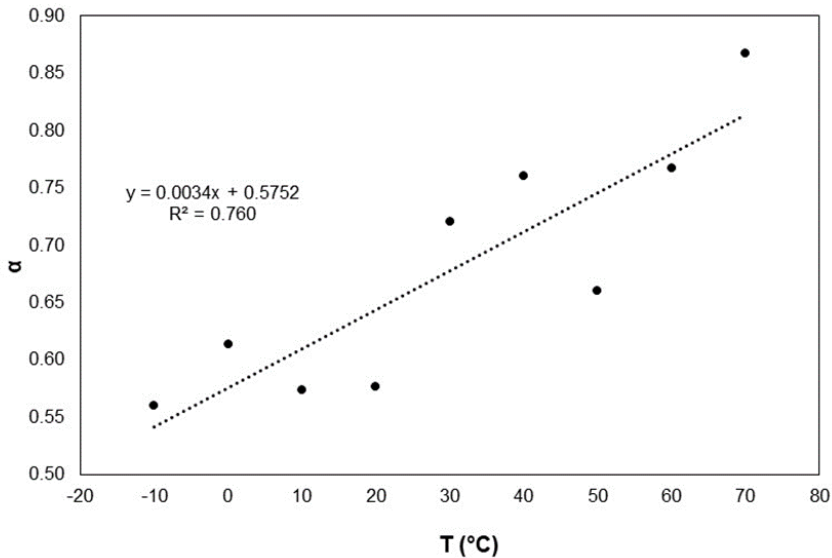


Figure 3. Influence of the air temperature (T) on the Weibull's shape parameter ( $\alpha$ ).

The Weibull parameter  $\beta$  was affected by the drying temperature; thus, the higher the drying temperature, the lower the  $\beta$  figures (Machado *et al.*, 1999). Therefore, at  $-10$  °C a value of  $\beta$  of  $402.3 \cdot 10^3$  s was obtained, at  $20$  °C one of  $61.3 \cdot 10^3$  s and at  $70$  °C the value obtained was of  $10.2 \cdot 10^3$  s (Table 1). It is complicated to compare  $\beta$  values with those obtained previously since they are affected by all the variables that influence the drying kinetics, such as sample geometry and mass load and distribution. The relationship of the kinetic parameter  $\beta$  of the Weibull model with the drying temperature followed an Arrhenius-type relationship, as observed in Figure 4, in which it may be seen that  $\beta$  departs from the linear trend marked by the rest of values at  $-10$  °C. This indicates that below  $0$  °C, dehydration occurs by sublimation (Ozuna *et al.*, 2014), while in the case of temperatures above the freezing point, water molecules are in a liquid state and are removed by evaporation (García-Pérez, 2007). The activation energy ( $E_a$ ) identified at temperatures from  $70$  °C to  $0$  °C was of  $29.56 \pm 2.49$  kJ/mol, a much lower figure than the one computed when considering only  $-10$  and  $0$  °C ( $64.36$  kJ/mol). Therefore, the process of removing water by lyophilisation consumed much more energy than in the case of evaporation. The latent heat of

sublimation for pure water at -10 °C is of 51.1 kJ/mol, which represents a figure lower than the  $E_a$  identified for low temperatures (-10 and 0 °C) (Rahman *et al.*, 2009). García-Pérez (2007) reported this difference between the  $E_a$  of evaporation and that of sublimation for the drying of cod fish, with values similar to those found in the present study on liver. Thus, an  $E_a$  of 67 kJ/mol was obtained for lyophilisation and 29.4 kJ/mol for drying at higher temperatures of cod fish (García-Pérez, 2007). Typical activation energy values lie between 12.7 and 110 kJ/mol for most of the food products (Zogzas *et al.*, 1996; Mirzaee *et al.*, 2009). Clemente (2003) obtained  $E_a$  values of 35.11 kJ/mol in pork meat dried at temperatures above the freezing point of water. Hii *et al.* (2014) reported values of between 16.3 and 22.8 kJ/mol for raw and cooked chicken meat samples, respectively, dried at 60, 70 and 80 °C. In the case of the convective drying of chicken meat, the  $E_a$  obtained was 27.85 kJ/mol (Ismail, 2017). However, in the drying kinetics of turkey breast meat samples at 60, 75 and 90 °C, a lower  $E_a$  (7.481 kJ/mol) was obtained (Elmas *et al.*, 2020).

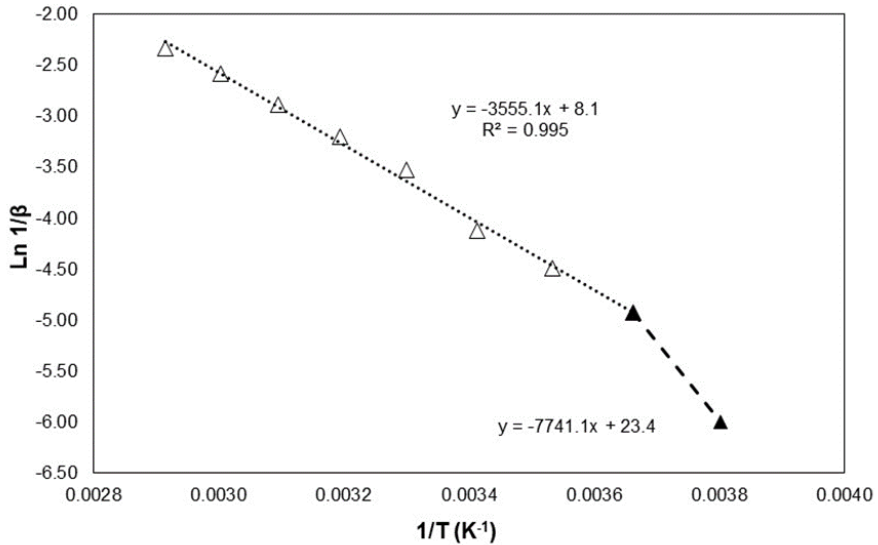


Figure 4. Influence of the air temperature (T) on the Weibull's kinetic parameter ( $\beta$ ).

### 3.2. Kinetics of ZnPP formation from pork liver dried at different temperatures

The kinetics of ZnPP formation using dried pork liver as a FeCH source (Figures 1B and 2B) was compared with the kinetics of ZnPP formation using raw pork liver with the aim of assessing the impact of drying on FeCH activity. The ZnPP formation kinetics from dried liver (Figures 1B and 2B) behaved in the same way as that of the raw product, previously observed in Abril *et al.* (2021), with an initial burst phase followed by a steady phase at constant rate. The kinetic of ZnPP formation using raw pork liver were very similar to the one reported by Abril *et al.* (2021) using a larger batch in terms of both y-intercept,  $0.213 \pm 0.077 \mu\text{M}$  (Table 1) and  $0.231 \pm 0.094 \mu\text{M}$  (Abril *et al.*, 2021), and slope ( $0.00428 \pm 0.00011 \mu\text{M}/\text{min}$  (Table 1) and  $0.0039 \pm 0.0001 \mu\text{M}/\text{min}$  (Abril *et al.*, 2021)). A narrower experimental variability was found in ZnPP kinetics when using dried pork liver than when studying raw pork liver, despite the fact that the same batch was used for the analysis. This fact could be linked to the high enzymatic activity in the raw liver, which increases the experimental variability. Despite this fact, noticeable differences were found between the raw pork liver and the livers dried at different temperatures as FeCH sources in ZnPP formation kinetics, as depicted in Figures 1B and 2B.



Table 2. Linear fit for the steady phase of ZnPP formation kinetics from FeCH extracts obtained from raw liver and liver dried at different temperatures.

	<b>EC<sub>app</sub></b> ( $\mu\text{M}$ )	<b>EA</b> ( $\mu\text{M} / \text{min}$ )	<b>r</b>	<b>ZnPP</b> ( $\mu\text{M}$ )
<b>Raw</b>	0.213 $\pm$ 0.077 <b>ABC</b>	0.00428 $\pm$ 0.00011 <b>v</b>	0.996	0.714
<b>-10 °C</b>	0.021 $\pm$ 0.002 <b>G</b>	0.00050 $\pm$ 0.00003 <b>y</b>	0.985	0.080
<b>0 °C</b>	0.150 $\pm$ 0.003 <b>DEF</b>	0.00091 $\pm$ 0.00005 <b>w</b>	0.989	0.252
<b>10 °C</b>	0.288 $\pm$ 0.005 <b>A</b>	0.00062 $\pm$ 0.00006 <b>xy</b>	0.950	0.358
<b>20 °C</b>	0.266 $\pm$ 0.007 <b>AB</b>	0.00068 $\pm$ 0.00009 <b>x</b>	0.991	0.343
<b>30 °C</b>	0.213 $\pm$ 0.007 <b>ABCD</b>	0.00067 $\pm$ 0.00009 <b>x</b>	0.920	0.289
<b>40 °C</b>	0.192 $\pm$ 0.006 <b>BCD</b>	0.00067 $\pm$ 0.00008 <b>x</b>	0.932	0.266
<b>50 °C</b>	0.164 $\pm$ 0.006 <b>CDE</b>	0.00062 $\pm$ 0.00008 <b>xy</b>	0.924	0.236
<b>60 °C</b>	0.109 $\pm$ 0.006 <b>EF</b>	0.00063 $\pm$ 0.00008 <b>xy</b>	0.917	0.181
<b>70 °C</b>	0.072 $\pm$ 0.004 <b>FG</b>	0.00033 $\pm$ 0.00005 <b>z</b>	0.882	0.108

Enzymatic activity (EA), apparent-FeCH concentration (EC<sub>app</sub>), correlation coefficient (r) and final ZnPP concentration at 120 min (ZnPP).

For EC<sub>app</sub> and EA, average values  $\pm$  LSD intervals are given.

(A, B, C, D, E, F, G) and (V, W, X, Y, Z) show homogeneous groups established from LSD intervals ( $p < 0.05$ ) for EC<sub>app</sub> and EA, respectively

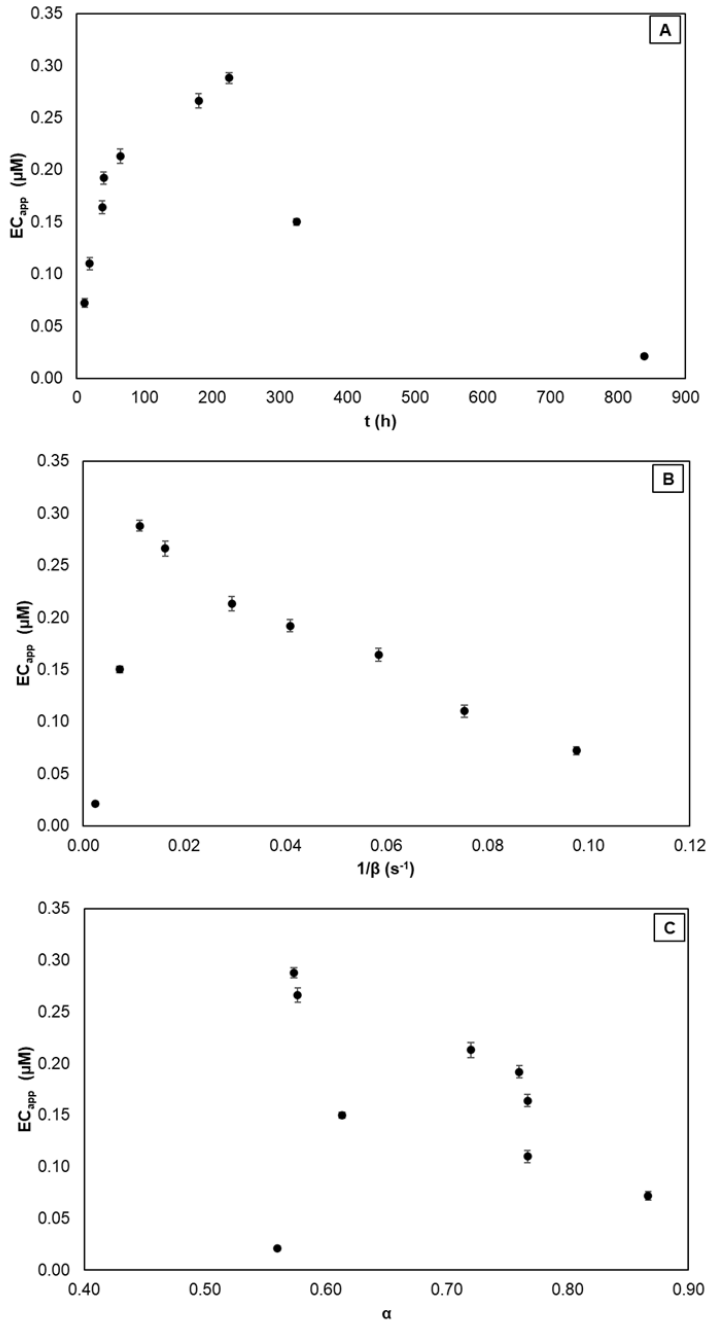


Figure 5. Relationship between drying time and Weibull parameters with the apparent-FeCH concentration ( $EC_{app}$ ).

Figure 1B shows that the apparent enzyme concentration ( $EC_{app}$ ) for samples dried at high temperatures ( $>20\text{ }^{\circ}\text{C}$ ) (Table 2), computed as the y-intercept of the linear relationships for the ZnPP kinetics, was dependent on the drying temperature. Thus, for the slowest drying kinetics (64.5 h to achieve 70% weight loss at  $30\text{ }^{\circ}\text{C}$ , Figure 1A) the highest  $EC_{app}$  was achieved ( $0.213\text{ }\mu\text{M}$ , Figure 5A), which gradually decreased as the drying temperature rose and, consequently, the drying time was shortened. Therefore, for liver dried at temperatures  $>20\text{ }^{\circ}\text{C}$ , the higher the drying temperature, the lower the  $EC_{app}$ , which illustrates a potential thermal degradation for the FeCH enzyme. However, in the case of drying at low temperatures ( $\leq 20\text{ }^{\circ}\text{C}$ ), the opposite behaviour was found (Figure 2B). Thus, pork livers dried at  $10\text{ }^{\circ}\text{C}$  (225.6 h) presented higher PFC ( $0.288\text{ }\mu\text{M}$ ) than those dried for longer times at  $0\text{ }^{\circ}\text{C}$  (325.1 h,  $0.150\text{ }\mu\text{M}$ ) and  $-10\text{ }^{\circ}\text{C}$  (838.8 h,  $0.021\text{ }\mu\text{M}$ ). This means that a prolonged time at excessively low temperatures and the consequent exposure to oxygen leads to a loss of FeCH (Wakamatsu *et al.*, 2007). Therefore, both drying at high temperatures for short times and drying at low temperatures for long times seem to lead to FeCH degradation and in order to better preserve the enzyme it would be more beneficial to conduct the drying process of pork liver at mild temperatures (around  $10\text{-}20\text{ }^{\circ}\text{C}$ ). The  $EC_{app}$  for the ZnPP kinetics of pork liver dried at  $10$  and  $20\text{ }^{\circ}\text{C}$  ( $0.288$  and  $0.266$ , respectively) was in the same order of magnitude as that of raw liver (Table 2 and Figure 5A). This indicates that when the drying kinetics approaches room temperature, the  $EC_{app}$  was similar to raw pork liver  $EC_{app}$ , preventing the enzyme degradation found at extreme temperatures ( $-10$  and  $70\text{ }^{\circ}\text{C}$ ) (Figure 5A). Thus, the  $EC_{app}$  for samples dried at  $70\text{ }^{\circ}\text{C}$  ( $0.072\text{ }\mu\text{M}$ ) was very similar to that obtained for samples dried at  $-10\text{ }^{\circ}\text{C}$  ( $0.021\text{ mM}$ ). The protein and enzyme degradation caused by the use of excessively high or low temperatures has already been reported (Amdadul Haque *et al.*, 2013).

Figure 5B shows the relationship between the drying rate, calculated as the inverse of the Weibull model kinetic parameter  $\beta$ , and  $EC_{app}$ . The highest  $EC_{app}$  values were obtained when  $1/\beta$  was between  $0.01$  and  $0.03\text{ (s}^{-1}\text{)}$ , obtaining values of  $0.288$  and  $0.266\text{ }\mu\text{M}$ . However, it should be noted that the extreme values of the kinetic parameter identified at the lowest ( $-10\text{ }^{\circ}\text{C}$ ) and the highest temperatures ( $70\text{ }^{\circ}\text{C}$ ) corresponded to the lowest values of  $EC_{app}$ ,  $0.021$  at  $-10\text{ }^{\circ}\text{C}$  and  $0.072\text{ }\mu\text{M}$  at  $70\text{ }^{\circ}\text{C}$ . As

previously mentioned, this indicates that the extreme values of temperature, and therefore of drying rate, negatively affect  $EC_{app}$ , inducing a degradation of the initial ZnPP concentration. Therefore, temperatures close to room conditions (10 and 20 °C) denote a maximum in the  $EC_{app}$  vs  $1/\beta$  figure, separating the region of low temperatures, in which the temperature rise led to an increase in both the drying rate and  $EC_{app}$ , from the high temperature range, in which the opposite behaviour was evidenced. However, in the case of the shape parameter of the Weibull model ( $\alpha$ ), no clear trend was observed with  $EC_{app}$  (Figure 5C).

As explained in the methodology (section 2.6.), the slope of the linear fit for the steady-state phase of ZnPP kinetics is proportional to the enzymatic activity (EA) expressed as the product formation rate. Figures 1B and 2B illustrates the different performance of the enzyme extracted from dried and raw pork livers in terms of EA. Thus, Table 2 shows that the values of EA for the kinetics of dried pork liver ranged between 0.00033 and 0.00091  $\mu\text{M}/\text{min}$ , while the values of EA for FeCH extracts from raw pork liver, of 0.00428  $\mu\text{M}/\text{min}$  which represents a figure one order of magnitude higher. A statistical analysis revealed that the influence of the drying temperature on EA was statistically significant ( $p < 0.05$ ), with the highest EA found at 0 °C (0.00091  $\mu\text{M}/\text{min}$ ). The lowest EA values, meanwhile, were obtained when drying was conducted at -10 and 70 °C, which presented EA figures that were 45.1% (0.00050  $\mu\text{M}/\text{min}$  at -10 °C) and 63.7% (0.00033  $\mu\text{M}/\text{min}$  at 70 °C) lower than those of the liver dried at 0 °C. Between 10 and 60 °C, the EA ranged between 0.00062 and 0.00067  $\mu\text{M}/\text{min}$ , and the temperature effect was negligible. This indicates that temperatures that are either excessively low (with the consequent long dehydration times) or high (with the consequent thermal degradation), cause a decrease in the catalytic activity in ZnPP formation.

There is no specific literature on the drying of pork liver and how drying affects the FeCH activity. However, there are studies that show that the FeCH, starts to reduce its activity at incubation temperatures above 40°C (Dailey *et al.*, 1994). While, Becker *et al.* (2012) postulated that at temperatures above 60°C the ZnPP was not formed in pork homogenates. In addition, regarding how drying affects the enzymatic activity

Perdana *et al.* (2012) demonstrated how enzymes are sensitive to heat and can, therefore, be inactivated during drying. In addition, Aksoy *et al.* (2019) and Baslar *et al.* (2014) demonstrated that high temperatures lead to the degradation of heat-sensitive components, such as proteins. Jaiswal *et al.* (2010) obtained similar results when evaluating the polyphenol oxidase (PPO) of arils from raw pomegranates dehydrated at 100 °C, obtaining a 68 % decrease in their activity (647.7 units/mL in raw arils compared to 205.7 units/mL in dry arils). Similarly, Parra Vergara (2013) observed an 89.5 % decrease in the enzymatic activity of peroxidase in dehydrated broccoli at 75 °C, compared to fresh broccoli. In addition, Maca *et al.* (2013) showed that the use of high drying temperatures influences the enzymatic activity of pectinmethylesterase in Tree Tomatoes (*Solanum betaceum*) and reported a 28 % decrease in the product concentration by increasing the drying temperature from 60 °C to 90 °C. Meanwhile, Shofian *et al.* (2011) highlighted that the freeze-drying process in tropical fruits, such as mango, papaya and carambola, accelerated the enzymatic reactions involved in the browning generated by polyphenoloxidases (PPO). In freeze-dried tomatoes, cell walls were shown to be altered, triggering the release of oxidative enzymes that destroyed antioxidant compounds in the fruit (Chang *et al.*, 2006). In the present study, low temperatures (-10 °C and 0 °C) had a detrimental effect on  $EC_{app}$ , compared to drying temperatures close to room temperature (10 °C and 20 °C) which provided a similar  $EC_{app}$  to that of raw pork liver (0.213  $\mu\text{M}$ ). In the case of pork liver dried at 10 and 20 °C, the EA was significantly reduced (0.00062 and 0.00068  $\mu\text{M}/\text{min}$ ) compared to that of raw pork liver (0.00428  $\mu\text{M}/\text{min}$ ), possibly due to conformational changes in the protein structure of the enzyme (Oyinloye & Yoon, 2020).

#### 4. Conclusions

Air drying has been proven to be an effective method to stabilise the pork liver and obtain a FeCH extract that can be used for ZnPP formation so it can be stored for a longer time at a moderate cost. However, it should be noted that drying significantly affects both the apparent-FeCH concentration and activity. Thus, high drying temperatures (> 30 °C), and low drying temperatures (< 0 °C), cause significant changes ( $p < 0.05$ ) in the concentration of FeCH as well as in its subsequent activity, both of which were completely dependent on the drying temperature. Drying conditions

close to room temperature (between 10 and 20 °C) were the most adequate conditions considering both apparent-FeCH concentration and activity. Further research should elucidate how drying affects the structure of FeCH, which would contribute to an understanding of the observed phenomena on its catalytic activity for ZnPP formation, as well as any further industrial application. In addition, it could be a relevant matter to gain insight into the use of drying techniques that minimise or avoid exposure to oxygen, such as vacuum drying or freeze drying. Two different applications of the dried pork liver as FeCH source could be envisioned: i) its incorporation to raw-cured products such as salami, fuet or sausage, to induce the formation of ZnPP and ii) the industrial production of ZnPP as a natural colorant for the food industry.

## Acknowledgements

The authors acknowledge the financial support from the “Ministerio de Economía y Competitividad (MINECO)” and “Instituto Nacional de Investigación y Tecnología Agraria y Alimentaria (INIA)” in Spain (Projects RTA2017-00024-C04-03 and RTA2017-00024-C04-02).

## References

- Abril, B., Sánchez-Torres, E. A., Bou, R., García-Pérez, J. V., & Benedito, J. (2021). Ultrasound intensification of Ferrochelatase extraction from pork liver as a strategy to improve ZINC-protoporphyrin formation. *Ultrasonics Sonochemistry*, 78, 105703. <https://doi.org/10.1016/j.ultsonch.2021.105703>
- Adamsen, C. E., Møller, J. K., Hismani, R., & Skibsted, L. H. (2004). Thermal and photochemical degradation of myoglobin pigments in relation to colour stability of sliced dry-cured Parma ham and sliced dry-cured ham produced with nitrite salt. *European Food Research and Technology*, 218(5), 403-409. <https://doi.org/10.1007/s00217-004-0891-8>

- Aksoy, Aslı; Karasu, Salih; Akcicek, Alican; Kayacan, Selma (2019). Effects of Different Drying Methods on Drying Kinetics, Microstructure, Color, and the Rehydration Ratio of Minced Meat. *Foods*, 8(6), 216–. doi:10.3390/foods8060216
- Amdadul Haque, M., Putranto, A., Aldred, P., Chen, J., & Adhikari, B. (2013). Drying and denaturation kinetics of whey protein isolate (WPI) during convective air drying process. *Drying Technology*, 31(13-14), 1532-1544. <https://doi.org/10.1080/07373937.2013.794832>
- AOAC. (1997). Official Methods 950.46. In Official Methods of Analysis (sixteenth ed.)
- Baque, M., Macías, B., & Cornejo, F. (2016). Influencia de pre tratamientos convencionales en el proceso de secado de manzana y en las características físicas del producto final. Escuela Superior Politécnica del Litoral. <http://www.dspace.espol.edu.ec/handle/123456789/8993>.
- Başlar, M., Kılıçlı, M., Toker, O. S., Sağdıç, O., & Arici, M. (2014). Ultrasonic vacuum drying technique as a novel process for shortening the drying period for beef and chicken meats. *Innovative Food Science & Emerging Technologies*, 26, 182-190. <https://doi.org/10.1016/j.ifset.2014.06.008>
- Becker, E. M., Westermann, S., Hansson, M., & Skibsted, L. H. (2012). Parallel enzymatic and non-enzymatic formation of zinc protoporphyrin IX in pork. *Food Chemistry*, 130(4), 832-840. <https://doi.org/10.1016/j.foodchem.2011.07.090>
- Buzrul, S. (2022). Reassessment of Thin-Layer Drying Models for Foods: A Critical Short Communication. *Processes*, 10(1), 118. <https://doi.org/10.3390/pr10010118>

- Clemente Polo, G. (2003). Efecto de la contracción en la cinética de secado de músculos de jamón. Tesis doctoral, Universidad Politécnica de Valencia, Valencia, España.
- Chang, C. H., Lin, H. Y., Chang, C. Y., & Liu, Y. C. (2006). Comparisons on the antioxidant properties of fresh, freeze-dried and hot-air-dried tomatoes. *Journal of Food Engineering*, 77(3), 478-485. <https://doi.org/10.1016/j.jfoodeng.2005.06.061>
- Chau, T. T., Ishigaki, M., Kataoka, T., & Taketani, S. (2010). Porcine ferrochelatase: the relationship between iron-removal reaction and the conversion of heme to Zn-protoporphyrin. *Bioscience, biotechnology, and biochemistry*, 74(7), 1415-1420. <https://doi.org/10.1271/bbb.100078>
- Chau, T. T., Ishigaki, M., Kataoka, T., & Taketani, S. (2011). Ferrochelatase catalyzes the formation of Zn-protoporphyrin of dry-cured ham via the conversion reaction from heme in meat. *Journal of agricultural and food chemistry*, 59(22), 12238-12245. <https://doi.org/10.1021/jf203145p>
- Cunha, L. M.; Oliveira, F. A. R.; Oliveira, J. C. (1998). Optimal experimental design for estimating the kinetic parameters of processes described by the Weibull probability distribution function. *Journal of Food Engineering*, 37, 175-191. [https://doi.org/10.1016/S0260-8774\(98\)00085-5](https://doi.org/10.1016/S0260-8774(98)00085-5)
- Dailey, H. A., Sellers, V. M., & Dailey, T. A. (1994). Mammalian ferrochelatase. Expression and characterization of normal and two human protoporphyrin ferrochelatases. *Journal of Biological Chemistry*, 269(1), 390-395.



- Echegaray, N., Gómez, B., Barba, F. J., Franco, D., Estévez, M., Carballo, J., ... & Lorenzo, J. M. (2018). Chestnuts and by-products as source of natural antioxidants in meat and meat products: A review. *Trends in Food Science & Technology*, 82, 110-121. <https://doi.org/10.1016/j.tifs.2018.10.005>
- EFPPA. Rendering in numbers (2021) <https://efpra.eu/wp-content/uploads/2021/07/Rendering-in-numbers-Infographic.pdf> (Accessed on 16 May 2022).
- Estévez, M., Morcuende, D., Ramirez, R., Ventanas, J., & Cava, R. (2004). Extensively reared Iberian pigs versus intensively reared white pigs for the manufacture of liver pâté. *Meat Science*, 67(3), 453-461. <https://doi.org/10.1016/j.meatsci.2003.11.019>
- Elmas, F., Bodruk, A., Köprüalan, Ö., Arikaya, Ş., Koca, N., Serdaroğlu, F. M., ... & Koc, M. (2020). Drying kinetics behavior of turkey breast meat in different drying methods. *Journal of Food Process Engineering*, 43(10), e13487. <https://doi.org/10.1111/jfpe.13487>
- García-Pérez, J.V. (2007). Contribución Al Estudio De La Aplicación De Ultrasonidos De Potencia En El Secado Convectivo De Alimentos. Tesis doctoral, Universidad Politécnica de Valencia.
- García-Pérez, J. V., Ozuna, C., Ortuño, C., Cárcel, J. A., & Mulet, A. (2011). Modeling ultrasonically assisted convective drying of eggplant. *Drying Technology*, 29(13), 1499-1509. <https://doi.org/10.1080/07373937.2011.576321>

- García-Pérez, J. V., Carcel, J. A., Riera, E., Rosselló, C., & Mulet, A. (2012). Intensification of low-temperature drying by using ultrasound. *Drying Technology*, 30(11-12), 1199-1208. <https://doi.org/10.1080/07373937.2012.675533>
- Guiné, R. (2018). The drying of foods and its effect on the physical-chemical, sensorial and nutritional properties. *International Journal of Food Engineering*, 2(4), 93-100. doi: 10.18178/ijfe.4.2.93-100
- Hii, C. L., Itam, C. E., & Ong, S. P. (2014). Convective air drying of raw and cooked chicken meats. *Drying Technology*, 32(11), 1304-1309. <https://doi.org/10.1080/07373937.2014.924133>
- Ismail, O. (2017). An experimental and modeling investigation on drying of chicken meat in convective dryer. *Studia Universitatis Babes-Bolyai Chemia*, 62(4), 459–469. <https://doi.org/10.24193/subbchem.2017.4.3>
- Jaiswal, V., DerMarderosian, A., & Porter, J. R. (2010). Anthocyanins and polyphenol oxidase from dried arils of pomegranate (*Punica granatum* L.). *Food Chemistry*, 118(1), 11-16. <https://doi.org/10.1016/j.foodchem.2009.01.095>
- Kuddus, M. (2019). Introduction to food enzymes. In *Enzymes in Food Biotechnology* (pp. 1-18). Academic Press. <https://doi.org/10.1016/B978-0-12-813280-7.00001-3>
- Maca, M. P., Osorio, O., & Mejía-España, D. F. (2013). Inactivación térmica de pectinmetilesterasa en tomate de árbol (*Solanum betaceum*). *Información tecnológica*, 24(3), 41-50. <http://dx.doi.org/10.4067/S0718-07642013000300006>

- Machado, M. F., Oliveira, F. A., & Cunha, L. M. (1999). Effect of milk fat and total solids concentration on the kinetics of moisture uptake by ready-to-eat breakfast cereal. *International journal of food science & technology*, 34(1), 47-57. <https://doi.org/10.1046/j.1365-2621.1999.00238.x>
- Meziane, S. (2011). Drying kinetics of olive pomace in a fluidized bed dryer. *Energy Conversion and Management*, 52(3), 1644-1649. <https://doi.org/10.1016/j.enconman.2010.10.027>
- Mirzaee, E., Rafiee, S., Keyhani, A., & Emam-Djomeh, Z. (2009). Determining of moisture diffusivity and activation energy in drying of apricots. *Research in Agricultural Engineering*, 55(3), 114-120.
- Morita, H., Niu, J., Sakata, R. and Nagata, Y. (1996). Red pigment of Parma ham and bacterial influence on its formation. *Journal Food Science.*, 61, 1021-1023. <https://doi.org/10.1111/j.1365-2621.1996.tb10924.x>
- Ozuna, C., Cárcel, J.A., Walde, P.M., & Garcia-Perez, J.V. (2014). Low temperature drying of salted cod (*Gadus morhua*) assisted by high power ultrasound: Kinetics and physical properties. *Innovative Food Science and Emerging Technologies*, 23, 146-155. <https://doi.org/10.1016/j.ifset.2014.03.008>
- Oyinloye, T. M., & Yoon, W. B. (2020). Effect of freeze-drying on quality and grinding process of food produce: A review. *Processes*, 8(3), 354. <https://doi.org/10.3390/pr8030354>
- Parra Vergara, J. C. (2013). Determinación de la cinética de liofilización en floretes de brócoli (*Brassica oleracea* L, var. Legacy) y evaluación del contenido de ácido L-ascórbico (L-AA) y actividad peroxidasa (POD). Duitama: Universidad Nacional Abierta y a Distancia.

- Perdana, J., Fox, M. B., Schutyser, M. A. I., & Boom, R. M. (2012). Enzyme inactivation kinetics: Coupled effects of temperature and moisture content. *Food Chemistry*, 133(1), 116-123. <https://doi.org/10.1016/j.foodchem.2011.12.080>
- Praestgaard, E., Elmerdahl, J., Murphy, L., Nymand, S., McFarland, K. C., Borch, K., & Westh, P. (2011). A kinetic model for the burst phase of processive cellulases. *The FEBS journal*, 278(9), 1547-1560. <https://doi.org/10.1111/j.1742-4658.2011.08078.x>
- Rahman, M. S., Machado-Velasco, M., Sosa-Morales, M. E., & Velez-Ruiz, J. F. (2009). Freezing point: measurement, data, and prediction. *Food Properties Handbook*, 2, 153-192.
- Roy, I., & Gupta, M. N. (2004). Freeze-drying of proteins: Some emerging concerns. *Biotechnology and applied biochemistry*, 39(2), 165-177. <https://doi.org/10.1042/BA20030133>
- Sánchez-Torres, E. A., Abril, B., Benedito, J., Bon, J., & García-Pérez, J. V. (2021). Water desorption isotherms of pork liver and thermodynamic properties. *LWT*, 149, 111857. <https://doi.org/10.1016/j.lwt.2021.111857>
- Santacatalina, J. V., Ozuna, C., Cárcel, J. A., Garcia-Perez, J. V., & Mulet, A. (2011). Quality assessment of dried eggplant using different drying methods: hot air drying, vacuum freeze drying and atmospheric freeze drying. *In Proceedings of the 11th International Congress on Engineering and Food*.
- Santacatalina, J. V., Rodríguez, O., Simal, S., Cárcel, J. A., Mulet, A., & García-Pérez, J. V. (2014). Ultrasonically enhanced low-temperature drying of apple: Influence on drying kinetics and antioxidant potential. *Journal of Food Engineering*, 138, 35-44. <https://doi.org/10.1016/j.jfoodeng.2014.04.003>

- Santacatalina, J. V., Contreras, M., Simal, S., Cárcel, J. A., & Garcia-Perez, J. V. (2016). Impact of applied ultrasonic power on the low temperature drying of apple. *Ultrasonics Sonochemistry*, 28, 100-109. <https://doi.org/10.1016/j.ultsonch.2015.06.027>
- Sassa, A., Beard, W. A., Shock, D. D., & Wilson, S. H. (2013). Steady-state, pre-steady-state, and single-turnover kinetic measurement for DNA glycosylase activity. *JoVE (Journal of Visualized Experiments)*, (78), e50695. doi:10.3791/50695
- Shofian, N. M., Hamid, A. A., Osman, A., Saari, N., Anwar, F., Pak Dek, M. S., & Hairuddin, M. R. (2011). Effect of freeze-drying on the antioxidant compounds and antioxidant activity of selected tropical fruits. *International Journal of molecular sciences*, 12(7), 4678-4692. <https://doi.org/10.3390/ijms12074678>
- Simal, S., Femenia, A., Garau, M. C., & Rosselló, C. (2005). Use of exponential, Page's and diffusional models to simulate the drying kinetics of kiwi fruit. *Journal of food engineering*, 66(3), 323-328. <https://doi.org/10.1016/j.jfoodeng.2004.03.025>
- Taketani, S., & Tokunaga, R. (1982). Purification and substrate specificity of bovine liver-ferrochelataase. *European journal of biochemistry*, 127(3), 443-447. <https://doi.org/10.1111/j.1432-1033.1982.tb06892.x>
- Wakamatsu, J., Nishimura, T., & Hattori, A. (2004a). A Zn-porphyrin complex contributes to bright red color in Parma ham. *Meat Science*, 67(1), 95-100. <https://doi.org/10.1016/j.meatsci.2003.09.012>

- Wakamatsu, J., Okui, J., Ikeda, Y., Nishimura, T., & Hattori, A. (2004b). Establishment of a model experiment system to elucidate the mechanism by which Zn–protoporphyrin IX is formed in nitrite-free dry-cured ham. *Meat Science*, *68*(2), 313-317. <https://doi.org/10.1016/j.meatsci.2004.03.014>
- Wakamatsu, J. I., Okui, J., Hayashi, N., Nishimura, T., & Hattori, A. (2007). Zn protoporphyrin IX is formed not from heme but from protoporphyrin IX. *Meat Science*, *77*(4), 580-586. <https://doi.org/10.1016/j.meatsci.2007.05.008>
- Wakamatsu, J. I., Murakami, N., & Nishimura, T. (2015). A comparative study of zinc protoporphyrin IX-forming properties of animal by-products as sources for improving the color of meat products. *Animal Science Journal*, *86*(5), 547-552. <https://doi.org/10.1111/asj.12326>
- Zogzas, N. P., Maroulis, Z. B., & Marinos-Kouris, D. (1996). Moisture diffusivity data compilation in foodstuffs. *Drying technology*, *14*(10), 2225-2253. <https://doi.org/10.1080/07373939608917205>



*Physicochemical and Techno-Functional Properties of Dried and Defatted Porcine Liver*

---

Blanca Abril<sup>1</sup>, Eduardo A. Sánchez Torres<sup>1</sup>, Mònica Todrà<sup>2</sup>, Jose Benedito<sup>1</sup> and Jose Vicente Garcia-Perez<sup>1</sup>

<sup>1</sup>Department of Food Technology, Universitat Politècnica de València, Camí de Vera, s/n, Valencia 46022, Spain

<sup>2</sup> Institute of Food and Agricultural Technology (INTEA), XIA (Catalonian Network on Food Innovation), Escola Politècnica Superior, University of Girona, C/ Maria Aurèlia Capmany 61, 17003 Girona, Spain;





## Physicochemical and Techno-Functional Properties of Dried and Defatted Porcine Liver

### Abstract

Porcine liver has a high nutritional value and is rich in proteins, minerals, and vitamins, making it an interesting co-product to alleviate the growing global demand for protein. The objective of this study was to analyze how the drying and defatting processes of porcine liver affect the physicochemical and techno-functional properties of its proteins. Two drying temperatures (40 and 70 °C) were studied, and dried samples were defatted using organic solvents. The drying process turned out to be an effective method for the stabilization of the protein fraction; however, when the drying temperature was high (70 °C), greater protein degradation was found compared to drying at a moderate temperature (40 °C). Regarding the defatting stage, it contributed to an improvement in certain techno-functional properties of the liver proteins, such as the foaming capacity (the average of the dried and defatted samples was 397 % higher than the dried samples), with the degree of foaming stability in the liver dried at 40 °C and defatted being the highest (13.76 min). Moreover, the emulsifying capacity of the different treatments was not found to vary significantly ( $p > 0.05$ ). Therefore, the conditions of the drying and defatting processes conducted prior to the extraction of liver proteins must be properly adjusted to maximize the stability, quality, and techno-functional properties of the proteins.

**Keywords:** Porcine liver, liver protein, drying, defatting, physicochemical characteristics, technofunctional properties

## 1. Introduction

In recent years, the consumption of pork-derived food products has been on the rise, which has stimulated its production in Europe. The main change that has taken place in the pork sector consisted of the transition from a multifunctional livestock, typical of organic-based livestock activity, to an intensive livestock model (García *et al.*, 2021). The more intensive production model is having a negative impact on the environment both in terms of the use of resources (nitrogen, phosphorus, land and water) and greenhouse gas emissions (Banco Mundial, 2019). Furthermore, a large number of co-products and a great amount of animal waste are generated in the meat industry, usually in slaughterhouses (Giroto & Cossu, 2017), which also increases its environmental impact. In this way, if we consider both economic and environmental issues, any action whose purpose is to revalue meat co-products is of great interest for this industry. In addition, the recovery and revalorisation of co-products is a current demand of our society.

The valorization of meat co-products depends on several factors, such as the country, culture, religion, economy, consumer preferences, etc. (Nollet & Toldrá, 2019). In general, hearts, tongues, livers, lungs and kidneys from animals, such as pigs, cows and lambs, have traditionally been consumed as food or as food ingredients in many countries (Toldra *et al.*, 2021). However, Llauger *et al.* (2021) conducted a study in Spain on the attitude of consumers towards the development of meat products from animal co-products and offal. The results reflected how society has a great interest in contributing to the environment by means of the valorisation of these co-products, but their typical flavour hinders their acceptability and consumption despite being considered healthy.

In general, the last few decades have witnessed a drop in the use of animal co-products for human consumption (FAO, 2021). Most co-product consumption is linked to their use as an ingredient in the manufacturing of traditional meat products, such as pâté (from the liver), blood sausages, or animal feed (Lynch *et al.*, 2018). In addition, meat co-products have been used in the development of new functional ingredients (Lafarga & Hayes, 2014), such as bioactive peptides obtained from the proteolysis

mechanisms of endogenous meat enzymes (calpains) or exogenous plant enzymes (papain, bromelain or ficin) (Albenzio *et al.*, 2017), and antimicrobial agents (Borrajo *et al.*, 2019). Co-products have also been used to produce biodiesel (Leal *et al.*, 2021). Moreover, the growth of world population and the increase in demand for food, combined with actions in favour of the sustainability of the meat industry, have highlighted the need to find alternative protein sources (pulses, cereals, insects, fungi, algae, and protein recovered from meat or fish by-products) of nutritional and sensory quality, with a milder environmental impact (Toldrà *et al.*, 2021). In this regard, the nutritional value of meat co-products is closely comparable to lean meat (Soladoye *et al.*, 2021), and they are sources of high-quality proteins with excellent techno-functional properties.

The use of proteins from meat co-products has attracted interest as a result of their use in human nutrition (Aspevik *et al.*, 2017). Protein hydrolysates can have various applications as food ingredients, due to their emulsifying properties or foaming agents (Toldrà *et al.*, 2012). These proteins may also be applied in nutritional formulas for special adult diets, in extra protein supplements for the elderly, in formulas for infants with allergies to intact food proteins or with congenital metabolic disorders, and as nutraceuticals (Wadhwa & Bakshi, 2016).

Porcine liver is an interesting co-product of the meat industry from a nutritional point of view, as it is rich in protein ( $22.05 \pm 1.38$  %), low in fat ( $2.94 \pm 0.50$  %) and contains minerals and nutrients, such as essential amino acids and fatty acids (Seong *et al.*, 2014). However, liver has  $71.59 \pm 3.42$  % moisture; therefore, in just the same way as meat and other offal, it is a perishable product and has a limited shelf life (Estévez *et al.*, 2004). Therefore, its previous dehydration is convenient in order to prolong its shelf life and facilitate its handling and storage before further use in applications, such as protein extraction (Sánchez-Torres *et al.*, 2021). Moreover, the removal of the fat fraction would also facilitate the recovery of the protein fraction, and would limit degradation reactions, such as lipid oxidation and rancidity. However, it is important to investigate how water and fat reduction affects protein quality and functionality. Proteins have functional properties of great technological interest, such

as their capacity to solubilise, gel, foam or emulsify, which makes them useful for the purposes of improving the creation of new products derived from meat co-products, as well as for reducing shear strength and improving the texture of meat products (Parés *et al.*, 2014).

Drying and defatting operations have been used for the isolation and subsequent extraction of proteins, mainly in vegetables such as lupine (Lo *et al.*, 2021), or from insect flour, in order to make meat analogues (Mishyna *et al.*, 2021). No references have been found to the effect of drying and defatting on liver protein quality. Depending on the matrix from which the protein fraction is extracted, the drying temperature is critical, directly affecting protein stability and, therefore, its techno-functional properties, such as solubility and foaming capacity. Thus, for example, temperatures above 80 °C negatively affected the solubility and foaming capacity and stability of lupine protein (Lo *et al.*, 2021). However, the defatting operation can cause changes in the amino acid composition and functionality of the proteins, such as an increase in the foaming and emulsifying capacity, as well as an increase in the quality of the insect protein in terms of essential amino acids (Kim *et al.*, 2020). Thus, the main objective of this study was to evaluate the effect of the drying and defatting processes on the physicochemical and techno-functional properties of porcine liver.

## **2. Materials and methods**

### **2.1. Raw material and sample preparation**

Raw porcine livers, from an industrial slaughterhouse were transported to the laboratory at 4 °C. Liver conditioning consisted of i) the separation of its 4 main lobes, ii) the splitting of each lobe into two parts, (iii) vacuum packaging (200 x 300 PA / PE, Sacoliva, Barcelona) and (iv) freezing (at -20 °C) until processing.

#### **2.1.1. Drying process**

Before drying, vacuum packaged samples were tempered at 2 °C for 2 h in order to facilitate further handling. Using a household device, cylinders of standardised dimensions (12.6 mm diameter x 15 mm height) were obtained. In each drying run, 8 cylinders, with a total weight of 15 g approximately, were used.

The drying experiments were carried out at moderate-low (40 °C) and moderate-high (70 °C) temperatures using a convective oven (FD 56, Binder, GmbH, Tuttlingen, Germany) with an air speed of 1.3 m·s<sup>-1</sup>. Then, 8 cylindrical porcine liver samples were placed in a porcelain crucible and their weight was recorded manually every 15 min. The finalization criterion was set at a weight loss of 70 % of the initial weight. At the end of the drying tests, the dried porcine liver samples were ground, vacuum packed in 200 x 300 PA/PE bags (Sacoliva, Barcelona), and stored under refrigeration at 4 °C until their physicochemical and techno-functional characterisation. The drying experiments were replicated 3 times at both temperatures. Subsequently, the porcine liver replicates dried at the same temperature (D-40 °C or D-70 °C) were ground and mixed, with the aim of obtaining a representative sample of each drying experiment and, thus, performing the analyses of the physicochemical and techno-functional properties of dried porcine liver.

### **2.1.2. Defatting process**

For liver defatting purposes, standard method 991.36 (AOAC, 1996) was used, based on the use of Soxhlet equipment and an organic solvent. Thus, 3 g of dried and ground porcine liver were weighed. Then, samples were placed in a filter paper cartridge (porous material). Subsequently, the sample was placed in the chamber of the Soxhlet extractor, which consisted of a balloon - flask (previously desiccated for 1 h at 125 °C, to eliminate ambient humidity), the chamber of the Soxhlet extractor (where the cartridge was inserted), a condenser and a water bath at a temperature above 70 °C (boiling point of the organic solvent used). 75 mL of organic solvent, petroleum ether (C<sub>6</sub>H<sub>6</sub>), was used in each extractor. Thus, the heated solvent, located in the flask-balloon immersed in the bath at 70 °C, evaporated on reaching the condenser and fell on the sample cartridge, extracting the fat. The condensed solvent returned to the boiling flask and the process was run continuously for 5 h. Afterwards, the balloons containing the fat dissolved in the organic solvent were rota-evaporated to separate the solvent from the fat. Meanwhile, in order to remove the solvent in the dried liver, the cartridges were placed in a vacuum oven at 70 °C for 4 h. Defatting experiments were replicated 3 times at both drying temperatures (40 and 70 °C). Subsequently, the dried

and defatted porcine liver was removed from the cartridge, and then the replicates (DD 40 °C and DD-70 °C) were ground and mixed with the aim of obtaining representative samples to perform the physicochemical and techno-functional analyses. The samples were vacuum packed in PA/PE bags and stored under refrigeration at 4 °C until characterisation.

## 2.2. Modelling of air-drying kinetics

For the mathematical description of the drying kinetics at 40 °C and 70 °C, the Weibull empirical model was used (Cunha *et al.*, 1998). The Weibull model is based on Equation 1.

$$W_t = W_e + (W_0 - W_e) \cdot \exp\left[-\left(\frac{t}{\beta}\right)^\alpha\right] \quad (\text{Equation 1})$$

Where  $W_t$  is the moisture content (kg water / kg dry matter) at time  $t$  (s),  $W_e$  is the equilibrium moisture content (kg water / kg dry matter) and  $W_0$  is the initial moisture content (kg water / kg dry matter) and  $\beta$  (s) and  $\alpha$  are the kinetic and shape parameters of the model, respectively.  $W_e$  was estimated from the equilibrium data reported by Sanchez-Torres *et al.* (2021).

When the value of  $\alpha$  is equal to 1, the model corresponds to first order kinetics, with a constant water loss rate. When  $\alpha > 1$ , the reaction rate for the Weibull model is increasing as a function of time and when  $\alpha < 1$ , it is decreasing (Marabi *et al.*, 2003). The Weibull model (Equation 1) was fitted to the experimental data and the kinetic and shape parameters were determined. The identification of Weibull parameters ( $\alpha$  and  $\beta$ ) was carried out using an optimisation procedure that minimised the sum of the squared differences between the experimental and calculated average moisture contents of the samples. For that purpose, the non-linear optimisation algorithm of the Generalised Reduced Gradient (GRG), available in a Microsoft Excel™ spreadsheet from MS Office 2019, was used (García-Pérez, 2007). The percentages of mean squared error (%MRE, Equation 2) and explained variance (%VAR, Equation 3) were determined to evaluate the model's goodness of fit.

$$\%MRE = \frac{100}{N} \left[ \sum_{i=1}^N \frac{|W_{exp} - W_{cal}|}{W_{exp}} \right] \quad (\text{Equation 2})$$

$$\%VAR = \left[ 1 - \frac{S_{xy}^2}{S_y^2} \right] 100 \quad (\text{Equation 3})$$

Where  $W_{exp}$  and  $W_{cal}$  are the experimental and the estimated moistures, respectively;  $N$  is the number of experimental data and  $S_{xy}$  and  $S_y$  are the standard deviations of the estimation and the sample deviation, respectively.

## 2.3. Physicochemical characteristics

### 2.3.1. Proximate analysis

Standard methods were used to analyse the proximate composition of dried porcine liver. Each sample was analysed in triplicate. Moisture, ash, protein, and fat contents were determined by following the procedures established by the Association of Official Analytical Chemists (AOAC, 2000). Moisture and ash contents were determined gravimetrically using a hot air oven and a muffle furnace, respectively. The protein content was estimated from the total Kjeldahl nitrogen (TKN x 6.25) by using a Gerhardt KB20 digestion system (C. Gerhardt GmbH & Co., KG, Königswinter Germany) and a Büchi K-314 distillation unit (Büchi Labortechnik AG, Flawil, Switzerland). The total fat content was determined gravimetrically by Soxhlet extraction with diethyl ether.

### 2.3.2. Colour parameters

The colour of dried liver samples was measured by determining the CIE  $L^*$ ,  $a^*$  and  $b^*$  colour parameters, with  $L^*$  representing the lightness on a scale of 0 (dark) to 100 (white);  $a^*$  the redness-greenness value; and  $b^*$  the yellowness-blueness value, using a Minolta Chroma Meter CR-300 with a CR-A33f glass light projection tube



(Minolta Co., Ltd., Osaka, Japan). The measurements were taken using diffuse illumination, a D65 light source and 2° standard observer. The colorimeter was calibrated using a standard white ceramic plate ( $L^*=97.15$ ,  $a^*=-5.28$  and  $b^*=+7.82$ ). The colour of each sample was measured in triplicate. The angular coordinates of Chroma ( $C^*$ ) and Hue angle ( $H^\circ$ ) were calculated according to Equations 4 and 5, respectively.

$$C^* = \sqrt{(a^{*2} + b^{*2})} \quad (\text{Equation 4})$$

$$H^\circ = \tan^{-1}\left(\frac{b^*}{a^*}\right) \quad (\text{Equation 5})$$

### **2.3.3. Differential Scanning Calorimetry (DSC) analysis**

Differential Scanning Calorimetry (DSC) analyses of samples were performed in a DSC (Q 2000 calorimeter, TA Instruments, New Castle, DE, USA), under a heating program from 20 to 100 °C and at a heating rate of 3 °C·min<sup>-1</sup>. Solutions of reconstituted dried liver samples with the same percentage of protein (w/v) as raw porcine liver (19.20 %) were analysed. From the DSC thermograms (heat flow curve as a function of temperature), the area of the endothermic transition peaks was calculated by integration and, by the use of a straight baseline, the variation in the global transition enthalpy of the protein denaturation ( $\Delta H$ , J/g) was also calculated. The initial temperature of the endothermic peak ( $T_i$ ) and the denaturation temperatures ( $T_{d1}$  and  $T_{d2}$ ) were also obtained, considering that they correspond to the temperatures at which the minimum of the two main endothermic peaks of denaturation were recorded in the thermograms. TA Instruments' Universal Analysis software was used.

## **2.4. Techno-functional properties**

### **2.4.1. Protein solubility**

The protein solubility of dried porcine liver samples was analysed using the method described by Morr *et al.* (1985), with slight modifications. 1 g of ground dried liver samples was diluted in distilled water (100 mL). The solutions were stirred for 30

min on a magnetic stirring plate, thus avoiding vortex formation. After stirring, aliquots of the solutions were centrifuged at  $20000 \times g$  for 30 min at  $20\text{ }^{\circ}\text{C}$  (Sorvall RC-SC plus, DuPont Co., Newton, CT, USA) and decanted. The protein solubility was calculated as the percentage of soluble protein content in the supernatant relative to the total protein content of dried liver samples. The protein content in both was determined by the Kjeldahl method AOAC 954.01 (AOAC, 2019). Each determination was carried out in duplicate for each drying condition.

#### **2.4.2. Foaming properties**

The foaming properties were determined as described in Toldrà *et al.* (2019). Three aliquots of 200 mL of dried liver protein solutions (5 g/L) from each sample were prepared in distilled water, and then transferred to 1000 mL volumetric flasks. The solutions were whipped in a mixer (Multimix M700, Braun Española S.A., Esplugues de Llobregat, Barcelona, Spain) with two whisks ( $\varnothing = 5\text{ cm}$ ) at 1000 rpm for 10 min. The flasks were placed on a rotational plate during mixing to form homogeneous foams. Afterwards, the foaming capacity (FC) was determined as the volume (mL) of foam after 2 min at rest. The foam stability was determined using a gravimetric method as follows: measured quantities of foam were carefully placed in three dry stainless steel sieves to let the released liquid drain, and the remaining foam was weighed every 10 min for a period of 60 min. The percentage of remaining foam versus time was plotted, and relative foam stability (RFS), defined as the time (min) needed for the disappearance of 50 % of the initial foam, was calculated by fitting an exponential decay function to the experimental data using Equation 6.

$$y = B_0 \cdot e^{(-B_1 \times t)} \quad (\text{Equation 6})$$

Where  $B_0$  is the initial foam percentage,  $t$  is the time (min) and  $B_1$  the foam disappearance rate ( $\text{min}^{-1}$ ). The measurements were taken in triplicate.

#### **2.4.3. Emulsifying properties**

The emulsifying properties were determined following the turbidimetric method described by Pearce & Kinsella (1978) and slightly modified by Parés & Ledward

(2001). The solutions of dried liver samples were prepared at 5 g/L of protein (w/v). 50 mL of liver protein solution was homogenised along with 50 mL of commercial corn oil using a hand-operated laboratory piston-type homogeniser (MFC Microfluidizer<sup>TM</sup> Series 5000, Microfluidics Corporation, Newton, MA, USA) at 12 MPa, giving 40 L/h output flow for 90 s, with recirculation. The temperature was maintained at 20 °C. The preparations were carried out in triplicate for each sample. The emulsions were diluted 2500-fold with 0.1 % sodium dodecyl sulphate (SDS), immediately after homogenisation (t=0) and after 10 min of emulsion rest (t=10). The absorbance of the diluted emulsions was then determined at 500 nm in a spectrophotometer (CE 7400, Cecil Instruments Ltd., England). Each determination was performed in duplicate. The results were reported as the Emulsifying Activity Index (EAI) and the Emulsion Stability Index (ESI). The EAI and ESI were calculated by means of Equation 7 and Equation 8, respectively.

$$EAI = \frac{2 \cdot T}{\phi \cdot C} \quad (\text{Equation 7})$$

$$ESI = \frac{T \times \Delta t}{\Delta T} \quad (\text{Equation 8})$$

Where T is the turbidity,  $\phi$  is the volume fraction of the dispersed phase (calculated as the volume of the oil phase divided by the total volume of the emulsion), C is the weight of protein per unit volume of aqueous phase before the emulsion is formed (g/mL), and  $\Delta T$  is the change in turbidity (T) occurring during  $\Delta t$  (10 min). The EAI has units of the area of stabilised interface per unit weight of protein.

## 2.5. Statistical analysis

To evaluate the significance of the differences identified between the Weibull parameters, an analysis of variance (ANOVA) was performed and the LSD (least significant differences) intervals were identified. Likewise, from the ANOVA and the LSD intervals, the influence of the drying temperature and the drying and subsequent defatting process on the physicochemical and techno-functional characteristics was analysed with a 95 % confidence level ( $p < 0.05$ ). A statistical analysis was performed using Centurion XVI software (Statpoint Technologies Inc., Warrenton, VA, USA).

## 3. Results and discussion

### 3.1. Modelling of porcine liver drying kinetics

The experimental drying kinetics of porcine liver at 40 °C and at 70 °C are shown in Figure 1. The moisture content varied between 2.704 and 0.115 (g water / g dry matter) for the liver dried at 40 °C and between 2.704 and 0.105 (g water / g dry matter) for the liver dried at 70 °C. Moreover, Figure 1 shows how the drying rate increased when the temperature rose (70 °C). Thus, in the drying kinetics at 40 °C, it took 56700 s to reach a moisture of 0.1 g water /g dry matter, while at 70 °C, the time was shortened to 32400 s. Therefore, a 42.9 % reduction in the drying time was manifested at 70 °C.

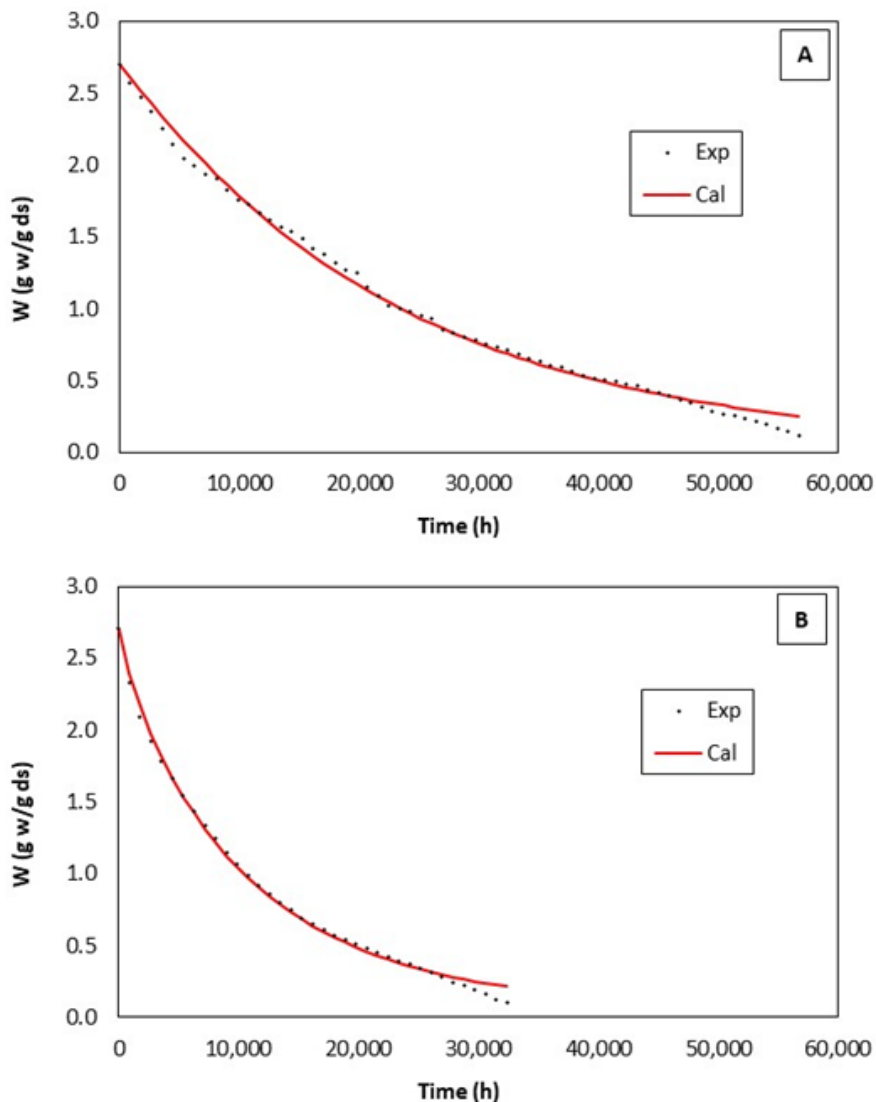


Figure 1. Experimental drying kinetics of porcine liver at 40 °C (A) and 70 °C (B) and the same drying kinetics calculated using the Weibull model.

The Weibull model provided a good description of drying kinetics, as shown in Figures 1A,B for the kinetics of dried porcine liver at 40 °C and 70 °C, respectively. The identified Weibull model parameters and goodness of fit estimators (%VAR and %MRE) are shown in Table 1. The percentages of explained variance obtained were high

( $99.5 \pm 0.1$  and  $99.6 \pm 0.1$  %, for 40 and 70 °C, respectively), and the MRE were equal to or lower than 10 % ( $9.36 \pm 0.33$  % and  $10.14 \pm 0.94$  %, for 40 and 70 °C, respectively), which indicates a reasonably satisfactory fit of the model (Table 1). On the one hand, as happened with the  $\alpha$  parameter, it was equal to 1 for the drying kinetics at 40 °C ( $1.02 \pm 0.03$ ), which indicates that the drying rate follows a first order kinetic pattern. In the case of the drying kinetics at 70 °C meanwhile, it was lower than 1 ( $0.86 \pm 0.02$ ), which indicated that the reaction rate was a decreasing function of time. On the other hand, the values of the  $\beta$  parameter were lower when drying porcine liver at 70 °C ( $1.1 \pm 0.4 \cdot 10^4$  s) they were  $2.3 \pm 0.4 \cdot 10^4$  s for the drying kinetics of porcine liver at 40 °C. As the  $\beta$  parameter is inversely proportional to the drying velocity, a reduction in this value indicates an increase in velocity (Cunha *et al.*, 1998); that is, drying velocity in the case of the kinetics at 70 °C is 54.17 % higher than at 40 °C (Figure 1).

Table 1. Weibull model parameters for porcine liver dried at 40 °C and 70 °C.

T (°C)	$\alpha$	$\beta$ ( $10^4$ s)	%VAR	%MRE
40	$1.02 \pm 0.03$	$2.3 \pm 0.4$	$99.5 \pm 0.1$	$9.36 \pm 0.33$
70	$0.86 \pm 0.02$	$1.1 \pm 0.4$	$99.6 \pm 0.1$	$10.14 \pm 0.94$

Weibull parameters ( $\alpha$  and  $\beta$ ) and statistical parameters (%VAR and %MRE). For Weibull parameters and %MRE, average values  $\pm$  LSD intervals are given (n = 3).

## 3.2. Physicochemical characterisation

### 3.2.1. Chemical composition

The chemical composition (moisture, protein, fat, and ash contents) of porcine liver samples is presented in Table 2. In general terms, dried samples presented a final moisture content of close to 10 % (Table 2), which is expected considering a moisture loss of 70 % during drying and an initial moisture content of nearly 73 % (Sánchez-Torres *et al.*, 2021). The observed differences between the moisture contents of the samples dried at 40 and 70 °C were related to minor changes in the weight loss during drying and the natural variability in the dried porcine liver. Defatting treatments also contributed to a reduction in the moisture content of the samples. The moisture contents of the dried and subsequently defatted samples were  $8.60 \pm 0.22$  % and  $6.62 \pm 0.31$  %, in DD-40 °C and DD-70 °C, respectively, which are lower values than those found for the samples that were only dried ( $11.24 \pm 0.40$  % in D-40 °C and  $7.86 \pm 0.27$  % in

D-70 °C). This difference was linked to the fact that the Soxhlet defatting method occurs at a high temperature (~70 °C) and, therefore, a greater dehydration of the samples could be expected.

Table 2. Chemical composition of porcine liver dried at 40 °C (D-40 °C) and 70 °C (D-70 °C) and subsequently defatted (DD-40 °C and DD-70 °C).

Sample	Moisture (%)	Protein (%)	Fat (%)	Ash (%)
D-40 °C	11.24 ± 0.40 <sub>A</sub>	61.10 ± 1.00 <sub>C</sub>	22.77 ± 1.57 <sub>A</sub>	3.99 ± 0.14 <sub>B</sub>
D-70 °C	7.86 ± 0.27 <sub>B</sub>	66.53 ± 0.06 <sub>B</sub>	19.60 ± 0.55 <sub>B</sub>	4.32 ± 0.10 <sub>B</sub>
DD-40 °C	8.60 ± 0.22 <sub>B</sub>	83.67 ± 1.15 <sub>A</sub>	3.36 ± 0.96 <sub>C</sub>	4.66 ± 0.88 <sub>AB</sub>
DD-70 °C	6.62 ± 0.31 <sub>C</sub>	82.98 ± 1.12 <sub>A</sub>	5.05 ± 0.05 <sub>C</sub>	5.39 ± 0.45 <sub>A</sub>

%: chemical composition (moisture, protein, fat, and ash) g/100 g product. Average values ± LSD intervals are given (n = 2). Different capital letters (A, B and C) show homogeneous groups established from LSD intervals ( $p < 0.05$ ) for moisture, protein, fat, and ash.

The defatting process enriched the protein content from around 16.5 to 22.6 % in the liver powders. A higher protein content was observed in the dried samples subjected to a defatting process (83.67 ± 1.15 % and 82.98 ± 1.12 % protein, in DD-40 °C and DD-70 °C, respectively), than in those that were only dried (61.10 ± 1.00 % and 66.53 ± 0.06 % protein in D-40 °C and D-70 °C, respectively).

Finally, the fat content in porcine liver samples dried at 40 °C and 70 °C was close to 20 % at both temperatures, but slightly higher in samples dried at 40 °C (22.70 ± 1.57 % fat in D-40 °C and 19.60 ± 0.55 % fat in D-70 °C). Defatting reduced the fat content by 85.2 % for the DD-40 °C (3.36 ± 0.96 % fat) and 74.2 % for the DD-70 °C (5.05 ± 0.05 % fat).

### 3.2.2. CIE L\*a\*b\* colour parameters

The colour modifications caused by drying and defatting treatments to porcine liver were analysed. On the one hand, the drying temperature did not lead to significant differences ( $p > 0.05$ ) in the Chroma (C\*) and yellowness from CIE L\*a\*b\* colour parameters. However, the drying temperature had a significant effect ( $p < 0.05$ ) on lightness, redness and Hue (H°) (Table 3). On the other hand, it is worth noting that

defatting induced noticeable modifications in the colour compared to those samples that were only dried, causing significant differences ( $p < 0.05$ ) in the different CIEL\*a\*b\* colour parameters. As seen in Table 3, the removal of fat caused an increase in luminosity ( $L^*$ ), obtaining values of  $73.95 \pm 0.48$  in DD-40 °C and  $67.99 \pm 0.53$  in DD-70 °C, compared to  $50.49 \pm 0.52$  in D-40 °C and  $53.95 \pm 1.37$  in D-70 °C and a decrease in the colour coordinate ( $a^*$ ) ( $4.39 \pm 0.08$  in DD-40 °C and  $4.97 \pm 0.09$  in DD-70 °C, compared to  $8.83 \pm 0.48$  in D-40 °C and  $7.09 \pm 0.29$  in D-70 °C). These changes were manifested in a tendency towards lightening (decrease in Chroma ( $C^*$ ) and increase in Hue ( $H^\circ$ )). In this regard, the  $C^*$  values obtained for the dried and defatted samples were  $16.23 \pm 0.04$  in DD-40 °C and  $17.66 \pm 0.03$  in DD-70 °C and the  $H^\circ$  values were  $74.97 \pm 0.31$  in DD-40 °C and  $73.66 \pm 0.28$  in DD-70 °C. Regarding the dried samples, the  $C^*$  values were  $19.60 \pm 0.59$  in D-40 °C and  $18.47 \pm 0.61$  in D-70 °C and the  $H^\circ$  were  $63.25 \pm 0.91$  in D-40 °C and  $67.44 \pm 0.28$  in D-70 °C.

Table 3. CIE L\*a\*b\* color parameters, chroma ( $C^*$ ) and hue ( $H^\circ$ ) of porcine liver dried at 40 °C (D-40 °C) and 70 °C (D-70 °C) and subsequently defatted (DD-40 °C and DD-70 °C).

Sample	$L^*$ (Lightness)	$a^*$ (Redness)	$b^*$ (Yellowness)	$C^*$ (Chroma)	$H^\circ$ (Hue)
D-40 °C	$50.49 \pm 0.52_A$	$8.83 \pm 0.48_A$	$17.50 \pm 0.46_A$	$19.60 \pm 0.59_A$	$63.25 \pm 0.91_A$
D-70 °C	$53.95 \pm 1.37_B$	$7.09 \pm 0.29_B$	$17.06 \pm 0.54_{AB}$	$18.47 \pm 0.61_A$	$67.44 \pm 0.28_B$
DD-40 °C	$73.95 \pm 0.48_C$	$4.39 \pm 0.08_C$	$16.35 \pm 0.06_B$	$16.93 \pm 0.04_B$	$74.97 \pm 0.31_C$
DD-70 °C	$67.99 \pm 0.53_D$	$4.97 \pm 0.09_D$	$16.94 \pm 0.04_B$	$17.66 \pm 0.03_C$	$73.66 \pm 0.28_D$

Average values  $\pm$  LSD intervals are given ( $n = 3$ ). Different capital letters (A, B, C and D) show homogeneous groups established from LSD intervals ( $p < 0.05$ ) for lightness, redness, yellowness, chroma, and hue.

### 3.2.3. Differential scanning calorimetry analysis

The thermograms obtained by DSC are shown in Figure 2, and they graphically represent the variations in total enthalpy and the maximum denaturation temperature. According to Agafonkina *et al.* (2019), the process of the irreversible thermal protein denaturation of different meat proteins could take place in the temperature range of 45 °C to 90 °C. Table 4 shows the calorimetric parameters obtained by DSC from samples of porcine liver dried at 40 °C and 70 °C, with and without subsequent defatting. In general terms, dried and defatted samples presented lower enthalpy values than raw



porcine liver (Table 4). This may reflect the structural modification in the protein matrix caused by drying and defatting. Moreover, differences in the endothermic heat flux were also found for dried samples (Figure 2). Drying at 40 °C resulted in a higher endothermic heat flux, which can be explained by considering the endothermic nature of the protein denaturation process. The samples dried at 70 °C have undergone greater irreversible denaturation leading to a lower total heat flux value during the calorimetric test. However, the liver dried at 40 °C presented a higher heat flux, because denaturation was milder than at 70°C. In addition, it is important to highlight that defatting did not cause noticeable changes in the degree of protein denaturation, since similar values were obtained in the total heat flux between the dried and subsequently defatted samples and those only dried (1.25 J/g in D-40 °C vs. 1.34 J/g in DD-40 °C and 0.54 J/g in D-70 °C vs. 0.46 J/g in DD-70 °C).

Table 4. DSC parameters (enthalpy of denaturation:  $\Delta H$ ; initial temperature:  $T_i$ ; denaturation points:  $T_{d1}$  and  $T_{d2}$ ) of porcine liver samples dried at 40 °C (D-40 °C) and 70 °C (D-70 °C), and subsequently defatted (DD-40 °C and DD-70 °C), reconstituted at 19.2% protein (w/v), as raw porcine liver.

Sample	$\Delta H_{total}$ (J/g)	$T_i$ (°C)	$T_{d1}$ (°C)	$T_{d2}$ (°C)
<b>D-40 °C</b>	1.25	49.16	65.87	85.10
<b>D-70 °C</b>	0.54	53.45	66.26	85.30
<b>DD-40 °C</b>	1.34	50.31	66.39	-
<b>DD-70 °C</b>	0.46	48.65	63.92	86.84
<b>Raw porcine liver</b>	3.46	52.29	66.44	86.90

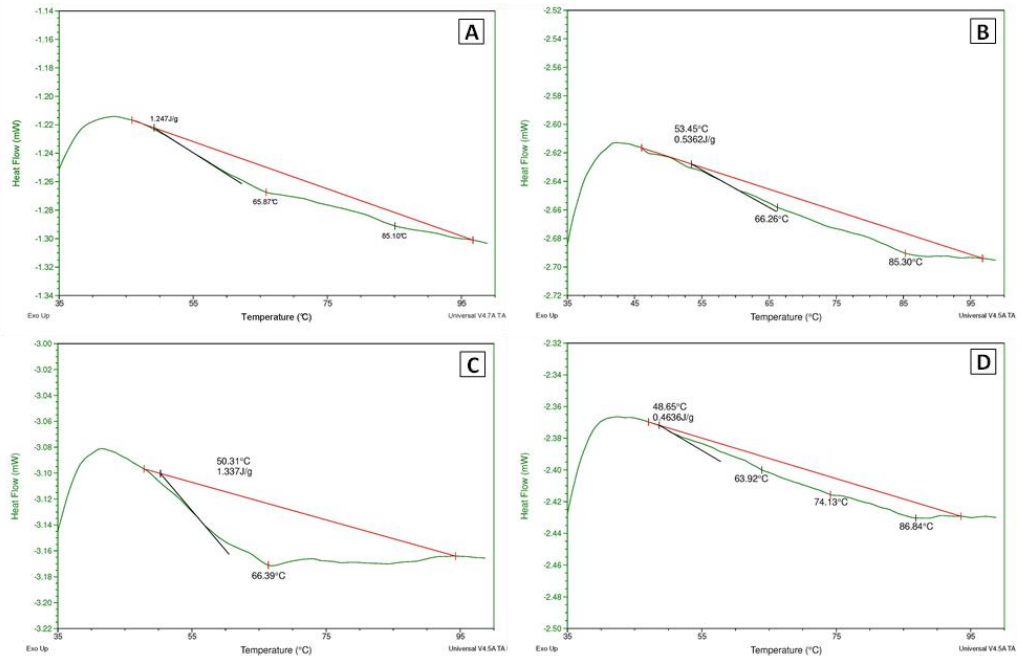


Figure 2. DSC thermograms of porcine liver samples dried at 40 °C (A) and 70 °C (B), and subsequently defatted (C,D) for samples dried at 40 and 70 °C, respectively, and reconstituted at 19.2% protein (w/v), as raw porcine liver. Endothermic heat flow (green lines); initial temperature ( $T_{in}$ ) at which heat flow is detected (black lines), and baseline (red lines) for calculating the total Enthalpy of denaturation ( $\Delta H$ ).

### 3.3. Techno-functional properties

#### 3.3.1. Protein solubility

The variation in the protein solubility of the different samples is a phenomenon that could be linked to the thermal denaturation produced by the drying and defatting treatments used. Thus, the drying temperature had a marked influence on the solubility of the proteins due to the fact that the samples dried at 70 °C were less soluble than those dried at 40 °C (Table 5). The variation in solubility is also explained by the results of the calorimetric analysis by DSC since, as commented on in section 3.2.3, a lower heat flux ( $H_{total}$ ) is obtained in the liver dried at 70 °C than those obtained at 40 °C and when using raw liver, which indicates that drying at high temperatures causes a greater structural modification of the proteins and, therefore, an irreversible protein denaturation.

Table 5. Soluble protein (%) and protein solubility (soluble protein/total protein, %) of porcine liver dried at 40 °C (D-40 °C) and 70 °C (D-70 °C) and subsequently defatted (DD-40 °C and DD-70 °C).

Sample	Soluble Protein (%)	Solubility (%)
D-40 °C	27.95 ± 0.31	45.74 ± 0.50
D-70 °C	12.43 ± 0.31	18.69 ± 0.46
DD-40 °C	35.63 ± 2.26	42.60 ± 2.91
DD-70 °C	14.64 ± 0.09	17.64 ± 0.30

Average values ± LSD intervals are given (n = 2).

Defatted samples presented a slight reduction in protein solubility compared to those samples that were only dried, but the differences were not significant ( $p > 0.05$ ), (45.74 ± 0.50 % in D-40 °C vs 42.60 ± 2.91 % in DD-40 °C and 18.69 ± 0.46 % in D-70 °C vs 17.64 ± 0.30 % in DD-70 °C). The addition of the solvent (ethyl ether) used for defatting caused the appearance of hydrophobic regions on the surface of the proteins (Jeantet *et al.*, 2006) that could slightly affect the protein solubility.

### 3.3.2. Surface functional properties (foaming and emulsifying)

The foaming and emulsifying properties of dried and defatted porcine liver are shown in Table 6. The porcine liver dried at 40 °C and subsequently defatted (DD-40 °C) was the one that presented the highest foaming capacity together with a high degree of stability compared to the rest of the treatments (Foam capacity: 700.31 ± 32.35 mL and RFS: 13.76 min). These results were consistent with the effects of liver processing treatments on protein solubility. The drying temperature affected the protein solubility of porcine liver; consequently, the foaming properties were reduced, and there was a sharp drop in the % of foam formation at 20 min for every treatment, the foam formed being under 60 % (Figure 3). Moreover, the defatting treatment contributed to the enhancement of the foaming properties of the protein fraction. This increase could be linked to the aforementioned effect provoked by the solvent used in defatting (ethyl ether) on the appearance of hydrophobic regions on the surface of the proteins, which enhances the surface-active properties of the proteins between the continuous and dispersed phases. Although there were no variations observed between the emulsifying

activity of the different treatments, a similar pattern to that found in the foaming properties was reproduced for the emulsifying stability. The ESI values of porcine liver fell as the drying temperature rose, whereas the defatting process did not contribute to an improvement in the emulsifying properties. However, when comparing the parameters of the functional surface properties obtained in the samples analysed in the present study with those of protein extracts from porcine hearts and spleens at pH 6.5 (Table 6), derived from other research (Camps *et al.*, 2019; Morera *et al.*, 2016; Parés *et al.*, 2020; Toldrà *et al.*, 2019), it can be seen how all the samples analysed have very poor surface functional properties, regardless of the treatment applied. However, the protein extracts from porcine heart and spleen did not undergo a prior drying or a drying and subsequent defatting process. Therefore, the functional properties of the proteins cannot be compared because the porcine liver proteins of the present study have undergone a structural modification brought about by denaturation as shown by the DSC and solubility results. For this reason, there are fewer functional properties of dried or dried/defatted porcine livers compared to protein extracts from raw porcine heart and spleen.

Table 6. Surface functional properties (foaming capacity; foam stability: RFS; emulsifying activity: EAI; emulsion stability: ESI) of porcine liver dried at 40 °C (D-40 °C) and 70 °C (D-70 °C) and subsequently defatted (DD-40 °C and DD-70 °C), compared to pork heart protein and pork spleen protein (pH 6.5).

Sample	Foaming Capacity (mL)	Foam Stability (RFS) (min)	Emulsifying Activity (EAI) (m <sup>2</sup> /g)	Emulsion Stability (ESI) (min)
<b>D-40 °C</b>	235.62 ± 34.2 <sub>B</sub>	7.43	74.85 ± 32.61 <sub>A</sub>	26.44 ± 0.42 <sub>B</sub>
<b>D-70 °C</b>	81.16 ± 4.53 <sub>A</sub>	27.79	92.51 ± 14.43 <sub>A</sub>	15.12 ± 2.83 <sub>A</sub>
<b>DD-40 °C</b>	700.31 ± 32.35 <sub>D</sub>	13.76	72.01 ± 36.08 <sub>A</sub>	22.56 ± 5.19 <sub>B</sub>
<b>DD-70 °C</b>	403.17 ± 4.53 <sub>C</sub>	7.23	72.01 ± 13.40 <sub>A</sub>	13.39 ± 0.27 <sub>A</sub>
<b>Pork heart protein (1)</b>	364.9	5.41	354.74	35.19
<b>Pork spleen protein (2)</b>	712.1	25.11	497.3	57.6

Average values ± LSD intervals are given (n = 3). Different capital letters (A, B, C and D) show homogeneous groups established from LSD intervals ( $p < 0.05$ ) for foaming capacity, foam stability, emulsifying activity, and emulsion stability. (1) Parés *et al.* (2020); (2) Toldrà *et al.* (2019).

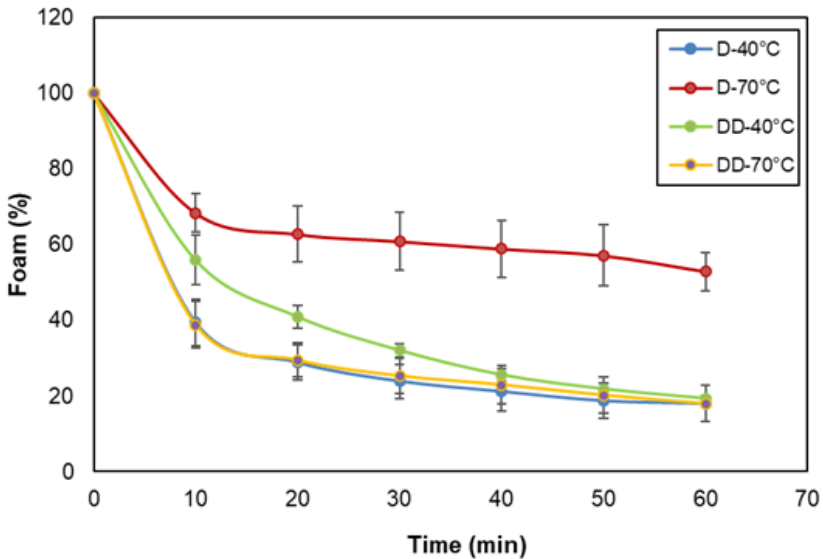


Figure 3. Foam stability (relative percentage of foam) of porcine liver protein solutions (0.5% w/v) of samples dried (D) at 40 and 70 °C and subsequently defatted (DD) (means  $\pm$  SD, n = 3).

#### 4. Conclusions

The drying temperature influenced the physicochemical and techno- functional parameters of the porcine livers, 40 °C being the temperature that presented less protein degradation compared to the porcine liver dried at 70 °C. At the same time, the defatting stage contributed to an enhancement of certain techno-functional characteristics, such as foaming capacity and stability. Therefore, the treatments applied to the liver protein fractions should be determined according to the subsequent use of the liver ingredients. Further research should also investigate the impact of the drying process at milder temperatures (10, 20, 30 °C) on the porcine liver in order to develop optimal thermal processing conditions that minimise the loss of quality and functionality in the protein matrix, while prolonging the shelf life of this highly perishable co-product.

## Acknowledgements

The authors acknowledge the financial support from the “Ministerio de Economía y Competitividad (MINECO)” and “Instituto Nacional de Investigación y Tecnología Agraria y Alimentaria (INIA)” in Spain (Projects RTA2017-00024-C04-03 and RTA2017-00024-C04-02). The authors acknowledge the contribution of the slaughterhouse “Carnes de Teruel S.A.” (D.O. Jamón de Teruel, Spain) for the supply of porcine livers.

## References

- AOAC (Association of Official Analytical Chemists), (2000). Official methods of analysis of AOAC international (17th ed.; International Association of Official Analytical, ed.). Arlington, VA, Washington DC.
- Agafonkina I.V., Korolev I.A., Sarantsev T.A. (2019). The study of thermal denaturation of beef, porcine, chicken and turkey muscle proteins using differential scanning calorimetry. *Theory and practice of meat processing*, 4 (3): 19-23. doi:10.21323/2414-438X-2019-4-3-19-23
- Albenzio, M., Santillo, A., Caroprese, M., Della Malva, A., & Marino, R. (2017). Bioactive peptides in animal food products. *Foods*, 6(5), 35. <https://doi.org/10.3390/foods6050035>
- Aspevik, T., Oterhals, Å., Rønning, S. B., Altintzoglou, T., Wubshet, S. G., Gildberg, A., ... & Lindberg, D. (2017). Valorization of proteins from co-and by-products from the fish and meat industry. *Chemistry and chemical technologies in waste valorization*, 123-150. [https://doi.org/10.1007/978-3-319-90653-9\\_5](https://doi.org/10.1007/978-3-319-90653-9_5)
- Banco Mundial. (2019). Guía de Invertir en ganadería sostenible. Obtained from <https://www.sustainablelivestockguide.org/>

- Borrajo, P., Pateiro, M., Barba, F. J., Mora, L., Franco, D., Toldrá, F., & Lorenzo, J. M. (2019). Antioxidant and antimicrobial activity of peptides extracted from meat by-products: A review. *Food Analytical Methods*, 12(11), 2401-2415. <https://doi.org/10.1007/s12161-019-01595-4>
- Camps, E. (2019). Determinació de les propietats tecnofuncionals d'extractes proteics solubles de cors de porc. Final Degree Project. Universitat de Girona.
- Cunha, L. M.; Oliveira, F. A. R.; Oliveira, J. C. (1998). Optimal experimental design for estimating the kinetic parameters of processes described by the Weibull probability distribution function. *Journal of Food Engineering*. 37, 175-191. [https://doi.org/10.1016/S0260-8774\(98\)00085-5](https://doi.org/10.1016/S0260-8774(98)00085-5)
- Estévez, M., Morcuende, D., Ramírez, R., Ventanas, J., & Cava, R. (2004). Extensively reared Iberian pigs versus intensively reared white pigs for the manufacture of liver pâté. *Meat Science*, 67(3), 453-461. <https://doi.org/10.1016/j.meatsci.2003.11.019>
- Food and Agricultural Organization of the United States. FAOSTAT Statistical Database. 1997. Available online: <http://www.fao.org/faostat/en/#data/CL> (accessed on 2 May 2022).
- García, R. G., Marín, C. E., Marín, R. G., & Álvarez, V. R. (2021). El sector del ganado porcino en España: caracterización, producción, comercio y repercusiones ambientales derivadas. The pig sector in Spain: characterization, production, trade and derived environmental problems. *TERRA: Revista de Desarrollo Local*, (8), 194-230.
- Giroto, F.; Cossu, C.A. (2017). Animal waste and waste animal by-products generated along the livestock breeding and meat food chain. *Waste Manag*, 70, 1–2. <https://doi.org/10.1016/j.wasman.2017.11.028>
- Jeanet, R., Croguennec, T., Schuck, P., & Burlé, G. (2006). Ciencia de los alimentos (La Voisier).



- Kim, T. K., Yong, H. I., Chun, H. H., Lee, M. A., Kim, Y. B., & Choi, Y. S. (2020). Changes of amino acid composition and protein technical functionality of edible insects by extracting steps. *Journal of Asia-Pacific Entomology*, 23(2), 298-305. <https://doi.org/10.1016/j.aspen.2019.12.017>
- Lafarga, T., & Hayes, M. (2014). Bioactive peptides from meat muscle and by-products: generation, functionality and application as functional ingredients. *Meat science*, 98(2), 227-239. <https://doi.org/10.1016/j.meatsci.2014.05.036>
- Leal, E. S., Ítavo, L. C. V., Ítavo, C. C. B. F., Nogueira, É., Franco, G. L., Gomes, M. D. N. B., ... & de Mello, J. A. T. (2021). Combinations of by-products from biodiesel production included in the supplement for finishing heifers on deferred pastures. *Tropical Animal Health and Production*, 53(2), 1-9. <https://doi.org/10.1007/s11250-021-02712-4>
- Llauger, M., Claret, A., Bou, R., López-Mas, L., & Guerrero, L. (2021). Consumer Attitudes toward Consumption of Meat Products Containing Offal and Offal Extracts. *Foods*, 10(7), 1454. <https://doi.org/10.3390/foods10071454>
- Lo, B., Kasapis, S., & Farahnaky, A. (2021). Lupin protein: Isolation and techno-functional properties, a review. *Food Hydrocolloids*, 112, 106318. <https://doi.org/10.1016/j.foodhyd.2020.106318>
- Lynch, S. A., Mullen, A. M., O'Neill, E., Drummond, L., & Álvarez, C. (2018). Opportunities and perspectives for utilisation of co-products in the meat industry. *Meat Science*, 144, 62-73. <https://doi.org/10.1016/j.meatsci.2018.06.019>
- Marabi, A., Livings, S., Jacobson, M., Saguy, I.S. (2003). Normalized Weibull distribution for modeling rehydration of food particulates. *Eur Food Res Technol* 217(4): 311–318. <https://doi.org/10.1007/s00217-003-0719-y>
- Mishyna, M., Keppler, J. K., & Chen, J. (2021). Techno-functional properties of edible insect proteins and effects of processing. *Current Opinion in Colloid & Interface Science*, 56, 101508. <https://doi.org/10.1016/j.cocis.2021.101508>

- Morera, X. (2016). Caracterització de melses de porcí com a font de proteïnes per la indústria alimentària. Final Degree Project. Universitat de Girona.
- Morr, C. V, German, B., Kinsella, J.E., Regenstein, J.M., Buren, J.P.V.A.N., Kilara, A., Lewis, B.A., Mangino, M.E., 1985. A Collaborative Study to Develop a Standardized Food Protein Solubility Procedure. *J. Food Sci.* 50, 1715-1718. <https://doi.org/10.1111/j.1365-2621.1985.tb10572.x>
- Nollet, L.M.L. and Toldrà, F. eds. (2019). Handbook of analysis of edible animal by-products. CRC Press.
- Parés, D. & Ledward, D.A. (2001). Emulsifying and gelling properties of porcine blood plasma as influenced by high-pressure processing. *Food Chemistry*, 74: 139-145. [https://doi.org/10.1016/S0308-8146\(01\)00105-4](https://doi.org/10.1016/S0308-8146(01)00105-4)
- Parés, D., Toldrà, M., Saguer, E., & Carretero, C. (2014). Scale-up of the process to obtain functional ingredients based in plasma protein concentrates from porcine blood. *Meat science*, 96(1), 304-310. <https://doi.org/10.1016/j.meatsci.2013.07.022>
- Parés, D., Toldrà, M., Camps, E., Geli, J., Saguer, E, Carretero, C. (2020). RSM Optimization for the Recovery of Technofunctional Protein Extracts from Porcine Hearts. *Foods*, 9 (12): 1733. <https://doi.org/10.3390/foods9121733>
- Pearce, K.N. & Kinsella, J.E. (1978). Emulsifying properties of proteins - evaluation of a turbidimetric technique. *Journal of Agricultural and Food Chemistry*, 26: 716-723.
- Sánchez-Torres, E. A., Abril, B., Benedito, J., Bon, J., & García-Pérez, J. V. (2021). Water desorption isotherms of porcine liver and thermodynamic properties. *LWT*, 149, 111857. <https://doi.org/10.1016/j.lwt.2021.111857>

- Seong, P. N., Park, K. M., Cho, S. H., Kang, S. M., Kang, G. H., Park, B. Y., ... & Van Ba, H. (2014). Characterization of edible pork by-products by means of yield and nutritional composition. *Korean Journal for Food Science of Animal Resources*, 34(3), 297. doi:10.5851/kosfa.2014.34.3.297
- Soladoye, P. O., Juárez, M., Estévez, M., Fu, Y., & Álvarez, C. (2022). Exploring the prospects of the fifth quarter in the 21 century. *Comprehensive Reviews in Food Science and Food Safety*, 1- 23. <https://doi.org/10.1111/1541-4337.12879>
- Toldrà, F., Aristoy, M. C., Mora, L., & Reig, M. (2012). Innovations in value-addition of edible meat by-products. *Meat science*, 92(3), 290-296. <https://doi.org/10.1016/j.meatsci.2012.04.004>
- Toldrà, M., Parés, D., Saguer, E., & Carretero, C. (2019). Recovery and extraction of technofunctional proteins from porcine spleen using response surface methodology. *Food and Bioprocess Technology*, 12 (2): 298-312. <https://doi.org/10.1007/s11947-018-2208-0>.
- Toldrà, F., Reig, M., & Mora, L. (2021). Management of meat by-and co-products for an improved meat processing sustainability. *Meat Science*, 108608. <https://doi.org/10.1016/j.meatsci.2021.108608>.
- Toldrà, M., Taberner, P., Parés, D., & Carretero, C. (2021). Surimi-like protein ingredient from porcine spleen as lean meat replacer in emulsion-type sausages, *Meat Science*, 182: 108640. <https://doi.org/10.1016/j.meatsci.2021.108640>
- Wadhwa, M., & Bakshi, M. P. S. (2016). Application of waste-derived proteins in the animal feed industry. In *Protein byproducts* (pp. 161-192). Academic press. <https://doi.org/10.1016/B978-0-12-802391-4.00010-0>



## **CAPÍTULO 3**

### *Desodorización de hígado de cerdo*



*Supercritical CO<sub>2</sub> deodorization of dried pork liver*

---

Blanca Abril<sup>1</sup>, José María Lorenzo<sup>2,3</sup>, José Vicente García-Pérez<sup>1</sup>,  
Marina Contreras<sup>1</sup> and José Benedito<sup>1</sup>

<sup>1</sup>Department of Food Technology, Universitat Politècnica de València, Camí de Vera, s/n, Valencia 46022, Spain

<sup>2</sup> Centro Tecnológico de la Carne de Galicia, Rúa Galicia No. 4, Parque Tecnológico de Galicia, San Cibrao das Viñas, Ourense, Spain

<sup>3</sup> Universidad de Vigo, Área de Tecnología de los Alimentos, Facultad de Ciencias de Ourense, 32004 Ourense, Spain





## Supercritical CO<sub>2</sub> deodorization of dried pork liver

### Abstract

Pork liver has excellent nutritional properties but is a highly perishable product often rejected by consumers due to its strong unpleasant flavour. The objective of this study was to analyze the feasibility of the deodorization of dried pork liver by means of vacuum steam distillation (VSD) and supercritical CO<sub>2</sub> (SC-CO<sub>2</sub>).

The results showed that both deodorization techniques were effective at reducing volatile organic compounds (VOCs). Through VSD, the VOC content was reduced by 67.6 % UA, while an 81.3% UA reduction was achieved by SC-CO<sub>2</sub>, with respect to dried pork liver. In addition, 3 characteristic compounds of raw pork liver were completely eliminated by applying SC-CO<sub>2</sub>, which could potentially reduce the characteristic mushroom (1-octen-3-ol), fatty and green (1-nonanol), and fishy ((E,E)-2,4-heptadienal) off-flavours. Therefore, SC-CO<sub>2</sub> could be considered a promising technique for the elimination of VOCs, and furthermore it leads to a reduction in the fat content (24.9 %).

**Keywords:** Pork liver, deodorization, steam distillation, supercritical CO<sub>2</sub>, volatile, off-flavour

## 1. Introduction

Pork liver, like other meat co-products and pork viscera, is a co-product of the porcine industry with a high nutritional value, being an important source of proteins (22.05 %), lipids (2.94 %), minerals and vitamins (Seong *et al.*, 2014). However, the commercial value of pork liver is very low at this moment (Seong *et al.*, 2021). In this context, it is of interest to valorize animal co-products, such as pork liver, searching for new products or ingredients in order to achieve a more competitive and sustainable industry (Lynch *et al.*, 2018). Different studies have reported the valorization of pork liver as a means of obtaining proteins and liver hydrolysates, which have excellent functional and technological (foaming, emulsifying and solubility) properties and biological activity as bioactive peptides (Seong *et al.*, 2021; López-Pedrouso *et al.*, 2020).

Nowadays, pork liver is mainly used as an ingredient in pâté products and animal feed (Lynch *et al.*, 2018), what is linked to two main aspects. The first issue is its highly perishable nature, since it contains a high water content (73 %) and many nutrients (Sánchez-Torres *et al.*, 2021). In order to address stability problems, air drying could be considered as a suitable preservation technique of moderate cost. In addition, dried pork liver facilitates storage and reduces weight and volume in liver processing and transportation (Sánchez Torres *et al.*, 2021). The second thing that explains its low commercial value, is linked to its strong, characteristic flavour, which leads to consumer rejection. The pork liver off-flavour has been described as intensely fishy and metallic (Im & Kurata, 2003). Several studies have aimed to improve liver acceptability using different culinary techniques to eliminate or mask liver's unpleasant odour (Kimura *et al.*, 1990). Thereby, a deep understanding of pork liver deodorization, using conventional or emerging techniques, would be a matter of relevant research and necessary in order to improve further uses of its protein fraction.

The issue related to off-flavours in pork liver is common to other novel protein sources, such as in the case of legumes or other vegetables (Kumar *et al.*, 2017; Damodaran & Arora, 2013; Wang *et al.*, 2021; Guldiken *et al.*, 2021). In addition to vegetable proteins, whey protein concentrates have also been associated with tastes

that are unpleasant for the consumer (Whetstine *et al.*, 2005). For these reasons, unless the flavour of the new protein isolates is improved, their direct use in human foodstuffs will remain very limited.

Deodorization consists of reducing or completely eliminating the content of those Volatile Organic Compounds (VOCs) associated with an unpleasant odour. Previous studies have applied deodorization to oils, either oilseed-based (Zehnder, 1995) or fish-based (De Oliveira *et al.*, 2016). Deodorization has also been applied to fish (Li *et al.*, 2020) and spices (Silva *et al.*, 2005) among other foods. However, to our knowledge, the application of deodorization techniques to meat products has not been addressed to date. To date, the most frequently-applied and efficient deodorization technique for the extraction of VOCs is distillation, which is based on the use of water as an extraction medium, either as a liquid or as vapour. Specifically, deodorization by steam distillation is the most common method (Silva *et al.*, 2005); this consists of generating steam at a high or moderate temperature (with or without vacuum) and putting it in contact with the sample to be deodorized (Zehnder, 1995). This method has been shown to be the most effective at deodorizing products, such as turmeric powder, reducing the odour to a greater extent than other methods, such as Kjeldahl, rotary evaporation or non-steam vacuum distillation (Silva *et al.*, 2005).

The use of supercritical CO<sub>2</sub> (SC-CO<sub>2</sub>) represents one of the few alternatives to distillation. The physical properties of SC-CO<sub>2</sub>, including high compressibility, liquid-like density, low viscosity, and high diffusivity (Mouahid *et al.*, 2017), allow its penetration into the solid matrix and the solubility of target compounds. Moreover, SC-CO<sub>2</sub> has other advantages: it has a low critical temperature (31 °C) and surface tension and better selectivity and is also non-toxic, non-flammable, economical and easily removable from the matrix to be deodorized (Reverchon & De Marco, 2006). SC-CO<sub>2</sub> has been used in the food industry for the extraction of different molecules, such as lipids and cholesterol (Vedaraman *et al.*, 2005), colorants such as tomato lycopene (Vasapollo *et al.*, 2004), caffeine from coffee or tea (Zabot, 2020) and various components (squalene, lipids, vitamin A and β carotene) from liver (Lee *et al.*, 2022; Kang *et al.*, 2017; Burri *et al.*, 1997). In addition to extracting compounds of interest,

SC-CO<sub>2</sub> has been used to reduce the fat content of high-protein food sources, such as meat and fish, preventing protein denaturation due to the mild temperatures used (King, 2014). Although the application of this technique for deodorization purposes is relatively expensive, its numerous advantages are in line with the demand for clean and safe technologies (King, 2014). SC-CO<sub>2</sub> has been applied for the deodorization of drinking water (Kobayashi *et al.*, 2006), custard apple seed powder (Panadare *et al.*, 2021), truffles (Tejedor-Calvo *et al.*, 2021), lavandin and thyme extracts (Oszagyan *et al.*, 1996), soy-protein isolate (Maheshwari *et al.*, 1995) and fish sauce (Shimoda *et al.*, 2000). However, so far, the use of SC-CO<sub>2</sub> for the extraction of VOCs in meat products has not been addressed. Therefore, the use of SC-CO<sub>2</sub> for the deodorization, and simultaneous defatting, of the pork liver would help to revalorize a product with a very relevant nutritional composition, taking advantage of its high protein content. Thus, the objective of this study was to analyze the feasibility of using supercritical CO<sub>2</sub> for the deodorization of dried pork liver comparing its performance with vacuum steam distillation.

## **2. Material and methods**

### **2.1. Raw material and sample preparation**

Raw pork livers (RPL), from an industrial slaughterhouse, were transported at 4 °C to the laboratory. Liver conditioning consisted of i) the separation of its 4 main lobes, ii) the splitting of each lobe into two parts, (iii) vacuum packaging (200 x 300 PA / PE, Sacoliva, Castellar del Vallès, Barcelona) and (iv) freezing (at -20 °C) until processing.

### **2.2. Drying process**

Before drying, vacuum packaged samples were tempered at 2 °C for 2 h in order to facilitate further handling. Using a household device, cylinders (12.6 mm diameter x 15 mm height) were obtained to be dried. Drying was carried out at a high temperature (105 °C) using a convective oven (FD 56, Binder, Germany) with an air speed of 1.3 m·s<sup>-1</sup> for 24 h until constant weight was reached (AOAC 950.46 B) (AOAC, 2016). Subsequently, the dried pork liver (DPL) samples were ground and mixed with

the aim of obtaining a representative sample. Then, the dried pork liver samples were vacuum packaged in 200 x 300 PA / PE bags (Sacoliva, Castellar del Vallès, Barcelona) of approximately  $3 \pm 0.05$  g for deodorization tests by vacuum steam distillation and  $30 \pm 0.05$  g for deodorization tests by supercritical CO<sub>2</sub>. Finally, the samples were stored in refrigeration at 4 °C until their subsequent deodorization.

## **2.3. Deodorization process**

### **2.3.1. Vacuum steam distillation**

Deodorization by vacuum steam distillation (VSD) was carried out using the experimental set-up shown in Figure 1. The distillation balloon (2, Figure 1), with 2 L of distilled water, was placed in the water bath (HB digital 115, IKA, Germany) (1, Figure 1) which was kept at 80 °C. The balloon was attached to the distillation column (3, Figure 1) in which 3 g of dried pork liver samples were placed into filter-paper cartridges. Thus, the steam generated rose in the column passing through the sample with a flow of 0.19 g/s. Afterwards, the steam passed through a condenser (4, Figure 1), which was connected to a cooling unit (5, Figure 1), and the condensate was collected in a small distillation balloon (6, Figure 1). The entire system was connected to a vacuum pump (MZ 2C, Vacuubrand, Germany) (7, Figure 1) (0.07 mbar) that allowed steam generation at low temperature ( $42 \pm 2$  °C). A water trap (8, Figure 1) was used to prevent the steam from reaching the vacuum pump. After the deodorization operation was completed, the volume of water collected was measured in order to compute the steam used (1100-1200 mL). The deodorization time was set at 90 min. Finally, the deodorized pork liver samples (DPL-VSD) were removed from the paper cartridge and stored frozen (-20 °C) until their VOCs analysis. Deodorization by VSD was replicated 3 times.

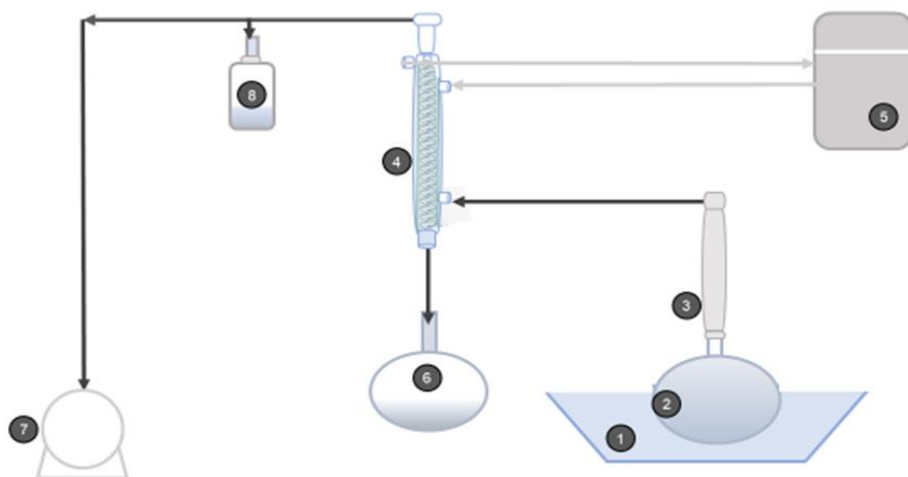


Figure 1. Deodorization by vacuum steam distillation: 1- Water bath; 2-Distillation balloon; 3-Distillation column; 4-Condenser; 5-Cooling system; 6-Condensate balloon; 7-Vacuum pump; 8-Water trap.

### 2.3.2. Supercritical CO<sub>2</sub>

Pork liver was treated with supercritical carbon dioxide (SC-CO<sub>2</sub>) for the purposes of removing the VOCs using laboratory-scale equipment. Figure 2 shows the SC-CO<sub>2</sub> system, which consisted of a deodorization vessel (1, Figure 2) into which a stainless steel cell, containing 30 g of dried pork liver, was placed (2, Figure 2). The stainless steel cell had filters on both sides, that allowed the sample to be retained and the SC-CO<sub>2</sub> to circulate at a pre-set temperature, and in pre-established pressure and time conditions. The vessel containing the sample to be deodorized was immersed in a thermostatic water bath (3, Figure 2) to maintain the temperature. In addition, the system was supplied with a separator tank (4, Figure 2) into which 90 g of activated carbon was placed for its ability to absorb volatile compounds (Pui *et al.*, 2019). The CO<sub>2</sub> tank (5, Figure 2) was connected to a cooling system, which maintained CO<sub>2</sub> at -18 °C (6, Figure 2) and a diaphragm dosing pump (LDB, LEWA, Tokyo, Japan) was used to achieve the desired pressure in the deodorization vessel (7, Figure 2). A manometer and a K-type thermocouple were installed inside the vessel to measure the temperature and pressure of the sample throughout the process (8, Figure 2).

Carbon dioxide was pumped from the cooling tank (6, Figure 2) to the deodorization vessel (1, Figure 2), where the sample to be deodorized was placed, changing states from liquid to supercritical. When the supercritical CO<sub>2</sub> leaves the deodorization vessel, it turns to vapour and passes through the separator tank containing active carbon (4, Figure 2). The CO<sub>2</sub> flow rate was constant during all the experiments ( $1 \pm 0.05$  kg CO<sub>2</sub>/h). The circuit was closed when the CO<sub>2</sub> vapour turned into liquid by passing it through the cooling reservoir (6, Figure 2) and recirculated again. Subsequently, the deodorized pork liver samples (DPL-SCCO<sub>2</sub>) were extracted from the stainless steel container and stored frozen (-20 °C) until their VOC analysis.

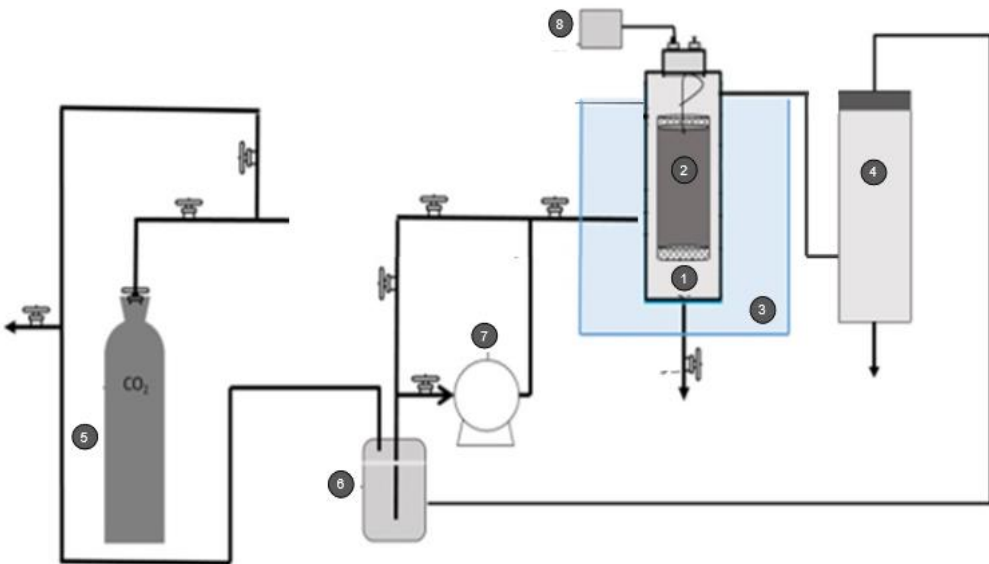


Figure 2. Deodorization by supercritical CO<sub>2</sub>: 1- Deodorization vessel, 2- Stainless steel cell containing the sample, 3- Bath, 4- Separator tank with active carbon, 5- CO<sub>2</sub> tank, 6- Reservoir/cooling tank, 7-Pump, 8- Manometer and a K-type thermocouple.

A Box Behnken experimental design was carried out for the optimization of the deodorization conditions, including the following variables: pressure (200, 325 and 450 bar), temperature (35, 50 and 65 °C) and time (30, 60 and 90 min). The design involved three levels for each factor and three replicates at the centre point (15 experimental runs) (Table 1).

Table 1. Box Behnken design for the SC-CO<sub>2</sub> deodorization experiments

<b>Treatment</b>	<b>Temperature (°C)</b>	<b>Pressure (bar)</b>	<b>Time (min)</b>
1	50	200	90
2	65	200	60
3	65	325	90
4	65	325	30
5	50	450	30
6	35	325	30
7	65	450	60
8	50	450	90
9	50	200	30
10	35	450	60
11	35	200	60
12	35	325	90
13	50	325	60
14	50	325	60
15	50	325	60

#### 2.4. Volatile organic compounds analysis

The volatile organic compounds (VOCs) were analysed following the methodology previously described by Domínguez *et al.* (2019) and consisting of solid phase microextraction with headspace (HS-SPME), coupled to gas chromatography (GC) and mass spectroscopy (MS) detection (HS-SPME-GC/MS).

For the HS-SPME, 10 mm long molten silica fiber coated with a 50/30 mm thick layer of divinylbenzene, carboxene and polydimethylsiloxane (Supelco, Bellefonte, PA,



USA) was used. Before carrying out the analysis, the fiber was conditioned by heat at 270 °C for 30 min. To perform the extraction,  $1 \pm 0.02$  g were introduced into 20 mL vials (Agilent Technologies, Santa Clara, CA, USA) and screwed with a laminated Teflon rubber disc. The samples were balanced for 15 min at 37 °C to ensure a homogeneous sample temperature and headspace. Then, the extractions were performed at 37 °C for 30 min.

Once the extraction was completed, the fiber was transferred to the injection zone of the system consisting of the gas chromatograph and the mass spectrometer (GC-MS). The HS-SPME fiber was desorbed and maintained in the injection site (splitless mode and a helium pressure of 9.59 psi) at 260 °C for 8 min. After each injection, the fiber was washed and conditioned at 270 °C for 2 min to ensure that it was clean before the next extraction. Helium was used as the carrier gas with a constant flow rate of 1.2 mL/min (9.59 psi). The column that was used for the separation of the volatile components was a DB-624 capillary column 30 m long, 250  $\mu$ m wide and 1.4  $\mu$ m film thickness (J&W Scientific, Folsom, CA, USA). A preheating was carried out to reach an isothermal temperature of 40 °C for 10 min, followed by a first heating where the temperature rose up to 200 °C to 5 °C/min. Finally, a second heating was carried out where the temperature rose up to 250 °C at 20 °C/min, which was maintained for 5 min. The analysis lasted 49.5 min.

As for the conditions of the MS, the transfer line was maintained at 260 °C. The ion source used was The Extraction Source Xtr EI 350 (Agilent Technologies, Santa Clara, CA, USA). The mass spectrum was obtained using the selective mass detector 5977B working with an electronic energy of 70 eV, with an electron multiplier voltage of around 900 V (gain factor = 1) and obtaining 2.9 scanners/s in the m/z range 40–550 in scan acquisition mode. The mass source was maintained at 230 °C while the mass quad was adjusted to 150 °C.

After the chromatographic analysis, all the data obtained were studied with the MassHunter Quantitative Analysis B.07.01 software. A comparison of these with bibliographic information was carried out. The integration of the peak areas was performed with the Agile2 algorithm, while the detection peak was obtained by

deconvolution. The compounds were identified by comparing the mass spectra obtained with those published in the NIST14 database. The compounds were considered correctly identified when they had a matching factor greater than 85 %.

From the chromatograms, the content of each compound was determined by the area of its peak, which were expressed by units of area (UA). In order to calculate the percentage of VOCs for the different families of chemical compounds, the ratio between the UA for each VOCs family and the total area (sum of the UA for all VOCs detected) was computed for each of the analysed samples: RPL, DPL, DPL-VSD and DPL-SCCO<sub>2</sub>. In order to calculate how the deodorization affects VOCs content, the loss (% UA) for each VOCs family was computed as the ratio of the UA for each family of the deodorized samples (VSD and SC-CO<sub>2</sub>) to the UA from dried pork liver (DPL).

## **2.5. Chemical composition**

To analyze the chemical composition (moisture, ash, protein, and fat contents) of DPL, DPL-VSD and DPL-SCCO<sub>2</sub>, the AOAC procedures (AOAC, 2016) were followed. The moisture and ash contents were determined gravimetrically using a hot air oven and a muffle furnace, respectively. The protein content was estimated from the total Kjeldahl nitrogen (TKN x 6.25) by using a Gerhardt KB20 digestion system (C. Gerhardt GmbH & Co., Königswinter, Germany) and a Büchi K-314 distillation unit (Büchi Labortechnik AG, Flawil, Switzerland). The total fat content was determined gravimetrically by Soxhlet extraction with diethyl ether as a solvent. Each sample was analyzed in triplicate.

## **2.6. Statistical analysis**

A response surface design (Box-Behnken) was employed using Statgraphics Centurion XVI (Statpoint Technologies Inc., Warrenton, VA, USA) to study how the temperature and pressure at which SC-CO<sub>2</sub> deodorization takes place and the length of time of the process (section 2.3.2) influence the VOC contents. In addition, to evaluate the differences between the VOC content and chemical composition of the

different samples (RPL, DPL, DPL-VSD and DPL-SCCO<sub>2</sub>), an analysis of variance (ANOVA) was performed and the LSD (least significant differences) intervals were identified (95 % confidence level) using Statgraphics Centurion XVI.

### **3. Results and Discussion**

#### **3.1. Drying of raw pork liver**

##### **3.1.1. *Impact on volatile organic compounds (VOCs)***

In the present study, a total of 136 volatile organic compounds (VOCs) were identified (Table 2). In raw pork liver (RPL), 58 VOCs were detected, while in dried pork liver (DPL), the number of VOCs increased up to 116.

Table 2. Profile of VOCs (UA = units area x 10<sup>5</sup>) in raw pork liver (RPL), dried pork liver (DPL) and dried pork deodorized by vacuum steam distillation (DPL-VSD) and supercritical CO<sub>2</sub> (DPL-SCCO<sub>2</sub>)

COMPOUND	RPL	DPL	DPL-VSD	DPL-SCCO <sub>2</sub>	ODOR	COMPOUND	RPL	DPL	DPL-VSD	DPL-SCCO <sub>2</sub>	ODOR
<b>Acids</b>						<b>Sulphur compounds</b>					
Acetic acid	nd <sub>A</sub>	120.78 ±24.87 D	9.19±1.3 6c	5.96±0. 71 <sub>B</sub>	sour, vinegar	Dimethyl sulfide	5.62±2. 70 <sub>B</sub>	nd <sub>A</sub>	nd <sub>A</sub>	nd <sub>A</sub>	cabbage , sulfur, gasoline
Propanoic acid	nd <sub>A</sub>	3.67±0. 73 <sub>c</sub>	1.15±0.5 B	nd <sub>A</sub>		Carbonyl sulfide	0.56±0. 34 <sub>B</sub>	0.38± 0.08 <sub>B</sub>	0.07±0. 01 <sub>A</sub>	0.06± 0.03 <sub>A</sub>	
Butanoic acid	nd <sub>A</sub>	14.04± 3.48 <sub>D</sub>	0.84±0.6 1c	0.20±0. 01 <sub>B</sub>	cheese	Dimethyl disulfide	0.02±0. 01 <sub>A</sub>	2.95± 0.91 <sub>D</sub>	0.51±0. 01 <sub>B</sub>	0.91± 0.12 <sub>c</sub>	onion, cabbage , putrid
<b>Alcohols</b>						Acetamide					
1-Propanol	0.59± 0.19 <sub>B</sub>	nd <sub>A</sub>	nd <sub>A</sub>	nd <sub>A</sub>		<b>Esters</b>					
Cyclopentanol	0.62± 0.22 <sub>B</sub>	nd <sub>A</sub>	nd <sub>A</sub>	nd <sub>A</sub>		Acetic acid, methyl ester	nd <sub>A</sub>	0.21± 0.08 <sub>c</sub>	0.33±0. 12 <sub>c</sub>	0.07± 0.05 <sub>B</sub>	
2-Butanol, 2,3-dimethyl-	0.43± 0.17 <sub>B</sub>	nd <sub>A</sub>	nd <sub>A</sub>	nd <sub>A</sub>		Acetic acid ethenyl ester	nd <sub>A</sub>	2.07± 0.55 <sub>D</sub>	0.04±0. 01 <sub>B</sub>	0.89± 012 <sub>c</sub>	
2-Pentanol, 2-methyl-	0.13± 0.16 <sub>B</sub>	nd <sub>A</sub>	nd <sub>A</sub>	nd <sub>A</sub>		Propanoic acid, ethyl ester	1.84±1. 00 <sub>B</sub>	nd <sub>A</sub>	nd <sub>A</sub>	nd <sub>A</sub>	
Glycidol	nd <sub>A</sub>	6.72±2. 03 <sub>c</sub>	1.15±0.5 0 <sub>B</sub>	1.14±0. 10 <sub>B</sub>		Formic acid, 2- propenyl ester	nd <sub>A</sub>	21.88 ±4.93 B	16.44± 0.74 <sub>B</sub>	nd <sub>A</sub>	

B. Abril, 2023

1-Propanol, 2-methyl-	nd <sub>A</sub>	0.17±0.06 <sub>C</sub>	0.03±0.01 <sub>B</sub>	nd <sub>A</sub>		Ethyl Acetate	nd <sub>A</sub>	0.73±0.32 <sub>C</sub>	1.62±0.04 <sub>D</sub>	0.32±0.01 <sub>B</sub>	pineapple
1-Butanol	0.24±0.03 <sub>B</sub>	0.42±0.09 <sub>C</sub>	0.28±0.12 <sub>BC</sub>	nd <sub>A</sub>	medicine, fruit, wine	<b>Ethers</b>					
2-Propen-1-ol	nd <sub>A</sub>	10.26±2.41 <sub>C</sub>	0.21±0.01 <sub>B</sub>	nd <sub>A</sub>		Dimethyl ether	71.91±45.21 <sub>C</sub>	2.55±0.75 <sub>A</sub>	3.06±0.61 <sub>A</sub>	8.14±0.69 <sub>B</sub>	
1-Butanol, 3-methyl-	2.11±1.77 <sub>D</sub>	0.21±0.02 <sub>C</sub>	0.06±0.0 <sub>B</sub>	nd <sub>A</sub>	whiskey, malt, burnt	<b>Furanes</b>					
1-Butanol, 2-methyl-	0.37±0.12 <sub>D</sub>	0.11±0.01 <sub>C</sub>	0.04±0.01 <sub>B</sub>	nd <sub>A</sub>	malt, wine, onion	Furan, 3-methyl-	0.07±0.04 <sub>A</sub>	0.74±0.19 <sub>C</sub>	0.15±0.04 <sub>A</sub>	0.25±0.05 <sub>B</sub>	mint
1-Pentanol	0.53±0.05 <sub>B</sub>	5.71±1.02 <sub>C</sub>	0.37±0.02 <sub>A</sub>	0.76±0.45 <sub>AB</sub>	fruit, balsamic	Tetrahydrofuran	nd <sub>A</sub>	0.54±0.11 <sub>C</sub>	nd <sub>A</sub>	0.04±0.03 <sub>B</sub>	
1-Butanol, 2,3-dimethyl-	0.06±0.01 <sub>B</sub>	nd <sub>A</sub>	nd <sub>A</sub>	nd <sub>A</sub>		Furan, 2-ethyl-	0.06±0.02 <sub>B</sub>	0.93±0.17 <sub>D</sub>	0.14±0.04 <sub>C</sub>	nd <sub>A</sub>	
(S)-(+)-1,2-Propanediol	nd <sub>A</sub>	1.87±0.25 <sub>C</sub>	1.18±0.07 <sub>B</sub>	nd <sub>A</sub>		3(2H)-Furanone, dihydro-2-methyl-	nd <sub>A</sub>	0.44±0.06 <sub>C</sub>	0.02±0.01 <sub>B</sub>	1.20±0.18 <sub>D</sub>	caramel, sweet
2,3-Butanediol	27.39±19.07 <sub>C</sub>	0.79±0.10 <sub>B</sub>	0.06±0.03 <sub>B</sub>	nd <sub>A</sub>		3-Furanmethanol	nd <sub>A</sub>	2.42±0.24 <sub>C</sub>	0.06±0.01 <sub>B</sub>	nd <sub>A</sub>	
1-Pentanol, 2-methyl-	1.01±0.66 <sub>B</sub>	nd <sub>A</sub>	nd <sub>A</sub>	nd <sub>A</sub>	pungent	Ethanone, 1-(2-furanyl)-	nd <sub>A</sub>	0.96±0.15 <sub>C</sub>	0.05±0.02 <sub>B</sub>	nd <sub>A</sub>	
1-Butanol, 3-methyl-, acetate	0.07±0.01 <sub>C</sub>	0.11±0.02 <sub>D</sub>	0.03±0.01 <sub>B</sub>	nd <sub>A</sub>		<b>Hydrocarbures</b>					
1-Hexanol	3.79±0.94 <sub>C</sub>	0.86±0.08 <sub>B</sub>	0.13±0.02 <sub>A</sub>	0.09±0.02 <sub>A</sub>	resin, flower, green, metallic	Butane, 1-chloro-	nd <sub>A</sub>	0.07±0.02 <sub>B</sub>	0.04±0.02 <sub>B</sub>	nd <sub>A</sub>	
Phenylethyl Alcohol	1.07±0.03 <sub>B</sub>	nd <sub>A</sub>	nd <sub>A</sub>	nd <sub>A</sub>	honey, spice,	Pentane	nd <sub>A</sub>	3.36±0.68 <sub>B</sub>	4.24±0.74 <sub>B</sub>	2.99±1.09 <sub>B</sub>	alkane

B. Abril, 2023

rose, lilac										
Ethanol, 2-butoxy-	nd <sub>A</sub>	0.41±0.03 <sub>C</sub>	0.32±0.01 <sub>B</sub>	nd <sub>A</sub>		Pentane, 3-methyl-	0.16±0.07 <sub>C</sub>	0.07±0.01 <sub>B</sub>	0.05±0.01 <sub>A</sub>	0.09±0.02 <sub>B</sub> c
(S)-(+)-5-Methyl-1-heptanol	nd <sub>A</sub>	0.46±0.13 <sub>D</sub>	0.02±0.01 <sub>B</sub>	0.10±0.04 <sub>C</sub>		Cyclopentane, methyl-	0.02±0.01 <sub>B</sub>	0.12±0.08 <sub>C</sub>	0.04±0.01 <sub>C</sub>	nd <sub>A</sub>
1-Octen-3-ol	3.16±0.71 <sub>B</sub>	53.01±1.12 <sub>C</sub>	4.95±1.22 <sub>B</sub>	nd <sub>A</sub>	mushroom	Benzene, 1,3-dimethyl-	nd <sub>A</sub>	nd <sub>A</sub>	nd <sub>A</sub>	0.21±0.01 <sub>B</sub>
Ethanol, 2,2'-oxybis-	nd <sub>A</sub>	0.37±0.06 <sub>B</sub>	0.42±0.04 <sub>B</sub>	nd <sub>A</sub>		Heptane, 3-methyl-	nd <sub>A</sub>	1.10±0.41 <sub>C</sub>	0.20±0.02 <sub>B</sub>	nd <sub>A</sub>
1,2-Propanediol, 1-phenyl-	nd <sub>A</sub>	0.18±0.06 <sub>C</sub>	0.05±0.01 <sub>B</sub>	nd <sub>A</sub>		Undecane	nd <sub>A</sub>	0.63±0.12 <sub>C</sub>	0.44±0.15 <sub>C</sub>	0.38±0.03 <sub>B</sub>
1-Nonanol	nd <sub>A</sub>	0.25±0.03 <sub>B</sub>	0.32±0.01 <sub>C</sub>	nd <sub>A</sub>	fatty, green	Dodecane	nd <sub>A</sub>	0.83±0.12 <sub>D</sub>	0.05±0.01 <sub>B</sub>	0.23±0.11 <sub>C</sub>
1-Tetradecanol	nd <sub>A</sub>	0.15±0.02 <sub>B</sub>	0.21±0.01 <sub>C</sub>	nd <sub>A</sub>	coconut	Cyclododecane	nd <sub>A</sub>	nd <sub>A</sub>	nd <sub>A</sub>	0.25±0.01 <sub>B</sub>
2,2,4-Trimethyl-1,3-pentanediol diisobutyrate	nd <sub>A</sub>	0.55±0.06 <sub>B</sub>	0.34±0.04 <sub>B</sub>	nd <sub>A</sub>		Cyclopropane, pentyl-	nd <sub>A</sub>	0.45±0.03 <sub>C</sub>	0.03±0.01 <sub>B</sub>	nd <sub>A</sub>
<b>Aldehydes</b>						Octane	nd <sub>A</sub>	7.93±1.25 <sub>C</sub>	1.26±0.74 <sub>B</sub>	2.33±0.66 <sub>B</sub>
Propanal	3.17±1.07 <sub>B</sub>	nd <sub>A</sub>	nd <sub>A</sub>	nd <sub>A</sub>	solvent, pungent	2-Octene, (E)-	1.37±0.97 <sub>C</sub>	nd <sub>A</sub>	nd <sub>A</sub>	0.31±0.12 <sub>B</sub>
Propanal, 2-methyl-	1.39±0.94 <sub>A</sub>	8.69±2.21 <sub>C</sub>	5.22±0.74 <sub>B</sub>	2.01±1.12 <sub>A</sub>	smoke, fatty	3-Octene, (E)-	0.67±0.32 <sub>C</sub>	nd <sub>A</sub>	nd <sub>A</sub>	0.16±0.01 <sub>B</sub>
Butanal	0.09±0.07 <sub>A</sub>	0.48±0.13 <sub>B</sub>	0.16±0.05 <sub>A</sub>	0.20±0.04 <sub>A</sub>	pungent, green	Heptane, 2,4-dimethyl-	2.20±1.01 <sub>C</sub>	0.01±0.01 <sub>B</sub>	nd <sub>A</sub>	nd <sub>A</sub>
Butanal, 3-methyl-	15.57±9.01 <sub>AB</sub>	17.38±4.12 <sub>B</sub>	16.66±3.97 <sub>B</sub>	7.12±1.81 <sub>A</sub>	malt	Hexane, 2,4,4-trimethyl-	nd <sub>A</sub>	0.19±0.02 <sub>B</sub>	nd <sub>A</sub>	nd <sub>A</sub>

B. Abril, 2023

Butanal, 2-methyl-	19.04 ±8.06 AB	30.55± 6.54B	23.66±5. 72B	9.63±1. 16A	cocoa, almond	Heptane, 2,2,4,6,6- pentamethyl-	333.45 ±151.4 4D	15.59 ±1.02 A	58.10± 1.02c	35.63 ±1.95 B
Pentanal	0.58± 0.18A	13.92± 2.84D	2.12±0.4 3B	5.03±1. 19c	almond, malt, pungent	Decane	ndA	0.39± 0.15B	14.85± 1.41Ac	ndA
2-Butenal, 2-methyl-	1.72± 0.41c	1.58±0. 51c	0.37±0.0 2B	0.14±0. 06A	green, fruit	Nonane	0.31±0. 24B	ndA	ndA	ndA
Hexanal	16.04 ±4.33 B	139.08 ±16.80 D	9.60±2.0 4A	26.39± 2.48c	green, grassy, tallow, fatty	2,2,4,4- Tetramethylocta ne	14.21± 8.92B	3.46± 0.26A	11.84± 0.84B	8.63± 0.33B
Heptanal	0.47± 0.29A	3.59±0. 29c	0.57±0.0 2A	0.83±0. 06B	fatty, citrus, rancid, unpleasa nt	Undecane, 5,5- dimethyl-	ndA	0.83± 0.41B	1.95±0. 06D	1.57± 0.05c
(E)-2-Nonenal	0.61± 0.14B	0.62±0. 12B	0.12±0.0 2A	0.18±0. 09A	cardboar d	Undecane	ndA	0.63± 0.23B	0.44±0. 04B	0.38± 0.02B
Benzaldehyde	9.05± 3.21c	ndA	ndA	0.70±0. 02B	almond, burnt sugar	Decane, 2,3,6- trimethyl-	ndA	0.28± 0.02B	0.24±0. 02B	ndA
2-Hexenal, 2-ethyl-	ndA	1.34±0. 10c	0.06±0.0 2B	ndA		Pentane, 3,3- diethyl-	ndA	0.16± 0.02B	0.34±0. 04c	0.15± 0.09B
2-Isopropyl-5-methylhex-2-enal	0.04± 0.02B	1.55±0. 04D	0.19±0.0 2c	ndA		Undecane, 3- methylene-	ndA	0.17± 0.01B	0.32±0. 12B	ndA
(E,E)-2,4-Heptadienal	5.63± 1.05c	2.26±0. 77B	1.79±0.6 3B	ndA	fishy	Hexane, 3,3- dimethyl-	ndA	0.29± 0.01c	0.26±0. 01B	ndA
<b>Halogen compounds</b>						Nonane, 5-(1- methylpropyl)-	ndA	0.41± 0.12B	0.39±0. 01B	ndA
Methane, oxybis[dichloro	1.63± 0.99c	0.27±0. 08B	0.13±0.0 4B	ndA		Cyclododecane	ndA	0.10± 0.01B	0.19±0. 01c	0.25± 0.02D

-											
<b>Nitrogen compounds</b>						Benzene, 1,3-dimethyl-	0.16±0.05 <sub>A</sub>	13.94±1.66 <sub>C</sub>	0.94±0.04 <sub>B</sub>	0.21±0.02 <sub>A</sub>	
Fumaronitrile	nd <sub>A</sub>	0.68±0.08 <sub>D</sub>	0.15±0.04 <sub>B</sub>	0.47±0.06 <sub>C</sub>		3-Ethyl-4-methyl-2-pentene	nd <sub>A</sub>	2.14±0.78 <sub>C</sub>	0.32±0.06 <sub>B</sub>	nd <sub>A</sub>	
Tetraethyl ammonium fluoride	nd <sub>A</sub>	2.45±0.91 <sub>C</sub>	0.01±0.0 <sub>B</sub>	nd <sub>A</sub>		Trimethylene oxide	nd <sub>A</sub>	5.52±1.48 <sub>C</sub>	0.63±0.05 <sub>B</sub>	nd <sub>A</sub>	
Propane, 2-nitro-	nd <sub>A</sub>	0.81±0.20 <sub>C</sub>	0.21±0.02 <sub>B</sub>	nd <sub>A</sub>		Diazene, dimethyl-	nd <sub>A</sub>	2.88±0.67 <sub>C</sub>	0.30±0.02 <sub>B</sub>	nd <sub>A</sub>	
Pyridine, 2-methyl-	nd <sub>A</sub>	0.84±0.07 <sub>C</sub>	0.02±0.00 <sub>B</sub>	nd <sub>A</sub>		Borane, diethyl(decyloxy)	nd <sub>A</sub>	nd <sub>A</sub>	nd <sub>A</sub>	0.24±0.02 <sub>B</sub>	
Pyrazine, methyl-	0.09±0.01 <sub>B</sub>	41.90±5.48 <sub>D</sub>	1.24±0.11 <sub>C</sub>	nd <sub>A</sub>	popcorn	2-Methyl-1-butene	nd <sub>A</sub>	0.09±0.04 <sub>B</sub>	0.11±0.02 <sub>B</sub>	nd <sub>A</sub>	
Cyclopentanone, 2-methyl-	nd <sub>A</sub>	0.25±0.02 <sub>C</sub>	0.03±0.01 <sub>B</sub>	nd <sub>A</sub>		D-Limonene	4.25±0.80 <sub>C</sub>	0.55±0.07 <sub>B</sub>	0.59±0.01 <sub>B</sub>	nd <sub>A</sub>	
2-Hexanone, 5-methyl-	nd <sub>A</sub>	2.92±0.36 <sub>C</sub>	0.17±0.02 <sub>B</sub>	nd <sub>A</sub>		<b>Ketones</b>					
Pyrazine, 2,6-dimethyl-	0.14±0.10 <sub>A</sub>	49.36±4.58 <sub>D</sub>	2.21±0.24 <sub>C</sub>	0.86±0.09 <sub>B</sub>	cocoa, roasted nut, roast beef, medicine	Acetone	13.43±7.41 <sub>B</sub>	13.87±3.62 <sub>B</sub>	3.56±1.11 <sub>A</sub>	10.02±1.01 <sub>B</sub>	
Pyrazine, ethyl-	nd <sub>A</sub>	4.22±0.27 <sub>C</sub>	0.12±0.02 <sub>B</sub>	nd <sub>A</sub>	peanut butter, wood	2-Butanone	3.06±1.98 <sub>A</sub>	11.33±2.37 <sub>B</sub>	2.97±1.05 <sub>A</sub>	1.95±0.33 <sub>A</sub>	blue cheese
Pyrazine, 2,3-dimethyl-	nd <sub>A</sub>	2.53±0.17 <sub>C</sub>	0.09±0.02 <sub>B</sub>	nd <sub>A</sub>		1-Penten-3-one	nd <sub>A</sub>	5.52±1.52 <sub>D</sub>	0.02±0.01 <sub>B</sub>	0.31±0.05 <sub>C</sub>	
Pyrazine, 2-ethyl-6-methyl-	0.14±0.07 <sub>A</sub>	30.29±0.79 <sub>C</sub>	1.07±0.55 <sub>B</sub>	0.41±0.08 <sub>B</sub>	fruit, sweet	2-Pentanone	0.26±0.04 <sub>B</sub>	0.36±0.06 <sub>B</sub>	0.09±0.01 <sub>A</sub>	0.10±0.02 <sub>A</sub>	butter, spicy, blue



## B. Abril, 2023

											cheese
Pyrazine, trimethyl-	nd <sub>A</sub>	11.23±0.58 <sub>D</sub>	0.33±0.12 <sub>C</sub>	0.14±0.04 <sub>B</sub>	roast, potato, must	3-Pentanone	0.29±0.04 <sub>B</sub>	9.14±2.31 <sub>D</sub>	1.15±0.06 <sub>C</sub>	nd <sub>A</sub>	
Pyrazine, 3-ethyl-2,5-dimethyl-	0.02±0.02 <sub>A</sub>	14.84±0.56 <sub>D</sub>	0.98±0.02 <sub>C</sub>	0.26±0.11 <sub>B</sub>	potato, roast	2,3-Pentanedione	nd <sub>A</sub>	5.97±1.46 <sub>D</sub>	0.14±0.02 <sub>B</sub>	0.80±0.03 <sub>C</sub>	
Pyrazine, 3,5-diethyl-2-methyl-	nd <sub>A</sub>	3.10±0.24 <sub>C</sub>	0.23±0.06 <sub>B</sub>	nd <sub>A</sub>		Methyl Isobutyl Ketone	nd <sub>A</sub>	0.95±0.13 <sub>C</sub>	0.15±0.02 <sub>B</sub>	nd <sub>A</sub>	
Pyrazine, 2,5-dimethyl-3-(2-methylpropyl)-	0.01±0.00 <sub>B</sub>	1.71±0.25 <sub>D</sub>	0.13±0.05 <sub>C</sub>	nd <sub>A</sub>		2-Hexanone	nd <sub>A</sub>	0.28±0.03 <sub>D</sub>	0.04±0.01 <sub>B</sub>	0.11±0.01 <sub>C</sub>	ether, grape
2-Isoamyl-6-methylpyrazine	nd <sub>A</sub>	8.46±1.69 <sub>C</sub>	0.43±0.05 <sub>B</sub>	nd <sub>A</sub>		2-Heptanone	0.35±0.01 <sub>A</sub>	16.73±1.80 <sub>D</sub>	1.31±0.04 <sub>C</sub>	0.97±0.01 <sub>B</sub>	soap, spicy and blue cheese
Ethanone, 1-(1H-pyrrol-2-yl)-	nd <sub>A</sub>	1.02±0.27 <sub>C</sub>	0.06±0.01 <sub>B</sub>	nd <sub>A</sub>		Butyrolactone	nd <sub>A</sub>	2.82±0.14 <sub>C</sub>	0.56±0.04 <sub>B</sub>	nd <sub>A</sub>	
Pantolactone	nd <sub>A</sub>	6.09±1.48 <sub>C</sub>	3.53±1.21 <sub>B</sub>	nd <sub>A</sub>		5-Hexen-3-one	nd <sub>A</sub>	0.22±0.04 <sub>B</sub>	0.40±0.08 <sub>C</sub>	0.33±0.09 <sub>B</sub>	
2-Pyrrolidinone	nd <sub>A</sub>	0.96±0.31 <sub>C</sub>	0.23±0.02 <sub>B</sub>	nd <sub>A</sub>		1-Octen-3-one	2.25±1.23 <sub>C</sub>	1.82±0.14 <sub>C</sub>	0.03±0.01 <sub>A</sub>	0.66±0.22 <sub>B</sub>	metallic
2-Decanone	nd <sub>A</sub>	2.05±0.15 <sub>C</sub>	0.50±0.02 <sub>B</sub>	nd <sub>A</sub>		3,5-Octadien-2-one	nd <sub>A</sub>	2.88±0.10 <sub>D</sub>	0.02±0.01 <sub>B</sub>	0.44±0.04 <sub>C</sub>	
2(4H)-Benzofuranone, 5,6,7,7a-tetrahydro-4,4,7a-trimethyl-, (R)-	nd <sub>A</sub>	0.31±0.09 <sub>B</sub>	0.14±0.09 <sub>B</sub>	nd <sub>A</sub>		Acetoin	192.49±67.46 <sub>C</sub>	0.05±0.10 <sub>A</sub>	1.54±0.01 <sub>B</sub>	0.02±0.01 <sub>A</sub>	butter, cream
Pyrazine	0.05±	3.02±0.	0.45±0.0	0.05±0.		Cyclobutanone,	nd <sub>A</sub>	2.17±	0.20±0.	0.22±	

B. Abril, 2023

	0.02 <sub>A</sub>	54 <sub>C</sub>	4 <sub>B</sub>	01 <sub>A</sub>	2,3,3-trimethyl-		0.02 <sub>C</sub>	01 <sub>B</sub>	0.04 <sub>B</sub>
Pyrolo[3,2-d]pyrimidin-2,4(1H,3H)-dione	nd <sub>A</sub>	5.83±0.57 <sub>B</sub>	5.94±0.74 <sub>B</sub>	4.25±0.88 <sub>B</sub>	2-Heptanone, 6-methyl-	nd <sub>A</sub>	1.22±0.04 <sub>B</sub>	1.75±0.07 <sub>C</sub>	1.12±0.31 <sub>B</sub>
Methylamine, N,N-dimethyl-	nd <sub>A</sub>	30.10±7.22 <sub>D</sub>	4.72±0.71 <sub>B</sub>	13.54±0.94 <sub>C</sub>					

\*Odour description obtained from database available on the web at <https://www.flavornet.org/flavornet.html>.

\*nd, not detected.

Average values ± LSD intervals are given (n=5).

Different capital letters show homogeneous groups established from LSD intervals (p<0.05) for each VOC.

A significant variation in the results of the VOC quantification can be observed in Table 2. As illustrated in Figure 3, the results of the quantitative analysis in terms of the percentages of units of area (UA) of the main VOC families in RPL were: hydrocarbons (46.6 % UA), ketones (27.7 % UA), aldehydes (9.6 % UA), ethers (9.4 % UA), alcohols (5.4 % UA), sulphur compounds (0.8 % UA), halogen compounds (0.2 % UA), esters (0.2 % UA), nitrogen compounds (0.06 % UA) and furans (0.02 % UA). As is illustrated in Figure 3, there are great differences between the content of the main VOC families in RPL and DPL. Thus, the acid family was not detected in RPL. However, after the drying process, as a result of lipid hydrolysis (Pugliese *et al.*, 2015) and from the degradation of the carbohydrates and aldehydes formed from the Strecker reaction (Merlo *et al.*, 2021), acids (15.9 % UA) were formed (Johansson *et al.*, 1994).

As for the aliphatic alcohols, an increase was found when comparing RPL and DPL (from 5.4 to 9.5 % UA). These compounds contribute to the flavour of the meat through unsaturated alcohols, and of these, 1-octen-3-ol must be highlighted. This was present in RPL and DPL, and its content increased after the drying process (from 3.16 to 53.01 UA) probably as a result of the degradation of fatty acids catalyzed by the lipoxygenase (Sun *et al.*, 2021). As in aliphatic alcohols, in aliphatic aldehydes, the VOC content increased in DPL compared to RPL (from 9.6 to 25.3 % UA). In DPL, the content of every saturated aldehyde increased when compared to the content in RPL, such as pentanal (from 0.58 to 13.92 UA), hexanal (from 16.04 to 139.08 UA) and heptanal (from 0.47 to 3.59 UA). However, the content of unsaturated aldehydes did not increase in the same magnitude, in some cases even falling, such as 2-butenal, 2-methyl- (from 1.72 to 1.58 UA) or (E,E)-2,4-heptadienal (from 5.63 to 2.26 UA). This was probably linked to the fact that unsaturated aldehydes are more reactive than saturated aldehydes and, therefore, more likely to participate in the Maillard reactions and give rise to other compounds (Wei *et al.*, 2020).

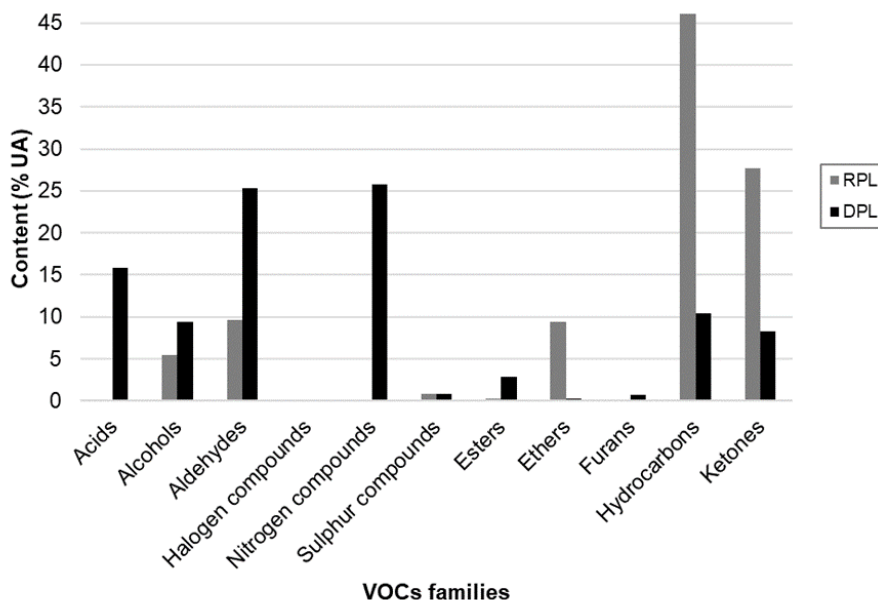


Figure 3. Content (% UA) of the main VOCs families detected in raw pork liver (RPL) and in dried pork liver (DPL).

Ketones are also one of the major flavour-related chemical families and are generated from lipid oxidation, alkane degradation and the dehydrogenation of alcohols by bacteria (Casaburi *et al.*, 2015). After drying, there was a smaller content of ketones (8.3 % UA) than in RPL (27.7 % UA).

One of the most noticeable changes in VOCs caused by drying was the increase in heterocyclic compounds, such as nitrogen compounds (pyrazines, 25.7 % UA) and furans (0.7 % UA) (Table 2). These heterocyclic compounds are generated through the Maillard reactions and are generally formed at high temperatures. Pyrazines contribute to the aroma of grilled meat (Cardinal *et al.*, 2020; Wei *et al.*, 2020). As for furans, they were formed by reactions that take place at temperatures of over 100 °C, usually from fatty acid oxidation (Liu *et al.*, 2015). In the DPL, therefore, new compounds appeared, such as 3 (2H)-furanone, dihydro-2-methyl-, which present a sweet caramel odour (Li *et al.*, 2018).

In contrast, the content of other VOC families in DPL dropped after drying: halogenated compounds (from 0.21 to 0.03 % UA), ethers (from 9.39 to 0.29 % UA) and hydrocarbons (from 46.58 to 10.40 % UA). This decrease is possibly due to the reactions that take place during drying, such as lipid oxidation, the participation of proteins and sugars in the Maillard reaction, protein degradation, and amino acid condensation with Maillard intermediates in Strecker degradation, among others.

### **3.1.2. Off-flavor removal**

Im *et al.* (2004) characterized the off-flavour of the VOCs present in pork liver as fishy, metallic and fatty, with hints of cardboard, nuts, such as almonds, oil, and nature, such as grass (green) and mushroom. The following compounds are those that contribute to the complexity of the unpleasant notes of pork liver:

- (E,E)-2,4-heptadienal (Fishy odour)
- 1-octen-3-one and 1-hexanol (Metallic odour)
- (E)-2-nonenal (Cardboard odour)
- Butanal, 2-methyl, benzaldehyde and pentanal (Almond odour)
- Propanal 2-methyl, hexanal and heptanal (Fatty odour)
- Hexanal, butanal, 2-butenal, 2-methyl- and 1-hexanol (Green-nature odour).
- 1-octen-3-ol (Mushroom-nature odour)

It has to be considered that the significant unpleasant aroma of pork liver is not only the result of a single odour, but the combination of the different ones, especially the metallic and fishy odours (Im & Kurata, 2003).

The drying process eliminated one of the characteristic compounds of the liver odour, the benzaldehyde (almond odour). However, the quantity of the two compounds to which the nutty odour is linked rose: butanal, 2-methyl- (from 19.04 to 30.55 UA) and

pentanal (from 0.58 to 13.92 UA), (Table 2). Likewise, the units of the characteristic fatty odours increased: propanal 2-methyl from 1.39 to 8.69 UA, hexanal from 16.04 to 139.08 UA and heptanal from 0.47 to 3.59 UA (Table 2). As for the nature odour, identified as the green odour, two of the characteristic compounds of liver increased their content compared to RPL, hexanal (already shown) and butanal from 0.09 to 0.48 UA. However, 1-hexanol decreased from 3.79 to 0.86 UA and the content of 2-butenal, 2 methyl (1.58 UA) was similar to that of RPL (1.72 UA). In addition, 1-nonanol, a compound also characteristic to fatty, green odours that are undetected in RPL, was found in DPL. The units of the other characteristic nature odour, mushroom, attributed to 1-octen- 3-ol, increased from 3.16 to 53.01 UA after drying. This alcohol is usually described as an important volatile that contributes to the typical aroma of dry-cured meat products (Narváez-Rivas *et al.*, 2012). Finally, the fishy and metallic odours of the pork liver were not completely removed after the drying process. In this regard, (E,E)-2,4-heptadienal, a compound related to a fishy odour, decreased in quantity from 5.63 UA in RPL to 2.26 UA in DPL and the content of 1-octen-3-one, related to a metallic odour, remained similar to that in RPL (2.25 UA in RPL and 1.82 UA in DPL).

### **3.2. . Dried pork liver deodorization by vacuum steam distillation**

#### **3.2.1. Impact on volatile organic compounds (VOCs)**

Overall, the VOC content detected in DPL-VSD fell if compared to DPL (Figure 4): the content of acids dropped by 91.9 % UA, alcohols by 87.7 % UA, aldehydes by 72.6 % UA, halogen compounds by 51.9 % UA, nitrogen compounds by 89.8 % UA, sulphur compounds by 84.5 % UA, esters by 26 % UA, furans by 93 % UA and ketones by 81.5 % UA. In the families of ethers and hydrocarbons however, there was an increase of 20 % UA and 55.9 % UA, respectively. The increase in hydrocarbons as a result of the VSD technique was also observed in the deodorization of fish sauce (9.4 % UA) (Song *et al.*, 2018). It should be noted that the compounds of heptane, 2,4-dimethyl; hexane, 2,4,4-trimethyl- (hydrocarbons) and tetrahydrofuran (furan) were eliminated from DPL after VSD deodorization (Table 2).

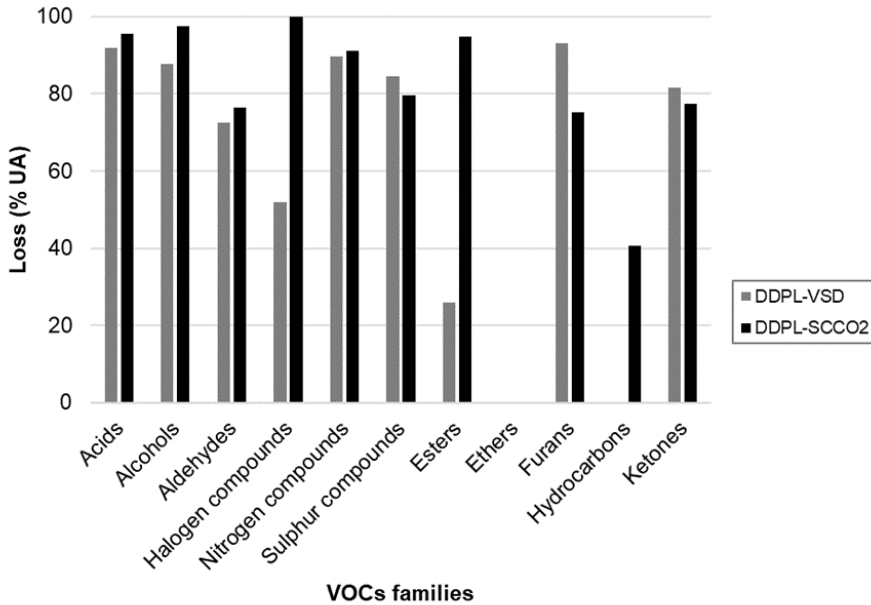


Figure 4. Loss (% UA) of the main VOCs families in dried pork liver (DPL) after vacuum steam distillation (DPL-VSD) and supercritical CO<sub>2</sub> (DPL-SCCO<sub>2</sub>) deodorization.

### 3.3. Supercritical CO<sub>2</sub> deodorization of dried pork liver.

#### 3.3.1. Impact on volatile organic compounds (VOCs)

The factors analyzed in SC-CO<sub>2</sub> deodorization (temperature, pressure and time) did not significantly ( $P < 0.05$ ) affect the VOC content. Thus, the statistical model evaluated fitted ( $R^2 < 40\%$ ) the experimental results poorly. Therefore, the average VOC values for the different experimental conditions analyzed were considered. Thereby, as illustrated in Figure 4, SC-CO<sub>2</sub> deodorization resulted in the complete removal of halogen compounds, and the following VOC families were greatly reduced if compared to DPL: acids by 95.6 % UA, alcohols by 97.5 % UA, aldehydes by 76.4 % UA, nitrogen compounds by 91.1 % UA, sulphur compounds by 79.6 % UA, esters by 94.9 % UA, furans by 75.3 % UA, hydrocarbons by 40.6 % UA and ketones by 81.5 % UA.

As for the reduction of sulphur compounds, Shimoda *et al.* (2000) carried out the SC-CO<sub>2</sub> deodorization of fish sauce and observed a remarkable reduction in sulphur compounds, which could contribute to the attenuation of the unpleasant odour produced by these compounds. Specifically, dimethyl disulphide in fish sauce was

reduced by 37 % UA when using SC-CO<sub>2</sub>, while in the present study it was reduced by 69.2 % UA (from 2.95 to 0.91 UA) (Table 2).

As for the ketones, 2-butanone and 2-pentanone were efficiently separated, and only 17.2 and 27.8 % UA were found after the SC-CO<sub>2</sub> deodorization, respectively (Table 2). A similar reduction was observed in the deodorization of fish sauce, with a UA retention of 12 and 40 %, respectively, after the SC-CO<sub>2</sub> deodorization (Shimoda *et al.*, 2000). However, the UA in dimethyl ether, the only ether compound, increased fourfold compared to its value in DPL (from 2.55 to 8.14 UA) (Table 2), which could be linked to the chemical reactions taking place in the SC-CO<sub>2</sub> medium.

### 3.4. Chemical composition

As in the VOC analysis, no significant ( $P>0.05$ ) effect was found for any of the factors (temperature, time and pressure) considered in the Box Behnken design. Therefore, an average value for all the SC-CO<sub>2</sub> treated samples was also considered and compared with DPL and DPL-VSD (Table 3).

Table 3. Proximate analysis of dried pork liver (DPL) and dried pork deodorized by vacuum steam distillation (DPL-VSD) supercritical CO<sub>2</sub> (DPL-SCCO<sub>2</sub>).

Samples	Moisture (%)	Protein (%)	Fat (%)	Ash (%)
DPL	2.77 ± 0.18 <sub>c</sub>	73.18 ± 0.07 <sub>B</sub>	19.33 ± 0.10 <sub>A</sub>	2.69 ± 0.21 <sub>B</sub>
DPL-VSD	45.00 ± 0.31 <sub>A</sub>	35.79 ± 1.01 <sub>c</sub>	17.15 ± 0.64 <sub>B</sub>	2.29 ± 0.4 <sub>B</sub>
DPL-SCCO <sub>2</sub>	3.56 ± 0.21 <sub>B</sub>	75.71 ± 0.44 <sub>A</sub>	14.52 ± 0.70 <sub>c</sub>	5.02 ± 0.22 <sub>A</sub>

%; chemical composition (moisture, protein, fat and ash) g / 100 g product. Average values ± LSD intervals are given.

Different capital letters show homogeneous groups established from LSD intervals ( $p<0.05$ ) for moisture, protein, fat and ash content.

The fat content of the samples treated with SC-CO<sub>2</sub> was significantly ( $p<0.05$ ) lower than in the untreated samples, decreasing from 19.33 % in DPL to 14.52 % in DPL-SCCO<sub>2</sub>. SC-CO<sub>2</sub> has been used for fat removal in foods with a high protein



content, as an alternative to other conventional techniques using undesirable organic solvents (Mouahid *et al.*, 2017). Thus, it has been used for the extraction of lipids in ground beef (39 % lipids extracted, 172 bar and 50 °C) (Chao *et al.*, 1991). In bovine heart, the SC-CO<sub>2</sub> treatment (at 40 MPa and 40 °C) reduced the fat content from 154.22 to 9.87 g/kg (Rahman *et al.*, 2019). In the case of lamb meat, SC-CO<sub>2</sub> (45 °C, 500 bar, 3 mL CO<sub>2</sub>/min) allowed the initial fat content to be reduced by 87.4 % (Taher *et al.*, 2011). Compared to these previous results, the fat content reduction in the DPL treated by SC-CO<sub>2</sub> was smaller (24.9 %) than in the analyses mentioned above. This could be linked to the experimental conditions employed and probably to the flow rate and extraction time used in the present study, which were not optimum for fat removal purposes.

As a result of the fat content reduction in the DPL-SCCO<sub>2</sub>, the content of the rest of the components was different from that in DPL and DPL-VSD (Table 3). Thus, the protein content increased from 73.18 % in DPL to 75.71 % in DPL-SCCO<sub>2</sub>. However, in DPL-VSD, the protein content was significantly lower (35.79 %), mainly due to the increase in moisture (45.0 %), caused by water adsorption during VSD, in comparison to DPL (2.77 %) and DPL-SCCO<sub>2</sub> (3.56 %). VSD would require further drying in order to reduce its moisture content to values close to DPL. As for the ash content, there were no significant differences ( $p < 0.05$ ) between DPL and DPL-VSD (2.69 % in DPL and 2.29 % in DPL-VSD); however, in DPL-SCCO<sub>2</sub>, the ash content increased by 5.02 %.

### **3.5. Comparison between vacuum steam distillation and supercritical CO<sub>2</sub> deodorization techniques**

If the two deodorization techniques are compared, SC-CO<sub>2</sub> allowed for the complete removal of a greater number of VOCs than VSD, as illustrated in Table 2. In addition, some VOC families presented a greater % loss after SC-CO<sub>2</sub> deodorization than the sample deodorized by VSD: acids (3.6 % UA), alcohols (9.8 % UA), aldehydes (3.8 % UA), halogenated compounds (48.2 % UA), nitrogenous compounds (1.3 % UA), esters (69.9 % UA) and hydrocarbons (40.6 % UA). Otherwise, VSD was more effective

at reducing sulphur compounds, presenting a greater % loss than the sample deodorized by SC-CO<sub>2</sub> (4.9 % UA), furans (17.7 % UA) and ketones (4.1 % UA) (Figure 4). However, neither of the two techniques was able to reduce dimethyl ether, whose content increased after the deodorization processes compared to DPL (20 % UA in DPL-VSD and 219.2 % UA in DPL- SCCO<sub>2</sub>).

Both techniques, VSD and SC-CO<sub>2</sub>, led to a relevant modification of the dried pork liver off-flavour (Table 2). SC-CO<sub>2</sub> treatment removed 3 characteristic compounds from the typical odour of pork liver, unlike VSD: 1-octen-3-ol, characteristic of the mushroom odour, 1-nonanol, a compound attributed to a fatty, green odour, and the (E,E)-2,4-heptadienal with a fishy odour. However, after SC-CO<sub>2</sub> deodorization, benzaldehyde was formed, a compound that had been eliminated by drying. This compound is attributed to the almond odour. In this sense, the content of the almond-like odour characteristic of pentanal was 137.3 % UA higher and that of 2-methylbutanal was 59.3 % UA lower in SC-CO<sub>2</sub> deodorization, compared to deodorization by VSD. In relation to the cardboard odour, (E)-2-nonenal content was 50% UA higher compared to DPL-VSD. Regarding the fatty odour, typical of hexanal and heptanal, its content after deodorization by SC-CO<sub>2</sub> was 174.9 % UA and 45.6 % UA, higher, respectively, compared to DPL-VSD; however, the propanal 2-methyl content was 61.5 % UA lower. Finally, as regards the nature aroma (green odour), the VOC content of 1-hexanol, and 2-butenal-2-methyl-, was 30.8 % UA and 62.2 % UA lower, respectively using SC-CO<sub>2</sub>, if compared to VSD. However, the butenal and hexanal content after SC-CO<sub>2</sub> deodorization was 25 % and 174.9 % UA higher, respectively, than in VSD. In this regard, high levels of hexanal can be associated with a rancid off-flavour, while low levels of hexanal have been associated with a green and nature aromatic note (Flores & Olivares, 2014). Therefore, after the application of SC-CO<sub>2</sub>, the typical metallic and fishy odours (Im *et al.*, 2004; Im & Kurata, 2003) were reduced to metallic, leaving the pork liver without a fishy odour. The effect of VSD and SC-CO<sub>2</sub> treatment on the deodorization of meat products has not been previously addressed.

## 4. Conclusions

Deodorization by vacuum steam distillation (VSD) and supercritical CO<sub>2</sub> (SC-CO<sub>2</sub>) have proven to be reliable techniques for the reduction and removal of VOCs in dried pork liver. The VSD showed more affinity to eliminate or reduce the content of sulphur compounds, furans and ketones, while SC-CO<sub>2</sub> showed a higher capacity for the elimination or reduction of acids, alcohols, aldehydes, halogenated compounds, nitrogenous compounds, esters and hydrocarbons. Thereby, it has been demonstrated that compounds responsible for the liver off-flavour, such as (E,E)- 2,4-heptadienal (fishy), 1-octen-3-ol (mushroom) and 1-nonanol (fatty and green), can be efficiently removed by SC-CO<sub>2</sub>. Moreover, it should be noted that SC-CO<sub>2</sub> led to a remarkable reduction in fat and a slight reduction in the moisture content compared to dried pork liver. Thus, further studies should assess the cost of SC-CO<sub>2</sub> deodorization in order to both evaluate its implementation in the industrial recovery of pork liver proteins or in protein isolates as a strategy to mitigate undesirable flavours, as well as look at its potential application in other matrices.

## Acknowledgements

The authors acknowledge the financial support from the “Ministerio de Economía y Competitividad (MINECO) and Instituto Nacional de Investigación y Tecnología Agraria y Alimentaria (INIA)” in Spain (Project RTA2017-00024-C04-03). The authors acknowledge the contribution of the slaughterhouse “Carnes de Teruel S.A.”, (D.O. Jamón de Teruel, Spain) for the supply of pork livers.

## References

AOAC, G. (2016). Official methods of analysis of AOAC International. Rockville, MD: AOAC International, ISBN: 978-0-935584-87-5

- Burri, B.J., Neidlinger, T.R., Lo, A.O., Kwan, C. & Wong, M.R. (1997). Supercritical fluid extraction and reversed-phase liquid chromatography methods for vitamin A and beta-carotene Heterogeneous distribution of vitamin A in the liver. *Journal of Chromatography A* 762: 201-206.
- Casaburi, A., Piombino, P., Nychas, G. J., Villani, F., & Ercolini, D. (2015). Bacterial populations and the volatilome associated to meat spoilage. *Food microbiology*, 45, 83-102. <https://doi.org/10.1016/j.fm.2014.02.002>
- Cardinal, M., Chaussy, M., Donnay-Moreno, C., Cornet, J., Rannou, C., Fillonneau, C., ... & Courcoux, P. (2020). Use of random forest methodology to link aroma profiles to volatile compounds: application to enzymatic hydrolysis of Atlantic salmon (*Salmo salar*) by-products combined with Maillard reactions. *Food Research International*, 134, 109254. <https://doi.org/10.1016/j.foodres.2020.109254>
- Chao, R. R., Mulvaney, S. J., Bailey, M. E., & Fernando, L. N. (1991). Supercritical CO<sub>2</sub> conditions affecting extraction of lipid and cholesterol from ground beef. *Journal of Food Science*, 56(1), 183-187. <https://doi.org/10.1111/j.1365-2621.1991.tb08007.x>
- Damodaran, S., & Arora, A. (2013). Off-flavor precursors in soy protein isolate and novel strategies for their removal. *Annual Review of Food Science and Technology*, 4(1), 327-346. doi: 10.1146/annurev-food-030212-182650
- De Oliveira, D. A., Minozzo, M. G., Licodiedoff, S., & Waszczynskyj, N. (2016). Physicochemical and sensory characterization of refined and deodorized tuna (*Thunnus albacares*) by-product oil obtained by enzymatic hydrolysis. *Food Chemistry*, 207, 187-194. <https://doi.org/10.1016/j.foodchem.2016.03.069>
- Domínguez, R., Purriños, L., Pérez-Santaescolástica, C., Pateiro, M., Barba, F.J., Tomasevic I., ... & Lorenzo, J.M. (2019). Characterization of volatile compounds of dry-cured meat products using HS-SPME-GC/MS technique. *Food Analytical Methods*, 12(6), 1263-1284. <https://doi.org/10.1007/s12161-019-01491-x>

- Flores, M., & Olivares, A. (2014). Flavor. *Handbook of fermented meat and poultry*, 217-225. <https://doi.org/10.1002/9781118522653.ch25>
- Guldiken, B., Green, R., & Nickerson, M. T. (2021). The impact of different adsorbents on flavor characteristics of a lentil protein isolate. *European Food Research and Technology*, 247(3), 593-604. <https://doi.org/10.1007/s00217-020-03648-z>
- Im, S., Hayakawa, F., & Kurata, T. (2004). Identification and sensory evaluation of volatile compounds in oxidized porcine liver. *Journal of Agricultural and Food Chemistry*, 52(2), 300-305. <https://doi.org/10.1021/jf030337v>
- Im, S., & Kurata, T. (2003). Characterization of off-flavors in porcine liver collected by SDE. *Food science and technology research*, 9(4), 338-341. <https://doi.org/10.3136/fstr.9.338>
- Johansson, G., Berdagué, J. L., Larsson, M., Tran, N., & Borch, E. (1994). Lipolysis, proteolysis and formation of volatile components during ripening of a fermented sausage with *Pediococcus pentosaceus* and *Staphylococcus xylosus* as starter cultures. *Meat Science*, 38(2), 203-218. [https://doi.org/10.1016/0309-1740\(94\)90110-4](https://doi.org/10.1016/0309-1740(94)90110-4)
- Kang, S. W., Kim, H. M., Rahman, M. S., Kim, A. N., Yang, H. S., & Choi, S. G. (2017). Nutritional quality and physicochemical characteristics of defatted bovine liver treated by supercritical carbon dioxide and organic solvent. *Korean Journal for Food Science of Animal Resources*, 37(1), 29. doi: 10.5851/kosfa.2017.37.1.29
- Kimura, T., Kagaya, M., Fukuya, Y., & Kosugi, S. (1990). Properties of chicken liver preserved in Miso. *Journal of Home Economics of Japan*, 41(7), 629-636. <https://doi.org/10.11428/jhej1987.41.629>
- King, J. W. (2014). Modern supercritical fluid technology for food applications. *Annual review of food science and technology*, 5, 215-238. <https://doi.org/10.1146/annurev-food-030713-092447>

- Kobayashi, F., Hayata, Y., Kohara, K., Muto, N., Miyake, M., & Osajima, Y. (2006). Application of supercritical CO<sub>2</sub> bubbling to deodorizing of drinking water. *Food science and technology research*, 12(2), 119-124. <https://doi.org/10.3136/fstr.12.119>
- Kumar, P., Chatli, M. K., Mehta, N., Singh, P., Malav, O. P., & Verma, A. K. (2017). Meat analogues: Health promising sustainable meat substitutes. *Critical reviews in food science and nutrition*, 57(5), 923-932. <https://doi.org/10.1080/10408398.2014.939739>
- Domínguez, R., Purriños, L., Pérez-Santaescolástica, C., Pateiro, M., Barba, F.J., Tomasevic I., ... & Lorenzo, J.M. (2019). Characterization of volatile compounds of dry-cured meat products using HS-SPME-GC/MS technique. *Food Analytical Methods*, 12(6), 1263-1284. <https://doi.org/10.1007/s12161-019-01491-x>
- Li, Y., Zhou, W., Cao, Y., Gong, X., Li, J., Lu, X., & Dai, Y. (2020). Analysis of volatile components of Tilapia enzymolysis solution after different deodorization treatments. In *IOP Conference Series: Earth and Environmental Science* (Vol. 571, No. 1, p. 012121). IOP Publishing. doi:10.1088/1755-1315/571/1/012121
- Li, X., Zhu, J., Li, C., Ye, H., Wang, Z., Wu, X., & Xu, B. (2018). Evolution of volatile compounds and spoilage bacteria in smoked bacon during refrigeration using an E-Nose and GC-MS combined with partial least squares regression. *Molecules*, 23(12), 3286. <https://doi.org/10.3390/molecules23123286>
- Liu, J., Liu, M., He, C., Song, H., & Chen, F. (2015). Effect of thermal treatment on the flavor generation from Maillard reaction of xylose and chicken peptide. *LWT- Food Science and Technology*, 64(1), 316-325. doi: <https://doi.org/10.1016/j.lwt.2015.05.061>
- López-Pedrouso, M., Borrajo, P., Pateiro, M., Lorenzo, J. M., & Franco, D. (2020). Antioxidant activity and peptidomic analysis of porcine liver hydrolysates using alcalase, bromelain, flavourzyme and papain enzymes. *Food Research International*, 137, 109389 <https://doi.org/10.1016/j.foodres.2020.109389>.

- Lynch, S. A., Mullen, A. M., O'Neill, E., Drummond, L., & Álvarez, C. (2018). Opportunities and perspectives for utilisation of co-products in the meat industry. *Meat Science*, *144*, 62-73. <https://doi.org/10.1016/j.meatsci.2018.06.019>
- Maheshwari, P., Ooi, E. T., & Nikolov, Z. L. (1995). Off-flavor removal from soy-protein isolate by using liquid and supercritical carbon dioxide. *Journal of the American Oil Chemists' Society*, *72*(10), 1107-1115. <https://doi.org/10.1007/BF02540975>
- Merlo, T. C., Lorenzo, J. M., Saldaña, E., Patinho, I., Oliveira, A. C., Menegali, B. S., ... & Contreras-Castillo, C. J. (2021). Relationship between volatile organic compounds, free amino acids, and sensory profile of smoked bacon. *Meat Science*, *181*, 108596. <https://doi.org/10.1016/j.meatsci.2021.108596>
- Mouahid, A., Boivin, P., Diaw, S., & Badens, E. (2022). Widom and extrema lines as criteria for optimizing operating conditions in supercritical processes. *The Journal of Supercritical Fluids*, *186*, 105587. <https://doi.org/10.1016/j.supflu.2022.105587>
- Narváez-Rivas, M., Gallardo, E., & León-Camacho, M. (2012). Analysis of volatile compounds from Iberian hams: a review. *grasas y aceites*, *63*(4), 432-454.
- Oszagyan, M., Simandi, B., Sawinsky, J., Kery, A., Lemberkovics, E., & Fekete, J. (1996). Supercritical fluid extraction of volatile compounds from lavender and thyme. *Flavour and Fragrance journal*, *11*(3), 157-165. [https://doi.org/10.1002/\(SICI\)1099-1026\(199605\)11:3<157::AID-FFJ559>3.0.CO;2-6](https://doi.org/10.1002/(SICI)1099-1026(199605)11:3<157::AID-FFJ559>3.0.CO;2-6)
- Panadare, D., Dialani, G., & Rathod, V. (2021). Extraction of volatile and non-volatile components from custard apple seed powder using supercritical CO<sub>2</sub> extraction system and its inventory analysis. *Process Biochemistry*, *100*, 224-230. <https://doi.org/10.1016/j.procbio.2020.09.030>

- Pugliese, C., Sirtori, F., Škrlep, M., Piasentier, E., Calamai, L., Franci, O., & Čandek-Potokar, M. (2015). The effect of ripening time on the chemical, textural, volatile and sensorial traits of Biceps femoris and Semimembranosus muscles of the Slovenian dry-cured ham Kraški pršut. *Meat Science*, *100*, 58-68. <https://doi.org/10.1016/j.meatsci.2014.09.012>
- Pui, W. K., Yusoff, R., & Aroua, M. K. (2019). A review on activated carbon adsorption for volatile organic compounds (VOCs). *Reviews in Chemical Engineering*, *35*(5), 649-668. <https://doi.org/10.1515/revce-2017-0057>
- Rahman, M. S., Gul, K., Yang, H. S., Chun, J., Kerr, W. L., & Choi, S. G. (2019). Thermal and functional characteristics of defatted bovine heart using supercritical CO<sub>2</sub> and organic solvent. *Journal of the Science of Food and Agriculture*, *99*(2), 816-823. <https://doi.org/10.1002/jsfa.9250>
- Reverchon, E., & De Marco, I. Supercritical fluid extraction and fractionation of natural matter. (2006). *The Journal of Supercritical Fluids*, *38*(2), 146-166. <https://doi.org/10.1016/j.supflu.2006.03.020>
- Sánchez-Torres, E. A., Abril, B., Benedito, J., Bon, J., & García-Pérez, J. V. (2021). Water desorption isotherms of pork liver and thermodynamic properties. *LWT*, *149*, 111857. <https://doi.org/10.1016/j.lwt.2021.111857>
- Shimoda, M., Yamamoto, Y., Cocunubo-Castellanos, J., Yoshimura, T., Miyake, M., Ishikawa, H. & Osajima, Y. (2000). Deodorization of fish sauce by continuous-flow extraction with microbubbles of supercritical carbon dioxide. *Journal of Food Science* *65*: 1349-1351. <https://doi.org/10.1111/j.1365-2621.2000.tb10610.x>
- Seong, P. N., Park, K. M., Cho, S. H., Kang, S. M., Kang, G. H., Park, B. Y., ... & Van Ba, H. (2014). Characterization of edible pork by-products by means of yield and nutritional composition. *Korean Journal for Food Science of Animal Resources*, *34*(3), 297. doi:10.5851/kosfa.2014.34.3.297



- Seong, P. N., Park, K. M., Cho, S. H., Kang, S. M., Kang, G. H., Park, B. Y., ... & Van Ba, H. (2021). Values-added utilization of protein and hydrolysates from animal processing by-product livers: A review. *Trends in Food Science & Technology*, 110,(2021),432-442. <https://doi.org/10.1016/j.tifs.2021.02.033>
- Song, G., Zhang, M., Peng, X., Yu, X., Dai, Z., & Shen, Q. (2018). Effect of deodorization method on the chemical and nutritional properties of fish oil during refining. *LWT*, 96, 560-567. <https://doi.org/10.1016/j.lwt.2018.06.004>
- Silva, L. V., Nelson, D. L., Drummond, M. F. B., Dufossé, L., Glória, M. B. A. (2005). Comparison of hydrodistillation methods for the deodorization of turmeric. Elsevier. *Food Research International*. 38 (8–9), 1087-1096. <https://doi.org/10.1016/j.foodres.2005.02.025>
- Sun, L., Xin, G., Hou, Z., Zhao, X., Xu, H., Bao, X., ... & Li, L. (2021). Biosynthetic Mechanism of Key Volatile Biomarkers of Harvested *Lentinula edodes* Triggered by Spore Release. *Journal of Agricultural and Food Chemistry*, 69(32), 9350-9361. <https://doi.org/10.1021/acs.jafc.1c02410>
- Taher, H., Al-Zuhair, S., AlMarzouqui, A., & Hashim, I. (2011), Extracted fat from lamb meat by supercritical CO<sub>2</sub> as feedstock for biodiesel production. *Biochemical Engineering Journal*,55(1), 23-31. <https://doi.org/10.1016/j.bej.2011.03.003>
- Tejedor-Calvo, E., García-Barreda, S., Sánchez, S., Morales, D., Soler-Rivas, C., Ruiz-Rodríguez, A., ... & Marco, P. (2021). Supercritical CO<sub>2</sub> extraction method of aromatic compounds from truffles. *LWT*, 150, 111954. <https://doi.org/10.1016/j.lwt.2021.111954>
- Vasapollo, G., Longo, L., Rescio, L., & Ciurlia, L. (2004). Innovative supercritical CO<sub>2</sub> extraction of lycopene from tomato in the presence of vegetable oil as co-solvent. *The Journal of Supercritical Fluids*,29(1-2), 87-96. [https://doi.org/10.1016/S0896-8446\(03\)00039-1](https://doi.org/10.1016/S0896-8446(03)00039-1)

- Vedaraman, N., Srinivasakannan, C., Brunner, G., Ramabrahmam, B. V., & Rao, P. G. (2005). Experimental and modeling studies on extraction of cholesterol from cow brain using supercritical carbon dioxide. *The Journal of supercritical fluids*, 34(1), 27-34. <https://doi.org/10.1016/j.supflu.2004.10.004>
- Wang, B., Zhang, Q., Zhang, N., Bak, K. H., Soladoye, O. P., Aluko, R. E., ... & Zhang, Y. (2021). Insights into formation, detection and removal of the beany flavor in soybean protein. *Trends in Food Science & Technology*, 112, 336-347. <https://doi.org/10.1016/j.tifs.2021.04.018>
- Wei, C. K., Ni, Z. J., Thakur, K., Liao, A. M., Huang, J. H., & Wei, Z. J. (2020). Aromatic effects of immobilized enzymatic oxidation of chicken fat on flaxseed (*Linum usitatissimum* L.) derived Maillard reaction products. *Food chemistry*, 306, 125560. <https://doi.org/10.1016/j.foodchem.2019.125560>
- Whetstine, M. C., Croissant, A. E., & Drake, M. A. (2005). Characterization of dried whey protein concentrate and isolate flavor. *Journal of Dairy Science*, 88(11), 3826-3839. [https://doi.org/10.3168/jds.S0022-0302\(05\)73068-X](https://doi.org/10.3168/jds.S0022-0302(05)73068-X)
- Zabot, G. L. (2020). Decaffeination using supercritical carbon dioxide. In *Green Sustainable Process for Chemical and Environmental Engineering and Science* (pp. 255-278). Elsevier.doi: <https://doi.org/10.1016/B978-0-12-817388-6.00011-8>
- Zehnder, C. T. (1995). Practical Handbook of Soybean Processing and Utilization. *Chapter 14 – Deodorization*. AOCS PRESS. 239-257. <https://doi.org/10.1016/B978-0-935315-63-9.50018-8>



## **5. DISCUSIÓN GENERAL**



El hígado de cerdo es un coproducto de origen animal de gran relevancia en la industria porcina, en cuanto a volumen generado y composición. Como resultado de las nuevas tendencias de consumo, se ha producido una disminución en la demanda de este producto por parte de los consumidores, por lo que hoy en día tiene un bajo valor comercial. Sin embargo, el hígado tiene unas excelentes propiedades nutricionales, destacando su alto contenido proteico, presentando además estas proteínas unas propiedades tecno-funcionales muy interesantes para su uso en la industria alimentaria. Además, el hígado tiene una elevada concentración de ferroquelatasa (FeQ), que es la enzima que cataliza la formación de zinc-protoporfirina (ZnPP), pigmento rojo natural que, debido a su estabilidad a la luz y al calor, podría ser útil como medio para mejorar el color de los productos cárnicos. Los métodos tradicionales de extracción de enzimas y de formación enzimática de productos son, en general, lentos y, en algunas ocasiones, poco eficientes. En este sentido, el uso de nuevas tecnologías, como los ultrasonidos de potencia (US), podría contribuir a mejorar el rendimiento y la velocidad, tanto en los procesos de extracción de enzimas, como en las reacciones enzimáticas. En la presente Tesis Doctoral, se abordó la aplicación de US, por un lado, en la extracción de FeQ y, por otro lado, durante la formación enzimática de ZnPP catalizada por la FeQ. Además, se llevó a cabo la deshidratación a diferentes temperaturas del hígado para aumentar su vida útil y facilitar la extracción de la fracción proteica, analizándose también el efecto de la temperatura de secado sobre la actividad de la FeQ. Por otra parte, el hígado deshidratado se desgrasó mediante el método Soxhlet y se analizaron y compararon las propiedades fisicoquímicas y tecno-funcionales de la fracción proteica desgrasada y el hígado deshidratado. Finalmente, el hígado deshidratado se desodorizó mediante dos técnicas: arrastre por vapor con aplicación de vacío (AVV) y la aplicación de CO<sub>2</sub> supercrítico (CO<sub>2</sub>-SC). El objetivo de estos tratamientos fue el de reducir o incluso eliminar compuestos orgánicos volátiles (COVs) característicos del olor desagradable del hígado de cerdo, el cual es considerado como el principal factor de rechazo por el consumidor.

## **5.1 Aplicación de ultrasonidos para mejorar la formación del pigmento zinc protoporfirina a partir de hígado de cerdo como fuente de ferroquelatasa (CAPÍTULO 1)**

### **5.1.1 Intensificación mediante US de la extracción de FeQ de hígado de cerdo**

Los US han demostrado ser una tecnología eficaz para intensificar la extracción de enzimas (Delgado-Povedano y De Castro, 2015; Medina-Torres *et al.*, 2017). También han sido utilizados como una estrategia para incrementar la velocidad de las reacciones enzimáticas y obtener mejores rendimientos (Soria *et al.*, 2010). Ambas estrategias se han abordado en esta Tesis Doctoral con el objetivo de mejorar la formación de ZnPP utilizando fracciones enzimáticas de FeQ obtenidas a partir de hígado de cerdo.

La efectividad de la aplicación de US para la intensificación de la extracción de FeQ del hígado de cerdo se abordó comparando la cinética de formación del pigmento ZnPP, con fracciones FeQ obtenidas mediante extracción convencional, sin aplicación de US, y mediante extracción asistida por US. Para las extracciones con US se diseñó un plan experimental con diferentes tiempos (1, 2.5 y 5 min) y modos (continuo y pulsado) de aplicación de US, a una misma potencia de 400 W. Independientemente del procedimiento utilizado para la extracción de FeQ (convencional, sin aplicación de US o asistido por US), la cinética de formación de ZnPP mostró el mismo patrón, una fase de velocidad de reacción constante (lineal), precedida por una fase inicial que en la bibliografía se le conoce como “burst phase”, que se podría traducir como una fase de ráfaga o estallido, con una velocidad de reacción muy alta. La existencia de esta fase inicial se demuestra a través de la intersección con el eje “y” de la fase de reacción constante, que, en todos los casos, fue significativamente ( $p < 0.05$ ) diferente de cero. La “burst phase” indica una etapa inicial en la reacción enzimática a una velocidad muy alta, que está relacionada con el primer recambio de los sitios activos (Praestgaard *et al.*, 2011). Posteriormente, la reacción enzimática entró en la fase de estado estacionario, en la que se manifiesta una velocidad de reacción constante debido a limitaciones en la cinética de reacción, probablemente asociadas a la difusión de los

sustratos al sitio activo del enzima y la salida del producto. Este mismo patrón se manifiesta en reacciones enzimáticas como la del tungsteno para la reducción de ácidos carboxílicos y  $\text{NAD}^+$  a partir de hidrógeno, donde se observa una “burst phase” (1-5 min) seguida de un aumento lineal hasta los 30 min de reacción (Winiarska *et al.*, 2022). Otro ejemplo de este comportamiento en la reacción enzimática se da en la hidrólisis de la celulosa insoluble catalizada por endoglucanasas de *Trichoderma reesi*, en la cual se manifiesta una “burst phase” de aproximadamente 8 s, seguida de una fase constante de 20 min de reacción (Murphy *et al.*, 2012). De acuerdo con el modelo de Michaelis-Menten, la pendiente del ajuste lineal para la fase de estado estacionario es proporcional a la concentración de enzima activa (E) y a la constante de velocidad de liberación del producto ( $K_2$ ), mientras que la intersección con el eje “y” es solo proporcional a la concentración de enzima activa (Sassa *et al.*, 2013). La duración de la “burst phase” inicial comprendida entre 0 y 15 min no se evaluó al estar fuera de los objetivos del trabajo, pero de acuerdo a la literatura previa su duración podrá ser únicamente de unos pocos segundos (Johnson, 2013).

Respecto a la extracción mediante US, se encontró que el tiempo de proceso se podía reducir de los 30 min de la extracción convencional a 1 min, mejorándose la formación de ZnPP con los extractos enzimáticos obtenidos tras la sonicación. De igual forma, Pakhale y Bhagwat (2016) observaron que la aplicación de US acortaba el tiempo de extracción de la serratiopeptidasa de *Serratia marcescens* a 5 min, en comparación con la extracción convencional, cuya duración era de 60 min, y, además, se incrementaba también la actividad enzimática. La aplicación de US mejoró la tasa de formación de ZnPP del extracto enzimático hasta en un 33.3 %, en comparación con la extracción convencional, sin aplicación de US. Los US no aumentaron la cantidad de FeQ extraída, pero sí mejoraron su actividad enzimática, probablemente debido a cambios estructurales que podrían favorecer tanto la localización de los sustratos en el sitio activo, la difusión del producto o ambos procesos. Se puso de manifiesto que tiempos de aplicación de US superiores a 1 min, podrían causar la degradación de la FeQ. Además, el sistema de aplicación de US pulsado permitió modular la energía liberada en el medio, sin embargo, en términos generales, condujo a un empeoramiento del rendimiento de extracción, en comparación con la aplicación continua. Pan *et al.* (2012) obtuvieron resultados similares en la extracción de



antioxidantes de la cáscara de granada. Mediante la extracción con aplicación de US pulsado, obtuvieron un 2 % menos de rendimiento y un 3 % menos de reducción en el tiempo de extracción, en comparación con la extracción asistida con US en modo continuo. Otra estrategia para mejorar la cinética de reacción de FeQ, es aplicar US durante el proceso de formación de ZnPP catalizado por FeQ en homogeneizado de hígado de cerdo e hígado de cerdo con adición de oxihemoglobina porcina, siendo un proceso de larga duración, el cual conlleva una degradación de la enzima. Por ello, la aplicación de US a potencias bajas o moderadas resulta de gran interés para la intensificación de dicho proceso.

### **5.1.2 Influencia de la aplicación de US en la formación de ZnPP**

La aplicación de US a potencias bajas y moderadas durante la reacción enzimática de la FeQ para la formación de ZnPP, mejoró notablemente la actividad enzimática, tanto en el homogeneizado de hígado de cerdo (Hhc), como en el homogeneizado de hígado de cerdo con adición de oxihemoglobina porcina (Hhc+OxiHb). Sin embargo, el efecto de los US dependió principalmente de la potencia ultrasónica aplicada. Así, la aplicación de US a potencia moderada (36.53 W/L) no permitió controlar la temperatura del medio de reacción en su valor óptimo (37 °C), alcanzándose temperaturas entre 45 y 50 °C. El aumento de temperatura, y la aplicación de US, dificultaron la formación de ZnPP, obteniéndose una concentración final de únicamente 0.037 mmol/L después de 24 h de incubación. Becker *et al.* (2012), observaron que por encima de los 60 °C no se observaba formación de ZnPP en carne de cerdo homogeneizada. Además, la intensidad del campo ultrasónico también pudo dificultar la formación de ZnPP. En este sentido, Tian *et al.* (2004) también observaron el mismo comportamiento en la reacción enzimática de hidrólisis de la tripsina utilizando éster metílico de N $\alpha$ -p-tosil-L-arginina (TAME) como sustrato al aumentar la potencia ultrasónica de 20 W/mL a 100 W/mL, en tiempos de tratamiento cortos (de 1 a 20 min). Según estos autores, el rendimiento de la reacción disminuyó debido al aumento de la temperatura, la presión y la formación de radicales libres inducidos por la disociación térmica del agua, consecuencia de la aplicación de US, que afectó a la conformación de la enzima y su estabilidad.

Por otro lado, la aplicación de US a baja potencia (7.05 W/L) fue un método efectivo para la intensificación de la reacción enzimática, obteniendo una mayor concentración de ZnPP (0.405 mmol/L en Hhc y 0.449 mmol/L en Hhc+OxiHb) con respecto al método convencional, sin aplicación de US (0.322 mmol/L en Hhc y 0.430 mmol/L en Hhc+OxiHb). Además, la aplicación de US provocó una reducción del 50 % en el tiempo necesario para alcanzar la concentración máxima de ZnPP (12 h a baja potencia de US y 24 h sin aplicación de US). En este sentido, Becker *et al.* (2012) demostraron que, en homogeneizado de jamón de Parma (*Biceps femoris*), la concentración máxima de ZnPP se alcanzó a las 48 h de incubación anaerobia a 37 °C. Por otro lado, Wakamatsu *et al.* (2007) observó que la concentración máxima de ZnPP en muestras de homogeneizado de lomo de cerdo aumentó rápidamente hasta 72 h de incubación anaerobia 25 °C y tras dicho tiempo de incubación el aumento de la concentración se atenuó, lo que concuerda con el tiempo de incubación para la obtención de la máxima concentración de ZnPP en el homogeneizado de *Longissimus lumborum* de carne de cerdo (Khozroughi *et al.*, 2017). Sin embargo, la máxima formación de ZnPP en el Hhc del presente trabajo tuvo lugar en un menor tiempo (24 h). Esto podría deberse al hecho de que la cantidad de FeQ fue mayor en los homogeneizados de hígado de cerdo que en los músculos de cerdo, como *Longissimus* o *Biceps femoris*. Otra hipótesis podría ser que, al estar el hígado homogeneizado en medio líquido y en el jamón de Parma desarrollarse la reacción enzimática en medio sólido, en el hígado existe una mayor facilidad de contacto entre la enzima y el sustrato, mejorándose la velocidad de la reacción enzimática.

## 5.2 Secado y desgrasado del hígado de cerdo (CAPÍTULO 2)

En la presente Tesis Doctoral se estudió por primera vez la influencia del proceso de secado en la actividad enzimática de ferroquelatasa (FeQ) para la formación del pigmento zinc protoporfirina (ZnPP), así como el efecto del secado y el desgrasado en las propiedades fisicoquímicas y tecno-funcionales del hígado de cerdo.

### 5.2.1 Influencia del secado en la actividad de la FeQ

El secado por convección es un método eficaz para estabilizar el hígado de cerdo y poder obtener posteriormente un extracto enzimático de FeQ para la formación de ZnPP. Por ello, se estudió el efecto de la temperatura de secado sobre la cinética de formación de ZnPP a partir de extractos de hígado deshidratado, comparándola con la del hígado fresco, obtenida siguiendo en mismo procedimiento que en el Capítulo 1. Así, la cinética de formación de ZnPP a partir de extractos de FeQ obtenido de hígado deshidratado a temperaturas comprendidas entre -10 y 70 °C, mostró el mismo comportamiento que a partir de hígado de cerdo fresco, estudiada en el Capítulo 1, es decir, una fase de velocidad de reacción constante (fase estacionaria), precedida por una “burst phase” inicial. Sin embargo, se observó que, independientemente de la temperatura, el secado disminuyó significativamente ( $p < 0.05$ ) tanto la concentración de FeQ aparente como su actividad. Por otra parte, la temperatura de secado afectó significativamente ( $p < 0.05$ ) a la concentración de enzima aparente obtenida a partir del hígado de cerdo deshidratado. La concentración más baja de FeQ se encontró a temperaturas extremas de secado. Así, se observó una marcada degradación térmica de la enzima a altas temperaturas ( $> 30$  °C), por ejemplo, a 70 °C se obtuvo una concentración de 0.072  $\mu\text{mol/L}$ , mientras que a bajas temperaturas de secado ( $< 0$  °C), la reducción de FeQ podría estar ligada a los largos tiempos de deshidratación y, en consecuencia, a la larga exposición al oxígeno, lo cual conduce a una pérdida de FeQ (Wakamatsu *et al.*, 2007). Así, a -10 °C se obtuvo una concentración de FeQ aparente de 0.021  $\mu\text{mol/L}$ . Las condiciones de secado cercanas a la temperatura ambiente, entre 10 y 20 °C (0.288 y 0.266  $\mu\text{mol/L}$ , respectivamente), fueron las más adecuadas para la conservación de la enzima, obteniéndose una concentración de enzima aparente del mismo orden de magnitud que la obtenida en el hígado fresco (0.213  $\mu\text{mol/L}$ ).

En cuanto a la actividad enzimática, se encontró que era aproximadamente igual para todas las temperaturas de secado ( $0.00063 \pm 0.00006$   $\mu\text{mol/L}\cdot\text{min}$ ) excepto a 70 °C, que fue la más baja (0.00033  $\mu\text{mol/L}\cdot\text{min}$ ), y a 0 °C, en la que se encontró una mayor actividad (0.00091  $\mu\text{mol/L}\cdot\text{min}$ ). Sin embargo, si se compara la actividad enzimática con la obtenida para el hígado de cerdo fresco (0.00428  $\mu\text{mol/L}\cdot\text{min}$ ) se

observa que la actividad enzimática del hígado fresco es de un orden de magnitud superior a la de las muestras deshidratadas, posiblemente debido a cambios conformacionales en la estructura proteica de la enzima durante la deshidratación (Oyinloye y Yoon, 2020). Por lo tanto, el secado provocó cambios significativos ( $p < 0.05$ ) en la actividad enzimática de la FeQ. No existe bibliografía previa sobre el secado del hígado de cerdo y cómo el mismo afecta a la actividad de la FeQ. Sin embargo, Jaiswal *et al.* (2010) obtuvieron resultados similares al evaluar la actividad de la polifenol oxidasa (PPO) de arilos procedentes de granadas frescas deshidratadas a 100 °C, observando una disminución del 68 % de su actividad enzimática tras el secado. Del mismo modo, Parra Vergara (2013) observó una disminución del 89.5 % en la actividad enzimática de la peroxidasa en el brócoli deshidratado a 75 °C, en comparación con el brócoli fresco. En conclusión, el proceso de secado fue un método efectivo para la estabilización del hígado de cerdo, sin embargo, el secado afectó la actividad enzimática de la FeQ. Por lo tanto, si se pretende aprovechar al máximo la fracción enzimática, una alternativa sería efectuar la extracción de la FeQ sobre el hígado en fresco, para posteriormente tras un proceso de separación, aprovechar la fracción proteica.

### **5.2.2 Efecto del secado y desgrasado sobre las propiedades fisicoquímicas y tecno-funcionales del hígado**

La temperatura de secado, así como el proceso posterior de desgrasado influyeron en los parámetros fisicoquímicos del hígado de cerdo. En términos generales, el proceso de desgrasado contribuyó a una mayor reducción en el contenido de humedad de las muestras deshidratadas, respecto a las solamente deshidratadas. En este sentido, y a modo de ejemplo, el contenido de humedad de las muestras deshidratadas-desgrasadas a 40 °C fue de  $8.60 \pm 0.22$  %, mientras que el de las muestras solo deshidratadas a 40 °C fue de  $11.24 \pm 0.40$  %. Esta diferencia se relacionó con el hecho de que el método de desgrasado Soxhlet se lleva a cabo a una temperatura alta (~ 70 °C) (Frangopoulos, 2022) y, por lo tanto, se podría esperar una mayor deshidratación de las muestras. Respecto al contenido proteico, se observó un mayor porcentaje en las muestras que habían recibido un proceso de desgrasado ( $83.67 \pm 1.15$  % y  $82.98 \pm 1.12$  % de proteína, en muestras deshidratadas a 40 °C y

70 °C, respectivamente), respecto a las que solo se deshidrataron ( $61.10 \pm 1.00$  % y  $66.53 \pm 0.06$  % de proteína en muestras deshidratadas a 40 °C y 70 °C, respectivamente). El aumento del porcentaje de proteína es debido a la reducción del porcentaje de grasa, siendo el contenido en grasa de las muestras deshidratadas a 40 y 70 °C cercano al 20 %, mientras que el de las muestras deshidratadas-desgrasadas un 4 %, y a la eliminación de una parte del agua, lo cual conlleva un aumento de la concentración del resto de componentes y en particular de la proteína. Respecto al color, la temperatura de secado y el proceso de desgrasado causaron cambios significativos ( $p < 0.05$ ) en las muestras de hígado de cerdo. Así, en los parámetros de color CIE  $L^*a^*b^*$ , la temperatura de secado tuvo un efecto significativo ( $p < 0.05$ ), aumentando la luminosidad ( $L^*$ ) y la tonalidad ( $H^0$ ) y disminuyendo el contenido rojo/verde ( $a^*$ ). Sin embargo, la temperatura de secado no dio lugar a diferencias significativas ( $p > 0.05$ ) en el croma ( $C^*$ ), ni en el contenido amarillo/azul ( $b^*$ ). Por otro lado, cabe destacar que el desgrasado indujo modificaciones notables en el color en comparación con aquellas muestras que solo se deshidrataron, aumentando significativamente ( $p < 0.05$ ) la luminosidad ( $L^*$ ) y la tonalidad ( $H^0$ ) y disminuyendo significativamente ( $p < 0.05$ ) el croma ( $C^*$ ) y la coordenada  $a^*$ . En cuanto a la degradación proteica, la temperatura de 40 °C fue la que dio lugar a una menor degradación proteica, en comparación con el hígado porcino fresco (flujo de calor total: 1.25 J/g a 40 °C vs 3.46 J/g en hígado fresco), siendo la temperatura de 70 °C la que mayor degradación proteica presentó, tal y como se observó en la prueba calorimétrica donde se observó un menor valor de flujo de calor total (0.54 J/g). Además, el proceso de desgrasado no causó cambios apreciables en el grado de desnaturalización proteica ya que se obtuvieron valores similares en el flujo de calor total entre las muestras las deshidratadas y las deshidratadas-desgrasadas.

Respecto a las propiedades tecno-funcionales, la solubilidad de la proteína fue dependiente de la temperatura de secado, siendo las muestras deshidratadas a 70 °C las que presentaron una menor solubilidad. Finalmente, el proceso de desgrasado contribuyó a potenciar ciertas características tecno-funcionales como la capacidad espumante y la estabilidad de la espuma, siendo la muestra deshidratada-desgrasada a 40 °C la que presentó mayor capacidad espumante junto con un alto grado de

estabilidad de la espuma, comparado con el resto de los tratamientos (capacidad espumante:  $700.31 \pm 32.35$  mL y estabilidad de la espuma RFS: 13.76 min). Sin embargo, el proceso de desgrasado no contribuyó a una mejora en las propiedades emulsionantes, disminuyendo los valores de estabilidad de la emulsión a medida que aumentaba la temperatura de secado. En resumen, la temperatura de secado influyó en los parámetros fisicoquímicos y tecno-funcionales de los hígados porcinos deshidratados, siendo 40 °C la temperatura que presentó menor degradación proteica en comparación con el hígado porcino secado a 70 °C. Al mismo tiempo, la etapa de desgrasado contribuyó a la mejora de ciertas características tecno-funcionales, como la capacidad espumante y la estabilidad de la espuma. Por lo tanto, la deshidratación y el desgrasado permitieron mejorar la estabilidad del hígado, potenciando algunas de sus propiedades tecno-funcionales, sin embargo, para el posterior aprovechamiento de la fracción proteica, se analizó el efecto del secado sobre los compuestos orgánicos volátiles (COVs) y en particular sobre aquellos característicos del olor desagradable del hígado de cerdo, así como de diferentes estrategias de desodorización.

### **5.3 Desodorización del hígado de cerdo (CAPÍTULO 3)**

#### **5.3.1 Desodorización de hígado de cerdo deshidratado mediante arrastre por vapor a vacío y CO<sub>2</sub> supercrítico.**

El secado se ha considerado una técnica de conservación, que permite mejorar la estabilidad de los productos con alto contenido de humedad a un costo moderado. Además, el secado facilita el almacenamiento y reduce el peso y el volumen en el procesamiento y transporte del hígado de cerdo (Sánchez-Torres *et al.*, 2021). Ante la problemática del olor característico del hígado de cerdo para el posterior aprovechamiento de su fracción proteica, en este capítulo se comparó la efectividad de dos técnicas de desodorización, arrastre por vapor a vacío (AVV) y CO<sub>2</sub> supercrítico (CO<sub>2</sub>-SC) para la eliminación de compuestos orgánicos volátiles (COVs) característicos del olor desagradable en el hígado de cerdo. Ambas técnicas redujeron la concentración de COVs, e incluso eliminaron algunos de ellos, en hígado de cerdo deshidratado. Además, la técnica de micro-extracción en fase sólida, con espacio de cabeza combinado con cromatografía de gases y detección por espectrómetro de masas (HS-SPME-GC/MS) permitió identificar y cuantificar los COVs para verificar la

reducción de su contenido, o su total eliminación, tras el proceso de desodorización. Im *et al.* (2004) describió el olor de los COVs presentes en el hígado de cerdo fresco como olor a pescado, metálico, graso y con toques de cartón, almendras, naturaleza como hierba (verde) y hongos. Estos aromas están asociados a los siguientes COVs en el hígado deshidratado: (E,E)-2,4-heptadienal (pescado), 1-octen-3-one y 1-hexanol (metálico), (E)-2-nonenal (cartón) butanal, 2-metil, benzaldehído, pentanal (almendras), 2-metil, hexanal y heptanal (grasa), hexanal, butanal, 2-butenal, 2-metil y 1-hexanol (naturaleza, verde), 1-octen-3-ol (setas).

Tras la deshidratación del hígado de cerdo se produjo un aumento de 58 COVs detectados en hígado fresco a 116 COVs en hígado deshidratado. Así pues, tras el proceso de secado se forman muchos COVs característicos de la carne cocinada, estos COVs se forman a través de procesos de oxidación lipídica, degradación de Strecker (degradación de aminoácidos para dar lugar a aldehídos) y reacciones de Maillard, donde tiene lugar la condensación de un azúcar reductor y un aminoácido no libre (Bassam *et al.*, 2022).

Respecto a la técnica de AVV, mostró más afinidad para eliminar y/o reducir COVs de las siguientes familias: compuestos azufrados, furanos y cetonas. Sin embargo, las familias de los éteres y los hidrocarburos aumentaron tras la aplicación de la AVV. El aumento de hidrocarburos por la técnica AVV también fue observado en la desodorización de salsa de pescado (Song *et al.*, 2018). Por otra parte, la técnica de CO<sub>2</sub>-SC, que usaba CO<sub>2</sub> en estado supercrítico como solvente de extracción, mostró una alta capacidad de eliminación y/o reducción de COVs de las siguientes familias: ácidos, alcoholes, aldehídos, compuestos halogenados, compuestos nitrogenados, ésteres e hidrocarburos. En cuanto a la reducción de compuestos azufrados, esta fue mayor con la técnica de AVV (84.5 % UA), aunque con CO<sub>2</sub>-SC también se redujo un alto porcentaje (79.6 % UA). Shimoda *et al.* (2000) también observaron una notable reducción de los compuestos azufrados en la desodorización de la salsa de pescado utilizando CO<sub>2</sub>-SC, lo que podrían contribuir a atenuar el olor desagradable generado por estos compuestos. En concreto, el disulfuro de dimetilo se redujo en un 37 % UA en la salsa de pescado, mediante el uso de CO<sub>2</sub>-SC, mientras que en el presente trabajo se redujo en un 69.2 % UA. Además, se observó que, de

las dos tecnologías estudiadas, el CO<sub>2</sub> supercrítico fue la que redujo una mayor cantidad de COVs (81.3 % UA respecto al hígado deshidratado). Asimismo, la técnica de CO<sub>2</sub>-SC fue capaz de eliminar completamente COVs característicos del aroma desagradable del hígado, como (E,E)- 2,4-heptadienal (pescado), 1-octen-3-ol (hongo) y 1-nonanol (grasa y verde). Por último, cabe señalar que, además de eliminar ciertos COVs del olor típico del hígado de cerdo, fue una técnica eficaz en la reducción del contenido de grasa. En este sentido, el contenido de grasa de las muestras tratadas con CO<sub>2</sub>-SC fue significativamente ( $p < 0.05$ ) menor con respecto a las muestras no tratadas, pasando de  $19.33 \pm 0.10$  % en hígado deshidratado, a  $14.52 \pm 0.71$  % en hígado deshidratado-desodorizado mediante CO<sub>2</sub>-SC. En este sentido, el CO<sub>2</sub>-SC se ha utilizado para la extracción de grasa en alimentos con alto contenido proteico, como alternativa a otras técnicas convencionales (Soxhlet) (Awasthi *et al.*, 2022). Así pues, y a modo de ejemplo, se ha utilizado el CO<sub>2</sub>-SC para la extracción de lípidos en carne picada (39 % de lípidos extraídos, 172 bar y 50 °C) (Chao *et al.*, 1991) o para desgrasar coproductos como el corazón bovino (490 bar y 40 °C), reduciéndose un 93.6 % el contenido de grasa, con el fin de revalorizar su fracción proteica (Rahman *et al.*, 2019) Sin embargo, la reducción del contenido de grasa en hígado deshidratado-desodorizado mediante CO<sub>2</sub>-SC respecto al hígado deshidratado fue menor (24.9 %) que en los trabajos mencionados anteriormente. Esto podría estar relacionado con las condiciones experimentales empleadas y probablemente con el caudal y tiempo de extracción utilizados en el presente trabajo, que no fueron los óptimos para la eliminación de grasa.





## **6. CONCLUSIONES**



A partir del análisis de los resultados obtenidos en la presente Tesis Doctoral, se enumeran las principales conclusiones, divididas en base a los tres capítulos de la sección de Resultados y Discusión. Además, al final de esta sección, se plantea una conclusión general de la Tesis.

## **6.1 Aplicación de ultrasonidos para mejorar la formación del pigmento zinc protoporfirina a partir de hígado de cerdo como fuente de ferroquelatasa (CAPÍTULO 1)**

### **6.1.1 Intensificación mediante ultrasonidos (US) de la extracción de ferroquelatasa (FeQ) de hígado de cerdo**

- La extracción asistida por US mejoró la actividad enzimática de los extractos de FeQ, proporcionando estos mayor concentración de zinc protoporfirina (ZnPP) que los extractos control (sin US). Además, la aplicación de US permitió reducir el tiempo de extracción de la enzima.
- El tiempo de aplicación de los US afectó a la actividad enzimática de la FeQ, obteniéndose los mejores rendimientos a tiempos cortos y con aplicación de US en continuo.
- La aplicación de US en modo pulsado permitió modular la energía liberada en el medio, pero, en términos generales, condujo a menores rendimientos de extracción, en comparación con la aplicación en modo continuo.
- Los extractos de FeQ obtenidos a partir del hígado de cerdo podrían ser añadidos a productos cárnicos, donde tendría lugar la reacción enzimática de formación de ZnPP, colorante natural que permitiría mejorar el color de dichos productos.

### **6.1.2 Influencia de la aplicación de US a baja y moderada potencia en la formación de ZnPP**

- El efecto de los US sobre la formación enzimática de ZnPP, a partir de hígado de cerdo, dependió de la potencia ultrasónica aplicada.
- La aplicación de US a potencia moderada (36.53 W/L) no permitió controlar la

temperatura del medio de reacción en su valor óptimo (37 °C), fluctuando alrededor de 50 °C. Esto conllevó una actividad enzimática muy baja debido a que la enzima pudo desnaturalizarse o disminuir notablemente su capacidad catalítica a esta temperatura.

- La aplicación de US a baja potencia (7.05 W/L) fue un método efectivo para la intensificación de la reacción enzimática, reduciendo el tiempo de formación del máximo de ZnPP al 50 % y obteniendo una mayor concentración de ZnPP, respecto a la formación sin aplicación de US.
- La sangre, y en concreto, la oxihemoglobina porcina obtenida de la misma, fue un buen sustrato para la FeQ del hígado de cerdo, aumentándose la concentración de ZnPP al adicionarla al homogeneizado de hígado.
- La aplicación de US mejoró la reacción enzimática de formación de ZnPP catalizada por la FeQ a partir de coproductos de la industria cárnica (hígado y sangre de cerdo). Así, su producción industrial y uso como colorante natural para la industria alimentaria puede considerarse de interés.

## **6.2 Secado y desgrasado del hígado de cerdo (CAPÍTULO 2)**

### **6.2.1 Influencia del secado en la actividad de la FeQ**

- El secado convectivo ha demostrado ser un método eficaz para estabilizar el hígado de cerdo y obtener un extracto de FeQ que puede usarse para la formación de ZnPP.
- La temperatura de secado influyó en la concentración de FeQ aparente. Así, el secado a altas temperaturas (> 30 °C) pudo dar lugar a una posible degradación térmica de la enzima, y el secado a bajas temperaturas (< 0 °C), conllevó tiempos prolongados de secado, con la consiguiente exposición al oxígeno, lo cual pudo también pudo afectar negativamente a la FeQ.
- Las condiciones de secado cercanas a la temperatura ambiente (entre 10 y 20 °C) fueron las más adecuadas para la conservación de la FeQ, considerando tanto la concentración aparente, como la actividad de la misma.

### **6.2.2 Efecto del secado y del desgrasado sobre las propiedades fisicoquímicas y tecno-funcionales del hígado**

- El proceso de secado resultó ser un método eficaz para la estabilización de la fracción proteica.
- El proceso de desgrasado concentró el contenido de proteína y redujo en aproximadamente el contenido de grasa en un 80 % respecto al hígado deshidratado sin desgrasar.
- La temperatura de secado no produjo diferencias en el croma ( $C^*$ ) y ni en el contenido de amarillo/azul ( $b^*$ ) de los parámetros de color CIE  $L^*a^*b^*$ . Sin embargo, la temperatura aumentó la luminosidad ( $L^*$ ) y la tonalidad ( $H^\circ$ ) y disminuyó el contenido rojo/verde ( $a^*$ ). Además, el proceso de desgrasado provocó un aumento de la luminosidad ( $L^*$ ) y la tonalidad ( $H^\circ$ ) y una disminución del contenido rojo/verde ( $a^*$ ) y del croma ( $C^*$ ).
- Las muestras deshidratadas a 70 °C sufrieron una mayor desnaturalización proteica lo que disminuyó su solubilidad respecto a las deshidratadas a 40 °C. Sin embargo, el desgrasado no provocó cambios relevantes en la desnaturalización proteica.
- El proceso de desgrasado contribuyó a mejorar la capacidad espumante y la estabilidad de la espuma, siendo la muestra deshidratada a 40 °C y desgrasada, la que mejores propiedades tecno-funcionales presentó.
- La temperatura de secado (40 °C y 70 °C) y el proceso de desgrasado no varió la actividad emulsionante, sin embargo, cuando la temperatura de secado fue alta (70 °C), la estabilidad de la emulsión disminuyó. Respecto al proceso de desgrasado, éste no contribuyó a mejorar las propiedades emulsionantes.

## **6.3 Desodorización de hígado de cerdo (CAPÍTULO 3)**

### **6.3.1 Desodorización de hígado de cerdo deshidratado mediante arrastre por vapor con aplicación de vacío y CO<sub>2</sub> supercrítico**

- Tras el proceso de deshidratación del hígado de cerdo, los compuestos orgánicos volátiles (COVs) aumentaron de 58 en hígado fresco, a 116 en hígado

deshidratado.

- La técnica de arrastre por vapor con aplicación de vacío (AVV) redujo la mayor cantidad de COVS de los compuestos azufrados, furanos y cetonas en comparación con la técnica de CO<sub>2</sub> supercrítico (CO<sub>2</sub>-SC).
- La técnica de CO<sub>2</sub>-SC disminuyó la cantidad de COVs de ácidos, alcoholes, aldehídos, compuestos halogenados, compuestos nitrogenados, ésteres e hidrocarburos en mayor medida que mediante AVV.
- Tras la aplicación de CO<sub>2</sub>-SC, se eliminaron COVs característicos del olor desagradable del hígado de cerdo: (E,E)- 2,4-heptadienal (pescado), 1-octen-3-ol (setas) y 1-nonanol (grasa y verde de naturaleza).
- El tratamiento con CO<sub>2</sub>-SC conllevó también una reducción de aproximadamente el 25 % del contenido de grasa respecto al hígado deshidratado sin desodorizar.

## 6.4 Conclusión general

De los resultados obtenidos en el trabajo, se puede concluir que la revalorización del hígado de cerdo para la obtención del pigmento ZnPP puede mejorarse mediante el uso de US. La aplicación de US intensificó la extracción de la enzima FeQ, mejorando la actividad enzimática y la concentración final de ZnPP obtenida. Además, el uso de US a baja potencia intensificó la reacción enzimática de formación de ZnPP a partir de hígado de cerdo como fuente de FeQ. Esto se evidenció en una reducción del tiempo de formación de ZnPP en un 50 % y en la obtención de una mayor concentración de ZnPP, respecto a la formación sin aplicación de US. Además, la adición de oxihemoglobina, derivada de la sangre del cerdo, al homogeneizado de hígado, resultó ser un buen sustrato para la formación de ZnPP, obteniéndose una mayor concentración de ZnPP. Así pues, la revalorización de estos dos coproductos en un nuevo ingrediente natural y sostenible, que ofrecería excelentes propiedades colorantes, puede resultar de gran interés para la industria cárnica.

El proceso de secado resultó ser un método efectivo en la estabilización del hígado de cerdo. Además, mediante el secado a temperaturas cercanas a la temperatura ambiente, entre 10 y 20 °C, se logró obtener una concentración de FeQ aparente del mismo orden que en el hígado fresco y se minimizaron las pérdidas de

actividad enzimática. Por otro lado, el análisis de las propiedades fisicoquímicas y tecno-funcionales confirmó que el proceso de secado era un método eficaz para la extracción de la fracción proteica, siendo la temperatura de 40 °C la que conllevó una menor degradación proteica. Finalmente, el proceso de desgrasado tras la deshidratación del hígado de cerdo puede minimizar las reacciones de oxidación y de enranciamiento en el producto y, contribuye a mejorar las propiedades espumantes de la proteína (capacidad espumante y estabilidad de la espuma), respecto a las muestras solamente deshidratadas.

Respecto al tratamiento de desodorización, las técnicas de AVV y CO<sub>2</sub>-SC fueron útiles para la eliminación y reducción de COVs característicos del olor desagradable del hígado fresco, en hígado deshidratado. Siendo el tratamiento de CO<sub>2</sub>-SC la técnica que redujo una mayor cantidad de COVs (81.3 % respecto al hígado deshidratado) y a su vez, eliminó 3 COVs característicos del olor desagradable del hígado de cerdo fresco: (E,E)- 2,4-heptadienal (pescado), 1-octen-3-ol (setas) y 1-nonanol (grasa y verde de naturaleza). Además, la técnica de CO<sub>2</sub>-SC permitió realizar un desgrasado simultáneo a la desodorización.

Por lo tanto, las tecnologías emergentes estudiadas para la revalorización del hígado de cerdo (US y CO<sub>2</sub>-SC), podrían ser una alternativa a las técnicas convencionales en la obtención del pigmento ZnPP, la extracción de la FeQ, la obtención de la fracción proteica del hígado de cerdo, así como en su desodorización. Además, estas técnicas podrían emplearse en revalorizar otros coproductos o vísceras de origen animal con alto contenido proteico, de interés para la industria alimentaria, minimizando los costes, el tiempo de proceso y mejorando la calidad del producto.





## **7. RECOMENDACIONES**



De acuerdo con los resultados obtenidos en la presente Tesis Doctoral y con el fin de mejorar el conocimiento relacionado con el uso de tecnologías emergentes en la revalorización del hígado de cerdo, se podrían explorar los siguientes aspectos en futuras investigaciones.

### **Extracción de ferroquelatasa (FeQ)**

- Determinar la duración y los mecanismos que ocurren durante la fase inicial de alta velocidad de la reacción enzimática de formación de zinc protoporfirina (ZnPP) catalizada por la FeQ.
- Profundizar en el uso de diferentes solventes para la extracción de la FeQ en hígado de cerdo.
- Abordar la extracción de FeQ del hígado de cerdo asistida por ultrasonidos (US) de modo continuo, para tiempos de tratamiento inferiores a 1 min.
- Evaluar la vida útil del extracto de FeQ del hígado de cerdo bajo diferentes condiciones de almacenamiento.
- Evaluar el uso de otras tecnologías emergentes como los pulsos eléctricos de alta intensidad (PEF) y/o campos eléctricos moderados (MEF) para la mejora de la extracción de FeQ.
- Búsqueda de nuevos coproductos de origen animal que puedan ser fuente de FeQ y aplicación de tecnologías emergentes para mejorar la extracción de la enzima.

### **Formación de ZnPP a partir de homogeneizado de hígado de cerdo**

- Llevar a cabo un estudio microbiológico del medio de reacción con ácidos, para verificar que no existe crecimiento microbiano durante la formación del pigmento.
- Evaluar la vida útil del pigmento ZnPP, en términos de estabilidad microbiana y fisicoquímica, bajo diferentes condiciones de almacenamiento.
- Estudiar la extracción y posterior purificación del pigmento ZnPP a partir de metodologías que utilicen disolventes aptos para la industria alimentaria con el fin de poder ser incorporado de forma segura en alimentos.
- Abordar el escalado de la formación de ZnPP asistida por US.

### **Formación de ZnPP en productos cárnicos**

- Estudiar la incorporación del extracto de FeQ del hígado de cerdo en productos cárnicos crudo-curados como el salchichón, fuet o la longaniza, para la mejora del color a partir de la formación de ZnPP.
- Evaluar la aplicación de US para mejorar la formación de ZnPP en productos cárnicos crudo-curados a los que se les ha añadido el extracto enzimático rico en FeQ, procedente del hígado de cerdo.

### **Secado del hígado de cerdo**

- Determinar cómo afecta la temperatura de secado a la estructura de la FeQ, con el objetivo de comprender cómo y por qué disminuye la actividad enzimática para la formación de ZnPP.
- Determinar cómo afecta la conservación del hígado deshidratado a diferentes temperaturas sobre la actividad de la FeQ.
- Estudiar el uso de otras técnicas de secado que minimicen o eviten la exposición al oxígeno, como el secado a vacío o la liofilización.
- Estudiar el impacto del proceso de secado a temperaturas más suaves (10, 20 y 30°C) sobre la pérdida de calidad y funcionalidad en la matriz proteica.

### **Desodorización de hígado**

- Evaluar el uso de nuevos materiales adsorbentes para la separación de compuestos volátiles durante la desodorización con CO<sub>2</sub> supercrítico (CO<sub>2</sub>-SC).
- Estudiar el uso del tratamiento combinado de US y CO<sub>2</sub>-SC, para aumentar la efectividad del proceso de desodorización.
- Evaluar la incorporación de hígado desgrasado y desodorizado a la formulación de nuevos productos.
- Realizar un análisis nutricional y sensorial de los nuevos productos formulados, determinando su aceptación por parte del consumidor.



## **8. CONTRIBUCIONES CIENTÍFICAS**





**ARTÍCULOS EN REVISTAS CIENTÍFICAS**

- Abril, B., Sánchez-Torres, E. A., Bou, R., García Pérez, J. V., & Benedito, J. (2021). Ultrasound intensification of Ferrochelatase extraction from pork liver as a strategy to improve ZINC-protoporphyrin formation. *Ultrasonics Sonochemistry*, *78*, 105703. <https://doi.org/10.1016/j.ultsonch.2021.105703>.
- Abril, B., Contreras, M., Bou, R., Llauger, M., García Pérez, J. V., & Benedito, J. Influence of Ultrasonic Application at Low and Moderate Power on the Formation of Zinc Protoporphyrin.
- Abril, B., Sánchez-Torres, E. A., Bou, R., Benedito, J., & García-Pérez, J. V. (2022). Influence of pork liver drying on ferrochelatase activity for zinc protoporphyrin formation. *LWT*, *171*, 114128. <https://doi.org/10.1016/j.lwt.2022.114128>.
- Abril, B., Sánchez-Torres, E. A., Toldrà, M., Benedito, J., & García-Pérez, J. V. (2022). Physicochemical and techno-functional properties of dried and defatted porcine liver. *Biomolecules*, *12*(7), 926. <https://doi.org/10.3390/biom12070926>.
- Abril, B., Lorenzo, J.M., García-Pérez, J.V., Contreras, M., and Benedito, J. Deodorization of dried pork liver using vacuum steam and supercritical CO<sub>2</sub>.
- Abril, B., Bou, R., García Pérez, J. V., & Benedito, J. Role of enzymatic reactions in meat processing and use of emergent technologies for process intensification.

## CONTRIBUCIONES EN CONGRESOS

- Abril, B., Pedrero, J.V., Bou, R., Benedito, J. & García Pérez, J. V. (2020). Ultrasonically assisted extraction of ferrochelataze. ENVII International Student Congress of Food Science and Technology, Valencia, España.
- Abril, B., Benedicic, S, Bou, R., García Pérez, J. V.& Benedito, J. (2020). Influence of ultrasound on the formation protoporphyrin in pork liver. EN VII International Student Congress of Food Science and Technology, Valencia, España.
- Abril, B., Alba, J.F., Sánchez-Torres, E.A., Bou, R., Benedito, J. & García Pérez, J. V. (2020). Influence of pork liver drying on the enzyme activity of ferrochelataze and the formation of zinc protoporphyrin. EN VII International Student Congress of Food Science and Technology, Valencia, España.
- Abril-Gisbert, Blanca (2022). Influencia de los ultrasonidos en la formación de zinc protoporfirina en hogenizado de hígado de cerdo. EN I Jornadas de Investigación: Doctorado de Ciencia, Tecnología y Gestión Alimentaria. Valencia, España.
- Abril-Gisbert, Blanca; J. F. Alba; Sanchez-Torres, E.A.; Mulet Pons, Antonio; R.Bou; Benedito Fort, José Javier; Garcia-Perez, J.V. (2022). Influence of pork liver drying on the enzyme activity of Ferrochelataze and the formation of Zinc protoporphyrin. EN 22nd International Drying Symposium (IDS 2022). Worcester, USA.
- Abril-Gisbert, Blanca; Lorenzo; J.M., García-Pérez, J.V.; Benedito, J. (2022). Desodorización de hígado de cerdo deshidratado mediante hidrodestilación y CO<sub>2</sub> supercrítico. EN XI Congreso Nacional de Ciencia y Tecnología de los Alimentos (CyTA/CESIA 2022). Zaragoza, España.
- Abril-Gisbert, Blanca; Bou; R., García Pérez, J.V.; Benedito, J., (2022). Formación del colorante zinc protoporfirina asistida por ultrasonidos a partir de coproductos cárnicos. .EN XI Congreso Nacional de Ciencia y Tecnología de los Alimentos (CyTA/CESIA 2022). Zaragoza, España.
- Abril-Gisbert, Blanca (2022). Aplicación de Tecnologías Emergentes para la Obtención de Zinc-Protoporfirina y Proteínas Funcionales a Partir de Co-Productos Cárnicos. EN VII Encuentro de Estudiantes de Doctorado de la Universitat Politècnica de València. Valencia, España.



## **9. REFERENCIAS**



- Adamsen, C. E., Moller, J. K. S., Hismani, R., & Skibsted, L. H. (2004). Thermal and photochemical degradation of myoglobin pigments in relation to colour stability of sliced dry-cured Parma ham and sliced dry-cured ham produced with nitrite salt. *European Food Research and Technology*, 218(5), 403–409: <https://doi.org/10.1007/s00217-004-0891-8>
- Adamsen, C. E., Møller, J. K., Laursen, K., Olsen, K., & Skibsted, L. H. (2006). Zn-porphyrin formation in cured meat products: Effect of added salt and nitrite. *Meat Science*, 72(4), 672-679. <https://doi.org/10.1016/j.meatsci.2005.09.017>
- Ahmad-Qasem, M. H., Cánovas, J., Barrajón-Catalán, E., Micol, V., Cárcel, J. A., & García-Pérez, J. V. (2013). Kinetic and compositional study of phenolic extraction from olive leaves (var. Serrana) by using power ultrasound. *Innovative Food Science & Emerging Technologies*, 17, 120-129. <https://doi.org/10.1016/j.ifset.2012.11.008>
- Aksoy, A., Karasu, S., Akcicek, A., & Kayacan, S. (2019). Effects of different drying methods on drying kinetics, microstructure, color, and the rehydration ratio of minced meat. *Foods*, 8(6), 216. <https://doi.org/10.3390/foods8060216>
- Allahdad, Z., Nasiri, M., Varidi, M., & Varidi, M. J. (2019). Effect of sonication on osmotic dehydration and subsequent air-drying of pomegranate arils. *Journal of Food Engineering*, 244, 202-211. <https://doi.org/10.1016/j.jfoodeng.2018.09.017>
- Amaral, A. B., Silva, M. V. D., & Lannes, S. C. D. S. (2018). Lipid oxidation in meat: mechanisms and protective factors—a review. *Food Science and Technology*, 38, 1-15. <https://doi.org/10.1590/fst.32518>
- Amid, M., Murshid, F.S., Manap, M.Y. & Islam Sarker, Z. (2016). Optimization of ultrasound-assisted extraction of pectinase enzyme from guava (*Psidium guajava*) peel: Enzyme recovery, specific activity, temperature, and storage stability. *Preparative Biochemistry and Biotechnology* 46: 91-99. doi: 10.1080/10826068.2015.1031396
- AOAC. 1996. Official methods of analysis. 16th ed. Washington DC: Association of Analytical Chemists. 1298 p.

- AOAC (Association of Official Analytical Chemists). (2000). Official methods of analysis of AOAC international (17th ed.; International Association of Official Analytical, ed.). Arlington, VA, Washington DC.
- Asiri, A. M., & Isloor, A. M. (Eds.). (2019). Green sustainable process for chemical and environmental engineering and science: supercritical carbon dioxide as green solvent. *Elsevier*.
- Aspevik, T., Oterhals, Å., Rønning, S. B., Altintzoglou, T., Wubshet, S. G., Gildberg, A., ... & Lindberg, D. (2017). Valorization of proteins from co-and by-products from the fish and meat industry. *Chemistry and chemical technologies in waste valorization*, 123-150. [https://doi.org/10.1007/978-3-319-90653-9\\_5](https://doi.org/10.1007/978-3-319-90653-9_5)
- Awasthi, T., Singh, N., Viridi, A. S., Mahendru Singh, A., & Ahlawat, A. K. Effect of solvents and supercritical-CO<sub>2</sub> extraction of lipids on physico-chemical, functional, pasting and rheological properties of hard, medium hard and soft wheat varieties. *International Journal of Food Science & Technology*. <https://doi.org/10.1111/ijfs.15813>
- Bansode, S.R. & Rathod, V.K. (2017). An investigation of lipase catalysed sonochemical synthesis: A review. *Ultrasonics Sonochemistry* 38: 503-529. <https://doi.org/10.1016/j.ultsonch.2017.02.028>
- Barbosa, L. A. P., Gerke, K. M., Munkholm, L. J., Keller, T., & Gerke, H. H. (2022). Discrete element modeling of aggregate shape and internal structure effects on Weibull distribution of tensile strength. *Soil and Tillage Research*, 219, 105341. <https://doi.org/10.1016/j.still.2022.105341>
- Barreiro, J. A., & Sandoval, A. J. (2006). Operaciones de conservación de alimentos por bajas temperaturas. *Equinoccio*.
- Bassam, S. M., Noleto-Dias, C., & Farag, M. A. (2022). Dissecting grilled red and white meat flavor: Its characteristics, production mechanisms, influencing factors and chemical hazards. *Food Chemistry*, 371, 131139. <https://doi.org/10.1016/j.foodchem.2021.131139>
- Becker, E. M., Westermann, S., Hansson, M., & Skibsted, L. H. (2012). Parallel enzymatic and non-enzymatic formation of zinc protoporphyrin IX in pork. *Food Chemistry*, 130(4), 832-840. <https://doi.org/10.1016/j.foodchem.2011.07.090>

- Benedini, R., Raja, V., & Parolari, G. (2008). Zinc-protoporphyrin IX promoting activity in pork muscle. *Food Science and Technology*, 41(7), 1160–1166. <https://doi.org/10.1016/j.lwt.2007.08.005>
- Bhatta, S., Stevanovic Janezic, T., & Ratti, C. (2020). Freeze-drying of plant-based foods. *Foods*, 9(1), 87. <https://doi.org/10.3390/foods9010087>
- Blasco, M., García-Pérez, J. V., Bon, J., Carreres, J. E., & Mulet, A. (2006). Effect of blanching and air flow rate on turmeric drying. *Food Science and Technology International*, 12(4), 315-323. <https://doi.org/10.1177/1082013206067352>
- Borrajó, P., Pateiro, M., Munekata, P. E., Franco, D., Domínguez, R., Mahgoub, M., & Lorenzo, J. M. (2021). Pork liver protein hydrolysates as extenders of pork patties shelf-life. *International Journal of Food Science & Technology*, 56(12), 6246-6257. <https://doi.org/10.1111/ijfs.15359>
- Bou, R., Hanquet, N., Codony, R., Guardiola, F., & Decker, E. A. (2010). Effect of heating oxyhemoglobin and methemoglobin on microsomes oxidation. *Meat science*, 85(1), 47-53. <https://doi.org/10.1016/j.meatsci.2009.12.002>
- Bou, R., Llauger, M., Joosse, R., & García-Regueiro, J. A. (2019). Effect of high hydrostatic pressure on the oxidation of washed muscle with added chicken hemoglobin. *Food chemistry*, 292, 227-236. <https://doi.org/10.1016/j.foodchem.2019.04.067>
- Bou, R., Llauger, M., Arnau, J., Olmos, A., & Fulladosa, E. (2022). Formation of Zn-protoporphyrin during the elaboration process of non-nitrified serrano dry-cured hams and its relationship with lipolysis. *Food Chemistry*, 374, 131730. <https://doi.org/10.1016/j.foodchem.2021.131730>
- Brannegan, D. R., Ashraf-Khorassani, M., & Taylor, L. T. (2001). Supercritical fluid extraction of ethoxyquin from a beef matrix. *Chromatographia*, 54(5), 399-401. <https://doi.org/10.1007/BF02492691>
- Burri, B.J., Neidlinger, T.R., Lo, A.O., Kwan, C. & Wong, M.R. (1997). Supercritical fluid extraction and reversed-phase liquid chromatography methods for vitamin A and beta-carotene Heterogeneous distribution of vitamin A in the liver. *Journal of Chromatography A* 762: 201-206. [https://doi.org/10.1016/S0021-9673\(96\)00705-4](https://doi.org/10.1016/S0021-9673(96)00705-4)



- Camadro, J. M., & Labbe, P. (1982). Kinetic studies of ferrochelatase in yeast: Zinc or iron as competing substrates. *Biochimica et Biophysica Acta (BBA)-Protein Structure and Molecular Enzymology*, 707(2), 280-288. [https://doi.org/10.1016/0167-4838\(82\)90362-4](https://doi.org/10.1016/0167-4838(82)90362-4)
- Capriotti, A. L., Caruso, G., Cavaliere, C., Samperi, R., Ventura, S., Chiozzi, R. Z., & Laganà, A. (2015). Identification of potential bioactive peptides generated by simulated gastrointestinal digestion of soybean seeds and soy milk proteins. *Journal of Food Composition and Analysis*, 44, 205-213. <https://doi.org/10.1016/j.jfca.2015.08.007>
- Carrera, C., Aliaño-González, M. J., Valaityte, M., Ferreiro-González, M., Barbero, G. F., & Palma, M. (2021). A Novel Ultrasound-Assisted Extraction Method for the Analysis of Anthocyanins in Potatoes (*Solanum tuberosum* L.). *Antioxidants*, 10(9), 1375. <https://doi.org/10.3390/antiox10091375>
- Catchpole, O.J., vonKamp, J.C. & Grey, J.B. (1997). Extraction of squalene from shark liver oil in a packed column using supercritical carbon dioxide. *Industrial & Engineering Chemistry Research* 36: 4318-4324. <https://doi.org/10.1021/ie9702237>
- Chao, R. R., Mulvaney, S. J., Bailey, M. E., & Fernando, L. N. (1991). Supercritical CO<sub>2</sub> conditions affecting extraction of lipid and cholesterol from ground beef. *Journal of Food Science*, 56(1), 183-187. <https://doi.org/10.1111/j.1365-2621.1991.tb08007.x>
- Chau, T. T., Ishigaki, M., Kataoka, T., & Taketani, S. (2011). Ferrochelatase Catalyzes the Formation of Zn-protoporphyrin of Dry-Cured Ham via the Conversion Reaction from Heme in Meat. *Journal of Agricultural and Food Chemistry*, 59(22), 12238–12245. <https://doi.org/10.1021/jf203145p>
- Chemat, F., Rombaut, N., Sicaire, A.G., Meullemiestre, A., Fabiano-Tixier, A.S. & Abert-Vian, M. (2017). Ultrasound assisted extraction of food and natural products. Mechanisms, techniques, combinations, protocols and applications. A review. *Ultrasonics Sonochemistry* 34: 540-560. doi: 10.1016/j.ultsonch.2016.06.035

- Chen, X., Luo, Y., Qi, B., Luo, J., & Wan, Y. (2017). Improving the hydrolysis efficiency of soy sauce residue using ultrasonic probe-assisted enzymolysis technology. *Ultrasonics Sonochemistry*, 35, 351–358. <https://doi.org/10.1016/j.ultsonch.2016.10.013>
- Contreras, M., Benedito, J., Bon, J., & Garcia-Perez, J. V. (2018). Accelerated mild heating of dry-cured ham by applying power ultrasound in a liquid medium. *Innovative Food Science and Emerging Technologies*, 50, 94–101. <https://doi.org/10.1016/j.ifset.2018.10.010>
- Crowell, R., Ferris, A. M., Wood, R. J., Joyce, P., & Slivka, H. (2006). Comparative Effectiveness of Zinc Protoporphyrin and Hemoglobin Concentrations in Identifying Iron Deficiency in a Group of Low-Income, Preschool-Aged Children: Practical Implications of Recent Illness. *PEDIATRICS*, 118(1), 224–232. <https://doi.org/10.1542/peds.2006-0156>
- Cunha, L. M.; Oliveira, F. A. R.; Oliveira, J. C. (1998). Optimal experimental design for estimating the kinetic parameters of processes described by the Weibull probability distribution function. *Journal of Food Engineering*, 37, 175-191. [https://doi.org/10.1016/S0260-8774\(98\)00085-5](https://doi.org/10.1016/S0260-8774(98)00085-5)
- De Maere, H., Chollet, S., Claeys, E., Michiels, C., Govaert, M., De Mey, E., ... Fraeye, I. (2017). In Vitro Zinc Protoporphyrin IX Formation in Different Meat Sources Related to Potentially Important Intrinsic Parameters. *Food and Bioprocess Technology*, 10(1), 131–142. <https://doi.org/10.1007/s11947-016-1804-0>
- de Souza Soares, A., Augusto, P. E. D., Júnior, B. R. D. C. L., Nogueira, C. A., Vieira, É. N. R., de Barros, F. A. R., ... & Ramos, A. M. (2019). Ultrasound assisted enzymatic hydrolysis of sucrose catalyzed by invertase: Investigation on substrate, enzyme and kinetics parameters. *LWT*, 107, 164-170. <https://doi.org/10.1016/j.lwt.2019.02.083>
- de Souza Soares, A., Júnior, B. R. D. C. L., Tribst, A. A. L., Augusto, P. E. D., & Ramos, A. M. (2020). Effect of ultrasound on goat cream hydrolysis by lipase: Evaluation on enzyme, substrate and assisted reaction. *LWT*, 130, 109636. <https://doi.org/10.1016/j.lwt.2020.109636>

- de Oliveira, D. A., Minozzo, M. G., Licodiedoff, S., & Waszczynskyj, N. (2016). Physicochemical and sensory characterization of refined and deodorized tuna (*Thunnus albacares*) by-product oil obtained by enzymatic hydrolysis. *Food Chemistry*, 207, 187-194. <https://doi.org/10.1016/j.foodchem.2016.03.069>
- Delgado-Povedano, M.M. & de Castro, M.D.L. (2015). A review on enzyme and ultrasound: A controversial but fruitful relationship. *Analytica Chimica Acta* 889: 1-21. <https://doi.org/10.1016/j.aca.2015.05.004>
- Di Bernardini, R., Harnedy, P., Bolton, D., Kerry, J., O'Neill, E., Mullen, A. M., & Hayes, M. (2011). Antioxidant and antimicrobial peptidic hydrolysates from muscle protein sources and by-products. *Food Chemistry*, 124(4), 1296-1307. <https://doi.org/10.1016/j.foodchem.2010.07.004>
- Domínguez, R., Pateiro, M., Gagaoua, M., Barba, F. J., Zhang, W., & Lorenzo, J. M. (2019a). A comprehensive review on lipid oxidation in meat and meat products. *Antioxidants*, 8(10), 429. <https://doi.org/10.3390/antiox8100429>
- Domínguez, R., Purriños, L., Pérez-Santaescolástica, C., Pateiro, M., Barba, F. J., Tomasevic, I., ... & Lorenzo, J. M. (2019b). Characterization of volatile compounds of dry-cured meat products using HS-SPME-GC/MS technique. *Food Analytical Methods*, 12(6), 1263-1284. <https://doi.org/10.1007/s12161-019-01491-x>
- Echegaray, N., Gómez, B., Barba, F. J., Franco, D., Estévez, M., Carballo, J., ... & Lorenzo, J. M. (2018). Chestnuts and by-products as source of natural antioxidants in meat and meat products: A review. *Trends in Food Science & Technology*, 82, 110-121. <https://doi.org/10.1016/j.tifs.2018.10.005>
- EFPPRA. Rendering in numbers (2021) <https://efpra.eu/wp-content/uploads/2021/07/Rendering-in-numbers-Infographic.pdf> (Accessed on 16 february 2022)
- EFSA Panel on Food Additives and Nutrient Sources added to Food (ANS), Mortensen, A., Aguilar, F., Crebelli, R., Di Domenico, A., Dusemund, B., ... & Younes, M. (2017). Re-evaluation of potassium nitrite (E 249) and sodium nitrite (E 250) as food additives. *Efsa journal*, 15(6), e04786. <https://doi.org/10.2903/j.efsa.2017.4786>

- FDA | Generally Recognized as Safe (GRAS). (n.d.). Retrieved May 19, 2021, from <https://www.fda.gov/food/food-ingredients-packaging/generally-recognized-safe-gras>
- Fersht, A. R. (1997). Nucleation mechanisms in protein folding. *Current opinion in structural biology*, 7(1), 3-9. [https://doi.org/10.1016/S0959-440X\(97\)80002-4](https://doi.org/10.1016/S0959-440X(97)80002-4)
- Fito, P., Grau, A. M. A., Sorolla, A. M. A., & Baviera, J. M. B. (2001). Introducción al secado de alimentos por aire caliente (pp. 43-49). Ed. Universidad Politécnica de Valencia, Valencia. España.
- Food and Agricultural Organization of the United States. FAOSTAT Statistical Database. 1997. Available online: <http://www.fao.org/faostat/en/#data/CL> (accessed 20 on April 2022).
- Frangopoulos, T. (2022). Incorporation of Trigonella Foenum-Graecum seed powder in meat emulsion systems with olive oil: effects on physicochemical, texture, and color characteristics. *Journal of Food Science and Technology*, 59(5), 2060-2070. <https://doi.org/10.1007/s13197-021-05220-3>
- Freire, F. B., Vieira, G. N., Freire, J. T., & Mujumdar, A. S. (2014). Trends in modeling and sensing approaches for drying control. *Drying Technology*, 32(13), 1524-1532. <https://doi.org/10.1080/07373937.2014.925471>
- García-Pérez, J.V. (2007). Contribución Al Estudio De La Aplicación De Ultrasonidos De Potencia En El Secado Convectivo De Alimentos. Tesis doctoral, Universidad Politécnica de Valencia.
- García-Pérez, J. V., Carcel, J. A., Riera, E., Rosselló, C., & Mulet, A. (2012). Intensification of low-temperature drying by using ultrasound. *Drying Technology*, 30(11-12), 1199-1208. doi: <https://doi.org/10.1080/07373937.2012.675533>
- García-Pérez, J. V., Ozuna, C., Ortuño, C., Cárcel, J. A., & Mulet, A. (2011). Modeling ultrasonically assisted convective drying of eggplant. *Drying Technology*, 29(13), 1499-1509. <https://doi.org/10.1080/07373937.2011.576321>
- Gimenes, N. C., Silveira, E., & Tambourgi, E. B. (2021). An overview of proteases: production, downstream processes and industrial applications. *Separation & Purification Reviews*, 50(3), 223-243. <https://doi.org/10.1080/15422119.2019.1677249>

- Graham, J. M. (2001). Isolation of Golgi membranes from tissues and cells by differential and density gradient centrifugation. *Current protocols in cell biology*, 10(1), 3-9. <https://doi.org/10.1002/0471143030.cb0303s04>
- Guimarães, B., Polachini, T. C., Augusto, P. E., & Telis-Romero, J. (2020). Ultrasound-assisted hydration of wheat grains at different temperatures and power applied: Effect on acoustic field, water absorption and germination. *Chemical Engineering and Processing-Process Intensification*, 155, 108045. <https://doi.org/10.1016/j.cep.2020.108045>
- Hardy, Z., & Jideani, V. A. (2017). Foam-mat drying technology: A review. *Critical reviews in food science and nutrition*, 57(12), 2560-2572. <https://doi.org/10.1080/10408398.2015.1020359>
- Henchion, M., Hayes, M., Mullen, A. M., Fenelon, M., & Tiwari, B. (2017). Future protein supply and demand: strategies and factors influencing a sustainable equilibrium. *Foods*, 6(7), 53. <https://doi.org/10.3390/foods6070053>
- Ilias, M. K. M., Balakrishnan, V., Zuknik, M. H., Al-Gheethi, A., Ghfar, A. A., & Hossain, M. (2021). Supercritical CO<sub>2</sub> separation of lipids from chicken by-product waste for biodiesel production: Optimization, kinetics, and thermodynamics modeling. *Biomass Conversion and Biorefinery*, 1-15. <https://doi.org/10.1007/s13399-021-02092-7>
- Im, S., Hayakawa, F., & Kurata, T. (2004). Identification and sensory evaluation of volatile compounds in oxidized porcine liver. *Journal of Agricultural and Food Chemistry*, 52(2), 300-305. <https://doi.org/10.1021/jf030337v>
- Ishikawa, H., Yoshihara, M., Baba, A., Kawabuchi T., Sato, M., Numata, M., & Matsumoto, K. (2006). Formation of Zinc Protoporphyrin IX from Myoglobin in Porcine Heart Extract. *Food Science and Technology Research*, 12(2), 125–130. <https://doi.org/10.3136/fstr.12.125>
- Jaiswal, V., DerMarderosian, A., & Porter, J. R. (2010). Anthocyanins and polyphenol oxidase from dried arils of pomegranate (*Punica granatum* L.). *Food Chemistry*, 118(1), 11-16. <https://doi.org/10.1016/j.foodchem.2009.01.095>
- Johnson, K. A. (2013). A century of enzyme kinetic analysis, 1913 to 2013. *FEBS letters*, 587(17), 2753-2766. <https://doi.org/10.1016/j.febslet.2013.07.012>

- Kadim, I. T., Mahgoub, O., Baqir, S., Faye, B., & Purchas, R. (2015). Cultured meat from muscle stem cells: A review of challenges and prospects. *Journal of Integrative Agriculture*, 14(2), 222-233. [https://doi.org/10.1016/S2095-3119\(14\)60881-9](https://doi.org/10.1016/S2095-3119(14)60881-9)
- Kang, S.W., Kim, H.M., Rahman, M.S., Kim, A.N., Yang, H.S. & Choi, S.G. (2017). Nutritional Quality and Physicochemical Characteristics of Defatted Bovine Liver Treated by Supercritical Carbon Dioxide and Organic Solvent. *Korean Journal for Food Science of Animal Resources* 37: 29-37. doi:[10.5851/kosfa.2017.37.1.29](https://doi.org/10.5851/kosfa.2017.37.1.29)
- Khadhraoui, B., Ummat, V., Tiwari, B. K., Fabiano-Tixier, A. S., & Chemat, F. (2021). Review of ultrasound combinations with hybrid and innovative techniques for extraction and processing of food and natural products. *Ultrasonics Sonochemistry*, 76, 105625. <https://doi.org/10.1016/j.ultsonch.2021.105625>
- Khozroughi, A. G., Jander, E., Schirrmann, M., Rawel, H., Kroh, L. W., & Schlüter, O. (2017). The role of myoglobin degradation in the formation of zinc protoporphyrin IX in the longissimus lumborum of pork. *LWT-Food Science and Technology*, 85, 22-27. <https://doi.org/10.1016/j.lwt.2017.06.047>
- King, J. W. (2014). Modern supercritical fluid technology for food applications. *Annual review of food science and technology*, 5, 215-238. <https://doi.org/10.1146/annurev-food-030713-092447>
- Kobayashi, F., Hayata, Y., Kohara, K., Muto, N., Miyake, M., & Osajima, Y. (2006). Application of supercritical CO<sub>2</sub> bubbling to deodorizing of drinking water. *Food science and technology research*, 12(2), 119-124. <https://doi.org/10.3136/fstr.12.119>
- Kumar, K., Srivastav, S., & Sharanagat, V. S. (2021). Ultrasound assisted extraction (UAE) of bioactive compounds from fruit and vegetable processing by-products: A review. *Ultrasonics Sonochemistry*, 70, 105325. <https://doi.org/10.1016/j.ultsonch.2020.105325>
- Kuvendziev, S., Lisichkov, K., Zeković, Z., Marinkovski, M., & Musliu, Z. H. (2018). Supercritical fluid extraction of fish oil from common carp (*Cyprinus carpio* L.) tissues. *The Journal of Supercritical Fluids*, 133, 528-534. <https://doi.org/10.1016/j.supflu.2017.11.027>

- Lafarga, T., & Hayes, M. (2014). Bioactive peptides from meat muscle and by-products: generation, functionality and application as functional ingredients. *Meat science*, 98(2), 227-239. <https://doi.org/10.1016/j.meatsci.2014.05.036>
- Laursen, K., Adamsen, C. E., Laursen, J., Olsen, K., & Møller, J. K. (2008). Quantification of zinc-porphyrin in dry-cured ham products by spectroscopic methods: Comparison of absorption, fluorescence and X-ray fluorescence spectroscopy. *Meat science*, 78(3), 336-341. <https://doi.org/10.1016/j.meatsci.2007.06.014>
- Lewis, W. K. (1921). The rate of drying of solid materials. *Industrial & Engineering Chemistry*, 13(5), 427-432.
- Li, H., Chen, Q., Zhang, X., Finney, K. N., Sharifi, V. N., & Swithenbank, J. (2012). Evaluation of a biomass drying process using waste heat from process industries: A case study. *Applied Thermal Engineering*, 35, 71-80. <https://doi.org/10.1016/j.applthermaleng.2011.10.009>
- Li, Y., Zhou, W., Cao, Y., Gong, X., Li, J., Lu, X., & Dai, Y. (2020). Analysis of volatile components of Tilapia enzymolysis solution after different deodorization treatments. In *IOP Conference Series: Earth and Environmental Science* (Vol. 571, No. 1, p. 012121). IOP Publishing. doi:10.1088/1755-1315/571/1/012121
- Li, Z., Xu, Z., Zhao, D., Chen, S., & Yan, J. (2021). Ultrasonic cavitation at liquid/solid interface in a thin Ga-In liquid layer with free surface. *Ultrasonics Sonochemistry*, 71, 105356. <https://doi.org/10.1016/j.ultsonch.2020.105356>
- Li, J., Pettinato, M., Casazza, A. A., & Perego, P. (2022). A Comprehensive Optimization of Ultrasound-Assisted Extraction for Lycopene Recovery from Tomato Waste and Encapsulation by Spray Drying. *Processes*, 10(2), 308. <https://doi.org/10.3390/pr10020308>
- Liu, X., Zhou, S., Jiang, Y., & Xu, X. (2021). Optimization of Deodorization Design for Four Different Kinds of Vegetable Oil in Industrial Trial to Reduce Thermal Deterioration of Product. *Journal of the American Oil Chemists' Society*, 98(4), 475-483. <https://doi.org/10.1002/aocs.12453>
- Llauger, M., Claret, A., Bou, R., López-Mas, L., & Guerrero, L. (2021). Consumer Attitudes toward Consumption of Meat Products Containing Offal and Offal Extracts. *Foods*, 10(7), 1454. <https://doi.org/10.3390/foods10071454>

- Lynch, S. A., Mullen, A. M., O'Neill, E., Drummond, L., & Álvarez, C. (2018). Opportunities and perspectives for utilisation of co-products in the meat industry. *Meat Science*, *144*, 62-73. <https://doi.org/10.1016/j.meatsci.2018.06.019>
- MAGRAMA. Encuesta de sacrificio de ganado. 2021; Available from: <https://www.mapa.gob.es/es/estadistica/temas/estadisticas-agrarias/ganaderia/encuestas-sacrificio-ganado/>
- Maluf, J. U., Fiorese, M. L., Maestre, K. L., Dos Passos, F. R., Finkler, J. K., Fleck, J. F., & Borba, C. E. (2020). Optimization of the porcine liver enzymatic hydrolysis conditions. *Journal of Food Process Engineering*, *43*(4), e13370. <https://doi.org/10.1111/jfpe.13370>
- Marabi, A., Livings, S., Jacobson, M., Saguy, I.S. (2003). Normalized Weibull distribution for modeling rehydration of food particulates. *Eur Food Res Technol* *217*(4): 311–318. <https://doi.org/10.1007/s00217-003-0719-y>
- Martinez-Solano, K. C., Garcia-Carrera, N. A., Tejada-Ortigoza, V., García-Cayuela, T., & Garcia-Amezquita, L. E. (2021). Ultrasound application for the extraction and modification of fiber-rich by-products. *Food Engineering Reviews*, *13*(3), 524-543. <https://doi.org/10.1007/s12393-020-09269-2>
- Martins, M. P., Cortés, E. J., Eim, V., Mulet, A., & Cárcel, J. A. (2019). Stabilization of apple peel by drying. Influence of temperature and ultrasound application on drying kinetics and product quality. *Drying 2012Technology*, *37*(5), 559-568. <https://doi.org/10.1080/07373937.2018.1474476>
- Medina-Torres, N., Ayora-Talavera, T., Espinosa-Andrews, H., Sánchez-Contreras, A., & Pacheco, N. (2017). Ultrasound Assisted Extraction for the Recovery of Phenolic Compounds from Vegetable Sources. *Agronomy*, *7*(3), 47. <https://doi.org/10.3390/agronomy7030047>
- Miller, R. (2020). Drivers of consumer liking for beef, pork, and lamb: A review. *Foods*, *9*(4), 428. <https://doi.org/10.3390/foods9040428>



- Ministerio de Agricultura, Pesca y Alimentación (MAPA). Informe sobre el consumo de carne y tendencias. Año 2020; Editorial MAPA: Madrid, España, 2020; Disponible en línea: [https://www.mapa.gob.es/es/alimentacion/temas/consumo-tendencias/consumo-carne-y-tendencias-2020\\_tcm30-584118.pdf](https://www.mapa.gob.es/es/alimentacion/temas/consumo-tendencias/consumo-carne-y-tendencias-2020_tcm30-584118.pdf) (consultado el 18 de mayo de 2022).
- Mora, L., Reig, M., & Toldrá, F. (2014). Bioactive peptides generated from meat industry by-products. *Food Research International*, 65, 344-349. <https://doi.org/10.1016/j.foodres.2014.09.014>
- Morr, C. V, German, B., Kinsella, J.E., Regenstein, J.M., Buren, J.P.V.A.N., Kilara, A., Lewis, B.A., Mangino, M.E. (1985). A Collaborative Study to Develop a Standardized Food Protein Solubility Procedure. *J. Food Sci.* 50, 1715-1718. <https://doi.org/10.1111/j.1365-2621.1985.tb10572.x>
- Mulet, A. (1994). Drying modelling and water diffusivity in carrots and potatoes. *Journal of Food Engineering*, 22(1-4), 329-348.
- Murphy, L., Cruys-Bagger, N., Damgaard, H. D., Baumann, M. J., Olsen, S. N., Borch, K., ... & Westh, P. (2012). Origin of initial burst in activity for *Trichoderma reesei* endo-glucanases hydrolyzing insoluble cellulose. *Journal of Biological Chemistry*, 287(2), 1252-1260. <https://doi.org/10.1074/jbc.M111.276485>
- Møller, J. K., Adamsen, C. E., Catharino, R. R., Skibsted, L. H., & Eberlin, M. N. (2007). Mass spectrometric evidence for a zinc–porphyrin complex as the red pigment in dry-cured Iberian and Parma ham. *Meat science*, 75(2), 203-210. <https://doi.org/10.1016/j.meatsci.2006.07.005>
- Nadar, S. S., & Rathod, V. K. (2017). Ultrasound assisted intensification of enzyme activity and its properties: a mini-review. *World Journal of Microbiology and Biotechnology*, 33(9), 1-12. <https://doi.org/10.1007/s11274-017-2322-6>
- Nollet, L. M. L., & Toldra, F. (2011). Handbook of analysis of edible animal by-products. Boca Raton, Fla.: CRC Press.

- Nunes, P., Fraga, J. L., Ratier, R. B., Rocha-Leão, M. H. M., Brígida, A. I., Fickers, P., & Amaral, P. F. (2021). Waste soybean frying oil for the production, extraction, and characterization of cell-wall-associated lipases from *Yarrowia lipolytica*. *Bioprocess and Biosystems Engineering*, 44(4), 809-818. <https://doi.org/10.1007/s00449-020-02489->
- Oszagyan, M., Simandi, B., Sawinsky, J., Kery, A., Lemberkovics, E., & Fekete, J. (1996). Supercritical fluid extraction of volatile compounds from lavender and thyme. *Flavour and Fragrance journal*, 11(3), 157-165. [https://doi.org/10.1002/\(SICI\)1099-1026\(199605\)11:3<157::AID-FFJ559>3.0.CO;2-6](https://doi.org/10.1002/(SICI)1099-1026(199605)11:3<157::AID-FFJ559>3.0.CO;2-6)
- Oyinloye, T. M., & Yoon, W. B. (2020). Effect of freeze-drying on quality and grinding process of food produce: A review. *Processes*, 8(3), 354. <https://doi.org/10.3390/pr8030354>
- Pakhale, S. V., & Bhagwat, S. S. (2016). Purification of serratiopeptidase from *Serratia marcescens* NRRL B 23112 using ultrasound assisted three phase partitioning. *Ultrasonics sonochemistry*, 31, 532-538. <https://doi.org/10.1016/j.ultsonch.2016.01.037>
- Pan, Z., Qu, W., Ma, H., Atungulu, G. G., & McHugh, T. H. (2012). Continuous and pulsed ultrasound-assisted extractions of antioxidants from pomegranate peel. *Ultrasonics sonochemistry*, 19(2), 365-372. <https://doi.org/10.1016/j.ultsonch.2011.05.015>
- Panadare, D., Dialani, G., & Rathod, V. (2021). Extraction of volatile and non-volatile components from custard apple seed powder using supercritical CO<sub>2</sub> extraction system and its inventory analysis. *Process Biochemistry*, 100, 224-230. <https://doi.org/10.1016/j.procbio.2020.09.030>
- Parés, D. & Ledward, D.A. (2001). Emulsifying and gelling properties of porcine blood plasma as influenced by high-pressure processing. *Food Chemistry*, 74: 139-145. [https://doi.org/10.1016/S0308-8146\(01\)00105-4](https://doi.org/10.1016/S0308-8146(01)00105-4)

- Parolari, G., Benedini, R., & Toscani, T. (2009). Color formation in nitrite-free dried hams as related to Zn-protoporphyrin IX and Zn-chelatase activity. *Journal of Food Science*, 74(6), C413-C418. <https://doi.org/10.1111/j.1750-3841.2009.01193.x>
- Parolari, G., Aguzzoni, A., & Toscani, T. (2016). Effects of processing temperature on color properties of dry-cured hams made without nitrite. *Foods*, 5(2), 33. <https://doi.org/10.3390/foods5020033>
- Parra Vergara, J. C. (2013). Determinación de la cinética de liofilización en floretes de brócoli (*Brassica oleracea* L, var. Legacy) y evaluación del contenido de ácido L-ascórbico (L-AA) y actividad peroxidasa (POD). Duitama: *Universidad Nacional Abierta y a Distancia. Grecco*, <https://repository.unad.edu.co/handle/10596/2094>
- Pateiro, M., Vargas, F. C., Chinchá, A. A., Sant'Ana, A. S., Strozzi, I., Rocchetti, G., ... & Lorenzo, J. M. (2018). Guarana seed extracts as a useful strategy to extend the shelf life of pork patties: UHPLC-ESI/QTOF phenolic profile and impact on microbial inactivation, lipid and protein oxidation and antioxidant capacity. *Food Research International*, 114, 55-63. <https://doi.org/10.1016/j.foodres.2018.07.047>
- Pearce, K.N. & Kinsella, J.E. (1978). Emulsifying properties of proteins - evaluation of a turbidimetric technique. *Journal of Agricultural and Food Chemistry*, 26: 716-723. <https://doi.org/10.1021/jf60217a041>
- Pearman, N. A., Ronander, E., Smith, A. M., & Morris, G. A. (2020). The identification and characterisation of novel bioactive peptides derived from porcine liver. *Current research in food science*, 3, 314-321. <https://doi.org/10.1016/j.crfs.2020.11.002>
- Peighambardoust, S. H., Karami, Z., Pateiro, M., & Lorenzo, J. M. (2021). A review on health-promoting, biological, and functional aspects of bioactive peptides in food applications. *Biomolecules*, 11(5), 631. <https://doi.org/10.3390/biom11050631>

- Pellicanò, T. M., Sicari, V., Loizzo, M. R., Leporini, M., Falco, T., & Poiana, M. (2019). Optimizing the supercritical fluid extraction process of bioactive compounds from processed tomato skin by-products. *Food Science and Technology*, *40*, 692-697. <https://doi.org/10.1590/fst.16619>
- Petrova, I.; Bantle, M.; Eikevik, T. M. (2015). Manufacture of dry-cured ham: A review. Part 2. Drying kinetics, modeling and equipment. *European Food Research and Technology*, *241*, 447–458. <https://doi.org/10.1007/s00217-015-2485-z>
- Phong, W. N., Show, P. L., Ling, T. C., Juan, J. C., Ng, E. P., & Chang, J. S. (2018). Mild cell disruption methods for bio-functional proteins recovery from microalgae—Recent developments and future perspectives. *Algal research*, *31*, 506-516. <https://doi.org/10.1016/j.algal.2017.04.005>
- Praestgaard, E., Elmerdahl, J., Murphy, L., Nymand, S., McFarland, K. C., Borch, K., & Westh, P. (2011). A kinetic model for the burst phase of processive cellulases. *FEBS Journal*, *278*(9), 1547-1560. <https://doi.org/10.1111/j.1742-4658.2011.08078.x>
- Priya, & Gogate, P. R. (2021). Ultrasound-Assisted Intensification of Activity of Free and Immobilized Enzymes: A Review. *Industrial & Engineering Chemistry Research*, *60*(27), 9650-9668. <https://doi.org/10.1021/acs.iecr.1c01217>
- Pui, W. K., Yusoff, R., & Aroua, M. K. (2019). A review on activated carbon adsorption for volatile organic compounds (VOCs). *Reviews in Chemical Engineering*, *35*(5), 649-668. <https://doi.org/10.1515/revce-2017-0057>
- Rahman, M. S., Gul, K., Yang, H. S., Chun, J., Kerr, W. L., & Choi, S. G. (2019). Thermal and functional characteristics of defatted bovine heart using supercritical CO<sub>2</sub> and organic solvent. *Journal of the Science of Food and Agriculture*, *99*(2), 816-823. <https://doi.org/10.1002/jsfa.9250>
- Rajeeva, S., & Lele, S. S. (2011). Three-phase partitioning for concentration and purification of laccase produced by submerged cultures of *Ganoderma* sp. WR-1. *Biochemical Engineering Journal*, *54*(2), 103-110. <https://doi.org/10.1016/j.bej.2011.02.006>

- Ramalingam, V., Song, Z., & Hwang, I. (2019). The potential role of secondary metabolites in modulating the flavor and taste of the meat. *Food research international*, 122, 174-182. <https://doi.org/10.1016/j.foodres.2019.04.007>
- Rodrigues, D., Sousa, S., Silva, A., Amorim, M., Pereira, L., Rocha-Santos, T.A.P., Gomes, A.M.P., Duarte, A.C. & Freitas, A.C. (2015). Impact of Enzyme- and Ultrasound-Assisted Extraction Methods on Biological Properties of Red, Brown, and Green Seaweeds from the Central West Coast of Portugal. *Journal of Agricultural and Food Chemistry* 63: 3177-3188. <https://doi.org/10.1021/jf504220e>
- Rodríguez-Jimenes, G. C., Vargas-García, A., Espinoza-Pérez, D. J., Salgado-Cervantes, M. A., Robles-Olvera, V. J., & García-Alvarado, M. A. (2013). Mass transfer during vanilla pods solid liquid extraction: Effect of extraction method. *Food and Bioprocess Technology*, 6(10), 2640-2650. <https://doi.org/10.1007/s11947-012-0975-6>
- Rosas-Mendoza, M. E., Coria-Hernández, J., Meléndez-Pérez, R., & Arjona-Román, J. L. (2017). Characteristics of chia (*Salvia hispanica* L.) seed oil extracted by ultrasound assistance. *Journal of the Mexican Chemical Society*, 61(4), 326-335.
- Saavedra, J., Córdova, A., Navarro, R., Díaz-Calderón, P., Fuentealba, C., Astudillo-Castro, C., ... & Galvez, L. (2017). Industrial avocado waste: Functional compounds preservation by convective drying process. *Journal of Food Engineering*, 198, 81-90. <https://doi.org/10.1016/j.jfoodeng.2016.11.018>
- Sánchez-Torres, E. A., Abril, B., Benedito, J., Bon, J., & García-Pérez, J. V. (2021). Water desorption isotherms of pork liver and thermodynamic properties. *LWT*, 149, 111857. <https://doi.org/10.1016/j.lwt.2021.111857>
- Sánchez-Torres, E. A., Abril, B., Benedito, J., Bon, J., Toldrà, M., Pares, D., & García-Pérez, J. V. (2022). Airborne ultrasonic application on hot air-drying of pork liver. Intensification of moisture transport and impact on protein solubility. *Ultrasonics Sonochemistry*, 106011. <https://doi.org/10.1016/j.ultsonch.2022.106011>

- Santacatalina, J. V., Rodríguez, O., Simal, S., Cárcel, J. A., Mulet, A., & García-Pérez, J. V. (2014). Ultrasonically enhanced low-temperature drying of apple: Influence on drying kinetics and antioxidant potential. *Journal of Food Engineering*, 138, 35-44. <https://doi.org/10.1016/j.jfoodeng.2014.04.003>
- Sassa, A., Beard, W. A., Shock, D. D., & Wilson, S. H. (2013). Steady-state, pre-steady-state, and single-turnover kinetic measurement for DNA glycosylase activity. *Journal of Visualized Experiments: JoVE*, (78). doi:10.3791/50695.
- Seong, P. N., Park, K. M., Cho, S. H., Kang, S. M., Kang, G. H., Park, B. Y., ... & Van Ba, H. (2014). Characterization of edible pork by-products by means of yield and nutritional composition. *Korean Journal for Food Science of Animal Resources*, 34(3), 297. doi:10.5851/kosfa.2014.34.3.297
- Şener, N., Apar, D. K., & Özbek, B. (2006). A modelling study on milk lactose hydrolysis and  $\beta$ -galactosidase stability under sonication. *Process Biochemistry*, 41(7), 1493-1500. <https://doi.org/10.1016/j.procbio.2006.02.008>
- Shahidi, F., & Pegg, R. B. (2017). Processing of Nitrite-Free Cured Meats. In *Advanced Technologies for Meat Processing* (pp. 513-534). CRC Press.
- Sherwood, T. K. (1929). The drying of solids—II. *Industrial & Engineering Chemistry*, 21(10), 976-980.
- Shimizu, M., Tanabe, S., Morimatsu, F., Nagao, K., Yanagita, T., Kato, N., & Nishimura, T. (2006). Consumption of pork-liver protein hydrolysate reduces body fat in Otsuka Long-Evans Tokushima Fatty rats by suppressing hepatic lipogenesis. *Bioscience, biotechnology, and biochemistry*, 70(1), 112-118. <https://doi.org/10.1271/bbb.70.112>
- Shimoda, M., Yamamoto, Y., Cocunubo-Castellanos, J., Yoshimura, T., Miyake, M., Ishikawa, H. & Osajima, Y. (2000). Deodorization of fish sauce by continuous-flow extraction with microbubbles of supercritical carbon dioxide. *Journal of Food Science* 65: 1349-1351. <https://doi.org/10.1111/j.1365-2621.2000.tb10610.x>
- Shivamathi, C. S., Moorthy, I. G., Kumar, R. V., Soosai, M. R., Maran, J. P., Kumar, R. S., & Varalakshmi, P. (2019). Optimization of ultrasound assisted extraction of pectin from custard apple peel: Potential and new source. *Carbohydrate polymers*, 225, 115240. <https://doi.org/10.1016/j.carbpol.2019.115240>

- Siddiqui, K. S., Ertan, H., Poljak, A., & Bridge, W. J. (2022). Evaluating Enzymatic Productivity—The Missing Link to Enzyme Utility. *International Journal of Molecular Sciences*, 23(13), 6908. <https://doi.org/10.3390/ijms23136908>
- Silva, L. V., Nelson, D. L., Drummond, M. F. B., Dufossé, L., & Glória, M. B. A. (2005). Comparison of hydrodistillation methods for the deodorization of turmeric. *Food Research International*, 38(8-9), 1087-1096. <https://doi.org/10.1016/j.foodres.2005.02.025>
- Snell, S. M., & Marini, M. A. (1988). A convenient spectroscopic method for the estimation of hemoglobin concentrations in cell-free solutions. *Journal of biochemical and biophysical methods*, 17(1), 25-33. [https://doi.org/10.1016/0165-022X\(88\)90075-9](https://doi.org/10.1016/0165-022X(88)90075-9)
- Soladoye, P. O., Juárez, M., Estévez, M., Fu, Y., & Álvarez, C. (2022). Exploring the prospects of the fifth quarter in the 21 century. *Comprehensive Reviews in Food Science and Food Safety*, 1- 23. <https://doi.org/10.1111/1541-4337.12879>
- Song, G., Zhang, M., Peng, X., Yu, X., Dai, Z., & Shen, Q. (2018). Effect of deodorization method on the chemical and nutritional properties of fish oil during refining. *LWT*, 96, 560-567. <https://doi.org/10.1016/j.lwt.2018.06.004>
- Soria, A. C., & Villamiel, M. (2010). Effect of ultrasound on the technological properties and bioactivity of food: a review. *Trends in Food Science & Technology*, 21(7), 323–331. <https://doi.org/10.1016/J.TIFS.2010.04.003>
- Soyer, A., Özalp, B., Dalmış, Ü., & Bilgin, V. (2010). Effects of freezing temperature and duration of frozen storage on lipid and protein oxidation in chicken meat. *Food chemistry*, 120(4), 1025-1030. <https://doi.org/10.1016/j.foodchem.2009.11.042>
- Sunkar, B., Kannoju, B., & Bhukya, B. (2020). Optimized production of xylanase by *Penicillium purpurogenum* and ultrasound impact on enzyme kinetics for the production of monomeric sugars from pretreated corn cobs. *Frontiers in Microbiology*, 11, 772. <https://doi.org/10.3389/fmicb.2020.0077>

- Szabo, O.E., Csiszar, E., Toth, K., Szakacs, G. & Koczka, B. (2015). Ultrasound assisted extraction and characterization of hydrolytic and oxidative enzymes produced by solid state fermentation. *Ultrasonics Sonochemistry* 22: 249-256. doi: [10.1016/j.ultsonch.2014.07.001](https://doi.org/10.1016/j.ultsonch.2014.07.001)
- Taheri-Garavand, A., & Meda, V. (2018). Drying kinetics and modeling of savory leaves under different drying conditions. *International Food Research Journal*, 25(4).
- Taketani, S., & Tokunaga, R. (1981). Rat liver ferrochelataze. Purification, properties, and stimulation by fatty acids. *Journal of Biological Chemistry*, 256(24), 12748-12753. [https://doi.org/10.1016/S0021-9258\(18\)42958-4](https://doi.org/10.1016/S0021-9258(18)42958-4)
- Taketani S., & Tokunaga, R. (2005). Purification and Substrate Specificity of Bovine Liver-Ferrochelataze. *European Journal of Biochemistry*, 127(3), 443–447. <https://doi.org/10.1111/j.1432-1033.1982.tb06892.x>
- Taipa, M. Â., Fernandes, P., & de Carvalho, C. C. (2019). Production and purification of therapeutic enzymes. *Therapeutic Enzymes: Function and Clinical Implications*, 1-24. [https://doi.org/10.1007/978-981-13-7709-9\\_1](https://doi.org/10.1007/978-981-13-7709-9_1)
- Taylor, R. A., Mordecai, E. A., Gilligan, C. A., Rohr, J. R., & Johnson, L. R. (2016). Mathematical models are a powerful method to understand and control the spread of Huanglongbing. *PeerJ*, 4, e2642. doi: 10.7717/peerj.2642
- Tejedor-Calvo, E., García-Barreda, S., Sánchez, S., Morales, D., Soler-Rivas, C., Ruiz-Rodriguez, A., ... & Marco, P. (2021). Supercritical CO<sub>2</sub> extraction method of aromatic compounds from truffles. *LWT*, 150, 111954. <https://doi.org/10.1016/j.lwt.2021.111954>
- Tian, Z. M., Wan, M. X., Wang, S. P., & Kang, J. Q. (2004). Effects of ultrasound and additives on the function and structure of trypsin. *Ultrasonics Sonochemistry*, 11(6), 399-404. doi: <https://doi.org/10.1016/j.ultsonch.2003.09.004>
- Tomasevic, I., Djekic, I., Font-i-Furnols, M., Terjung, N., & Lorenzo, J. M. (2021). Recent advances in meat color research. *Current Opinion in Food Science*, 41, 81-87. <https://doi.org/10.1016/j.cofs.2021.02.012>
- Toldrá, F., Mora, L., & Reig, M. (2016). New insights into meat by-product utilization. *Meat science*, 120, 54-59. <https://doi.org/10.1016/j.meatsci.2016.04.021>



- Toldrà, M., Parés, D., Saguer, E., & Carretero, C. (2019). Recovery and extraction of technofunctional proteins from porcine spleen using response surface methodology. *Food and Bioprocess Technology*, 12 (2): 298-312. <https://doi.org/10.1007/s11947-018-2208-0>.
- Traffano-Schiffo, M. V., Castro-Giráldez, M., Fito, P. J., & Balaguer, N. (2014). Thermodynamic model of meat drying by infrared thermography. *Journal of Food engineering*, 128, 103-110. <https://doi.org/10.1016/j.jfoodeng.2013.12.024>
- UNIPROT | FECH - Ferrochelatase - Sus scrofa (Pig). (n.d.). Retrieved May 18, 2022, from <https://www.uniprot.org/uniprot/F1S1X4>
- Uribe, E., Lemus-Mondaca, R., Vega-Gálvez, A., Zamorano, M., Quispe-Fuentes, I., Pasten, A., & Di Scala, K. (2014). Influence of process temperature on drying kinetics, physicochemical properties and antioxidant capacity of the olive-waste cake. *Food chemistry*, 147, 170-176. <https://doi.org/10.1016/j.foodchem.2013.09.121>
- Vafaei, N., Rempel, C. B., Scanlon, M. G., Jones, P. J., & Eskin, M. N. (2022). Application of Supercritical Fluid Extraction (SFE) of Tocopherols and Carotenoids (Hydrophobic Antioxidants) Compared to Non-SFE Methods. *AppliedChem*, 2(2), 68-92. <https://doi.org/10.3390/appliedchem2020005>
- Van Boekel, M. A. (2008). Kinetic modeling of food quality: a critical review. *Comprehensive Reviews in Food Science and Food Safety*, 7(1), 144-158. <https://doi.org/10.1111/j.1541-4337.2007.00036.x>
- Vatanserver, S., & Hall, C. (2020). Flavor modification of yellow pea flour using supercritical carbon dioxide+ ethanol extraction and response surface methodology. *The Journal of Supercritical Fluids*, 156, 104659. <https://doi.org/10.1016/j.supflu.2019.104659>
- Vázquez-Espinosa, M., V. González-de-Peredo, A., Espada-Bellido, E., Ferreiro-González, M., Toledo-Domínguez, J. J., Carrera, C., ... & F. Barbero, G. (2019). Ultrasound-assisted extraction of two types of antioxidant compounds (TPC and TA) from black chokeberry (*Aronia Melanocarpa* L.): Optimization of the individual and simultaneous extraction methods. *Agronomy*, 9(8), 456. <https://doi.org/10.3390/agronomy9080456>

- Verma, A. K., Chatli, M. K., Kumar, P., & Mehta, N. (2019). Antioxidant and antimicrobial activity of porcine liver hydrolysate in meat emulsion and their influence on physico-chemical and color deterioration during refrigeration storage. *Journal of food science*, *84*(7), 1844-1853. <https://doi.org/10.1111/1750-3841.14683>
- Vioque, J., Sánchez-Vioque, R., Pedroche, J., del Mar Yust, M., & Millán, F. (2001). Production and uses of protein concentrates and isolates. *Grasas y aceites*, *52*(2), 127-131. doi: 10.3989/gya.2001.v52.i2.384
- Waghmare, G. V., & Rathod, V. K. (2016). Ultrasound assisted enzyme catalyzed hydrolysis of waste cooking oil under solvent free condition. *Ultrasonics sonochemistry*, *32*, 60-67. <https://doi.org/10.1016/j.ultsonch.2016.01.033>
- Wakamatsu, J., Nishimura, T., & Hattori, A. (2004a). A Zn-porphyrin complex contributes to bright red color in Parma ham. *Meat Science*, *67*(1), 95-100. <https://doi.org/10.1016/j.meatsci.2003.09.012>
- Wakamatsu, J., Okui, J., Ikeda, Y., Nishimura, T., & Hattori, A. (2004b). Establishment of a model experiment system to elucidate the mechanism by which Zn-protoporphyrin IX is formed in nitrite-free dry-cured ham. *Meat Science*, *68*(2), 313-317. <https://doi.org/10.1016/j.meatsci.2004.03.014>
- Wakamatsu, J., Okui, J., Hayashi, N., Nishimura, T., & Hattori, A. (2007). Zn protoporphyrin IX is formed not from heme but from protoporphyrin IX. *Meat Science*, *77*(4), 580-586. <https://doi.org/10.1016/j.meatsci.2007.05.008>
- Wakamatsu, J., Murakami, N., & Nishimura, T. (2015). A comparative study of zinc protoporphyrin IX-forming properties of animal by-products as sources for improving the color of meat products. *Animal Science Journal*, *86*(5), 547-552. <https://doi.org/10.1111/asj.12326>
- Wakamatsu, J. I., Akter, M., Honma, F., Hayakawa, T., Kumura, H., & Nishimura, T. (2019). Optimal pH of zinc protoporphyrin IX formation in porcine muscles: Effects of muscle fiber type and myoglobin content. *LWT*, *101*, 599-606. <https://doi.org/10.1016/j.lwt.2018.11.040>
- Wakamatsu, J. I. (2022). Evidence of the mechanism underlying zinc protoporphyrin IX formation in nitrite/nitrate-free dry-cured Parma ham. *Meat Science*, *192*, 108905. <https://doi.org/10.1016/j.meatsci.2022.108905>

- Wang, D., Yan, L., Ma, X., Wang, W., Zou, M., Zhong, J., ... & Liu, D. (2018). Ultrasound promotes enzymatic reactions by acting on different targets: Enzymes, substrates and enzymatic reaction systems. *International journal of biological macromolecules*, 119, 453-461. <https://doi.org/10.1016/j.ijbiomac.2018.07.133>
- Wang, D., Hou, F., Ma, X., Chen, W., Yan, L., Ding, T., ... & Liu, D. (2020). Study on the mechanism of ultrasound-accelerated enzymatic hydrolysis of starch: Analysis of ultrasound effect on different objects. *International Journal of Biological Macromolecules*, 148, 493-500. <https://doi.org/10.1016/j.ijbiomac.2020.01.064>
- Wen, C., Zhang, J., Zhang, H., Dzah, C. S., Zandile, M., Duan, Y., ... & Luo, X. (2018). Advances in ultrasound assisted extraction of bioactive compounds from cash crops—A review. *Ultrasonics sonochemistry*, 48, 538-549. <https://doi.org/10.1016/j.ultsonch.2018.07.018>
- Winiarska, A., Hege, D., Gemmecker, Y., Kryściak-Czerwenka, J., Seubert, A., Heider, J. y Szaleniec, M. (2022). A tungsten enzyme using hydrogen as an electron donor to reduce carboxylic acids and NAD+. <https://doi.org/10.21203/rs.3.rs-1462116/v2>
- Wong, S. T., Tan, M. C., & Geow, C. H. (2019). Optimization of ultrasound-assisted ethanol extraction of hazelnut oil. *Journal of Food Processing and Preservation*, 43(10), e14138. <https://doi.org/10.1111/jfpp.14138>
- Xue, Z., Wen, H., Zhai, L., Yu, Y., Li, Y., Yu, W., ... & Kou, X. (2015). Antioxidant activity and anti-proliferative effect of a bioactive peptide from chickpea (*Cicer arietinum* L.). *Food Research International*, 77, 75-81. <https://doi.org/10.1016/j.foodres.2015.09.027>
- Yousefi, M., Rahimi-Nasrabadi, M., Pourmortazavi, S. M., Wysokowski, M., Jesionowski, T., Ehrlich, H., & Mirsadeghi, S. (2019). Supercritical fluid extraction of essential oils. *TrAC Trends in Analytical Chemistry*, 118, 182-193. <https://doi.org/10.1016/j.trac.2019.05.038>
- Yu, Z. L., Zeng, W. C., & Lu, X. L. (2013). Influence of ultrasound to the activity of tyrosinase. *Ultrasonics sonochemistry*, 20(3), 805-809. <https://doi.org/10.1016/j.ultsonch.2012.11.006>

- Zabot, G. L. (2020). Decaffeination using supercritical carbon dioxide. In *Green Sustainable Process for Chemical and Environmental Engineering and Science* (pp. 255-278). Elsevier. <https://doi.org/10.1016/B978-0-12-817388-6.00011-8>
- Zhao, X., Liang, K., & Zhu, H. (2022). Carotenoids in Cereals and Related Foodstuffs: A Review of Extraction and Analysis Methods. *Food Reviews International*, 1-16. <https://doi.org/10.1080/87559129.2022.2027438>
- Zhu, Z.Z., He, J.R., Liu, G., Barba, F.J., Koubaa, M., Ding, L.H., Bals, O., Grimi, N. & Vorobiev, E. (2016). Recent insights for the green recovery of inulin from plant food materials using non-conventional extraction technologies: A review. *Innovative Food Science & Emerging Technologies* 33: 1-9. <https://doi.org/10.1016/j.ifset.2015.12.023>
- Zou, Y., Shahidi, F., Shi, H., Wang, J., Huang, Y., Xu, W., & Wang, D. (2021). Value-added utilization of protein and hydrolysates from animal processing by-product livers: A review. *Trends in Food Science & Technology*, 110, 432-442. <https://doi.org/10.1016/j.tifs.2021.02.033>
- Zou, Y., Wang, L., Li, P., Cai, P., Zhang, M., Sun, Z., ... & Wang, D. (2017). Effects of ultrasound assisted extraction on the physiochemical, structural and functional characteristics of duck liver protein isolate. *Process Biochemistry*, 52, 174-182



# **ANEXOS**



*Role of enzymatic reactions in meat processing and use of emerging technologies for process intensification*

---

Blanca Abril<sup>1</sup>, Ricard Bou<sup>2</sup>, José Vicente García-Pérez<sup>1</sup> and José Benedito<sup>1</sup>

<sup>1</sup>Department of Food Technology, Universitat Politècnica de València, Camí de Vera, s/n, Valencia 46022, Spain

<sup>2</sup>IRTA, XaRTA, Food Technology, Finca Camps i Armet, Monells, Girona E-17121, Spain





**Abstract**

Meat processing involves different transformations in the animal muscle after slaughtering, which results into changes in tenderness, aroma and colour, determining the quality of the final meat product. Several enzyme reactions, such as glycolysis, proteolysis and lipolysis, play a key role on the muscle conversion into meat. The accurate control of enzyme reactions in meat muscle is complicated due to the numerous factors affecting, as well as its low reaction rate. Moreover, exogenous enzymes are also used in the meat industry to produce restructured meat, to obtain bioactive peptides and to promote meat tenderization.

Emerging technologies have been used to intensify enzymatic reactions in different food applications, such as ultrasound, pulsed electric fields (PEF), moderate electric fields (MEF), high pressure (HPP) or supercritical CO<sub>2</sub> (SC-CO<sub>2</sub>). This review aims to provide an overview of some enzymatic reactions taking place during the processing of meat products and how this have been intensified by using emerging technology, as well as to online novel applications.

**Key words:** enzymes, enzyme reaction, meat, emerging technologies, intensification.

## 1. Introduction

A combination of transformations that originate in the muscle of the animal after slaughtering occur, which result into changes in color, tenderness and aroma (Lonergan *et al.*, 2018). These transformations continue during the aging process. The biochemical processes that occur during meat aging are especially caused by endogenous enzymes, which catalyze glycolysis, proteolysis and lipolysis reactions, among others. In the glycolysis reactions, glucose is metabolized to produce lactic acid, which lowers muscle pH and depletes the energy reserves (ATP). The energy depletion leads to the degradation of myofibrillar proteins by the action of endopeptidases, such as calpains, lysosomal cathepsins and the ubiquitin-proteasome system, and the action of exopeptidases. Endopeptidases and exopeptidases are enzymes that play a key role in the proteolysis of meat, giving rise to peptides of different sizes and amino acids (Sentandreu *et al.*, 2002). Another reaction that takes place during the meat aging is the lipolysis in the muscle and the adipose tissue (Toldrá *et al.*, 2000). The products resulting from the degradation of proteins and lipids are precursors of the flavor and aroma compounds characteristic of the meat and meat products (Khan *et al.*, 2016). In addition, the fragmentation of the myofibrils also leads to changes in texture that result into the meat softening (Bekhit *et al.*, 2014). Therefore, post-mortem changes in the muscle, which affects the organoleptic properties of meat, are mostly related to the action of enzymes. Moreover, the enzymatic reactions that take place in muscle transformation to meat have low reaction rates and are affected by numerous intrinsic (animal breed, age or feeding) and extrinsic factors (such as temperature). On the other hand, exogenous enzymes are also used in the meat industry to produce restructured meat, obtain bioactive peptides and induce meat tenderization.

The application of emerging technologies in meat processing could be used for the intensification of enzymatic reactions involving endogenous and exogenous enzymes. In this sense, during the last years, there has been a growing interest in non-thermal techniques capable of accelerating enzymatic reactions, without affecting the quality of meat and guaranteeing food safety (Sunil *et al.*, 2018). Currently, some of the emerging technologies that have been used to improve the enzymatic reactions are ultrasound, pulsed electric fields (PEF), moderate electric fields (MEF), high pressure (HPP) or supercritical CO<sub>2</sub> (SC-CO<sub>2</sub>) which have shown its ability to preserve the quality

and safety of the processed products (Chemat *et al.*, 2017).

In this context, the aim of this paper is to review the enzymatic reactions taking place during the processing of meat products, and to identify and describe those emerging technologies that have been used to intensify enzymatic reactions in different food matrices and especially in meat products. Potential uses of these emerging technologies for enzymatic intensification in meat processing, not covered in the literature, will be also outlined.

## **2. Enzymatic reactions in meat processing. Endogenous enzymes.**

During the processing of meat, a series of biochemical reactions, mainly catalyzed by enzymes, occur. These reactions involve enzymes responsible for post-mortem glycolysis and muscle enzymes responsible for the conformational changes in proteins. Proteolytic enzymes involved include first muscle endopeptidases: calpains ( $\mu$ -calpain and m-calpain) and cathepsins (B, H, L and D), the ubiquitin-proteasome system and, subsequently, exopeptidases such as dipeptidases, aminopeptidases, and carboxypeptidases (Sentandreu *et al.*, 2002), which degrade the polypeptides generated by endopeptidases into peptides and free amino acids (Toldrá & Aristoy, 2010). In addition to proteolytic changes, hydrolysis reactions of triglycerides and phospholipids occur due to the action of lipases, which contribute to the characteristic flavor and aroma of meat (Toldrá, 2006).

### **2.1. Conversion of muscle into meat**

Meat is the result of a series of transformations that the muscle tissue of the animal undergoes after slaughtering. This process entails structural transformations and biochemical reactions, which will produce changes affecting the technological and sensory quality of the meat. The process of converting muscle into meat comprises three stages: *pre-rigor mortis*, *rigor mortis* and *post-rigor mortis* (Braden, 2013). The first stage, *pre-rigor mortis*, is the survival phase of the nervous system (Ouali *et al.*, 2006). In the *rigor mortis*, the depletion of energy components takes place, that is, adenosine triphosphate (ATP), phosphocreatinine and glucose. Finally, in *the post-rigor mortis*, the disintegration of the muscle structure of the myofibrils by endogenous proteolytic systems, that induce meat tenderization, takes place. The duration of the stages of *rigor mortis* depends on the animal species, on the glycogen reserves at the

time of sacrifice of the animal and on the storage temperature. Thus, the completion of the three stages of *rigor mortis* takes at least in 14 days in cattle, 7 to 10 days in lamb, 5 to 7 days in pigs, and approximately 6 hours in poultry (Nowak, 2011). The three proteolytic system involved in the three stages are calpains, cathepsins and the ubiquitin-proteasome system (Salmerón *et al.*, 2015).

In the first phase, *pre-rigor mortis*, which occurs immediately after exsanguination, the meat must be kept at a temperature above 10 °C until reaching the *rigor mortis* phase. Thus, the "cold shortening" does not occur during *rigor mortis* avoiding the meat hardening (Dadgar, 2010). In *pre-rigor mortis*, the metabolism of the animal muscle changes from aerobic to anaerobic and therefore undergoes a gradual decrease in energy intake. Muscle needs glycogen and phosphocreatine to synthesize ATP from glucose. Under these circumstances, the enzymes that lead the muscle metabolism begin to act, that is, those responsible for glycolysis. Among the enzymes that participate in anaerobic glycolysis, glucose 6 phosphate and phosphocreatine kinase are particularly relevant. These enzymes act until the glycogen and phosphocreatine reserves are depleted. After which ATP is reduced to form, firstly, adenosine diphosphate (ADP) and subsequently adenosine monophosphate (AMP), which can be deaminated by the enzymes responsible for the degradation of ATP. The degradation of ATP gives rise to the final product xanthine, which can subsequently give rise to uric acid, responsible for the microbial flora of meat (Aristoy & Toldrá, 2009). On the other hand, after the progressive reduction of ATP levels, inorganic phosphate is generated, which stimulates the degradation of glucose to pyruvate and subsequently, lactic acid is generated from the enzyme lactate dehydrogenase. Lactic acid causes the muscle pH to drop from 7.2 to 5.5 and the enzymes responsible for anaerobic metabolism (glycolysis) will be inactivated (Chauhan & England, 2018). The decrease in muscle pH is one of the most significant post-mortem changes, leading to the start of the *rigor mortis* stage. After the depletion of ATP, there is a depolarization of the membranes due to an ionic increase linked to the  $\text{Ca}^{2+}$ ,  $\text{Na}^{+}$  and  $\text{K}^{+}$  pumps standstill, that depend on ATP. That is why, the  $\text{Ca}^{2+}$  ions react with troponin which modifies the configuration of the active sites of actin and then, myosin binds to actin giving rise to the irreversible formation of actomyosin, which causes a reduction in water retention capacity (WRC) and therefore a hardening of the muscle. The stage of *rigor*

*mortis* ends with the formation of actomyosin, which is characterized by muscle tension and stiffness.

In the third stage, *post-rigor mortis*, the enzymatic reactions responsible for the tenderization of meat take place. First, the proteolytic system of calpain plays a central role in post-mortem proteolysis and softening (Koochmarai, 1996). The calpain system, dependent on  $\text{Ca}^{2+}$  and its endogenous inhibitors calpastatins, has been described as the main factor responsible for proteolysis in the early post-mortem period (0-24 h) and meat tenderization, since calpain system acts at neutral pH and its activity declines when the pH drops. Caballero *et al.* (2007) postulated that the synergistic action of calpains with cathepsins was the result of meat softening. Cathepsins, lysosomal enzymes, are activated at lower pH than calpains and therefore, becomes more important in later phases of *post-mortem*, as well as, their endogenous inhibitors, cystatins. Finally, the proteasome is responsible for the degradation of most intracellular proteins, with the ubiquitin-proteasome complex responsible for the intracellular turnover of damaged proteins (Ouali *et al.*, 2013). However, to date, the role of the proteasome in tenderization has not been fully clarified, although it is known that its activation is one of the first cellular responses to oxidative stress.

The evolution of pH after slaughtering has a great effect on the technological properties of the meat, affecting the texture (tenderization), color and aroma, due to the generation of volatile compounds resulting from the proteolytic and lipid degradation of the meat (Toldrá, 1998). Reactions that will be discussed more extensively in section 2.2, since they have a greater importance in the maturation and curing of meat. In addition, it should be noted that some factors related to genetics, nutrition, and pre-mortem and post-mortem handling, can drastically influence the conversion of muscle into meat (Matarneh *et al.*, 2017).

In addition, color is one of the meat characteristics that plays an important role, as it is the attribute indicative of the meat freshness and is therefore a key factor for consumers' acceptability (Brewer & McKeith, 1999). The color depends on the concentration and oxidation state of the hemic compounds, mainly myoglobin. Myoglobin is a globular protein, which can be found in four chemical forms, deoxymyoglobin, carboxymyoglobin, metmyoglobin and oxymyoglobin (Mancini &

Hunt, 2005). Myoglobin is a water-soluble protein and among the amino acid residues that contains, histidine has received the most attention due to its key role in the structure and function of myoglobin. In addition, there are heme proteins such as hemoglobin and cytochrome C that may also play a role in the color of beef, lamb, pork, and poultry. However, the mechanisms that control color stability remain unclear (Giddings & Solberg, 1977). The bright red color of fresh meat depends on a triple balance of biochemical factors: respiratory activities (O<sub>2</sub> uptake rate), auto-oxidation of myoglobin and enzymatic reduction of MetMb, which in turn can be affected by time, temperature, and muscle pH history (Ledward, 1985).

## **2.2. Raw cured meat products**

The main muscle enzymes associated with the curing and aging process of meat are the muscle endopeptidase enzymes: calpains ( $\mu$ -calpain and m-calpain) and cathepsins (B, H, L and D), the ubiquitin-proteasome system, and muscle exopeptidases: dipeptidases, aminopeptidases and carboxypeptidases (Sentandreu *et al.*, 2002). The two types of enzymes will give rise to a large number of peptides and free amino acids, which contribute to the flavor, aroma, texture and final quality of cured meat products (Lametsch *et al.*, 2003).

Unlike the conversion of muscle into meat, meat curing is a long process, which can be extended up to 12 months or more in cured ham, with enzymatic reactions being particularly relevant. As previously mentioned in section 2.1., calpains are the enzymes that act first. These enzymes are very unstable and have an optimal pH and temperature of 5.5-6.5 and 2-6 °C, respectively (Sentandreu *et al.*, 2002). Calpains are able to hydrolyze proteins, such as titin, nebulin, troponins T and I, tropomyosin and desmin (Koochmaraire, 1994). On the other hand, cathepsins, along with calpains, also play an important role in the meat softening during post-mortem, as previously mentioned. Cathepsins are mostly active at acidic pH (5.0 - 6.0). While cathepsins B, H and L are stable and active during the whole meat curing process, cathepsin D disappears throughout the process. To a large degree, the disappearance of cathepsin D is due to the addition of salts (NaCl), a stage that takes place in the meat curing (Rico *et al.*, 1991). In addition, cathepsins D and L release fragments of proteins from the degradation of myofibrillary proteins such as titin, troponins T and I and tropomyosin

that degrade calpains and myosin, as well as cathepsin B degrades actin and also myosin.

As for exopeptidases, pyroglutamyl, alanyl, leucyl, arginyl aminopeptidases are enzymes that have the greatest activity during the processing of raw cured meat. They present a good stability during curing, although NaCl is also an inhibitory factor of these enzymes (Toldrá *et al.*, 1997). The amino acids and peptides generated during this stage by exopeptidases (glutamic acid, alanine, arginine, lysine and leucine) are the compounds that give the characteristic aroma and flavor to raw-cured products (Flores, 1997).

As for the enzymatic activity of lipases, it consists of the enzymatic hydrolysis of muscle lipids and adipose tissue to generate free fatty acids. These free fatty acids are susceptible to oxidation, which gives rise to some of the aromatic compounds typical of cured products (Toldrá & Flores, 2000). As for lipases, we can differentiate between lipases (lysosomal and neutral) and muscle phospholipases (Motilva *et al.*, 1993). Neutral lipases act at the beginning of the curing process, forming free fatty acids. Subsequently, lysosomal acid lipase is the one that acts on triglycerides giving rise to mono and diglycerides and free fatty acids. Phospholipases act during the first 6 months of curing, forming free fatty acids, especially oleic, stearic, linoleic and palmitic (Motilva & Toldrá, 1993).

The proteolytic activity in raw cured meat products depends on temperature, pH and also on sodium chloride (NaCl), which affects the proteolytic activity during the process and the final texture of the cured meat (Arnau *et al.*, 1998). Arnau *et al.* (1998) and García-Rey *et al.* (2004) studied the texture of *Biceps femoris*, salted at different levels of NaCl content. They observed that pastiness in *Biceps femoris* increased when NaCl content decreased. Ruiz-Ramírez *et al.* (2005) observed that the hardness, cohesiveness and springiness of *Semimembranosus* and *Biceps femoris* muscles were affected by NaCl content. Raw cured muscles with lower NaCl contents showed lower hardness, cohesiveness and springiness due to NaCl acts as a strong inhibitor of proteolytic activity (Sárraga *et al.*, 1989).

Raw cured meat products can be obtained from meat pieces made from whole



muscles, with anatomical integrity (cured ham or shoulder) or meat derivatives formed by pieces of lean tissue and fat, without anatomical integrity (“salchichón”, “longaniza”, “salami” or “chorizo”, among others), being the enzymatic reactions specific for each type of meat product (Toldrá, 2008).

#### 2.1.1. *Raw cured meat products with anatomical integrity*

Nitrates and nitrites play an important role in curing raw cured meat products, particularly cured ham. The function of these nitrifying agents is to provide food stability and safety from a microbiological point of view. Apart from offering food safety to these products, they are responsible for the formation and stability of the characteristic color of cured meat. During the processing of cured products with anatomical integrity, the reaction of nitric oxide with myoglobin leads to the formation nitrosilmyoglobin (NOMb), which is the pigment responsible for the reddish coloration of the cured ham, highly appreciated by consumers. NOMb formation requires the presence of nitrites, which generate nitrogen monoxide (NO), which under reducing conditions, either directly combined with myoglobin (Mb) or indirectly in combination with metamyoglobin (MetMb), give rise to NOMb. This pigment is very stable, maintaining its reddish color even in very long-lasting hams (Cordoba *et al.*, 1994). On the other hand, Zinc protoporphyrin (ZnPP) is a natural red pigment known for the typical color that provides to the Italian dry-cured Parma ham, which is manufactured without the use of nitrifying agents. In this pigment, the iron atom of the porphyrin ring has been replaced by a zinc atom. There is evidence that ZnPP is formed endogenously in meat under anaerobic conditions and in the presence of endogenous microorganisms and the enzyme Ferrochelatase (FeCH) (Wakamatsu *et al.*, 2004). It has been shown that ZnPP accumulates in Iberian ham and Parma ham during maturation (Adamsen *et al.*, 2006, Møller *et al.*, 2007) and *Longissimus lumborum* muscle after a few days of storage at room temperature (Khozroughi *et al.*, 2017). On the other hand, Abril *et al.* (2021) reported that pork liver, an important by-product in the meat industry, contains the FeCH enzyme that catalyzes the ZnPP formation.

As mentioned in section 2.2., the taste in raw cured meat products and specifically in cured ham is associated with non-volatile compounds, such as free amino acids and peptides appearing during processing (Toldrá *et al.*, 1995), while flavor is

associated with the generation of volatile compounds related to the onset of lipid oxidation after lipolysis and proteolytic activity (Toldrá *et al.*, 1997). Glutamic and aspartic acids, alanine, leucine, lysine and valine appear to be some of the amino acids undergoing the largest increases during the processing of dry cured ham (Toldrá & Aristoy, 1993). The combination of all these free amino acids and small peptides contribute to the characteristic flavor of dry cured ham (Aristoy & Toldrá, 1995).

### 2.1.2. *Fermented sausages*

There is a wide variety of raw cured products without anatomical integrity, with or without fermentation. The enzymatic reactions of products without fermentation are similar to those of raw cured products with anatomical integrity, explained in section 2.2.1. On the other hand, products that undergo a fermentation stage during their processing undergo additional enzymatic reactions that will be described in this section. The final characteristics and quality of these fermented products depend on the raw material, the microbial population as well as the processing conditions during fermentation (temperature between 18-26 °C, 90-95 % relative humidity and time 24-72 h) (Demeyer *et al.*, 1992). Microorganisms involved in fermentation include the microbiota of the raw meat or microorganisms added as starter cultures (lactic acid bacteria (*Lactobacillus*), Gram-positive catalase-positive cocci (*Staphylococcus*), yeasts and moulds). Lactic acid bacteria, essentially *Lactobacillus sakei*, play an important role in the technological properties and microbial stability of the final product, through the production of lactic and acetic acids and the consequent decrease in pH to approximately 5. At this pH value, muscle proteins coagulate, lose their water-holding capacity and result into an increase in the firmness and cohesivity of the final product. In addition, the accumulation of lactic and acetic acids inhibits the growth of pathogenic and spoilage microorganisms. On the other hand, *Staphylococcus* also has an important role in the fermentation since it contributes to the development of the characteristic flavor and color together with the acidic pH caused by the lactic acid bacteria, which improve the color stability of the fermented products. The action of these microorganisms is due to endopeptidase and exopeptidase enzymes generated by these microorganisms. In general, these endopeptidases and exopeptidases contribute to increasing the concentration of free amino acids that affect flavor development (Flores & Toldrá, 2011). Finally, yeasts and moulds participate in

fermentation through lactate oxidation, proteolysis, and lipolysis (Talon *et al.*, 2007).

During the fermentation of sausages, muscle proteins (actin and myosin) begin to degrade to peptides mainly by cathepsin D and at the same time, lipolysis begins. Both, microorganisms added as starter cultures, and endogenous enzymes of meat (lysosomal lipases and phospholipases, explained in section 2.2), produce lipolysis generating free fatty acids, which due to successive modifications give rise to esters, aldehydes and ketones, among other compounds and participate in the final aroma of the fermented product (Andrade, 2009).

Once the fermentation stage of sausages is finished, the maturation stage begins. This stage implies the maintenance of the sausages during variable periods under controlled humidity and temperature. The most common procedures usually consist of 5 - 10 days at 18 - 22 °C and relative humidity between 80 - 90 % and, subsequently, they are kept at 12 - 15 °C and a relative humidity of 65 - 80 %. The maturation stage can range from 20 to 90 days, depending on the type of sausage (Flores, 1997). During maturation, proteolysis initiated in the fermentation stage continues with the action of exopeptidases, both endogenous and microbial origin, which release peptides and free amino acids (Molly *et al.*, 1997). In addition, lipolysis initiated in the fermentation continues. Oxidative processes that involve the release of free fatty acids and the oxidation of unsaturated fatty acids, particularly polyunsaturated acids, with the production of carbonyl compounds follows (Demeyer *et al.*, 1992).

### **3. Enzymatic reactions in meat processing. Exogenous enzymes.**

#### **3.1. Restructured meat products**

Due to consumer's demand for nutritious and higher quality products, meat industries are currently processing innovative products such as restructured meat. By means of restructured meat, an attempt is made to imitate the appearance of meat muscle. Thereby, restructured meat is considered an intermediate product between minced meat and a piece of meat with anatomical integrity. Its production begins with meat particles of different sizes to achieve a consistent product by joining these particles. With this process, it is possible to produce products of better quality, from portions of meat of low nutritional value, with poor texture and difficult commercialization. Restructuration technology is applied to all types of meat.

Different non-meat ingredients are used in the manufacturing of restructured meat products. One of the most important ingredients is the enzyme transglutaminase (Anzani *et al.*, 2020). Transglutaminase is an enzyme produced by the microorganism *Streptoverticillium mobaraense*, which is naturally found in most tissues of living organisms. This enzyme has a range of action between 0 and 60 °C, being the optimal at 50 °C and pH 7. In addition, unlike endopeptidase enzymes such as calpain, it is independent of  $\text{Ca}^{2+}$  and has the ability to improve the functional characteristics of protein, including water retention, water solubility, and functional properties, such as food taste and toughness (Yang & Zhang, 2019). Transglutaminase is a transferase enzyme that is characterized by catalyzing cross-breeding reactions between the residual  $\gamma$ -carboxamide residual groups of glutamine and the residual  $\epsilon$ -amino groups of lysine, resulting in a molecular cross of proteins by forming  $\epsilon$ - $\gamma$  glutamyl lysine bonds (Tarté, 2009). The inter and intramolecular bonds they form are highly resistant to proteolysis, which is why transglutaminase becomes an important ingredient that enhances the physical and functional properties of meat products (Kaufmann *et al.*, 2012). Transglutaminase has been tested on a large number of meat products with different targets. One of the objectives is to develop new meat products or enriched meat products. Thus, Baugreet *et al.* (2018) optimized a restructured beef fillet enriched with vegetable protein (lentil and rice) through the action of transglutaminase, from which meat with a high protein value (28 g protein / 100 g meat) was obtained. Ahhmed *et al.* (2007), investigated the improvement of the physical properties of meat products, such as the texture of chicken and beef sausages. In addition, there are several studies that show how a good bond of meat pieces can be achieved using transglutaminase, without the need of using salt and phosphates, for the manufacturing of cooked ham (Fulladosa *et al.*, 2009) and sausages (Colmenero *et al.*, 2005), aiming to reduce the salt content. This enzyme has also been used in restructured unsalted and low-fat kebab meat (Askin & Kilic, 2009), improving its functional properties.

### 3.2. Bioactive peptides

It is known that bioactive peptides are generated through enzymatic hydrolysis of whole protein molecules. The activity of bioactive peptides derived from meat proteins depends on the amino acid sequence, and can affect the cardiovascular, immune, nervous and digestive systems (Jakubczyk *et al.*, 2020). Bioactive peptides

derived from meat proteins have an effect and biological activity in humans on the cardiovascular system, with antihypertensive activity. Peptides with antihypertensive activity act by inhibiting the Angiotensin I Converting Enzyme (ACE). The muscle proteins of pork (myosin, actin, troponin T and titin) are a source of antihypertensive peptides, after gastrointestinal digestion these bioactive peptides are generated by the action of gastrointestinal enzymes (pepsin and pancreatin) (Muguruma *et al.*, 2009; Arihara *et al.*, 2021). Kim *et al.* (2001) studied that the enzymatic activity of five proteases (akalasa, chymotripsin, neutral, pronase E and trypsin) of bovine gelatin, contributed to the formation of bioactive peptides, inhibitors of ACE. Arrutia *et al.* (2016) studied serum albumin, the main blood protein. The hydrolysis of this protein by trypsin resulted in bioactive peptides that had inhibitory activity of ACE (antihypertensive activity), inhibition of DPP-IV (glucose regulation) and antioxidant activity.

In addition to the generation of peptides by digestive enzymes from meat, hydrolysates can be obtained using enzymes such as papain, bromelain, thermolysine, actinase E or proteinase K (Toldrá *et al.*, 2012). The peptides resulting from the enzymatic action of papain and actinase E on the myofibrillary proteins of pork have antioxidant activity in a peroxidation system with linolenic acid induced by Fe<sup>2+</sup>, in addition to their functional ability to improve the texture of certain meat products (Saiga *et al.*, 2003). Li *et al.* (2020) and Wang *et al.* (2020) purified and characterized bioactive peptides with antioxidant activity from duck and mutton meat, respectively. Kim *et al.* (2009) reported the antioxidant activity of bioactive peptides from venison, to obtain these peptides, six enzymes were used (papain, pepsin, trypsin, chemotrypsin, alkalase and neutral), being the papain hydrolysates, the ones with the greatest antioxidant activity. Therefore, the purification of the antioxidant peptides of deer was carried out to obtain new healthy foods.

### **3.3. Tenderization**

Tenderness has been rated by consumers as the most important organoleptic attribute of fresh meat. Various enzymatic systems have been identified to be involved in the softening of meat through the degradation of muscle proteins, caused by endogenous enzyme systems (discussed in section 2) or exogenous ones (Koochmaraie & Geesink, 2006). Regarding exogenous enzyme systems, they are

mostly formed by enzymes of plant origin, being the papain, bromelain and ficin, the most studied. Other enzymes less studied in the literature are zingibain, cucumis and actinidin.

Papain can be found in the latex of the papaya plant, *Carica papaya*, and is an enzyme that protects the papaya plant from insects (Konno *et al.*, 2004). Papain is a very heat-stable enzyme and therefore, it is not easily deactivated, allowing a continuous change of product texture even after cooking (Dransfield & Etherington, 1981). The application of papain for beef tenderization has been studied at different concentrations (0.003, 0.005, 0.007 and 0.01 mg/100 g meat) leaving the enzyme to act from 24 to 48 h at 4 °C and subsequently carrying out a heat treatment at 83 °C for 10 min. The results showed an increase in tenderness and juiciness as the concentration and application time increased. Ashie *et al.* (2002) showed how, in beef, the application of papain to obtain a residual level of 0.002 to 0.05 units of proteolytic activity/100 g meat, improved the tenderness of the meat by 25 - 30 %. However, high doses of papain are not recommended because they can lead to meat pastiness (Istrati, 2008).

Bromelain is a complex of proteolytic enzymes found in some fruits, specifically in the stem of pineapple (*Ananas comosus*). As for its enzymatic activity, it is slightly lower than that of papain. The profile of proteins subjected to enzymatic action indicates that papain degrades myosin and actin at similar rates, while bromelain mainly degrades myosin (Kim & Taub, 1991). Ionescu *et al.* (2008) studied the effect of applying different concentrations of papain and bromelain (10, 15 and 20 mg enzyme/100 g of meat) to beef for 24 and 48 h at 4 °C and subsequently cooking, resulting in an improvement of meat softening more noticeable in the application of the enzyme papain compared to bromelain. The optimal concentration applied was 10 mg enzyme (papain or bromelain)/100 g meat for a tenderization time of 24 h at 4 °C, in order to avoid excessive structural degradation of the meat caused by the enzymatic treatment.

Ficin, is a proteolytic substance obtained from the latex of trees of the genus *Ficus*. The cysteine proteases of *Ficus glabrata* and *Ficus carica* have demonstrated an ability to increase the solubilization of proteins and to improve the tenderness of

meat products. Ramezani *et al.* (2003) observed how the quality of beef sausages could be improved by using the enzyme ficin together with chemically modified soy proteins. 3 kg of ground beef was mixed with 4 mL of enzyme solution containing 30 units of ficin activity. It was observed how the enzyme ficin increased the solubility of meat proteins by degrading them into units of smaller molecular weight. In addition, the joint action of ficin and soy proteins increased the softening effect of the meat compared to the individual effects.

Zingibain, is a vegetable proteolytic enzyme isolated from the ginger rhizome. The ginger rhizome is mainly used as a flavoring agent, but its application as a softening agent in meat products is of great interest. In this regard, zingibain showed a good potential for beef softening, however, the injection level was limited due to problems associated with taste (Naqvi *et al.*, 2021). That is why, if the enzyme could be purified, its application in meat would be more promising (Sullivan & Calkins, 2010).

On the other hand, cucumis is a proteolytic enzyme of *Cucumis trigonus Roxb* (Kachri) plants that grow wild in India, Afghanistan and Persia (Mali & Chavan, 2016). Naveena *et al.* (2004), studied the application of the enzymes cucumis, zingibain and papain in buffalo meat. The results obtained showed the softening effect of the three enzymes and that the samples treated with zingibain were rated as superior, attributed to a desired ginger taste. Regarding the samples treated with cucumis and papain, they were rated equally. Therefore, cucumis and zingibain, which are cheaper enzymes, could be used as an alternative to the use of papain.

The enzyme actinidin is obtained from kiwi juice. Actinidin hydrolyzes microfibrillary proteins, leading to new peptides and activation of m-calpain, during the *post-mortem* aging period (Han *et al.*, 2009). The effect of raw extracts and purified actinidin of the Xuxiang cultivar was studied at a concentration of 0.25 and 0.5 mg/100 g meat in pork and rabbit *Longissimus dorsi*. After the injection of the enzyme, a period of action (3 h at 20 °C) and the meat cooking (75 °C for 30 min), samples treated with actinidin showed a higher shear force in the texture tests than those treated with papain, especially in the pork samples, with lower shear forces compared to the control sample without the addition of exogenous enzymes (Zhang *et al.*, 2017). Moreover, Christensen *et al.* (2009) showed that an actinidin injection accelerated the muscle-to-

meat conversion process, improving tenderness in *Biceps femoris* muscle of the pork, affecting the protein myofibrils and the proteins of the connective tissue, without affecting the flavor and juiciness of the meat. After an injection of 2.8 g/L of actinidin and storage for 2 days at 2 °C, the same tenderness was obtained as in 5 days of storage at 2 °C without enzymatic treatment.

In addition to exogenous enzymes of plant origin, there are also microbial enzymes, such as *Bacillus subtilis* elastase and *Aspergillus oryzae* enzymes, that can be used for meat softening. Qihe *et al.* (2006) compared the action of *Bacillus spp* elastase with that of papain proteases, observing a significant degradation of meat myofibrils indicating that it could be used as a substitute of papain. As for the applications of the microorganism *Aspergillus oryzae*, Ashie *et al.* (2002) studied the enzyme aspartic protease (AP) expressed in *Aspergillus oryzae*, which was shown to be interesting in softening beef compared to papain. The softening effect of AP occurs mainly during cooking, and not in the cold storage, as in the case of papain. That is why the injection of this enzyme could be of interest in the storage of packaged fresh meat products. Sullivan & Calkins (2010) conducted a study on the level of beef softening of the muscles *Triceps brachii* and *supraspinous* using seven types of enzymes (papain, ficin, bromelain, zingibain, *Bacillus subtilis* protease and two proteases from *Aspergillus oryzae*: *Aspergillus oryzae* concentrate protease (ACONC) and *Aspergillus oryzae* 400 protease (A400). The results showed a high degree of meat softening for all the enzymes. Regarding the mode of action of proteases, those of vegetable origin degraded myofibrillary and collagen proteins in a balanced way, while those of microbial origin, tended to degrade more myofibrillary proteins, compared to collagen ones, and in turn, gave better sensory results than those of vegetable origin.

#### **4. Intensification of enzymatic reactions by emerging technologies**

Given the growing demand for products that guarantee food safety and the quality of the final product, as well as the interest of the meat industry in intensifying production processes, new technologies are emerging. These technologies aim at improving existing processes in terms of process rate, energy consumption or final product quality. The use of novel technologies may also pursue the development of new processes covering the lack of actual ones. this section, emerging technologies



focused on the intensification of enzymatic reactions, especially in meat products, will be addressed.

#### **4.1. Ultrasound**

Ultrasound is an emerging technology that has applications both in the analysis and in the intensification of food processes. Ultrasounds are elastic waves with frequencies higher than the human ear detection limit (20 kHz). Power ultrasound (US) applications, work in the frequency range from 20 to 100 kHz. When US waves are transmitted in liquid media and reach a power threshold, they produce a series of effects, bubbles can grow and collapse within liquids, a phenomenon known as cavitation. Another phenomenon resulting from the bubble size variation and subsequent collapse is the development of strong micro-streaming currents, associated with high-velocity gradients and shear stresses that alter the media characteristics. In addition, US can be broken water molecules generating highly reactive free radicals that may react with and modify other molecules (Soria & Villamiel, 2010). Another effect that US produce is an agitation in the fluid that can reduce the external resistance to mass transfer by increasing the bulk transport within the fluid. Thus, US interaction in the solid–fluid interfaces can produce a microstirring (Mulet et al., 2003). Therefore, the effects produced by US may induce physical and chemical effects, which can be used in the food industry to intensify extraction processes, heating/cooling processes, microbial inactivation, drying and chemical and enzymatic reactions, among other applications.

Table 1. Influence of ultrasound (US) treatment on enzymatic reactions of non-meat and meat products.

Non-meat products			
Sample	US parameters (power, frequency, temperature, pH, time)	US effects	Reference
Milk ( $\beta$ -Galactosidase from <i>Kluyveromyces marzianus</i> )	20 W and 20 kHz, 37 °C, pH 6.7, 30 min	Increased degree of lactose hydrolysis (14 %) compared to the treatment without US	Sener <i>et al.</i> (2006)
Sugar (invertase)	22 W/L, 25 Hz, 40 °C	Increased degree of carbohydrates hydrolysis (33 %) with invertase compared to the treatment without US	de Souza Soares <i>et al.</i> (2019)
Starch (glucoamylase)	7.2 W/mL, 22 kHz, 35 °C, 40 min	Accelerated the degree of enzymatic hydrolysis, decreasing the molecular weight of starch by 80.19 % and increasing solubility by 136.5 %.	Wang <i>et al.</i> (2017)
Soy sauce (protein)	126.4 W/cm <sup>2</sup> , 50 °C, for 20 min and 240 min	Accelerated the degree of protein hydrolysis in 20 min 4.98 % and in 240 min 8.48 %.	Chen <i>et al.</i> (2017)
Pectinase from <i>Aspergillus niger</i> ,	4.5 W/mL, 22 kHz, 20 °C for 10 min	Improved the reaction rate of the enzymatic hydrolysis process of citrus peel pectin (32.59 %) to obtain galacturonic acid	Ma <i>et al.</i> (2016)
Meat products			
Sample	US parameters (power, frequency, temperature, pH, time)	US effects	Reference
Beef <i>Semimembranosus</i> muscles (lysosomal enzyme and $\beta$ -glucuronidase)	10 W/cm <sup>2</sup> , 2.6 MHz, 2 consecutive periods of 15 s allowing a rest period of 2 min	Accelerated the release of the lysosomal enzyme, and $\beta$ -glucuronidase and weakened the muscle structure	Got <i>et al.</i> (1999)
Hen breast muscle (proteases)	12 W/cm <sup>2</sup> , 24 Hz, for 15 s	Increased of degradation of muscular proteases, improve tenderisation	Xiong <i>et al.</i> (2012)

In the field of enzymatic reactions, the application of an US treatment was applied to different food products (Table 1). Şener *et al.* (2006) reported that ultrasonic treatment in  $\beta$ -Galactosidase from *Kluyveromyces marzianus* achieved a lactose hydrolysis in milk of 90 % compared to 84 % without sonication. In addition, a residual enzymatic activity of 75 % was obtained (only 25 % of the enzyme activity was lost), under optimal operating conditions (37 °C, pH 6.7, 20 W and 20 kHz), after 30 min of sonication. Also, in the field of sugar hydrolysis, the application of US (25 Hz, 22 W/L, 40 °C) enhanced the reaction rate of the carbohydrates hydrolysis with invertase by 33.0 %, compared to the treatment without US (de Souza Soares *et al.*, 2019). On the other hand, Wang *et al.* (2017) reported that the application of US together with glucoamylase accelerated the degree of starch hydrolysis, decreasing the molecular weight of starch by 80.19 % and increasing solubility by 136.5 %. The optimal conditions were 35 °C, 40 min, an ultrasonic intensity of 7.2 W/mL and a frequency of 22 kHz. Another improvement of the application of US in hydrolyse carbohydrates, was on the hydrolysis of pectin, the application of US, together with pectinase from *Aspergillus niger*, improved the reaction rate of the enzymatic hydrolysis process of citrus peel pectin to obtain galacturonic acid, increasing the rate of hydrolysis by 32.59 % over the control. The process was carried out applying an intensity of 4.5 W/mL and a frequency of 22 kHz for 10 min at 20 °C (Ma *et al.*, 2016a). In addition to intensify the activity of enzymes that hydrolyse carbohydrates, ultrasound also has been used to accelerate protein hydrolysis. In this regard, Chen *et al.* (2017) reported that, in soy sauce, US accelerated the degree of protein hydrolysis from 10.46 % and an enzymatic recovery of 57 %, without US treatment (20 min, 50 °C), to a degree of hydrolysis of 15.44 % and a recovery of 61.94 % with the US treatment (126.4 W/cm<sup>2</sup>, 20 min, 50 °C). When the treatment time was extended to 240 min, the US increased the degree of hydrolysis by 3.5 % and the recovery by 4.79 %, compared to the 20 min treatment. In these applications, the great energy release caused by the acoustic waves (Khan *et al.*, 2021) helps to improve both hydrolysis and the enzyme extraction from the inner cell (Yao *et al.*, 2020) but the high power may also cause enzyme denaturation. However, another plausible strategy by which to improve the enzymatic reaction is low or moderate power US application in order to induce a mild cavitation, or only a micro-stirring, and promote the union of the substrates with the active sites, or even product

diffusion without altering the enzyme structure. Abril *et al.* (2021) postulated that the rate of ZnPP formation catalyzed by the FeCH, using exogenous porphyrins and  $Zn^{2+}$ , was controlled by the product diffusion in the steady phase.

US has also been used to improve different meat properties, promoting safer and better quality meat products (Gallo *et al.*, 2018). Specifically, US has been used to improve the texture of raw and processed meat (Table 1), by contributing to the release of myofibrillar proteins, which play a fundamental role in the formation of gels and are responsible for the water retention capacity, the emulsifying properties and the tenderness of meat (Xiong, 2018). US cavitation is also capable of breaking down cell components, causing softening of cell membranes. The alteration of the meat tissue results into the extraction of proteins and other compounds outside the cells and the consequent acceleration of the enzymatic activity (Jayasooriya *et al.*, 2004). Got *et al.* (1999) reported that in beef Semimembranosus muscles, when US was applied (2 consecutive periods of 15 s allowing a rest period of 2 min; 2.6 MHz; 10 W/cm<sup>2</sup>) in *pre-rigor mortis*, the treatment accelerated the release of the lysosomal enzyme, and  $\beta$ -glucuronidase and weakened the muscle structure. In addition, Xiong *et al.* (2012) observed a significant tenderisation of the hen breast muscle, following the application of US (24 Hz, 12 W/cm<sup>2</sup>, 15 s) and demonstrated that the effect was linked to muscle degradation by the combination of US and proteases (calpain and cathepsin).

In addition to the improvement of meat texture due to the combined action of ultrasound and enzymes, US has also been used in meat products to accelerate freezing (Bhatta *et al.*, 2020) and thawing (Gambuteanu & Alexe, 2015) or improve heat transfer in the ham curing process, which would correct ham pastiness defects (Contreras *et al.*, 2018) or to accelerate enzymatic extraction of enzymes from meat co-products. In this regard, US improved the extraction of Ferrochelatase from pork liver (Abril *et al.*, 2021). US has been also used to intensify the penetration of enzymes in meat. In this regard, Barekat & Soltanizadeh (2018) reported that ultrasonic treatment (20 kHz; at 100 W for 20 min) on beef, *Longissimus lumborum*, immersed in a 0.1 % papain solution, improved the enzyme diffusion in the deepest layer of the meat by 62 % compared to untreated meat. Finally, US enhanced the diffusion of salt and water in pork *Longissimus dorsi*, increasing the diffusion rates as the intensity of the US raised

(Ozuna *et al.*, 2013; Ojha *et al.*, 2016).

#### **4.2. High pressure**

High pressure processing (HPP) is a technique that is based on the application of an elevated and uniform pressure (300-700 MPa) for a short time (from a few seconds to several minutes) to a food product, by means of a transmitter liquid (Sukmanov *et al.*, 2019). By using HPP, food can be processed at room or even lower temperatures. This is an important advantage, which is common to other non-thermal technologies, since it allows maintaining the sensory and nutritional properties of the treated food (Torres Bello *et al.*, 2014).

Table 2. Influence of High-pressure processing (HPP) treatment on enzymatic reactions of non-meat and meat products.

<b>Non-meat products</b>			
<b>Sample</b>	<b>HPP parameters (pressure, time, temperature)</b>	<b>HPP effects</b>	<b>Reference</b>
Goat cheese (casein)	400 MPa for 5 min	Acceleration proteolysis process by which casein, the main protein in milk. The maturation was completed in 14 d with HPP, while normal maturation took 28 d	Saldo <i>et al.</i> (2000), Saldo <i>et al.</i> (2002) Messens <i>et al.</i> (1998)
$\beta$ -lactoglobulin	200 MPa for 180 min	Complete hydrolysis of $\beta$ -lactoglobulin was carried out by the enzyme thermolysin, observing that this enzyme only partially hydrolyzed $\beta$ -lactoglobulin in cow whey concentrate at atmospheric pressure and 25 °C.	Hayashi <i>et al.</i> (1987)
Peptinase cocktail and black garlic juice	50 MPa for 240 min at 55 °C	Increased the enzymatic activity of peptinase compared to treatment without HPP. The concentration of galacturonic acid released was higher than in the untreated black garlic juice.	Kim <i>et al.</i> (2019)
<b>Meat products</b>			
<b>Sample</b>	<b>HPP parameters (pressure, time, temperature)</b>	<b>HPP effects</b>	<b>Reference</b>
Beef <i>Biceps femoris</i> muscle (metmyoglobin reductase)	130 MPa, 10 °C	Enhanced reduction of myoglobin to methemoglobin, improved red color of fresh meat	Jung <i>et al.</i> (2003)

Mostly, this high pressure causes changes in the permeability of cell membranes, as well as denaturation of proteins and inactivation of some enzymes, reasons why it has been mainly used in food preservation processes (Mañas & Pagán, 2005). However, the enhancement of enzymatic reactions in food products using this emerging technology has also been studied (Table 2). Some of the enzymatic reactions that HPP enhances are those related to enzymatic hydrolysis of proteins in dairy products. Saldo *et al.* (2000), Saldo *et al.* (2002) and Messens *et al.* (1998) reported the acceleration of the maturation of goat cheese, in particular, the proteolysis process by which casein, the main protein in milk, is hydrolyzed into free peptides and amino acids. The maturation was completed in 14 days with HPP, while typical maturation took 28 days. The optimal conditions studied were 400 MPa for 5 min. Hayashi *et al.* (1987) reported the hydrolysis of the  $\beta$ -lactoglobulin by the thermolysin enzyme, observing that this enzyme only hydrolyzed partially the  $\beta$ -lactoglobulin in cow's whey concentrate at atmospheric pressure and 25 °C. However, after the HPP treatment at 200 MPa for 180 min the  $\beta$ -lactoglobulin was completely hydrolyzed. In addition to act on whey proteins, Kim *et al.* (2019) reported that the application of a pre-treatment with HPP (50 MPa for 240 min at 55 °C) to a mixture of a peptinase cocktail and black garlic juice, before its aging process, increased the enzymatic activity of peptinase to 5 units/mL compared to 3 units/mL without HPP. Furthermore, the concentration of galacturonic acid released was higher (4.5 mM) than in the untreated black garlic juice (2 mM). The applied pretreatment allowed to improve the extractability and clarification of the black garlic juice. In addition it enhanced the functional properties (antidiabetic activity) of black garlic.

Regarding the intensification of enzymatic reactions that take place in meat by using HPP (Table 2), Jung *et al.* (2003) reported the effect of high pressure on the color of the beef *Biceps femoris* muscle. These authors showed that at moderate pressures (130 MPa) and at low temperatures (10 °C); the enzymatic reaction that takes place through metmyoglobin reductase, that causes the reduction of myoglobin to methemoglobin, could be intensified. The HPP enhanced the enzymatic reaction and consequently the redness of the pieces, improving the typical color of fresh meat.

In addition to the enhancement of enzymatic reactions, it is worth highlighting the application of HPP in other meat processes, such as the tenderness improvement. Sikes *et al.* (2010) and Ma & Ledward (2004), showed that HPP treatment (200 MPa, 20 min and 60 °C) modified the structure of the myofibrils of *Sternomandibularis* and *Longissimus dorsi* muscles of beef and caused changes in tenderness. On the contrary, Jung *et al.* (2000) demonstrated that pressures between 100-600 MPa at low temperature (10 °C) modified the structure of the myofibrils of the *Biceps femoris* muscle of beef without producing changes in tenderness. Thus, HPP effect on meat tenderness seems to be temperature dependent.

### **4.3. Electrical stimulation**

In recent years, the use of electric fields for food processing is receiving special attention (Jemai & Vorobiev, 2002). Pulsed electric fields (PEF) and moderate electric fields (MEF) constitute the two main modes of electrical stimulation applied in the food industry.

#### **4.3.1. Pulsed electric fields (PEF)**

This emerging non-thermal technology is based on the application of electrical energy through high intensity electrical pulses, of short duration ( $\mu\text{s}$  or  $\text{ms}$ ) and high voltage (0.1-40 kV/cm) (Martín & Raso, 2018). By applying a high energy electric field, reversible or irreversible permeabilization of cell membranes is observed, phenomenon known as electroporation (Martínez *et al.*, 2020).



Table 3. Influence of Pulsed Electric Fields (PEF) treatment on enzymatic reactions of non-meat and meat products.

Non-meat product			
Sample	PEF parameters (electric field strength, pulse width, number of pulses, specific energy, time)	PEF effects	Reference
Papain	50 kV/cm with 500 pulses for 2 ms	Reduced enzyme activity due to oxidation of cysteine amino acid residue located in the active site of papain	Yeom <i>et al.</i> (1999)
Carrots (Ascorbic acid oxidase)	0.2 to 1.2 kV/cm, 5 to 300 Hz, 20 $\mu$ s	Reduced enzyme activity	Leong & Oey, (2014)
Tomato (pectin methylesterase)	24 kV/cm, 400 pulses of 0.02 ms pulse-width	Reduced enzyme activity	Giner <i>et al.</i> (2000)
Apple and pear (polyphenoloxidase)	Apple extract: 24 kV/ cm, 6 ms Pear extract: 22.3 kV/cm, 6 ms	Reduced enzyme activity	Giner <i>et al.</i> (2001)
Meat products			
Sample	PEF parameters (electric field strength, pulse width, number of pulses, specific energy, time)	PEF effects	Reference
Deer meat (calpain)	0.2 kV/cm, 1.93 kJ/kg, 20 $\mu$ s and 0.5 kV/cm, 70.2 kJ/kg and 20 $\mu$ s	Increased proteolysis of calpain	Bhat <i>et al.</i> (2019)
Beef <i>Semimembranosus</i>	10 kV, 90 Hz, 20 $\mu$ s	Improved tenderness. Due to the phenomenon of electroporation, that allows Ca <sup>2+</sup> release, which activates its dependent proteases, calpains	Carne <i>et al.</i> (2015) Bekhit <i>et al.</i> (2016) Warner <i>et al.</i> (2017)

---

Beef <i>Longissimus thoracis</i>	.2-0.6 kV/cm, 1-50 Hz, 20 $\mu$ s	Did not affect the activity of proteases, and therefore meat tenderness was not improved	Faridnia <i>et al.</i> (2014)
Chicken meat	3 kV/cm, 300 pulses of 20 $\mu$ s	Did not affect the activity of proteases, and therefore meat tenderness was not improved	Arroyo <i>et al.</i> (2015)

The electroporation of animal or plant tissue membranes has numerous applications in those processes of the food industry in which mass transfer takes place through cell membranes (Van *et al.*, 2001), such as solid-liquid extraction, pressure extraction, dehydration, osmotic dehydration or the curing and marinating of meat and fish (Raso & Heinz, 2010). However, PEF can also affect the activity of enzymatic reactions (Table 3). Electrochemical reactions might occur on the surface of the electrode causing electrolysis and therefore a change in pH, which leads to enzyme inactivation or slowdown of enzymatic activity (Soliva-Fortuny *et al.*, 2009). For example, papain activity was affected by the PEF treatment, due to oxidation of cysteine amino acid residue located in the active site of papain (Yeom *et al.*, 1999). Enzyme activity was also reduced by PEF in ascorbic acid oxidase in carrots (Leong & Oey, 2014), in pectin methylesterase from tomato (Giner *et al.*, 2000) and in polyphenoloxidase from apple and pears (Giner *et al.*, 2001).

PEF been used in the meat industry to improve meat tenderness (Table 3). In deer meat, a great proteolysis of calpain was observed in two different treatments (0.2 kV/cm, 1.93 kJ/kg, 20  $\mu$ s and 0.5 kV/cm, 70.2 kJ/kg and 20  $\mu$ s) (Bhat *et al.*, 2019). The application of high electric field strength PEF treatments (10 kV, 90 Hz, 20  $\mu$ s) in beef *Semimembranosus* improved tenderness after a 3-day post-mortem maturation period (Carne *et al.*, 2015). This is due to the phenomenon of electroporation, that allows  $Ca^{2+}$  release, which activates its dependent proteases, calpains (Bekhit *et al.*, 2016; Warner *et al.*, 2017). However, the application of PEF at lower electric field intensity (0.2-0.6 kV/cm, 1-50 Hz, 20  $\mu$ s) in *Longissimus thoracis* muscle of beef caused changes in the microstructure of the meat, but these changes did not affect the activity of proteases, and therefore meat tenderness was not improved after 1-3 d post-mortem (Faridnia *et al.*, 2014). On the other hand, Arroyo *et al.* (2015) showed that the application of PEF (3 kV/cm, 300 pulses of 20  $\mu$ s) did not improve the tenderness of chicken meat post-mortem (1 day). Thus, the application of PEF for improving the meat tenderness depends both on the electric field strength and on the state of the post-mortem maturation period.

In addition to enhance the enzymatic reactions to improve the texture of the meat, PEF treatments have been used to reduce the thermal stability of intramuscular

collagen, due to the physical alteration of the muscle fibers, and thus to improve the tenderness of the meat (Judge *et al.*, 1980). On the other hand, treatments of PEF (1.4 kV/cm, 90 Hz, 20  $\mu$ s) before freezing-thawing improved the volatile profile and sensory properties of cooked lamb meat (Ma *et al.*, 2016b). Kantono *et al.* (2021) showed that PEF application to frozen-thawed lamb meat after 7 days refrigerated storage produced an increase in the amino acid content and a reduction in the fatty acid content of these cuts of lamb.

#### 4.3.2. *Moderate electric fields (MEF)*

Moderate electric fields (MEF) are based on the application of electrical energy in a range of 1 to 1000 V/cm, using an alternating current with arbitrary frequencies (50-25000 Hz) and waveforms (Pereira *et al.*, 2019). Unlike the application of PEF, it can have ohmic heating effects, that is, a thermal process where the passage of a moderate electric current through the food causes heating (Gutiérrez, 2018). Through the application of MEF, although with a lower intensity than for PEF, cell electroporation can also take place (Moreno *et al.*, 2016).

Table 4. Influence of Moderate Electric Fields (MEF) treatment on enzymatic reactions of non-meat and meat products.

Non-meat products			
Sample	MEF parameters (electric field strength, frequency, temperature, time)	MEF effects	Reference
Corn starch (glucoamylase)	0-10 V/cm, 50 Hz, 30 min	Hydrolysis of corn starch, activating glucoamylase	Li <i>et al.</i> (2022).
Tomato homogenate (pectin methyl esterase (PME))	8 V/cm, 60 Hz sinusoidal wave, reaching 80 °C starting at 65 °C	Activated pectin methyl esterase (PME)	Samaranayake <i>et al.</i> (2016)
Sugarcane juice (peroxidase and polyphenol oxidase)	3.57 V/cm, 98 °C for 12 min	Inactivated enzymes peroxidase and polyphenol oxidase	Brochier <i>et al.</i> (2016)
Pea puree (peroxidase)	50 V/cm, 100 °C for 54 s	Inactivated enzyme peroxidase	Icier <i>et al.</i> (2006)
Meat products			
Sample	MEF parameters (electric field strength, frequency, temperature, time)	MEF effects	Reference
Bovine (glycolysis)	10-600 V, 50 Hz, 2-100 pulses/s, 5- 120 s	Accelerated <i>post-mortem</i> glycolysis, improving tenderization	Chrystall <i>et al.</i> (1978)
Beef (proteases)	550 V, 60 Hz, 1 s pulse and 0.5 s rest, during 120 s	Electroporation of the muscle cell membrane, affecting the release of Ca <sup>2+</sup> and the activation of calpain	Ducastaing <i>et al.</i> (1985)

The ohmic heating and the electroporation of cell membranes have allowed the use of MEF for intensifying extraction (Pereira *et al.*, 2016). In addition, it has also been reported that low intensity MEF increases enzymatic activity by improving molecular mobility associated with temperature (ohmic heating), thus improving mass transfer within the system (Durham & Sastry, 2020). In this sense, the application of MEF in non-meat products improved enzymatic reactions (Table 4). In the hydrolysis of corn starch (0-10 V/cm, 50 Hz, 30 min, temperature was not controlled), MEF caused an increase in hydrolysis, activating glucoamylase (Li *et al.*, 2022). Besides, it was observed that the application of MEF (5.8 V/cm, 60 Hz sinusoidal wave, reaching 80 °C starting at 65 °C) in tomato homogenate activated pectin methyl esterase (PME) (Samaranayake *et al.*, 2016). However, the application of MEF can lead to high temperatures reached might cause enzymatic inactivation due to conformational changes in the enzyme structure (Castro *et al.*, 2004). In the case of sugarcane juice treated with MEF (98 °C, 3.57 V/cm, for 12 min), peroxidase and polyphenol oxidase were completely inactivated (Brochier *et al.*, 2016), while in pea puree, the application of MEF (50 V/cm, for 54 s up to 100 °C) caused the peroxidase enzyme inactivation (Icier *et al.*, 2006).

In the meat industry, MEF has also been used to intensify the tenderization of meat (Table 4). It has been reported that the electroporation caused by MEF, can accelerate the post-mortem glycolysis process, in which the production of lactic acid takes place, ensuring that the pH of the meat drops below 6.0, before the muscle temperature reaches 10 °C (Álvarez *et al.*, 2022). In bovine *Sternomandibularis*, tenderness improvement and carcass hardening prevention by accelerated post-mortem glycolysis was demonstrated after the application of moderate electrical stimulation (10-600 V, 50 Hz, 2-100 pulses/s (pulse shapes: sinusoidal or square wave, polarities: alternating or unidirectional and stimulating periods of 5-120 s) and a subsequent aging period (Chrystall *et al.*, 1978). Moreover, it has been shown how the application of MEF caused the electroporation of the muscle cell membrane, affecting the release of Ca<sup>2+</sup> and the activation of calpain proteases in the post-mortem maturation period. In beef, this phenomenon was observed by applying 550 V, 60 Hz, 1 s pulse and 0.5 s rest, during 120 s (Ducastaing *et al.*, 1985).

In addition to enhance the enzymatic reactions to improve the meat texture, MEF has also been applied to improve the diffusion of sodium chloride in porcine muscle (Rinella, 2014), to improve the quality of the pork carcass during cold storage in modified atmosphere packaging (Hu *et al.*, 2020), and for cooking meat and meat products using ohmic heating (Icier *et al.*, 2014).

#### **4.4. Supercritical fluids**

The method is based on the use of a fluid, normally carbon dioxide, at temperatures and pressures above its critical point ( $P_c = 73.8$  bar and  $T_c = 31.1$  °C, for  $CO_2$ ). The most extended application of supercritical fluids in the food industry is the extraction of target compounds from vegetal or animal matrices.

Table 5. Influence of Supercritical carbon dioxide (SC-CO<sub>2</sub>) treatment on enzymatic reactions of non-meat products.

Non-meat products			
Sample	SC-CO <sub>2</sub> parameters (pressure, temperature, time, flow)	SC-CO <sub>2</sub> effects	Reference
Immobilized cellulase in a system consisting of enzyme aggregates cross-linked (CLEA) with solvents and glutaraldehyde.	10 MPa, 50 °C, 3 h	Increased the enzyme activity by 57 % compared to the enzyme not treated with CO <sub>2</sub>	Hojnik Podrepšek <i>et al.</i> (2019)
α-amylase	240 bar, 41 °C, 50 min, 4 g/min CO <sub>2</sub> flow	Increased the enzyme activity (67.7 %) compared to the enzyme not treated with CO <sub>2</sub>	Senyay-Oncel & Yesil-Celiktas (2011)



Applications involving supercritical fluids and enzymes in food-related processes include the improvement of the enzymatic activity of free enzymes in supercritical media (Table 5). In this regard, Song *et al.* (1993) investigated the enzymatic hydrolysis reaction with supercritical carbon dioxide (SC-CO<sub>2</sub>) as a reaction medium to produce glucose from starch. The rate of enzymatic reaction improved with the application of SC-CO<sub>2</sub>, being the optimal process conditions close to the critical point of SC-CO<sub>2</sub> (31 °C, 73.8 bar). Also, Hojnik Podrepšek *et al.* (2019), experimented with immobilized cellulase in a system consisting of enzyme aggregates cross-linked (CLEA) with solvents and glutaraldehyde. These authors determined the effects of SC-CO<sub>2</sub> on the free and immobilized enzyme and a control treatment without using SC-CO<sub>2</sub>, at different combinations of pressure (atmospheric, 10 and 20 MPa), temperature (40 and 50 °C) and different reaction times (1, 3, 4 and 24 h). The maximum enzymatic activity was reached with the immobilized enzyme, at 50 °C and 10 MPa, which increased the enzyme activity by 57 % after 3 h treatment, compared to a treatment without SC-CO<sub>2</sub>. All reactions in SC-CO<sub>2</sub> (with free and immobilized enzyme) showed higher enzymatic activity than those carried out in a non-supercritical medium. The better performance in the supercritical medium could be attributed to an increase in enzyme activity and stability due to changes in the conformational structure of the enzyme. On the other hand, Senyay-Oncel & Yesil-Celiktas (2011) evaluated the effect of supercritical SC-CO<sub>2</sub> as a pre-treatment on the enzymatic activity of α-amylase. The optimal process conditions were 240 bar, 41 °C, 4 g/min CO<sub>2</sub> flow and 150 min of treatment time, providing 67.7 % higher enzyme activity (29.728 μmol/mL x min) than in the enzyme not treated with CO<sub>2</sub> (17.726 μmol/mL x min). Thus, the use of SC-CO<sub>2</sub> as a pre-treatment also improves the enzymatic activity.

To our knowledge, there is no literature regarding enzymatic reactions enhanced by supercritical fluids in the meat industry. However, supercritical fluids have been applied for lipid extraction in pork and lamb meat (King *et al.*, 1989; Taher *et al.*, 2011). Also, for the extraction of traces of antibiotics in meat (Din *et al.*, 1997). SC-CO<sub>2</sub> can also be used combined with US and saline solution for microbial inactivation of *Escherichia coli* in dry-cured ham, with no significant changes in color, texture and pH (Castillo-Zamudio *et al.*, 2021). Also, Morbiato *et al.* (2019) combined US and SC-CO<sub>2</sub> technologies to dry chicken breast while preserving nutritional quality and inactivating

mesophilic bacteria, moulds, yeasts and *Salmonella spp.*

## **5. Conclusions and future trends in the intensification of enzymatic reactions in meat processing**

Emerging technologies enhance enzymatic reactions through different mechanisms. Specifically, the cycles of compression and expansion and the consequent cavitation caused by ultrasound, accelerate mass transfer and causes the rupture of cell walls, therefore improving the binding of the enzyme with the substrate and consequently enhancing the rate of enzymatic reaction. In addition, the micro-agitation caused by moderate intensity ultrasound (US) (without reaching cavitation that could result into enzyme inactivation), leads to an improvement in the diffusion of the products resulting from the enzymatic reaction, as well as to the diffusion and improved interaction between the enzyme and the substrate. However, the effect of US on enzyme activity depends on the power applied, so small variations in power may cause changes in activity and concentration enzymatic. As for high pressure (HPP), by applying a high static pressure (100-1000 MPa), the covalent bonds are broken, which causes a change in the internal structure of the matrix that can enhance the binding of the enzyme with the substrate. Regarding the application of electrical stimulation, electroporation may cause the rupture of cell membranes, which leads to a release of enzymes and substrates that facilitates their subsequent bond. Finally, supercritical fluids, particularly supercritical CO<sub>2</sub> (SC-CO<sub>2</sub>), increase the enzyme activity and stability due to changes in the conformational structure of the enzyme.

Emerging technologies can be used to shorten and intensify the enzymatic reactions that take place during meat processing. After the slaughter of the animal until *rigor mortis*, the first enzymatic reaction that occurs is glycolysis, a stage in which the energy reserves are depleted and the pH drops. To date, it has been shown that the application of MEF accelerates the process of formation of lactic acid from glycogen. In addition, moderate intensity US could be applied in order to reduce the activation energy of the enzymes involved in the glycolysis reactions and thus to promote the bond between the enzyme and the substrates, accelerating the rate of reaction and diffusion of lactic acid with the consequent drop the of the muscle pH. However, other emerging technologies could not be applied because they would have a negative effect.

For example, the application of SC-CO<sub>2</sub> would not be convenient since the temperature is a limiting factor in the *pre-rigor mortis* stage and SC-CO<sub>2</sub> treatments are applied above CO<sub>2</sub> critical point (31.1 °C).

Before reaching the *post-rigor mortis* stage the bond of actin and myosin takes place forming actomyosin which is responsible for the hardness and muscle tension that characterizes *rigor mortis*. So far, emerging technologies have not been used to accelerate this process. However, as for glycolysis, moderate intensity US could be applied with the same objective of decreasing the activation energy of enzymes and thus promoting the binding between the enzyme and proteins (actin and myosin).

In the *post-rigor mortis* stage, the proteolytic enzymatic reactions of endopeptidases (calpains and cathepsins) begin, improving meat tenderness, enzymatic reactions that extend during the curing of meat products. In this type of enzymatic reactions, US, HPP, as well as electrical stimulation by pulsed electric fields (PEF) and moderate electric fields (MEF) have been applied. Regarding US, its application causes the alteration of cell membranes, leading to the release of more myofibrillary proteins outside the cell membrane and its consequent enzymatic acceleration by calpain and cathepsin. HPP have also been used to modify the structure of muscle myofibrils to enhance contact with enzymes. Finally, the application of PEF and MEF, through the electroporation of the cell membranes, allows to release Ca<sup>2+</sup> and activate the calpain Ca<sup>2+</sup>-dependent enzymes. The SC-CO<sub>2</sub> has not been applied so far, however, its application could improve the proteolysis of endopeptidases by causing changes in the cell membrane structure enhancing the release of proteins into the medium.

Regarding the color of raw meat, HPP has been applied to intensify the enzymatic reaction of metmyoglobin reductase, which catalyzes the reduction of myoglobin to methemoglobin and enhances the redness of the meat. Another technology that could intensify the enzymatic reaction of metmyoglobin reductase would be US at moderate intensities, since it would limit the temperature increase and the micro-agitation generated by US could decrease the activation energy, intensifying the binding of metmyoglobin reductase with myoglobin.

In the curing and aging process of the meat, other proteolysis reactions catalyzed by exopeptidases (dipeptidases, aminopeptidases and carboxypeptidases) take place, giving rise to a large number of peptides and free amino acids, which contribute to the flavor, aroma, texture and final quality of the cured meat products. So far, emerging technologies have not been used to enhance exopeptidase reactions in meat. However, high power US could catalyze mass transfer and therefore accelerate enzymatic activity to carry out a high proteolytic degradation of peptides, which would contribute to enhancing the organoleptic characteristics of raw-cured products. Also, the electrical stimulation of PEF and MEF, through the electroporation of cell membranes, would facilitate the extraction of proteins to the medium and intensify the enzymatic activity of exopeptidases in the hydrolysis of peptides. In addition, the application of a SC-CO<sub>2</sub> medium could improve the performance and activity of enzymes since it could cause changes in the conformational structure of the enzyme, favoring the enzymatic reactions.

At the end of the curing process, lipolysis reactions take place from lipase enzymes and phospholipases, which cause the hydrolysis of fats to result in the release of compounds such as fatty acids and low molecular weight substances responsible for the taste and smell of the final product. As in the reactions of exopeptidases, emerging technologies could be applied following the aforementioned mechanisms.

Regarding the color in raw-cured products, it has been shown that in Parma ham the formation of Zinc Protoporphyrin (ZnPP) takes place from the reaction catalyzed by the enzyme Ferrochelatase (FeCH). Enzymatic reaction that takes place naturally over time. However, the application of HPP and moderate intensity US, could accelerate the enzymatic reaction following similar mechanisms as in the case of raw meat. In addition, US has been used to enhance the extraction of the enzyme FeCH from pork liver and to intensify the formation of ZnPP. This technology could also be used to accelerate the formation of ZnPP in raw-cured meat products.

In sausages, fermentation is carried out by endogenous microorganisms and microorganisms added as starter cultures (lactic acid bacteria, *Staphylococcus*, molds and yeasts). In this case, the application of SC-CO<sub>2</sub> could facilitate the mass transfer intensifying the enzymatic reactions related to the starter cultures.

Emerging technologies have not been applied yet in conjunction with transglutaminase for the manufacturing of restructured meat products. In this regard, moderate intensity US could enhance the binding between the enzyme and the substrate to develop new meat products. In addition, carrying out the enzymatic reaction in SC-CO<sub>2</sub> medium could cause an intensification of the process, since temperature is not a limiting factor.

Finally, there is no literature that applies emerging technologies to intensify the enzymatic generation of peptides with beneficial properties for health. Thus, the use of US could promote the breakdown of protein bonds and intensify the formation of peptides. Electrical stimulation (PEF and MEF) could cause electroporation of cell membranes, enhancing the exit of proteins to the medium and accelerating the enzymatic reaction with both exogenous and endogenous enzymes. However, the application of HPP could not be a favorable technology in the formation of bioactive peptides because high pressures could contribute to the denaturation of the formed peptides.

Most attributes defining meat and meat products' quality, such as taste, texture or appearance, are closely related to the meat's enzymatic reactions. Therefore, the use of emerging technologies, under controlled conditions, could allow an acceleration of the enzymatic processes and therefore an increase in production and quality of the meat products.

## **Acknowledgements**

The authors acknowledge the financial support from the "Ministerio de Economía y Competitividad (MINECO)" and "Instituto Nacional de Investigación y Tecnología Agraria y Alimentaria (INIA)" in Spain (Projects RTA2017-00024-C04-03 and RTA2017-00024-C04-02).

## References

- Abril, B., Sánchez-Torres, E. A., Bou, R., García-Pérez, J. V., & Benedito, J. (2021). Ultrasound intensification of FerrochelataSe extraction from pork liver as a strategy to improve ZINC-protoporphyrin formation. *Ultrasonics Sonochemistry*, *78*, 105703. <https://doi.org/10.1016/j.ultsonch.2021.105703>
- Adamsen, C. E., Møller, J. K., Parolari, G., Gabba, L., & Skibsted, L. H. (2006). Changes in Zn-porphyrin and proteinous pigments in italian dry-cured ham during processing and maturation. *Meat science*, *74*(2), 373-379. <https://doi.org/10.1016/j.meatsci.2006.04.003>
- Ahmed, A. M., Kawahara, S., Ohta, K., Nakade, K., Soeda, T., & Muguruma, M. (2007). Differentiation in improvements of gel strength in chicken and beef sausages induced by transglutaminase. *Meat Science*, *76*(3), 455-462. <https://doi.org/10.1016/j.meatsci.2007.01.002>
- Álvarez, C., Koolman, L., Whelan, M., & Moloney, A. (2022). Effect of Pre-Slaughter Practises and Early Post-Mortem Interventions on Sheep Meat Tenderness and Its Impact on Microbial Status. *Foods*, *11*(2), 181. <https://doi.org/10.3390/foods11020181>
- Andrade, M. J., Córdoba, J. J., Sánchez, B., Casado, E. M., & Rodríguez, M. (2009). Evaluation and selection of yeasts isolated from dry-cured Iberian ham by their volatile compound production. *Food Chemistry*, *113*(2), 457-463. <https://doi.org/10.1016/j.foodchem.2008.07.080>
- Anzani, C., Boukid, F., Drummond, L., Mullen, A. M., & Álvarez, C. (2020). Optimising the use of proteins from rich meat co-products and non-meat alternatives: Nutritional, technological and allergenicity challenges. *Food Research International*, 109575. <https://doi.org/10.1016/j.foodres.2020.109575>
- Arihara, K., Yokoyama, I., & Ohata, M. (2021). Bioactivities generated from meat proteins by enzymatic hydrolysis and the Maillard reaction. *Meat Science*, *180*, 108561. <https://doi.org/10.1016/j.meatsci.2021.108561>

- Aristoy, M. C., & Toldrá, F. (1995). Isolation of flavor peptides from raw pork meat and dry-cured ham. *In Developments in Food Science* (Vol. 37, pp. 1323-1344). Elsevier. [https://doi.org/10.1016/S0167-4501\(06\)80236-0](https://doi.org/10.1016/S0167-4501(06)80236-0)
- Aristoy, M. C., & Toldrá, F. (2009). Nucleotides and its derived compounds. *Handbook of muscle foods analysis*, 279-288.
- Arnau, J., Guerrero, L., & Sárraga, C. (1998). The effect of green ham pH and NaCl concentration on cathepsin activities and the sensory characteristics of dry-cured hams. *Journal of the Science of Food and Agriculture*, 77(3), 387-392. [https://doi.org/10.1002/\(SICI\)1097-0010\(199807\)77:3<387::AID-JSFA57>3.0.CO;2-H](https://doi.org/10.1002/(SICI)1097-0010(199807)77:3<387::AID-JSFA57>3.0.CO;2-H)
- Arroyo, C., Eslami, S., Brunton, N. P., Arimi, J. M., Noci, F., & Lyng, J. G. (2015). An assessment of the impact of pulsed electric fields processing factors on oxidation, color, texture, and sensory attributes of turkey breast meat. *Poultry Science*, 94(5), 1088-1095. <https://doi.org/10.3382/ps/pev097>
- Ashie, I. N. A., Sorensen, T. L., & Nielsen, P. M. (2002). Effects of papain and a microbial enzyme on meat proteins and beef tenderness. *Journal of food science*, 67(6), 2138-2142. <https://doi.org/10.1111/j.1365-2621.2002.tb09516.x>
- Askin, O. O., & Kilic, B. (2009). Effect of microbial transglutaminase, sodium caseinate and non-fat dry milk on quality of salt-free, low fat turkey döner kebab. *LWT-Food Science and Technology*, 42(10), 1590-1596. <https://doi.org/10.1016/j.lwt.2009.06.005>
- Barekat, S., & Soltanizadeh, N. (2018). Effects of ultrasound on microstructure and enzyme penetration in beef longissimus lumborum muscle. *Food and bioprocess technology*, 11(3), 680-693. <https://doi.org/10.1007/s11947-017-2043-8>

- Baugreet, S., Kerry, J. P., Brodkorb, A., Gomez, C., Auty, M., Allen, P., & Hamill, R. M. (2018). Optimisation of plant protein and transglutaminase content in novel beef restructured steaks for older adults by central composite design. *Meat science*, *142*, 65-77. <https://doi.org/10.1016/j.meatsci.2018.03.024>
- Bekhit, A. E. D. A., Carne, A., van de Ven, R., & Hopkins, D. L. (2016). Effect of repeated pulsed electric field treatment on the quality of hot-boned beef loins and topsides. *Meat Science*, *111*, 139-146. <https://doi.org/10.1016/j.meatsci.2015.09.001>
- Bekhit, A. A., Hopkins, D. L., Geesink, G., Bekhit, A. A., & Franks, P. (2014). Exogenous proteases for meat tenderization. *Critical reviews in food science and nutrition*, *54*(8), 1012-1031. <https://doi.org/10.1080/10408398.2011.623247>
- Bhat, Z. F., Morton, J. D., Mason, S. L., Mungure, T. E., Jayawardena, S. R., & Bekhit, A. E. D. A. (2019). Effect of pulsed electric field on calpain activity and proteolysis of venison. *Innovative Food Science & Emerging Technologies*, *52*, 131-135. <https://doi.org/10.1016/j.ifset.2018.11.006>
- Bhatta, S., Stevanovic Janezic, T., & Ratti, C. (2020). Freeze-drying of plant-based foods. *Foods*, *9*(1), 87. <https://doi.org/10.3390/foods9010087>
- Braden, K. W. (2013). Converting muscle to meat: the physiology of rigor. *The science of meat quality*, 79-97. <https://doi.org/10.1002/9781118530726.ch5>
- Brochier, B., Mercali, G. D., & Marczak, L. D. F. (2016). Influence of moderate electric field on inactivation kinetics of peroxidase and polyphenol oxidase and on phenolic compounds of sugarcane juice treated by ohmic heating. *LWT*, *74*, 396-403. <https://doi.org/10.1016/j.lwt.2016.08.001>
- Caballero, B., Sierra, V., Olivan, M., Vega-Naredo, I., Tomás-Zapico, C., Alvarez-García, Ó., ... & Coto-Montes, A. (2007). Activity of cathepsins during beef aging related to mutations in the myostatin gene. *Journal of the Science of Food and Agriculture*, *87*(2), 192-199. <https://doi.org/10.1002/jsfa.2683>



- Carne, A., van de Ven, R., Bekhit, A. E. D. A., & Hopkins, D. L. (2015). Effect of pulsed electric field on the proteolysis of cold boned beef *M. Longissimus lumborum* and *M. Semimembranosus*. *Meat science*, *100*, 222-226. <https://doi.org/10.1016/j.meatsci.2014.10.011>
- Castillo-Zamudio, R. I., Paniagua-Martínez, I., Ortuño-Cases, C., García-Alvarado, M. A., Larrea, V., & Benedito, J. (2021). Use of high-power ultrasound combined with supercritical fluids for microbial inactivation in dry-cured ham. *Innovative Food Science & Emerging Technologies*, *67*, 102557. <https://doi.org/10.1016/j.ifset.2020.102557>
- Castro, I., Macedo, B., Teixeira, J. A., & Vicente, A. A. (2004). The effect of electric field on important food-processing enzymes: Comparison of inactivation kinetics under conventional and ohmic heating. *Journal of Food Science*, *69*(9), C696-C701. <https://doi.org/10.1111/j.1365-2621.2004.tb09918.x>
- Chauhan, S. S., & England, E. M. (2018). Postmortem glycolysis and glycogenolysis: Insights from species comparisons. *Meat science*, *144*, 118-126. <https://doi.org/10.1016/j.meatsci.2018.06.021>
- Chemat, F., Rombaut, N., Meullemiestre, A., Turk, M., Perino, S., Fabiano-Tixier, A. S., & Abert-Vian, M. (2017). Review of green food processing techniques. Preservation, transformation, and extraction. *Innovative Food Science & Emerging Technologies*, *41*, 357-377. <https://doi.org/10.1016/j.ifset.2017.04.016>
- Chen, X., Luo, Y., Qi, B., Luo, J., & Wan, Y. (2017). Improving the hydrolysis efficiency of soy sauce residue using ultrasonic probe-assisted enzymolysis technology. *Ultrasonics Sonochemistry*, *35*, 351-358. <https://doi.org/10.1016/j.ultsonch.2016.10.013>

- Christensen, M., Tørngren, M. A., Gunvig, A., Rozlosnik, N., Lametsch, R., Karlsson, A. H., & Ertbjerg, P. (2009). Injection of marinade with actinidin increases tenderness of porcine M. Biceps femoris and affects myofibrils and connective tissue. *Journal of the Science of Food and Agriculture*, *89*(9), 1607-1614. <https://doi.org/10.1002/jsfa.3633>
- Chrystall, B. B., & Devine, C. E. (1978). Electrical stimulation, muscle tension and glycolysis in bovine sternomandibularis. *Meat science*, *2*(1), 49-58. [https://doi.org/10.1016/0309-1740\(78\)90021-9](https://doi.org/10.1016/0309-1740(78)90021-9)
- Colmenero, F. J., Ayo, M. J., & Carballo, J. (2005). Physicochemical properties of low sodium frankfurter with added walnut: effect of transglutaminase combined with caseinate, KCl and dietary fibre as salt replacers. *Meat Science*, *69*(4), 781-788. <https://doi.org/10.1016/j.meatsci.2004.11.011>
- Contreras, M., Benedito, J., Bon, J., & García-Pérez, J. V. (2018). Intensification of heat transfer during mild thermal treatment of dry-cured ham by using airborne ultrasound. *Ultrasonics Sonochemistry*, *41*, 206-212. <https://doi.org/10.1016/j.ultsonch.2017.09.019>
- Cordoba, J. J., Antequera, T., García, C., Ventanas, J., Lopez Bote, C., & Asensio, M. A. (1994). Evolution of free amino acids and amines during ripening of Iberian cured ham. *Journal of Agricultural and Food Chemistry*, *42*(10), 2296-2301.
- Dadgar, S. (2010). Effect of cold stress during transportation on post-mortem metabolism and chicken meat quality (Doctoral dissertation).
- de Souza Soares, A., Augusto, P. E. D., Júnior, B. R. D. C. L., Nogueira, C. A., Vieira, É. N. R., de Barros, F. A. R., ... & Ramos, A. M. (2019). Ultrasound assisted enzymatic hydrolysis of sucrose catalyzed by invertase: Investigation on substrate, enzyme and kinetics parameters. *LWT*, *107*, 164-170. <https://doi.org/10.1016/j.lwt.2019.02.083>
- Demeyer, D., Hoozee, J., & Mesdom, H. (1974). Specificity of lipolysis during dry sausage ripening. *Journal of Food Science*, *39*(2), 293-296. <https://doi.org/10.1111/j.1365-2621.1974.tb02878.x>

- Din, N., Bartle, K. D., Clifford, A. A., McCormack, A., & Castle, L. (1997). Supercritical fluid extraction of sulphamethazine and its metabolites from meat tissues. *Journal of chromatographic science*, 35(1), 31-37. <https://doi.org/10.1093/chromsci/35.1.31>
- Dransfield, E., & Etherington, D. (1981). *Enzymes and food precessing*. Birch, GG..
- Ducastaing, A., Valin, C., Schollmeyer, J., & Cross, R. (1985). Effects of electrical stimulation on post-mortem changes in the activities of two Ca dependent neutral proteinases and their inhibitor in beef muscle. *Meat Science*, 15(4), 193-202. [https://doi.org/10.1016/0309-1740\(85\)90075-0](https://doi.org/10.1016/0309-1740(85)90075-0)
- Durham, E. K., & Sastry, S. K. (2020). Moderate Electric Field Treatment Enhances Enzymatic Hydrolysis of Cellulose at Below-Optimal Temperatures. *Enzyme and Microbial Technology*, 142, 109678. <https://doi.org/10.1016/j.enzmictec.2020.109678>
- Faridnia, F., Bekhit, A. E. D. A., Niven, B., & Oey, I. (2014). Impact of pulsed electric fields and post-mortem vacuum ageing on beef longissimus thoracis muscles. *International Journal of Food Science & Technology*, 49(11), 2339-2347. <https://doi.org/10.1111/ijfs.12532>
- Flores, M., & Toldra, F. (2011). Microbial enzymatic activities for improved fermented meats. *Trends in Food Science & Technology*, 22(2-3), 81-90. <https://doi.org/10.1016/j.tifs.2010.09.007>
- Flores, J. (1997). Mediterranean vs northern European meat products. Processing technologies and main differences. *Food Chemistry*, 59(4), 505-510. [https://doi.org/10.1016/S0308-8146\(97\)00011-3](https://doi.org/10.1016/S0308-8146(97)00011-3)
- Fulladosa, E., Serra, X., Gou, P., & Arnau, J. (2009). Effects of potassium lactate and high pressure on transglutaminase restructured dry-cured hams with reduced salt content. *Meat Science*, 82(2), 213-218. <https://doi.org/10.1016/j.meatsci.2009.01.013>

- Gambuteanu, C., & Alexe, P. (2015). Comparison of thawing assisted by low-intensity ultrasound on technological properties of pork Longissimus dorsi muscle. *Journal of food science and technology*, 52(4), 2130-2138. <https://doi.org/10.1007/s13197-013-1204-7>
- Gallo, M., Ferrara, L., & Naviglio, D. (2018). Application of ultrasound in food science and technology: A perspective. *Foods*, 7(10), 164. <https://doi.org/10.3390/foods7100164>
- García-Rey, R. M., Garcia-Garrido, J. A., Quiles-Zafra, R., Tapiador, J., & De Castro, M. L. (2004). Relationship between pH before salting and dry-cured ham quality. *Meat Science*, 67(4), 625-632. <https://doi.org/10.1016/j.meatsci.2003.12.013>
- Giddings, G. G., & Solberg, M. (1977). The basis of color in muscle foods. *Critical Reviews in Food Science & Nutrition*, 9(1), 81-114. <https://doi.org/10.1080/10408397709527231>
- Giner, J., Gimeno, V., Espachs, A., Elez, P., Barbosa-Cánovas, G. V., & Martín, O. (2000). Inhibition of tomato (*Lycopersicon esculentum* Mill.) pectin methylesterase by pulsed electric fields. *Innovative Food Science & Emerging Technologies*, 1(1), 57-67. [https://doi.org/10.1016/S1466-8564\(00\)00003-5](https://doi.org/10.1016/S1466-8564(00)00003-5)
- Giner, J., Gimeno, V., Barbosa-Cánovas, G. V., & Martín, O. (2001). Effects of pulsed electric field processing on apple and pear polyphenoloxidases. *Food Science and Technology International*, 7(4), 339-345. <https://doi.org/10.1106/MJ46-8J9U-1H11-T0ML>
- Got, F., Culioli, J., Berge, P., Vignon, X., Astruc, T., Quideau, J. M., & Lethiecq, M. (1999). Effects of high-intensity high-frequency ultrasound on ageing rate, ultrastructure and some physico-chemical properties of beef. *Meat Science*, 51(1), 35-42. [https://doi.org/10.1016/S0309-1740\(98\)00094-1](https://doi.org/10.1016/S0309-1740(98)00094-1)
- Gutiérrez, F. F. V. (2018). Calentador óhmico para extracción de aceites esenciales de plantas aromáticas. *Scientia Et Technica*, 23(2), 160-167.

- Hayashi, R., Kawamura, Y., & Kunugi, S. (1987). Introduction of high pressure to food processing: preferential proteolysis of  $\beta$ -lactoglobulin in milk whey. *Journal of food science*, 52(4), 1107-1108. <https://doi.org/10.1111/j.1365-2621.1987.tb14289.x>
- Hojnik Podrepšek, G., Knez, Ž., & Leitgeb, M. (2019). Activation of cellulase cross-linked enzyme aggregates (CLEAs) in SCCO<sub>2</sub>. *Journal of Supercritical Fluids*, 154. <https://doi.org/10.1016/j.supflu.2019.104629>
- Hu, H., Zhang, L., Lu, L., Huang, F., Chen, W., Zhang, C., ... & Goto, K. (2020). Effects of the combination of moderate electric field and high-oxygen modified atmosphere packaging on pork meat quality during chill storage. *Journal of Food Processing and Preservation*, 44(1), e14299. <https://doi.org/10.1111/jfpp.14299>
- Icier, F., Sengun, I. Y., Turp, G. Y., & Arserim, E. H. (2014). Effects of process variables on some quality properties of meatballs semi-cooked in a continuous type ohmic cooking system. *Meat science*, 96(3), 1345-1354.. <https://doi.org/10.1016/j.meatsci.2013.11.013>
- Icier, F., Yildiz, H., & Baysal, T. (2006). Peroxidase inactivation and colour changes during ohmic blanching of pea puree. *Journal of Food Engineering*, 74(3), 424-429. <https://doi.org/10.1016/j.jfoodeng.2005.03.032>
- Istrati, D. (2008). The influence of enzymatic tenderization with papain on functional properties of adult beef. *Journal of Agroalimentary Processes and Technologies*, 14(1), 140-146.
- Ionescu, A., Aprodu, I., & Pascaru, G. (2008). Effect of papain and bromelin on muscle and collagen proteins in beef meat. *The Annals of the University Dunarea de Jos of Galati. Fascicle VI-Food Technology*, 32, 9-16.
- Jakubczyk, A., Karaś, M., Rybczyńska-Tkaczyk, K., Zielińska, E., & Zieliński, D. (2020). Current trends of bioactive peptides—New sources and therapeutic effect. *Foods*, 9(7), 846. <https://doi.org/10.3390/foods9070846>

- Jayasooriya, S. D., Bhandari, B. R., Torley, P., & D'arcy, B. R. (2004). Effect of high power ultrasound waves on properties of meat: a review. *International Journal of Food Properties*, 7(2), 301-319. <https://doi.org/10.1081/JFP-120030039>
- Jemai, A. B., & Vorobiev, E. (2002). Effect of moderate electric field pulses on the diffusion coefficient of soluble substances from apple slices. *International journal of food science & technology*, 37(1), 73-86. <https://doi.org/10.1046/j.1365-2621.2002.00516.x>
- Judge, M. D., Reeves, E. S., & Aberle, E. D. (1980). Effect of electrical stimulation on thermal shrinkage of bovine muscle collagen. In Proc. 26th European Meeting of Meat Research Workers, Colorado Springs J (Vol. 3, p. 74). <https://doi.org/10.2527/jas1981.523530x>
- Jung, S., de Lamballerie-Anton, M., & Ghoul, M. (2000). Modifications of ultrastructure and myofibrillar proteins of post-rigor beef treated by high pressure. *LWT-Food Science and Technology*, 33(4), 313-319. <https://doi.org/10.1006/fstl.2000.0654>
- Jung, S., Ghoul, M., & de Lamballerie-Anton, M. (2003). Influence of high pressure on the color and microbial quality of beef meat. *LWT-food science and technology*, 36(6), 625-631. [https://doi.org/10.1016/S0023-6438\(03\)00082-3](https://doi.org/10.1016/S0023-6438(03)00082-3)
- Kantono, K., Hamid, N., Ma, Q., Oey, I., & Farouk, M. (2021). Changes in the physicochemical properties of chilled and frozen-thawed lamb cuts subjected to pulsed electric field processing. *Food Research International*, 141, 110092. <https://doi.org/10.1016/j.foodres.2020.110092>
- Kaufmann, A., Köppel, R., & Widmer, M. (2012). Determination of microbial transglutaminase in meat and meat products. *Food Additives & Contaminants: Part A*, 29(9), 1364-1373. <https://doi.org/10.1080/19440049.2012.691557>

- Khan, M. K., Imran, M., Ahmad, M. H., Hassan, S., & Sattar, S. (2021). Ultrasound for beverage processing. *In Design and Optimization of Innovative Food Processing Techniques Assisted by Ultrasound*, 189-215 Academic Press. <https://doi.org/10.1016/B978-0-12-818275-8.00007-6>
- Khozroughi, A. G., Jander, E., Schirrmann, M., Rawel, H., Kroh, L. W., & Schlüter, O. (2017). The role of myoglobin degradation in the formation of zinc protoporphyrin IX in the longissimus lumborum of pork. *LWT-Food Science and Technology*, 85, 22-27. <https://doi.org/10.1016/j.lwt.2017.06.047>
- Kim, S. K., Byun, H. G., Park, P. J., & Shahidi, F. (2001). Angiotensin I converting enzyme inhibitory peptides purified from bovine skin gelatin hydrolysate. *Journal of Agricultural and Food Chemistry*, 49(6), 2992-2997. <https://doi.org/10.1021/jf001119u>
- Kim, J. H., Kim, J. W., Yu, S. H., Lee, J., Cho, H. T., Heo, W., ... & Kim, Y. J. (2019). Utilization of Pectinase Cocktail and High Hydrostatic Pressure for the Production of Aged Black Garlic Juice with Improved Nutritional Value. *Preventive nutrition and food science*, 24(3), 357. <https://doi.org/10.3746/pnf.2019.24.3.357>
- Kim, E. K., Lee, S. J., Jeon, B. T., Moon, S. H., Kim, B., Park, T. K., ... & Park, P. J. (2009). Purification and characterisation of antioxidative peptides from enzymatic hydrolysates of venison protein. *Food Chemistry*, 114(4), 1365-1370. <https://doi.org/10.1016/j.foodchem.2008.11.035>
- Kim, H. J., & Taub, I. A. (1991). Specific degradation of myosin in meat by bromelain. *Food chemistry*, 40(3), 337-343. [https://doi.org/10.1016/0308-8146\(91\)90117-7](https://doi.org/10.1016/0308-8146(91)90117-7)
- King, J. W., Johnson, J. H., & Friedrich, J. P. (1989). Extraction of fat tissue from meat products with supercritical carbon dioxide. *Journal of Agricultural and Food Chemistry*, 37(4), 951-954.

- Konno, K., Hirayama, C., Nakamura, M., Tateishi, K., Tamura, Y., Hattori, M., & Kohno, K. (2004). Papain protects papaya trees from herbivorous insects: role of cysteine proteases in latex. *The Plant Journal*, *37*(3), 370-378. <https://doi.org/10.1046/j.1365-313X.2003.01968.x>
- Koohmaraie, M. (1996). Biochemical factors regulating the toughening and tenderization processes of meat. *Meat science*, *43*, 193-201. [https://doi.org/10.1016/0309-1740\(96\)00065-4](https://doi.org/10.1016/0309-1740(96)00065-4)
- Koohmaraie, M., & Geesink, G. H. (2006). Contribution of postmortem muscle biochemistry to the delivery of consistent meat quality with particular focus on the calpain system. *Meat science*, *74*(1), 34-43. <https://doi.org/10.1016/j.meatsci.2006.04.025>
- Lametsch, R., Karlsson, A., Rosenvold, K., Andersen, H. J., Roepstorff, P., & Bendixen, E. (2003). Postmortem proteome changes of porcine muscle related to tenderness. *Journal of Agricultural and Food Chemistry*, *51*(24), 6992-6997. <https://doi.org/10.1021/jf034083p>
- Ledward, D. A. (1985). Post-slaughter influences on the formation of metmyoglobin in beef muscles. *Meat Science*, *15*(3), 149-171. [https://doi.org/10.1016/0309-1740\(85\)90034-8](https://doi.org/10.1016/0309-1740(85)90034-8)
- Leong, S. Y., & Oey, I. (2014). Effect of pulsed electric field treatment on enzyme kinetics and thermostability of endogenous ascorbic acid oxidase in carrots (*Daucus carota* cv. Nantes). *Food chemistry*, *146*, 538-547. <https://doi.org/10.1016/j.foodchem.2013.09.096>
- Li, T., Shi, C., Zhou, C., Sun, X., Ang, Y., Dong, X., ... & Zhou, G. (2020). Purification and characterization of novel antioxidant peptides from duck breast protein hydrolysates. *LWT*, *125*, 109215. <https://doi.org/10.1016/j.lwt.2020.109215>
- Li, D., Wu, Z., Wang, P., Xu, E., Cui, B., Han, Y., & Tao, Y. (2022). Effect of moderate electric field on glucoamylase-catalyzed hydrolysis of corn starch: Roles of electrophoretic and polarization effects. *Food Hydrocolloids*, *122*, 107120. <https://doi.org/10.1016/j.foodhyd.2021.107120>



- Loneragan, Steven M.; Topel, David G.; Marple, Dennis N. (2018). The science of animal growth and meat technology. Academic Press,
- Ma, X., Zhang, L., Wang, W., Zou, M., Ding, T., Ye, X., & Liu, D. (2016a). Synergistic effect and mechanisms of combining ultrasound and pectinase on pectin hydrolysis. *Food and Bioprocess Technology*, 9(7), 1249-1257. <https://doi.org/10.1007/s11947-016-1689-y>
- Ma, Q., Hamid, N., Oey, I., Kantono, K., Faridnia, F., Yoo, M., & Farouk, M. (2016b). Effect of chilled and freezing pre-treatments prior to pulsed electric field processing on volatile profile and sensory attributes of cooked lamb meats. *Innovative Food Science & Emerging Technologies*, 37, 359-374. <https://doi.org/10.1016/j.ifset.2016.04.009>
- Ma, H. J., & Ledward, D. A. (2004). High pressure/thermal treatment effects on the texture of beef muscle. *Meat science*, 68(3), 347-355. <https://doi.org/10.1016/j.meatsci.2004.04.001>
- Mali, A. M., & Chavan, N. S. (2016). In vitro rapid regeneration through direct organogenesis and ex-vitro establishment of Cucumis trigonus Roxb.—An underutilized pharmaceutically important cucurbit. *Industrial Crops and Products*, 83, 48-54. <https://doi.org/10.1016/j.indcrop.2015.12.036>
- Mancini, R. A., & Hunt, M. (2005). Current research in meat color. *Meat science*, 71(1), 100-121. <https://doi.org/10.1016/j.meatsci.2005.03.003>
- Mañas, P., & Pagán, R. (2005). Microbial inactivation by new technologies of food preservation. *Journal of applied microbiology*, 98(6), 1387-1399. <https://doi.org/10.1111/j.1365-2672.2005.02561.x>
- Martín Municio, E., & Raso Pueyo, J. (2018). Aplicaciones de los pulsos eléctricos de alto voltaje para el procesado y conservación de alimentos. Universidad de Zaragoza.

- Martínez, J. M., Delso, C., Álvarez, I., & Raso, J. (2020). Pulsed electric field-assisted extraction of valuable compounds from microorganisms. *Comprehensive Reviews in Food Science and Food Safety*, 19(2), 530-552. <https://doi.org/10.1111/1541-4337.12512>
- Matarneh, S. K., England, E. M., Scheffler, T. L., & Gerrard, D. E. (2017). The conversion of muscle to meat. In *Lawrie's Meat Science* (pp. 159-185). Woodhead Publishing. <https://doi.org/10.1016/B978-0-08-100694-8.00005-4>
- Messens, W., Dewettinck, K., Van Camp, J., & Huyghebaert, A. (1998). High pressure brining of Gouda cheese and its effect on the cheese serum. *LWT-Food Science and Technology*, 31(6), 552-558. <https://doi.org/10.1006/fstl.1998.0414>
- Møller, J. K., Adamsen, C. E., Catharino, R. R., Skibsted, L. H., & Eberlin, M. N. (2007). Mass spectrometric evidence for a zinc–porphyrin complex as the red pigment in dry-cured Iberian and Parma ham. *Meat science*, 75(2), 203-210. <https://doi.org/10.1016/j.meatsci.2006.07.005>
- Molly, K., Demeyer, D., Johansson, G., Raemaekers, M., Ghistelinck, M., & Geenen, I. (1997). The importance of meat enzymes in ripening and flavour generation in dry fermented sausages. First results of a European project. *Food chemistry*, 59(4), 539-545. [https://doi.org/10.1016/S0308-8146\(97\)00004-6](https://doi.org/10.1016/S0308-8146(97)00004-6)
- Morbiato, G., Zambon, A., Toffoletto, M., Poloniato, G., Dall'Acqua, S., de Bernard, M., & Spilimbergo, S. (2019). Supercritical carbon dioxide combined with high power ultrasound as innovate drying process for chicken breast. *The Journal of Supercritical Fluids*, 147, 24-32. <https://doi.org/10.1016/j.supflu.2019.02.004>
- Moreno, J., Espinoza, C., Simpson, R., Petzold, G., Nuñez, H., & Gianelli, M. P. (2016). Application of ohmic heating/vacuum impregnation treatments and air drying to develop an apple snack enriched in folic acid. *Innovative Food Science & Emerging Technologies*, 33, 381-386. <https://doi.org/10.1016/j.ifset.2015.12.014>

- Muguruma, M., Ahhmed, A. M., Katayama, K., Kawahara, S., Maruyama, M., & Nakamura, T. (2009). Identification of pro-drug type ACE inhibitory peptide sourced from porcine myosin B: Evaluation of its antihypertensive effects in vivo. *Food Chemistry*, 114(2), 516-522. <https://doi.org/10.1016/j.foodchem.2008.09.081>
- Mulet, A., Cárcel, J. A., Sanjuan, N., & Bon, J. (2003). New food drying technologies- Use of ultrasound. *Food Science and Technology International*, 9(3), 215-221. <https://doi.org/10.1177/1082013203034641>
- Naqvi, Z. B., Campbell, M. A., Latif, S., Thomson, P. C., McGill, D. M., Warner, R. D., & Friend, M. A. (2021). Improving tenderness and quality of M. biceps femoris from older cows through concentrate feeding, zingibain protease and sous vide cooking. *Meat Science*, 180, 108563. <https://doi.org/10.1016/j.meatsci.2021.108563>
- Nowak, D. (2011). Enzymes in tenderization of meat-the system of calpains and other systems-a review. *Polish Journal of Food and Nutrition Sciences*, 61(4).
- Naveena, B. M., Mendiratta, S. K., & Anjaneyulu, A. S. R. (2004). Tenderization of buffalo meat using plant proteases from *Cucumis trigonus* Roxb (Kachri) and *Zingiber officinale* roscoe (Ginger rhizome). *Meat Science*, 68(3), 363-369. <https://doi.org/10.1016/j.meatsci.2004.04.004>
- Ojha, K. S., Keenan, D. F., Bright, A., Kerry, J. P., & Tiwari, B. K. (2016). Ultrasound assisted diffusion of sodium salt replacer and effect on physicochemical properties of pork meat. *International journal of food science & technology*, 51(1), 37-45. <https://doi.org/10.1111/ijfs.13001>
- Ouali, A., Gagaoua, M., Boudida, Y., Becila, S., Boudjellal, A., Herrera-Mendez, C. H., & Sentandreu, M. A. (2013). Biomarkers of meat tenderness: present knowledge and perspectives in regards to our current understanding of the mechanisms involved. *Meat science*, 95(4), 854-870. <https://doi.org/10.1016/j.meatsci.2013.05.010>

- Ouali, A., Herrera-Mendez, C. H., Coulis, G., Becila, S., Boudjellal, A., Aubry, L., & Sentandreu, M. A. (2006). Revisiting the conversion of muscle into meat and the underlying mechanisms. *Meat science*, 74(1), 44-58. <https://doi.org/10.1016/j.meatsci.2006.05.010>
- Ozuna, C., Puig, A., García-Pérez, J. V., Mulet, A., & Cárcel, J. A. (2013). Influence of high intensity ultrasound application on mass transport, microstructure and textural properties of pork meat (*Longissimus dorsi*) brined at different NaCl concentrations. *Journal of Food Engineering*, 119(1), 84-93. <https://doi.org/10.1016/j.jfoodeng.2013.05.016>
- Pereira, R. N., Vicente, A. A., & Teixeira, J. A. (2019). Food Structure Development/Production Through Flexible Processes: The Use of Electric Fields to Enable Food Manufacturing. *Handbook of Food Structure Development*, 18, 422.
- Qihe, C., Guoqing, H., Yingchun, J., & Hui, N. (2006). Effects of elastase from a *Bacillus* strain on the tenderization of beef meat. *Food chemistry*, 98(4), 624-629. <https://doi.org/10.1016/j.foodchem.2005.06.043>
- Ramezani, R., Aminlari, M., & Fallahi, H. (2003). Effect of chemically modified soy proteins and ficin-tenderized meat on the quality attributes of sausage. *Journal of food science*, 68(1), 85-88. <https://doi.org/10.1111/j.1365-2621.2003.tb14119.x>
- Raso-Pueyo, J., & Heinz, V. (Eds.). (2010). Pulsed electric fields technology for the food industry: fundamentals and applications. Springer Science & Business Media.
- Rico, E., Toldrá, F., & Flores, J. (1991). Assay of cathepsin D activity in fresh pork muscle and dry-cured ham. *Meat science*, 29(4), 287-293. [https://doi.org/10.1016/0309-1740\(91\)90008-E](https://doi.org/10.1016/0309-1740(91)90008-E)

- Rinella, AL (2014). Efecto de campos eléctricos moderados sobre la difusión de cloruro de sodio en el músculo porcino (tesis doctoral, The Ohio State University).
- Ruiz-Ramírez, J., Arnau, J., Serra, X., & Gou, P. (2005). Relationship between water content, NaCl content, pH and texture parameters in dry-cured muscles. *Meat Science*, 70(4), 579-587. <https://doi.org/10.1016/j.meatsci.2005.02.007>
- Saiga, A. I., Tanabe, S., & Nishimura, T. (2003). Antioxidant activity of peptides obtained from porcine myofibrillar proteins by protease treatment. *Journal of agricultural and food chemistry*, 51(12), 3661-3667. <https://doi.org/10.1021/jf021156g>
- Saldo, J., Sendra, E., & Guamis, B. (2000). High hydrostatic pressure for accelerating ripening of goat's milk cheese: proteolysis and texture. *Journal of Food Science*, 65(4), 636-640. <https://doi.org/10.1111/j.1365-2621.2000.tb16064.x>
- Saldo, J., McSweeney, P. L. H., Sendra, E., Kelly, A. L., & Guamis, B. (2002). Proteolysis in caprine milk cheese treated by high pressure to accelerate cheese ripening. *International Dairy Journal*, 12(1), 35-44. [https://doi.org/10.1016/S0958-6946\(01\)00169-8](https://doi.org/10.1016/S0958-6946(01)00169-8)
- Salmerón, C., Navarro, I., Johnston, I. A., Gutiérrez, J., & Capilla, E. (2015). Characterisation and expression analysis of cathepsins and ubiquitin-proteasome genes in gilthead sea bream (*Sparus aurata*) skeletal muscle. *BMC research notes*, 8(1), 1-15. <https://doi.org/10.1186/s13104-015-1121-0>
- Samaranayake, C. P., & Sastry, S. K. (2016). Effects of controlled-frequency moderate electric fields on pectin methylesterase and polygalacturonase activities in tomato homogenate. *Food Chemistry*, 199, 265-272. <https://doi.org/10.1016/j.foodchem.2015.12.010>
- Sárraga, C., Gil, M., Arnau, J., Monfort, J. M., & Cussó, R. (1989). Effect of curing salt and phosphate on the activity of porcine muscle proteases. *Meat Science*, 25(4), 241-249. [https://doi.org/10.1016/0309-1740\(89\)90042-9](https://doi.org/10.1016/0309-1740(89)90042-9)

- Şener, N., Apar, D. K., & Özbek, B. (2006). A modelling study on milk lactose hydrolysis and  $\beta$ -galactosidase stability under sonication. *Process Biochemistry*, 41(7), 1493-1500. <https://doi.org/10.1016/j.procbio.2006.02.008>
- Sentandreu, M. A., Coulis, G., & Ouali, A. (2002). Role of muscle endopeptidases and their inhibitors in meat tenderness. *Trends in Food Science & Technology*, 13(12), 400-421. [https://doi.org/10.1016/S0924-2244\(02\)00188-7](https://doi.org/10.1016/S0924-2244(02)00188-7)
- Senyay-Oncel, D., & Yesil-Celiktas, O. (2011). Activity and stability enhancement of  $\alpha$ -amylase treated with sub-and supercritical carbon dioxide. *Journal of bioscience and bioengineering*, 112(5), 435-440. <https://doi.org/10.1016/j.jbiosc.2011.07.012>
- Sikes, A., Tornberg, E., & Tume, R. (2010). A proposed mechanism of tenderising post-rigor beef using high pressure–heat treatment. *Meat Science*, 84(3), 390-399. <https://doi.org/10.1016/j.meatsci.2009.09.007>
- Soliva-Fortuny, R., Balasa, A., Knorr, D., & Martín-Belloso, O. (2009). Effects of pulsed electric fields on bioactive compounds in foods: a review. *Trends in Food Science & Technology*, 20(11-12), 544-556. <https://doi.org/10.1016/j.tifs.2009.07.003>
- Soria, A. C., & Villamiel, M. (2010). Effect of ultrasound on the technological properties and bioactivity of food: a review. *Trends in food science & technology*, 21(7), 323-331. <https://doi.org/10.1016/j.tifs.2010.04.003>
- Sukmanov, V., Hanjun, M., & Li, Y. P. (2019). Effect of high pressure processing on meat and meat products. A review. *Ukrainian food journal*, (8, Issue 3), 448-469
- Sullivan, G. A., & Calkins, C. R. (2010). Application of exogenous enzymes to beef muscle of high and low-connective tissue. *Meat science*, 85(4), 730-734. <https://doi.org/10.1016/j.meatsci.2010.03.033>

- Sunil, N. C., Singh, J., Chandra, S., Chaudhary, V., & Kumar, V. (2018). "Non-thermal techniques: Application in food industries" A review. *Journal of Pharmacognosy and Phytochemistry*, 7(5), 1507-1518.
- Taher, H., Al-Zuhair, S., AlMarzouqui, A., & Hashim, I. (2011). Extracted fat from lamb meat by supercritical CO<sub>2</sub> as feedstock for biodiesel production. *Biochemical Engineering Journal*, 55(1), 23-31. <https://doi.org/10.1016/j.bej.2011.03.003>
- Talon, R., Leroy, S., & Lebert, I. (2007). Microbial ecosystems of traditional fermented meat products: The importance of indigenous starters. *Meat Science*, 77(1), 55-62. <https://doi.org/10.1016/j.meatsci.2007.04.023>
- Tarté, R. (Ed.). (2009). Ingredients in meat products: properties, functionality and applications. *Springer Science & Business Media*.doi: 10.1007/978-0-387-71327-4
- Toldrá, F. (2008). Dry-cured meat products. John Wiley & Sons.
- Toldrá, F. (2006). The role of muscle enzymes in dry-cured meat products with different drying conditions. *Trends in Food Science & Technology*, 17(4), 164-168. <https://doi.org/10.1016/j.tifs.2005.08.007>
- Toldrá, F., & Aristoy, M. C. (1993). Availability of essential amino acids in dry-cured ham. *International journal of food sciences and nutrition*, 44(3), 215-219. <https://doi.org/10.3109/09637489309017442>
- Toldrá, F., Aristoy, M. C., & Flores, M. (2000). Contribution of muscle aminopeptidases to flavor development in dry-cured ham. *Food Research International*, 33(3-4), 181-185. [https://doi.org/10.1016/S0963-9969\(00\)00032-6](https://doi.org/10.1016/S0963-9969(00)00032-6)
- Toldrá, F., Aristoy, M. C., Mora, L., & Reig, M. (2012). Innovations in value-addition of edible meat by-products. *Meat science*, 92(3), 290-296. <https://doi.org/10.1016/j.meatsci.2012.04.004>

- Toldrá, F., Flores, M., & Aristoy, M. C. (1995). Enzyme generation of free amino acids and its nutritional significance in processed pork meats. *In Developments in Food Science*, 37, 1303-1322. Elsevier. [https://doi.org/10.1016/S0167-4501\(06\)80235-9](https://doi.org/10.1016/S0167-4501(06)80235-9)
- Toldrá, F., Flores, M., & Sanz, Y. (1997). Dry-cured ham flavour: enzymatic generation and process influence. *Food Chemistry*, 59(4), 523-530. [https://doi.org/10.1016/S0308-8146\(97\)00013-7](https://doi.org/10.1016/S0308-8146(97)00013-7)
- Torres Bello, E. F., González Martínez, G., Klotz Ceberio, B. F., Rodrigo, D., & Martínez López, A. (2014). High pressure treatment in foods. *Foods*, 3(3), 476-490. <https://doi.org/10.3390/foods3030476>
- Wakamatsu, J., Okui, J., Ikeda, Y., Nishimura, T., & Hattori, A. (2004). Establishment of a model experiment system to elucidate the mechanism by which Zn-protoporphyrin IX is formed in nitrite-free dry-cured ham. *Meat Science*, 68(2), 313-317. <https://doi.org/10.1016/j.meatsci.2004.03.014>
- Wang, D., Ma, X., Yan, L., Chantapakul, T., Wang, W., Ding, T., Ye, X., & Liu, D. (2017). Ultrasound assisted enzymatic hydrolysis of starch catalyzed by glucoamylase: Investigation on starch properties and degradation kinetics. *Carbohydrate Polymers*, 175, 47–54. <https://doi.org/10.1016/j.carbpol.2017.06.093>
- Wang, J., Lu, S., Li, R., Wang, Y., & Huang, L. (2020). Identification and characterization of antioxidant peptides from Chinese dry-cured mutton ham. *Journal of the Science of Food and Agriculture*, 100(3), 1246-1255. <https://doi.org/10.1002/jsfa.10136>
- Warner, R. D., McDonnell, C. K., Bekhit, A. E. D., Claus, J., Vaskoska, R., Sikes, A., ... & Ha, M. (2017). Systematic review of emerging and innovative technologies for meat tenderisation. *Meat Science*, 132, 72-89. <https://doi.org/10.1016/j.meatsci.2017.04.241>



- 
- Xiong, Y. L. "Muscle proteins." *Proteins in food processing*. Woodhead Publishing, 2018. 127-148. <https://doi.org/10.1016/B978-0-08-100722-8.00006-1>
- Xiong, G. Y., Zhang, L. L., ZhanG, W., & Wu, J. (2012). Influence of ultrasound and proteolytic enzyme inhibitors on muscle degradation, tenderness, and cooking loss of hens during aging. *Czech Journal of Food Sciences*, 30(3), 195-205. <https://doi.org/10.17221/136/2011-CJFS>
- Yang, X., & Zhang, Y. (2019). Expression of recombinant transglutaminase gene in *Pichia pastoris* and its uses in restructured meat products. *Food chemistry*, 291, 245-252. <https://doi.org/10.1016/j.foodchem.2019.04.015>
- Yao, Y., Pan, Y., & Liu, S. (2020). Power ultrasound and its applications: A state-of-the-art review. *Ultrasonics sonochemistry*, 62, 104722. <https://doi.org/10.1016/j.ultsonch.2019.104722>
- Yeom, H. W., Zhang, Q. H., & Dunne, C. P. (1999). Inactivation of papain by pulsed electric fields in a continuous system. *Food Chemistry*, 67(1), 53-59. [https://doi.org/10.1016/S0308-8146\(99\)00109-0](https://doi.org/10.1016/S0308-8146(99)00109-0)
- Zhang, B., Sun, Q., Liu, H. J., Li, S. Z., & Jiang, Z. Q. (2017). Characterization of actinidin from Chinese kiwifruit cultivars and its applications in meat tenderization and production of angiotensin I-converting enzyme (ACE) inhibitory peptides. *LWT*, 78, 1-7. <https://doi.org/10.1016/j.lwt.2016.12.012>



